

**UNIVERSITY OF VERONA**  
**GRADUATE SCHOOL OF NATURAL AND ENGINEERING**  
**SCIENCES**

**PhD in Biotechnology**  
**(XXX cycle)**

**Myristic acid:**  
***in vivo* evaluation of connection with cardiovascular risk factors**  
**and *in vitro* proteomic investigations of its biochemical effects**

**S.S.D CHIM/01**

COORDINATOR

Prof. MASSIMO DELLEDONNE

TUTOR

Prof.ssa DANIELA CECCONI

PhD STUDENT  
Dott.ssa GIULIA SPEZIALI

# TABLE OF CONTENTS

<b>SUMMARY</b>	4
<b>LIST OF ABBREVIATIONS</b>	6
<b>SECTION 1</b>	
<b><u>CHAPTER 1: CORONARY ARTERY DISEASE AND FATTY ACIDS</u></b>	9
1. Coronary artery disease	9
1.1. The atherosclerotic process	10
1.2. CAD outcomes	13
2. Lipid metabolism: the importance of lipoproteins	16
2.1. Lipid components of lipoproteins	18
2.2. Protein components: focus on ApoA-I, B, C-III and E	22
3. CAD risk factors	31
3.1. Dyslipidemia	35
3.2. Fatty acids intake	37
4. <i>In vivo</i> studies on myristic acid role in CAD	39
<b><u>CHAPTER 2: IN VIVO INVESTIGATION OF POSSIBLE NEW ASSOCIATIONS BETWEEN CARDIOVASCULAR RISK FACTORS: THE EMERGING ROLE OF MYRISTIC ACID</u></b>	42
1. Introduction	42
2. Experimental design and procedures	44
2.1. Study subjects	44
2.2. Clinical chemistry analyses of plasma lipid parameters	46
2.3. Gas-chromatography analysis of plasma fatty acids levels	46
2.4. Statistical analysis	49
3. Results	50
3.1. Clinical characteristics of the studied population	50
3.2. Lipid profile and apolipoproteins levels of the studied population	51
3.3. Fatty acids levels in plasma of the studied population	52
3.4. Correlation analyses	54
3.5. Principal Component Analysis (PCA) results	63
3.6. Regression analyses	64
3.7. <i>In vivo</i> evaluation of myristic acid correlation with CAD risk factors: focus on triglycerides and ApoC-III plasma levels	66
4. Discussion	71

<b><u>CHAPTER 3: ANALYSIS OF THE ASSOCIATION BETWEEN MYRISTIC ACID AND APOC-III IN A HEPG2 CELL MODEL</u></b>	76
1. Introduction	76
2. Experimental design and procedures	78
2.1. Cell culture and myristic acid conditioning	78
2.2. Western Blot analyses on ApoC-III	79
2.3. Protein digestion for mass spectrometry analysis	80
2.4. LC-MS/MS targeted analysis of ApoC-III	80
2.5. Real Time PCR analysis of ApoC-III	82
3. Results	83
3.1. Effect of myristic acid treatments on HepG2 cells viability and growth	83
3.2. Modulation of ApoC-III protein in HepG2 cells treated with myristic acid	84
3.3. Modulation of ApoC-III mRNA in HepG2 cells treated with myristic acid	85
4. Discussion	87
5. Concluding remarks	89
<b>SECTION 2</b>	
<b><u>CHAPTER 1: PROTEOMICS AND FATTY ACIDS</u></b>	92
1. Proteomics investigations of fatty acids effects	92
2. <i>In-vitro</i> studies on myristic acid	97
<b><u>CHAPTER 2: IN-VITRO PROTEOMIC ANALYSIS OF HEPG2 CELLS TREATED WITH MYRISTIC ACID</u></b>	102
1. Introduction	102
2. Experimental design and procedure	103
2.1. Cell culture and treatment with myristic acid	103
2.2. Oil Red O staining	104
2.3. Proteome and Secretome sample preparation	104
2.4. LC-MS/MS and data analysis	105
2.5. Protein annotation, secretion prediction, protein networks and pathways analysis	107
2.6. Western Blot analysis of selected proteins	108
3. Results	110
3.1. Effects of myristic acid on HepG2 cells viability and on lipid droplets accumulation	110
3.2. Quantitative analysis of proteins deregulated by myristic acid in HepG2 cells proteome and secretome	112
3.3. Prediction of secretion pathways	119
3.4. Modulation of biological processes and pathways induced by myristic acid	121

3.5. Myristic acid influence on ER stress	126
4. Discussion	128
4.1. Myristic acid induces lipid droplet formation, cytoskeleton reorganization and ER stress	128
4.1.1. Lipid droplets	129
4.1.2. Cytoskeleton remodeling	130
4.1.3. ER stress and protein homeostasis	130
4.1.4. Other effects of myristic acid	134
4.2. Myristic acid causes deregulation of secreted proteins involved in exosome and extracellular miRNA sorting	135
4.2.1. Proteins related to exosomes	136
4.2.2. miRNA sorting	137
4.2.3. Other effects of myristic acid	137
<b>CHAPTER 3: COMPARATIVE PROTEOMIC STUDY OF THE BIOCHEMICAL EFFECTS INDUCED BY MYRISTIC, PALMITIC AND OLEIC ACIDS</b>	140
1. Introduction	140
2. Experimental design and procedures	143
2.1 Cell culture and fatty acids conditioning	143
2.2 Oil Red O staining	144
2.3 Samples preparation and mass spectrometry analysis	145
2.4 Comparative proteomic analysis to assess the effects of myristic, palmitic and oleic acid	146
3. Results	148
3.1 Effects of palmitic and oleic acid on HepG2 cell viability and lipid droplets	148
3.2 Quantitative analysis of proteins deregulated by palmitic and oleic acid in HepG2 cell proteome	151
3.3 Comparison between proteins modulated in HepG2 cells by myristic, palmitic and oleic acid	157
3.4 Biological processes exclusively modulated by myristic, palmitic and oleic acid	159
4. Discussion	165
4.1 Proteins modulated exclusively by myristic acid	166
4.2 Proteins modulated by both myristic and palmitic acid	169
4.3 Proteins modulated by both myristic and oleic acid	170
4.4 Proteins modulated exclusively by palmitic and oleic acid	170
5. Concluding remarks	174
Acknowledgements	175
Bibliography	176

## SUMMARY

Fatty acids (FAs) are fundamental constituents of cell structure, but they can also influence cellular functions and molecular mechanisms with different effects according to their chain length and degree of saturation. Different pathological conditions have been linked to FAs profile, including dyslipidemia and hypertriglyceridemia. However, data concerning the effects of FAs on lipid metabolism and cardiovascular disease are still scarce and controversial. Therefore, the aim of the first part of the present PhD thesis (Section 1) has been to investigate the presence of possible significant correlations between plasma FAs profile and lipid parameters (including levels of the major apolipoproteins) in a population of Coronary Artery Disease (CAD) patients and controls. The analysis, performed on plasma of 1,370 subjects, revealed that Myristic acid (C14:0) positively predicted both Triglycerides (TG) and Apolipoprotein C-III (ApoC-III) plasma levels, confirming the preliminary data obtained in my master's degree thesis on 57 CAD patients. ApoC-III being an important regulator of plasma TG levels, the influence of C14:0 on the expression of this protein has been investigated in a HepG2 cell model. Mass spectrometry results, together with Real Time PCR findings, suggest a slight but significant increase in ApoC-III protein and mRNA levels in C14:0 treated cells. Therefore, the *in vitro* investigations supported the positive connection observed *in-vivo* between C14:0, TG and ApoC-III plasma levels, suggesting a possible important role of this saturated FA in the onset of cardiovascular disease.

The effects of FAs on liver metabolism have been studied during the last few years for the influence they have on lipid metabolism, the onset of nonalcoholic fatty liver disease (NAFLD) and cardiovascular disease. However, proteomics investigations in this direction are still scarce and the influence of C14:0 on liver metabolism still needs to be elucidated. Therefore, in the second part of the present PhD thesis (Section 2) the effects of different concentrations of

C14:0 on HepG2 cells proteome and secretome have been investigated by means of high-resolution mass spectrometry. The results obtained highlighted the influence of this FA on proteins involved in lipid droplets formation, cytoskeleton organization, endoplasmic reticulum stress, exosome release and cell-cell stress communication. To highlight the proteome changes specifically related to C14:0, a comparative study of the proteomic modulations induced by C14:0, palmitic (C16:0) and oleic acid (C18:1) has been performed. Interestingly, the overlapping of modulated proteins induced by the three FAs treatments was limited to just one protein, highlighting their different mechanisms of action. 40 proteins were found to be deregulated specifically by C14:0. These results suggested a unique influence of this saturated FA on specific proteins involved in different biological processes, mainly protein homeostasis counteracting ER stress (e.g. ENTPD5, VAPB and SGTA) and lipid metabolism (e.g. ApoE).

In conclusion, the present PhD thesis highlights for the first time a possible *in-vivo* fundamental role of C14:0 on lipid metabolism, particularly on ApoC-III and TG plasma levels and represents the first investigation shedding light on the *in-vitro* C14:0 effects on a human hepatocyte-derived cell line.

## LIST OF ABBREVIATIONS

2-DE	Two-dimensional gel electrophoresis
ABCA1	ATP-binding cassette transporter A1
ACS	Acute Coronary Syndrome
ADRP	Perilipn-2
Apo	Apolipoprotein
BMI	Body mass index
BSA	Bovine serum albumin
C14:0	Myristic acid
C16:0	Palmitic acid
C18:1	Oleic acid
CAD	Coronary Artery Disease
CETP	Cholesteryl Ester Transfer Protein
CVD	Cardiovascular Diseases
DES1	Sphingolipid $\Delta$ 4 desaturase 1
DMSO	Dimethyl sulfoxide
DNM2	Dynammin-2
DSTN	Dextrin
ECs	Endothelial cells
EDTA	Ethylenediaminetetraacetic acid
ENTPD5	Ectonucleoside triphosphate diphosphohydrolase 5
ER	Endoplasmic Reticulum
ERAD	Endoplasmic reticulum associated degradation
FAs	Fatty acids
FASN	Fatty acid synthase
FBS	Fetal Bovine Serum
GO	Gene Ontology
HDL	High Density Lipoproteins
HSPs	Heat Shock Proteins
IDL	Intermediate Density Lipoproteins
LCAT	Lecithin-cholesterol Acyltransferase
LD	Lipid droplets
LDL	Low Density Lipoproteins
LDLR	Low Density Lipoprotein Receptor
LFQ	Label-free quantification
LPL	Lipoprotein lipase
LRP	Low density Lipoproteins receptor- related protein
MetS	Metabolic syndrome
MI	Myocardial infarction
MS	Mass-spectrometry
MUFA	Monounsaturated fatty acids
n-3 PUFA	Omega-3 polyunsaturated fatty acids
n-6 PUFA	Omega-6 polyunsaturated fatty acids
NAFLD	Nonalcoholic fatty liver disease
NASH	Nonalcoholic steatohepatitis
NMT	N-myristoyltransferase
NO	Nitric Oxide

oxLDL	Oxidized Low Density Lipoproteins
OXPHOS	Oxidative phosphorylation system
PBS	Phosphate-buffered saline
PPAR	Peroxisome Proliferator Receptors
PUFA	Polyunsaturated fatty acids
RBP	Retinol Binding Protein
RCT	Reverse cholesterol transport
ROS	Reactive Oxygen Species
SFA	Saturated fatty acids
SGTA	Small glutamine-rich tetratricopeptide repeat-containing protein alpha
SMCs	Smooth Muscle Cells
SR-BI	Scavenger receptor class B type I
T1DM	Type 1 diabetes mellitus
T2DM	Type 2 diabetes mellitus
TF	Transferrin
TFA	Trans fatty acids
TG	Triglycerides
TRLs	Triglycerides-rich lipoproteins
UPR	Unfolded Protein Response
VAPB	Vesicle-associated membrane protein associated protein B/C
VCAM-1	Vascular cell adhesion molecule 1
VLDL	Very Low-Density Lipoproteins
WHO	World Health Organisation



# **SECTION 1**

# CHAPTER 1

## **CORONARY ARTERY DISEASE AND FATTY ACIDS**

### **1. CORONARY ARTERY DISEASE**

Cardiovascular diseases (CVD) consist of group of health diseases involving heart, blood or vascular diseases of the brain (Mendis S., 2011). To date CVD account for nearly one-third of worldwide deaths and are still the main cause of mortality (<http://www.who.int>) (Fig.1A). In 2015 the World Health Organization (WHO) estimated that 17.7 million deaths were caused by CVD, which corresponds to 31% of global deaths (<http://www.who.int>).

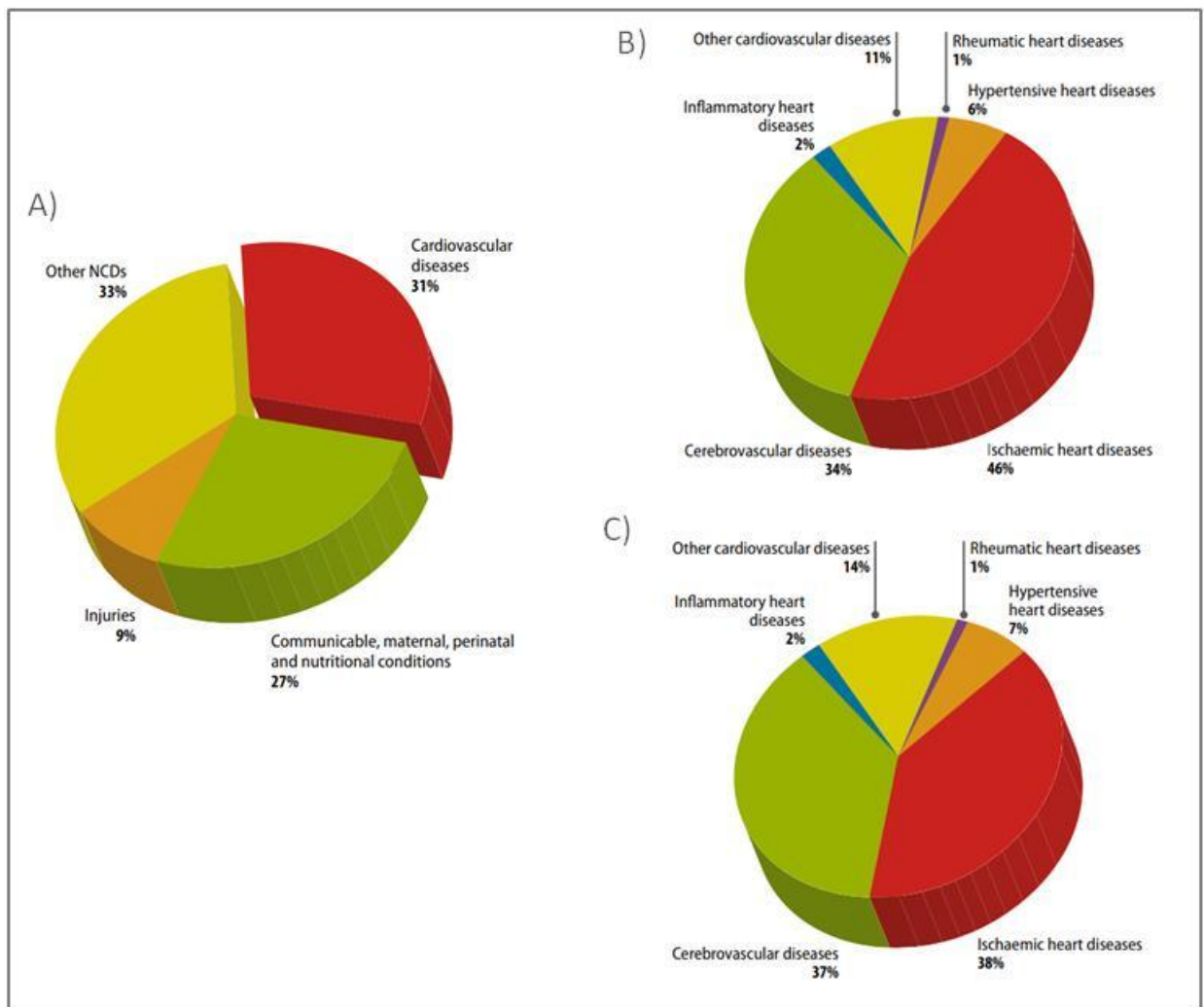


*Fig.1 CVDs incidence and distribution in the world population. Percentage of world deaths caused by CDVs (A) and their distribution among men (B) and women global populations (C) NCDs: non-communicable diseases (Mendis S., 2011).*

From the survey it emerged that the majority of those deaths (7.4 million) were caused by Coronary Artery Disease (CAD) (Fig.1B-C), including stable and unstable angina, myocardial infarction and coronary death, characterised by the progressive or even sudden occlusion of coronary arteries. Low and middle-income countries account for 80% of these deaths, with Eastern Europe and Central Asian countries having the highest number. Despite the decrease in CAD mortality by more than one half in wealthy countries over the last 25 years, the general tendency in low and middle-income countries is still flat or even rising due to a shift in lifestyle towards that seen in rich countries (Finegold et al., 2013). These data highlight that it is actually possible to prevent this pathology, but further research will be necessary in order to counteract the onset of CAD, which still also remains a major risk in wealthy countries.

## **1.1 THE ATHEROSCLEROTIC PROCESS**

Like stroke and peripheral vascular disease, CAD belongs to the group of CVD caused by the development of atherosclerosis inside blood vessels (Mendis S., 2011; Wong, 2014). While in the past it was seen just as a cholesterol storage disease, recent evolutions in our understanding of atherosclerosis allow us to describe atherosclerosis as a complex and progressive inflammatory process due to the accumulation of cells, connective-tissue elements, lipids and debris inside the intima, the innermost layer of vessel wall (Hansson, 2005; Libby et al., 2005). The first and trigger event of this process is the infiltration of circulating Low Density Lipoproteins (LDL), as well as of other Apolipoprotein B (ApoB) containing lipoproteins, inside the vessel walls, in areas of arterial branching or curvature, where disturbed flow permits an increased permeability (Lusis, 2000). LDL undergo a series of modifications including lipolysis, proteolysis, aggregation and oxidation. LDL oxidation is caused by the action of enzymes, such as myeloperoxidase and lipoxygenases, or by reactive oxygen species (ROS) that give rise to the pro-inflammatory oxLDL. These molecules inhibit the production of nitric oxide (NO), a molecule with antiatherogenic effects, and cause the release of phospholipids

that in turn activate the overlying endothelial cells (ECs) (Hansson et al., 2011). The activation induces ECs to produce pro-inflammatory molecules, growth factors and adhesion molecules (e.g. E-selectin and vascular cell adhesion molecule 1 (VCAM1)) that, in synergy with chemokines (e.g. CCL2), promote the sticking leucocytes, in particular monocytes and lymphocytes, to the inner surface of the artery wall, in correspondence with the endothelial lesion (Fig.2A) (Hansson et al., 2011). High density lipoproteins (HDL) play a protective role both by the removal of cholesterol from peripheral tissues and also by inhibiting lipoprotein oxidation through the action of paraoxonase on their surfaces (Lusis, 2000).

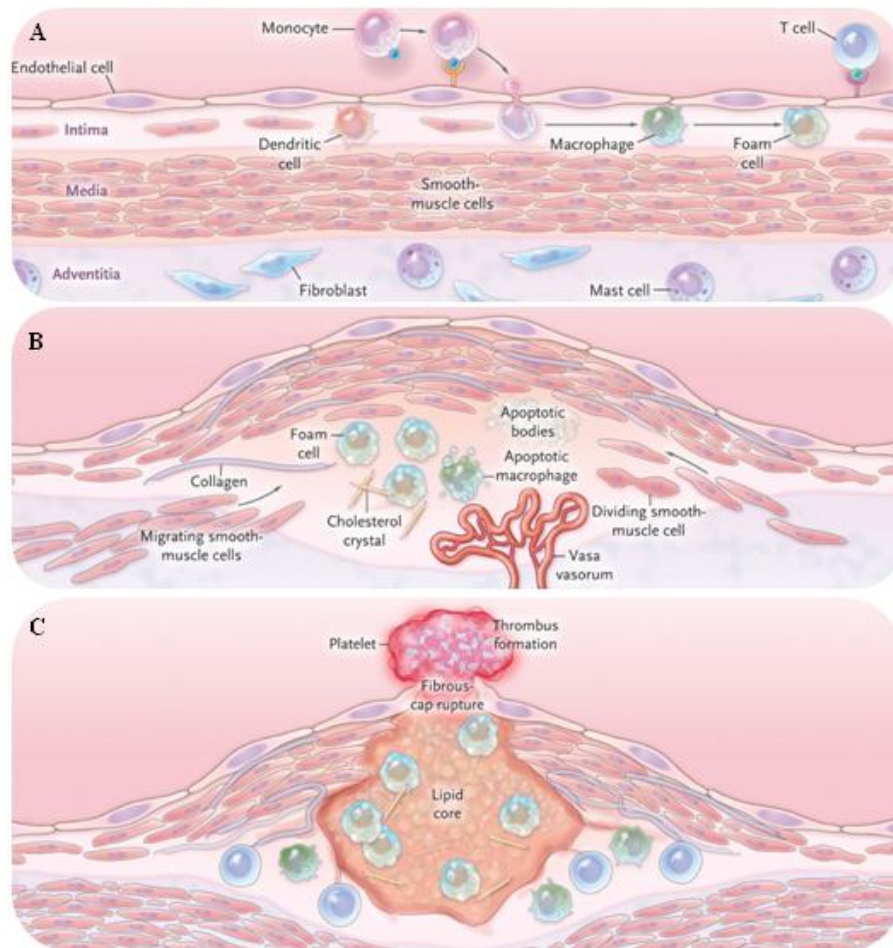


*Fig.2 Stages of atherosclerotic plaque development inside artery wall. Lesion formation implicates the sticking of monocytes to vessel endothelial cells (ECs) and their transformation in macrophages and foam cells (A). Smooth Muscle Cells (SMCs together with extracellular matrix molecules, lipids, microvessels and necrotic cells form the atherosclerotic plaque (B). Rupture of the fibrous cap expose tissue factor to the blood flow causing thrombus formation (C) (Nabel et al., 2012).*

Inside the inflamed intima, the Macrophage Colony-Stimulating factor (M-CSF) induces the differentiation of those monocytes in macrophages that, through the up-regulation of Scavengers Receptors and Toll like Receptors, internalise bacteria and toxins, apoptotic cell fragments and also oxLDL particles (Hansson, 2005). When lipids accumulate inside monocytes, they evolve into the so-called “foam cells” which have been defined as the hallmark of both early and late atherosclerotic lesions (Glass et al., 2001). Such “fatty streaks” are not clinically significant but they are the base for the formation of more dangerous “fibrous lesions” (Lusis, 2000) (Fig.2B). As a consequence of inflammatory situation, the underlying Smooth Muscle Cells (SMCs) migrate from the media layer to the intima or subendothelial space and, internalising oxLDL, they contribute to foam cells formation. In addition, SMCs synthesise the extracellular matrix proteins, like collagen and elastin, which contribute to the formation of a fibrous cap on the atherosclerotic lesion (Glass et al., 2001).

Clinical symptoms of the atherosclerotic plaque involve the progressive limitation of blood flow by stenoses or acute events that completely block blood flow, temporarily or permanently (Nabel et al., 2012). The rupture of the plaque and subsequent thrombosis (Fig.2C) provoke the latest situation. Unstable plaques seem to be those with thin fibrous caps, increased number of inflammatory cells and large necrotic cores (Lusis, 2000; Glass et al., 2001). Macrophages and SMCs in the plaque can undergo apoptotic or necrotic process, which also seems to be stimulated by the presence of oxLDL. Lipids released by these cells give rise to the formation of classical features of the advanced lesions and contribute to the thrombogenic potential of the atherosclerotic plaque (Glass et al., 2001). In addition, when the clearance of these dead cells through the efferocytosis process is inefficient or weak, the accumulation of cell debris and extracellular lipids form the necrotic core of the plaque (Libby et al., 2011). In addition to necrotic core formation, other events can contribute to plaque instability: for example, T cells produce  $\text{INF-}\gamma$  which inhibits the release of matrix

proteins by SMCs, while macrophages secrete proteases, in particular metalloproteinases (MMPs) and cysteine proteases (Lusis, 2000; Hansson, 2005), which contribute to extracellular matrix degradation, giving rise to unstable plaques prone to rupture. Moreover, neovascularisation phenomena contribute to plaque instability both with a physical destabilisation and also by allowing the entrance of additional inflammatory cells inside the lesion (Lusis, 2000). Furthermore, in response to inflammatory cytokines, pericytes, cells surrounding ECs, induce the production of a matrix scaffold that later becomes the base for the calcification process taking place inside the lesion. Taken together, all these events impair plaque stability and cause its rupture, exposing lipids and tissue factor. ECs and apoptotic macrophages can induce the accumulation of extracellular tissue factor which, when exposed to coagulation proteins and platelets present in the blood flow, can trigger thrombus formation (Libby et al., 2005).

## **1.2 CAD OUTCOMES**

In the case of CAD pathology, the atherosclerotic process affects coronary arteries, vessels accountable for oxygen supply to the myocardium. Due to the reduced oxygen supply, this complex disease gives rise to a wide range of clinically relevant manifestations, ranging from asymptomatic angina pectoris to acute events such as Acute Coronary Syndrome (ACS), heart failure and sudden cardiac death (Boudoulas et al., 2016).

CAD manifestations are frequently caused by the stenosis of coronary lumen, due to the increasing plaque formations. Most patients may live in this pathological condition for many years, even decades, without any symptoms. This happens because of the presence of an important vessels-balancing mechanism involving artery remodelling, aimed at counteracting plaque development. Therefore, despite the presence of the atherosclerotic plaque, the arteries preserve their original luminal area. The drawback of this compensation lies in the fact that the degree of stenosis is not directly correlated with the size and the dangerousness of the

atherosclerotic plaque, postponing its detection (Boudoulas et al., 2016). In some patients, however, the artery stenosis can cause stable angina pectoris, a pathological condition caused by myocardial ischemia. This manifestation follows the severe narrowing of one or more coronary arteries but also happens in the case of non-obstructive coronary arteries, or even angiographically normal coronary arteries. Stable angina pectoris is described as a recurring pressure or choking sensation in the chest or adjacent areas, often in association with physical or emotional stress. Affected patients have to reduce their activities and, as a consequence, their quality of life is definitely impaired (Rousan et al., 2017).

While in the past years CAD manifestations were thought to be dependent only on arterial narrowing and stenosis, today our understanding of the pathology has improved, and we now recognise that dangerous atherosclerotic lesions can also evolve inside artery walls without inducing arterial stenosis. Indeed, occurring in the late stages when plaque growth overtakes artery expansion mechanism, stenosis has been described as the “tip of the iceberg” of atherosclerosis, and atherosclerotic lesions are normally widespread when steatosis emerges (Libby et al., 2005; Libby, 2013). Studies on patients undergoing medical intervention following CAD manifestations demonstrated that only half of those cases were generated by stenosis (Libby, 2013). Many CAD symptoms arise from the subsequent appearance of ACS, due to plaque damaging rather than to stenosis. Tomography study on ACS patients showed that 44% of those events were caused by plaque rupture (Fig.3, top images), 31% by plaque erosion (Fig.3, lower images) and only 8% by the presence of calcified nodules (Santos-Gallego et al., 2014). Most studies aimed at disclosing the pathogenesis of coronary artery thrombus formation focused on the mechanism of plaque rupture, the main cause of ACS. Results highlighted that unstable plaques are characterised by large lipid pools, high concentrations of macrophages, minor amounts of collagen, thin caps (50 to 65  $\mu\text{m}$  thick) and spotty calcification (Libby, 2013; Boudoulas et al., 2016). Interestingly, while an unstable

plaque may become stabilised, a stable plaque may transform into an unstable plaque at any time. Rupture of the fibrous cap causes the exposure of coagulation factors to blood circulation.

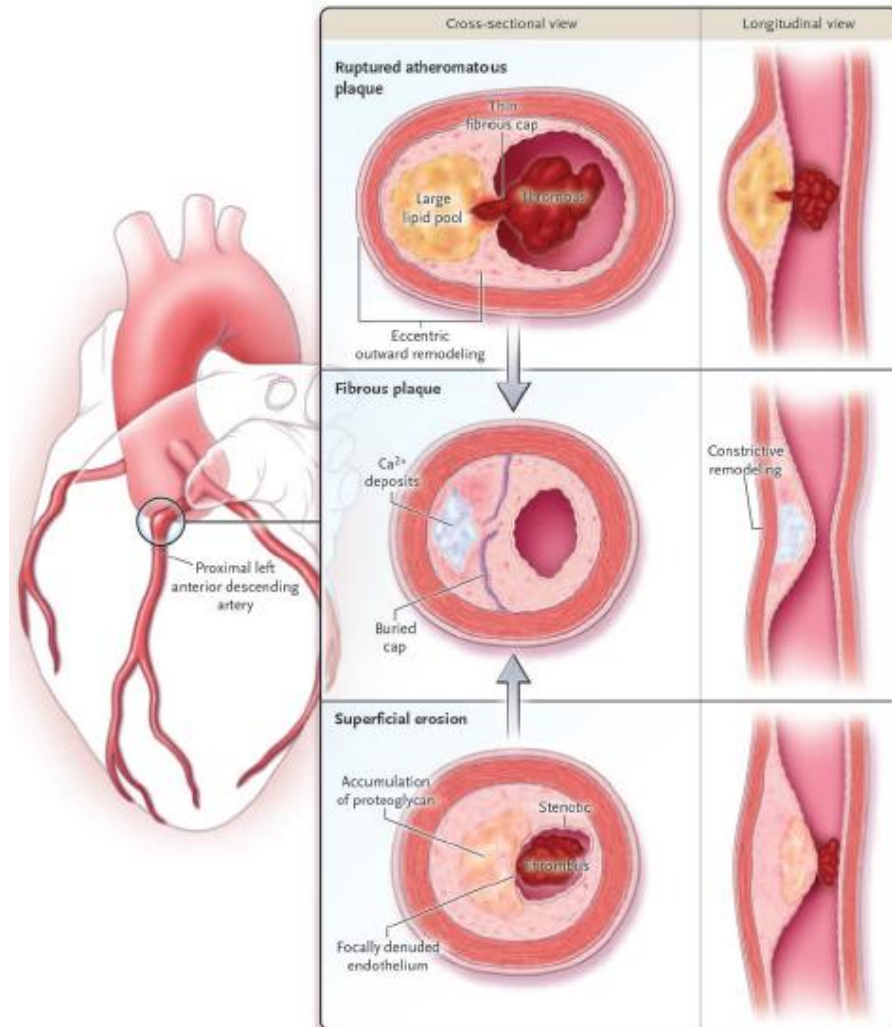


*Fig.3 Clinical events caused by Coronary Artery Disease evolution in coronary arteries. The atherosclerotic plaque is represented in a typical location, the proximal left anterior descending artery (on the left). On the right the three lesion types are shown. When a plaque rupture occurs, thrombus formation arises, occluding artery lumen (top images). Alternatively, thrombus can be generated by erosion of the proteoglycan rich plaque (bottom images). In both cases, myocardial infarction can arise or the healing of the lesion can promote the evolution to a more fibrous cap causing stable ischemic syndromes (Libby, 2013).*



This event has been described as a “solid state stimulus” for both coagulation and atherosclerosis, two pathways reinforcing each other (Libby et al., 2005). Subsequent thrombus formation may lead to the generation of lethal myocardial infarction (MI). For this reason, early diagnosis of those plaques is essential. Alternatively, if the thrombus formation does not occlude the artery, unstable angina events may occur (Boudoulas et al., 2016). Plaque erosion events can also cause thrombus formation and, even though less studied, these lesions have a lower content of inflammatory cells and more proteoglycan accumulation (Libby, 2013). Sometimes plaque rupture and erosion occur without any symptoms and the healing of these lesions gives rise to a progression in plaque volume, contributing therefore to the increase in artery steatosis (Fig.3, middle figures) (Libby, 2013; Santos-Gallego et al., 2014).

## **2. LIPID METABOLISM: THE IMPORTANCE OF LIPOPROTEINS**

The already mentioned LDL and HDL belong to the family of lipoproteins, highly heterogeneous macromolecules, accountable for the transport and emulsification of hydrophobic lipids in blood and organs. Because of this important function, since the discovery of lipoproteins (in 1929 for HDL and 1950 for LDL), efforts have been made in order to clearly elucidate their regulation and their relationship with CVD and also with CAD (Olson, 1998). Lipoproteins have an outer single phospholipid layer that protects the inner hydrophobic core composed of lipids that would have a lower solubility inside blood flow (Fig.4).

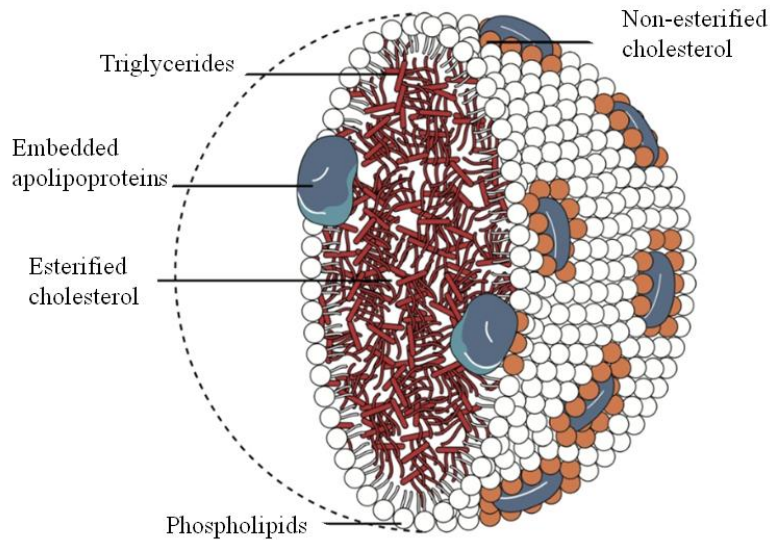


*Fig.4 Components of the inner core and outer shall of all lipoproteins*

The various lipoproteins mainly differ in their density and they have been classified based on their separation during ultracentrifugation steps (Fig.5). However, lipoproteins do not differ just in their density but also in their lipid composition, protein composition and dimensions. Chylomicrons, representing the largest and lowest density type of lipoprotein, rapidly flow on the top of plasma vial after ultracentrifugation. They are mainly responsible for the transport of triglycerides (TG) from the intestine to the liver. Also, Very Low Density (VLDL) lipoproteins transport TG and before the transformation into LDL, they turn into Intermediate Density Lipoproteins (IDL), surviving in the blood flow for a very short period. The smaller class of lipoproteins is represented by HDL, which are enriched mainly in protein component. In fact, while the dimensions of these macromolecules decrease, their density increases together with their protein content. The abovementioned lipoprotein classes are however only the main category of lipoproteins, which are composed of extremely heterogeneous molecules. Since the existence of lipoprotein subfractions has emerged, their connection with CVD has been investigated and still remains the object of many cardiovascular studies (Krauss, 2010).

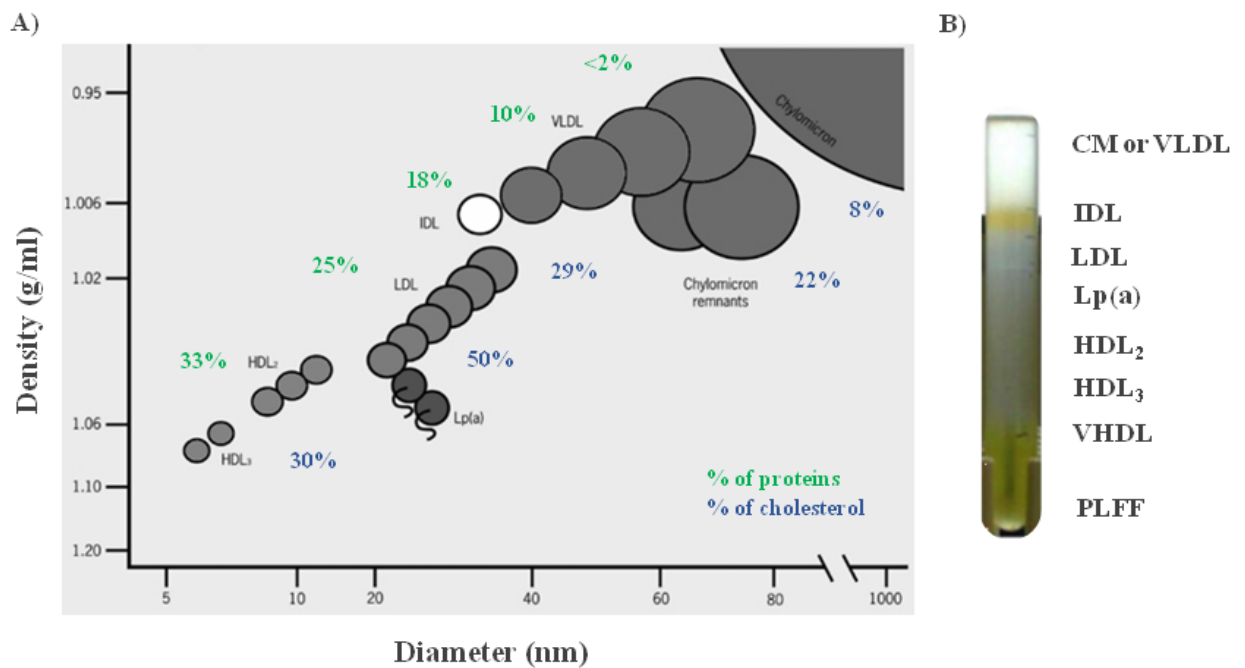


Fig.5 Different density and diameter of lipoprotein particles (A) (from *The British Journal of Cardiology*). As a consequence, they stratify in a peculiar order after plasma ultracentrifugation (B) (Dashti et al., 2011)(PLFF, plasma lipoprotein free fraction).

## 2.1 LIPID COMPONENTS OF LIPOPROTEINS

Lipoproteins have an outer single phospholipid layer in which cholesterol molecules as well as proteins are embedded. This shell protects the inner hydrophobic core composed mainly of TG and cholesterol esters. These compounds are essential for the correct maintenance of body function. Cholesterol represents an essential component of cell membranes, managing their fluidity, and it is necessary for the synthesis of steroid hormones. While some cholesterol derives from dietary intake, the majority comes from endogenous synthesis in the liver and needs to be redistributed to the other organs. TG may also derive from diets or from liver synthesis. TG, being esters of a molecule of glycerol and three of fatty acids (FAs), represent a way of FAs storage and transport, involved not only in phospholipid formation but also an important source of energy for the body. The main lipoproteins involved in TG transport are chylomicrons and VLDL: chylomicrons are involved in so-called “exogenous transport” (Fig.6), the transport of lipids coming from dietary intake from the intestine to the liver. TG composed of long chain FAs are decomposed by gastric and pancreatic lipase to form FAs and

2-monoacylglycerols (2-MG). Micellar solubilisation of FAs and 2-MG is essential for their uptake by enterocytes. Inside these cells they are transported toward the endoplasmic reticulum (ER), probably by the action of FAs-binding proteins. TG are then recreated and, together with diet cholesterol, phospholipids and Apolipoprotein B-48 (ApoB-48), are incorporated in chylomicrons (Kindel et al., 2010). Short chain FAs TG instead are hydrolysed and FAs are transported to the liver bounded to the albumin. While they are flowing into the bloodstream, chylomicrons undergo TG hydrolysis by lipoprotein lipases (LPL) bound to the wall of vessels. In this manner, FAs are delivered directly to peripheral tissue. As a result, new types of molecules are formed called chylomicrons remnants, enriched in cholesteryl esters, ApoB-48 and Apolipoprotein E (ApoE) and apolipoproteins C, originating from circulating HDL. Apolipoprotein A-I (ApoA-I), secreted by the intestine together with chylomicrons, is lost in the bloodstream and destined to the HDL surface. The acquired ApoE is essential for the absorption of chylomicron remnants by the liver, as through their binding to LDL receptor on the liver surface they start the chylomicrons endocytosis internalisation process. Part of the cholesterol adsorbed by the liver is then used for bile formation and is redistributed to the intestine for digestive processes. In the so-called “endogenous transport” (Fig.6) lipids are redistributed from the liver to other organs, following secretion of lipoproteins. TG and cholesterol esters are packed into VLDL particles, together with the liver-synthesised ApoB100, and releases into the blood circulation (Tiwari et al., 2012). These macromolecules contain only a small amount of ApoC, but they rapidly attract many ApoE and ApoC-II on their surfaces. The latest apolipoprotein is essential for VLDL metabolism, as it stimulates LPL activity inside capillaries. LPL hydrolyses TG inside the VLDL faction, allowing the distribution of FAs to peripheral muscles cells, where they are taken up and used for energy production, or to adipose cells where FAs are mainly stored.

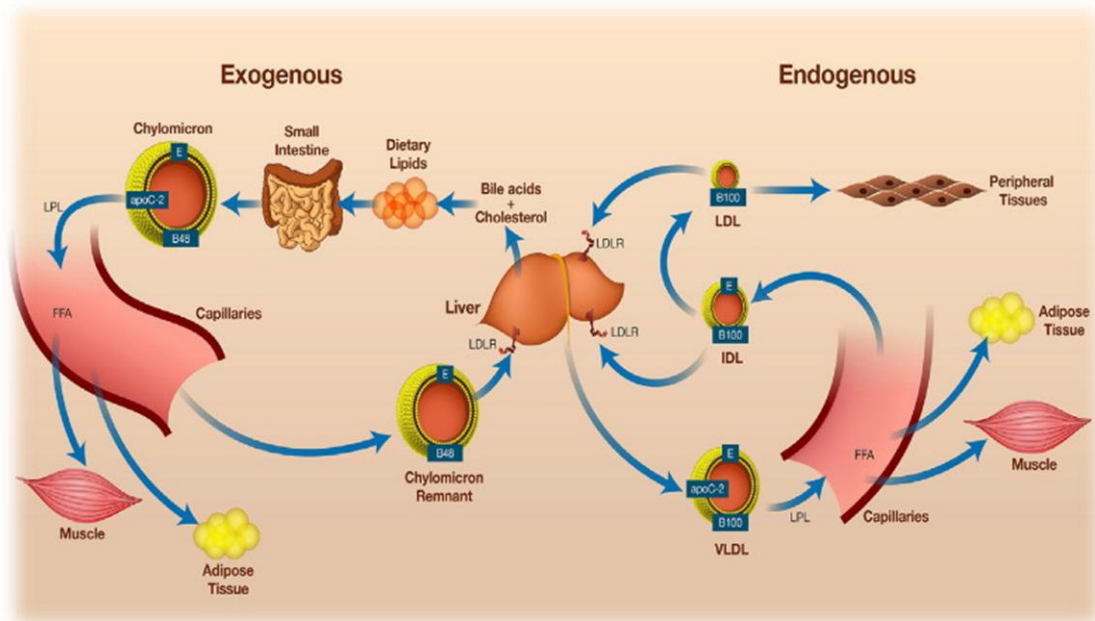


Fig.6 Schematic representation of exogenous and endogenous lipoprotein metabolism (Marais et al., 2015).

Remaining VLDL have fewer TG, phospholipids and proteins. These molecules can be absorbed by the liver or alternatively can remain in the blood circulation where they are called VLDL remnants, or IDL, floating in the blood circulation for a short period. IDL can also be internalised by the liver, because of the recognition of ApoE and ApoB100 by liver receptors, or, if exposed to LPL hydrolysis, can transform into LDL molecules. The smaller and denser LDL molecules are mainly composed of cholesterol and they have ApoB100 as unique apolipoprotein. As described in the first part of the chapter, if LDL remain in blood circulation they become extremely dangerous for cardiovascular health due to their atherogenic potential. LDL can be internalised again by the liver through an endocytosis process by LDL-receptor or they are absorbed by adipocytes or extra-hepatic cells, where they are used for cell membrane as well as for steroid hormone synthesis. Cholesterol intake is also associated with a reduction in endogenous cholesterol biosynthesis, in particular through the inhibition on the hydroxyl-3-methylglutaryl coenzyme A (HMG-CoA) reductase, inhibition of LDL receptor and the activation of acyl-coenzyme A cholesterol acyltransferase, which synthesise cholesterol esters for lipid storage (Goldstein et al., 2009). The final step in cholesterol metabolism is the so-

called “reverse cholesterol transport” (RCT), in which cholesterol is removed from peripheral tissues and returns to the liver. This process is mediated by the action of the HDL, the smallest and densest type of lipoprotein. These small lipoproteins may be secreted by the liver or small intestine (~70-80% of total HDL) or alternatively they may form through the action of ApoA-I. ApoA-I, representing the skeleton of HDL and 70% of its structure, has a pivotal role in the HDL assembly process. This apolipoprotein through its  $\alpha$ -helix structures has a high affinity to lipids and it can attract phospholipids and cholesterol, present in the blood flow or coming from cells. ATP- Binding cassette A1 are lipid transporters on cell surfaces, which only in presence of ApoA-I can mediate the efflux of cholesterol from cell. This is the rate-limiting step in HDL biosynthesis and generates the assembly of nascent HDL, heterogeneous in size, disc-shaped and containing 2-4 ApoA-I proteins. Under the stimulus of ApoA-I, Lecithin-cholesterol Acyltransferase (LCAT) converts free cholesterol molecules inside nascent HDL into cholesterol esters, increasing its hydrophobicity and allowing its redistribution inside the core of the lipoprotein. Together with the acquisition of other apolipoproteins, such as ApoA-II, A-IV, B, C-I and C-II, this process generates the mature form of the HDL. The liver is also involved in the production of Cholesteryl Ester Transfer protein (CETP), an enzyme involved in the exchange of lipids among HDL and LDL or VLDL. During this process that involves the formation of a ternary complex (HDL-CETP-LDL or HDL-CETP-VLDL), cholesterol esters of HDL are transported to TG-rich lipoproteins (TRLs), and TG from VLDL or LDL are targeted to mature HDL. This process is essential for the release of ApoA-I and the uptake of HDL from the liver, as TG-rich HDL are natural substrates for hepatic lipase, promoting HDL clearance from blood circulation. The cholesterol absorbed is used for bile acids synthesis and HDL can undergo a new cycle upon liver secretion (Zhou et al., 2015). Mainly because of this unique role in cholesterol clearance, HDL have been linked for decades to cardioprotective effects.

## **2.2 PROTEIN COMPONENTS: FOCUS ON APOA-I, B, C-III AND E**

The protein components of lipoprotein are called apolipoproteins. Apolipoproteins can be described as the proteins associated with lipoproteins, synthesised by the liver or the intestine, that increase the solubility of the lipophilic components of lipoproteins. A hallmark of apolipoproteins (except for ApoD and Apo[a]) is the presence of highly conserved amphipathic  $\alpha$ -helices, that facilitate the binding of lipids. Key features of these helices are one face inserted among phospholipid tails interacting with the hydrophobic core and the other interacting with phospholipid heads, in contact with the aqueous phase (Li et al., 1988; Elliott et al., 2010). More than one type of amphipathic helices have been described and variations in the number of these helices can define the high or low lipid affinity (Segrest et al., 1992). Unlike other apolipoproteins, ApoB has a relatively high content of  $\beta$ -sheet chain content, allowing a stronger and irreversible binding to the lipid components. In fact, ApoB is the only apolipoprotein that is not transferred among the lipoproteins particles (Li et al., 1988). Many apolipoproteins also contain additional domains such as signal peptides or receptor-binding domain: this is because apolipoproteins are not only structural components of the lipoproteins external shell, but they also have many essential roles in lipoprotein metabolism. Some apolipoproteins, such as ApoA-I, are needed for the assembly of the lipoproteins in which they are embedded. Another possible task performed by apolipoproteins is the regulation of enzymatic molecules. Many apolipoproteins can act as cofactor for enzymes and this is the case of the already mentioned ApoC-II that positively influences the activity of LPL or ApoA-I activating LCAT induced cholesterol esterification. Some other apolipoproteins are instead essential for the lipoprotein recognition by cellular receptors, such as ApoB-100 and ApoE recognized by LDL receptors.

Apolipoproteins are divided into seven classes and some of them have corresponding subclasses:

- A (apo A-I, apo A-II, apo A-IV, and apo A-V)
- (a)
- B (apo B48 and apo B100)
- C (apo C-I, apo C-II, apo C-III, and apo C-IV)
- D
- E
- H

The above information describes the general common features of apolipoproteins, but it is important to note that these are specialised molecules acting on different lipoproteins metabolism and guiding in some cases contrasting actions. Therefore, in the following part the features of the major and more studied apolipoproteins will be discussed, underlining their possible connections with CVD and CAD.

***Apolipoprotein A-I.*** ApoA-I is a protein of 243 amino acids, with an estimated weight of 28 KDa, generated by APOA1 gene that is located inside the APOA1/C3/A4/A5 gene cluster on chromosome 11. As described above, ApoA-I is not only a structural component of HDL but is also essential for their assembly process. In particular, ApoA-I represents 70% of HDL lipoproteins and is the most abundant human apolipoprotein in human blood (Dominiczak et al., 2011). The liver and the intestine synthesise it and when lipid-free ApoA-I acquires phospholipids and cholesterol they transform into pre- $\beta$ HDL, which contain 2 or 3 molecules of ApoA-I per particle. These molecules represent only a minor component of all HDL circulating in plasma and they suddenly transform into mature HDL (Rye et al., 2004). ApoA-I positively influence cholesterol efflux from peripheral cells and macrophages, through the stimulation of the ATP-binding cassette transporter A1 (ABCA1), contributing to the cardioprotective action of HDL. However, this important physiological function can be impaired by oxidative damage of HDL by myeloperoxidase (MPO) which, generating the oxidation of specific tyrosine and methionine residues in ApoA-I, induces the loss of ABCA1



stimulation, as observed in ACS patients (Shao, 2012; Rosenson et al., 2016). Moreover, ApoA-I also promotes the activity of LCAT and the binding of HDL to scavenger receptor class B type I (SR-BI), which are responsible for HDL liver recognition and internalisation. The binding of lipid-free ApoA-I to SR-BI was also observed but it seems to take place through a weaker interaction. In particular, it has been demonstrated that this binding happens through multiple interactions between  $\alpha$ -helices of ApoA-I and HDL binding is strictly connected with ApoA-I conformation (de Beer et al., 2001). Mainly because of this important function in RCT, ApoA-I strongly contributes to HDL cardioprotective effects, even though a recent analysis demonstrated that it does not represent a better indicator of CAD events when compared with HDL levels (van Capelleveen et al., 2017). The favourable cardiovascular effect of ApoA-I plasma levels induced researchers to focus their attention not only on the management of cholesterol biosynthesis with statins therapy but also on the stimulation of the RCT, as an alternative strategy to combat atherosclerosis. The increase of HDL levels would also promote their antioxidant and anti-inflammatory actions. In animal models HDL and ApoA-I administration significantly reduced atherosclerosis (Valenta et al., 2006; Puranik et al., 2008; Patel et al., 2010), therefore  $\alpha$ -helices ApoA-I mimetic peptides have been studied in order to simulate Apo A-I physiological functions and to promote cholesterol transport (Leman et al., 2014). Recent investigations demonstrated discrepancies among *in vitro* and *in vivo* effects of ApoA-I mimetic peptides administration, highlighting the necessity of further experimental studies to better predict and implement their *in vivo* cardioprotective effects (Ditiatkovski et al., 2017).

***Apolipoprotein B.*** ApoB represents the framework necessary for the correct assembly of TRLs in the liver and in the intestine. While the liver secretes VLDL enriched in Apo B-100, chylomicrons secreted by the intestine have ApoB-48 embedded on their surfaces. ApoB-48 corresponds to 48% of the ApoB-100 N-terminal part, and it is produced by a premature stop

codon inducing the termination of protein synthesis. ApoB is unique in its ability to associate with TG coming from cell stores; this process gives rise to new VLDL lipoproteins that normally contain just a single molecule of ApoB. ApoB as well as a substantial pool of neutral lipids and the microsomal TG transfer protein (MTP) are key ingredients for the assembly of such TG-rich lipoproteins. This process is strictly controlled by the degradation of ApoB co-translationally or even after complete protein production, through the ER associated degradation (ERAD) by ubiquitin proteasome system and autophagy. However, it is still unclear if these processes are independent or collaborate for ApoB degradation (Fisher et al., 2014). Once in blood flow ApoB remains on VLDL, IDL and finally LDL as, because of its irreversible binding with lipids, it cannot be exchanged with other lipoproteins. Interestingly, ApoB is the only apolipoprotein of the LDL fraction and is therefore essential for their recognition by LDL-receptors on cell surfaces. Mutations in the ApoB gene may reduce the binding affinity for LDL receptors triggering the development of an important autosomal dominant genetic disorder, the familial defective apolipoprotein B-100 (FDB), associated with hyperlipidemia and elevated risk for atherosclerosis (Andersen et al., 2016). These processes, secretion ApoB process and absorption are extremely important because of their strict connection with cardiovascular risk; increased hepatic secretion of ApoB, together with a decreased removal from blood circulation, lead to increased ApoB plasma concentration, correlated with the onset of the atherosclerotic process and CAD (St-Pierre et al., 2006). As mentioned in the first part of the chapter, circulating LDL can undergo oxidative modifications, also involving modification of ApoB fragment. Modified ApoB fragments are no longer recognised by LDL-receptors but interact with macrophages Scavenger Receptors, leading to the formation of the so-called foam cells, and fatty streak development (Witztum et al., 1991). This process has also been connected with immune system activation, leading to a rapid aggravation of plaque inflammation (Nilsson et al., 2012).

It has been discovered that atherosclerotic process seems to be more strictly connected with the number of circulating proteins rather than with cholesterol concentration. Accordingly, it has been suggested that ApoB could be a better predictor of cardiovascular risk than the content of cholesterol in LDL fraction. In the Copenhagen City Heart Study, ApoB was found to be a better predictor of cardiovascular events in both genders than LDL cholesterol (Benn et al., 2007). Later it was proposed that the ratio between fasting ApoB/A-I may be a better indicator of acute myocardial infarction risk -as assessed in the INTERHEART study- even when computationally inferred from serum total, HDL cholesterol and TG plasma levels (McQueen et al., 2008; Raitakari et al., 2013).

Other recent investigations also focused on the mechanisms to inhibit the synthesis of ApoB, using the strategy of antisense oligonucleotides which, having a complementary sequence to the ApoB, may promote its degradation, therefore inhibiting LDL production. Mipomersen is an FDA-approved antisense oligonucleotide-based drug for homozygous familial hypercholesterolemia that reduces ApoB and LDL levels in up to 76% of patients, but the risk of adverse effects including hepatotoxicity requires strategies for risk evaluation and management (Ellis et al., 2016).

***Apolipoprotein C-III.*** ApoC-III is a small apolipoprotein of just 79 amino acids, synthesised mainly by the liver and to a lesser extent by the intestine. ApoC-III gene is located on the long arm of chromosome 11, in cluster with ApoA-I and ApoA-V genes and is regulated by many factors. Insulin in particular can down-regulate the expression of ApoC-III, through binding to the IRE promoter (Insulin Responsive Element) and, as a consequence, ApoC-III expression was found to be increased in patients affected by metabolic syndrome (MetS) and type 2 diabetes, pathologies associated with insulin resistance conditions (Olivieri et al., 2003; Kawakami et al., 2009). Down regulation of this protein also occurs through the action of

Peroxisome Proliferator Receptors (PPAR), in particular PPAR $\alpha$ , following fibrates administration (Staels et al., 1995). On the contrary, activator of ApoC-III gene transcription is instead the transcription factor NF- $\kappa$ B (Ooi et al., 2008). After transcription ApoC-III exists in three isoforms: the non-glycosylated isoform (ApoC-III<sub>0</sub>) and the isoforms with one or two molecules of sialic acid (ApoC-III<sub>1</sub> and 2 respectively); the distribution of these glycoforms was found to be sensitive to the presence of pathological states, such as sepsis or liver diseases (Zhang et al., 2012). The presence of fucosylated forms of ApoC-III has also been established by mass spectrometry analysis (Nicolardi et al., 2013)

ApoC-III is associated with Apo-B containing lipoproteins and HDL and undergoes continuous exchanges among them. In particular, it is secreted by the liver on VLDL particles and after VLDL hydrolysis it is targeted to HDL surfaces, in order to be secreted again on TG-rich lipoparticles (Ooi et al., 2008). A higher number of ApoC-III molecules are normally on HDL fraction but it has been established that in hypertriglyceridemia conditions ApoC-III is found mainly on TG-rich lipoproteins (Huff et al., 1981).

Many studies have demonstrated the strict connection between ApoC-III and CVD (Sacks et al., 2000; Olivieri et al., 2003; Onat et al., 2003). In particular, ApoC-III is an important regulator of lipoproteins metabolism and, besides CVD progression, variations in ApoC-III levels are strongly associated with the severity of hypertriglyceridemia. ApoC-III is able to inhibit LPL activity, impairing TRLs, the formation of lipoprotein remnants and therefore their clearance from blood circulation (Wang et al., 1985) (Fig.7). In addition ApoC-III is responsible for the inhibition of the hepatic lipase, so reducing the possibilities of TRLs uptake by the liver (Kinnunen et al., 1976; Ooi et al., 2008). Moreover, the impaired uptake of lipoproteins by the liver is caused by ApoC-III inhibition of ApoB and ApoE binding to liver surface Low Density Lipoprotein Receptor (LDLR) and Low density Lipoproteins receptor-related protein 1 (LRP-1) (Fig.7) (Gordts et al., 2016). It has been demonstrated that ApoC-III

has the ability to stimulate the secretion of VLDL from the liver cells, increasing the amount of plasma TRLs (Ooi et al., 2008). It is important to note that not only are LDL levels risk factors for CVD but also TRLs remnants can penetrate in the intima layer of vessels and contribute to atherosclerotic process development (Nordestgaard et al., 2014).

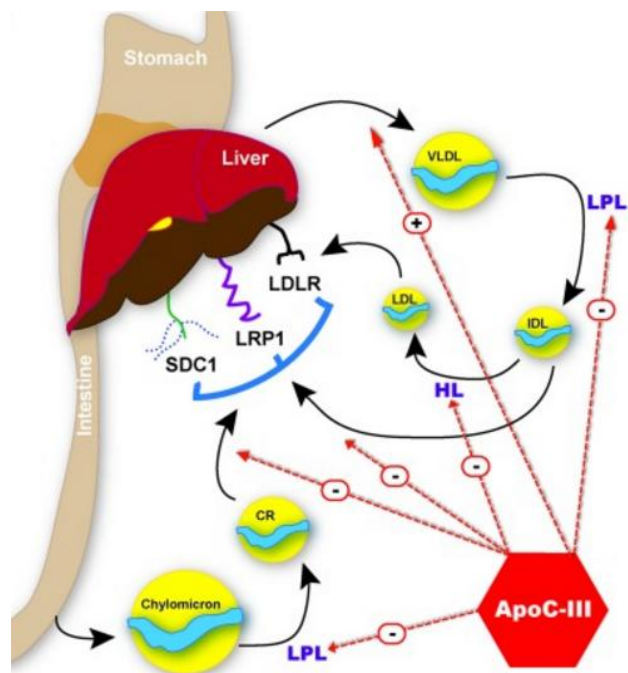


*Fig.7 ApoC-III plasma effects, contributing to the associated hypertriglyceridemia (Gordts et al., 2016).*

This evidence linking ApoC-III with TG plasma levels agrees with genome-wide association studies, where the role of ApoC-III gene polymorphisms was investigated. In particular, the TG and HDL Working Group of the Exome Sequencing Project reported that loss-of-function mutations on ApoC-III gene caused a reduction in ApoC-III levels together with decreased plasma TG levels (lower than 39% in carrier compared to non-carrier) and decreased CAD risk (Crosby et al., 2014). On the contrary, genetic variants increasing ApoC-III levels have been associated with higher plasma TG contents and increased CVD risk (Olivieri et al., 2002). Besides its role in VLDL secretion and clearance, connected with TG plasma content, ApoC-III

seems to be connected with the atherosclerotic process by many other direct mechanisms, such as the activation of NF- $\kappa$ B, expression of VCAM-1 and Intracellular adhesion molecule-1 (ICAM-1) and recruitment of monocytes to the artery wall (Kawakami et al., 2006; Kawakami et al., 2007). Finally, ApoC-III was positively linked to the coagulation process, also involved in the progression of atherosclerotic process (Olivieri et al., 2013). Recently the Bruneck study confirmed the association of ApoC-III with CVD and also with MI and stroke (Pechlaner et al., 2017). Taken together, all this evidence highlights the strong and direct link existing between ApoC-III plasma levels and CVD and suggests ApoC-III as a possible therapeutic target for lowering VLDL levels and preventing CVD. For many years the therapies used to decrease CVD risk were aimed at reducing only LDL cholesterol levels, considered the most dangerous risk factor. Even though this approach remains effective, many patients continue to be at high residual cardiovascular risk, therefore targeting ApoC-III to reduce cardiovascular risk has become the new challenge. Many molecules have been employed, including fibrates, n-3 FAs and statins. Antisense inhibition of ApoC-III synthesis by means of the Volanesorsen is currently in phase III study (Khetarpal et al., 2016). Recent evaluations of its therapeutic effects reported that approach reduced ApoC-III levels by more than 75% and there was a concurrent 50% decrease in plasma TG content (Pechlaner et al., 2017). These results highlighted the importance in ApoC-III targeting in CVD risk patients and opens the road to the use of new therapeutic approaches.

***Apolipoprotein E.*** ApoE is a protein of 299 amino acids and a potent modulator of plasma lipoprotein and cholesterol concentration. Liver cells account for 75% of total ApoE production, while the remaining portion is synthesised by many other organs such as the brain, spleen and kidneys but also macrophages and adipocytes where it is involved in lipid homeostasis (Dose et al., 2016). ApoE is present in a wide range of lipoproteins: chylomicrons, VLDL, IDL and in particular 60% are on HDL surfaces. It is therefore involved both in the

exogenous and endogenous lipoprotein pathways. It has an important structural role for lipoproteins and facilitates their solubility in blood circulation. However, its fundamental function is in lipid metabolism which derives from its ability to bind lipoprotein receptors such as LDLR and LRP (Dominiczak et al., 2011). Furthermore, lipid-bound ApoE is able to promote cholesterol efflux from peripheral cells through the stimulation of SR-B1, promoting RCT (Chroni et al., 2005). This function is particularly important in macrophages, where ApoE prevents foam cells formation. It also stimulates LPL, hepatic lipase and LCAT activity. Therefore, ApoE is absolutely involved in lipoprotein metabolism and explains about 20-40% of TG plasma levels variability (Dominiczak et al., 2011). Many other atheroprotective ApoE mechanisms have been described for their ability to inhibit platelet aggregation, the inhibition of SMC proliferation and the down regulation of VCAM-1 (Greenow et al., 2005). ApoE knockout mice have been widely used as a model for *in vivo* studies on CVD because they develop atherosclerosis (Meir et al., 2004). However, these studies also highlight many other functions of ApoE, not only related to lipid metabolism. Knockout mice developed neurological disorders, type II diabetes, defects in immunity response, age-related features and elevated marker of oxidative stress (Hayek et al., 1994; Roselaar et al., 1998; Robertson et al., 2000). Further *in vivo* studies revealed the antioxidant properties of ApoE, which is also isoform dependent (Miyata et al., 1996). ApoE has in fact three main isoforms E2, E3 and E4 which, despite differing by only one amino acid at positions 112 or 158, behave quite differently. It was reported that the distribution of these three variants is in the range from 0 to 20% for E2, 60-90% for E3 (the most common isoform) and 10-20% for E4 (Singh et al., 2006). The E4 isoform is associated with a decrease in its anti-oxidant activity and in general with a decreased response to stressors. E2 isoform differs for its lower affinity for the LDLR, having only 1% of the binding capacity shown by the other two isoforms. Due to this feature, ApoE2 has been connected with increased levels of plasma cholesterol and TG, causing type III hyperlipoproteinemia onset (Weisgraber et al., 1982). In particular, it has been observed that

while ApoE2 is connected with decreased levels of ApoB and cholesterol but increased levels of ApoE and TG, on the contrary ApoE4 is linked with increased ApoB and cholesterol and decreased ApoE levels: this is because the latter isoform is present mainly on TRLs accelerating their uptake and the consequent down-regulation of LDLR expression, increasing plasma LDL levels (Greenow et al., 2005). Compared to E3 the isoform E4 showed to be associated to the 42% increase in cardiovascular risk (Song et al., 2004).

The evidence mentioned above highlight the ApoE actions that can affect either indirectly, acting on receptors, and directly, acting on enzymes and cells involved in the atherosclerotic process. Isoforms of this protein need however to be considered as they also have important consequences on CVD and neurodegenerative diseases.

### **3. CAD RISK FACTORS**

Due to the high incidence of CVD and in particular of CAD, the study of cardiovascular risk factors has been carried out for a long time. The first study analysing elements involved in this pathology started in 1948 and was called the Framingham Heart Study (Dawber et al., 1951). Since then many interconnected cardiovascular risk factors, contributing to the progression of the atherosclerotic process, have been identified. CVD has been described as the most complex human disease, due to the interplay of a high number of risk factors involving genes, lifestyle and environment (Messner et al., 2014). The WHO listed cardiovascular risk factors as follows (Mendis S., 2011):

#### **Behavioural risk factors:**

1. *Smoking*: cigarette smoking represents one of the most important and preventable cardiovascular risk factors. The WHO estimated that tobacco smoking is responsible for 10% of all deaths caused by CVD (WHO, 2012). It seems that it is not the presence of a single



compound that provokes adverse health effects, but rather the complex mix of compounds used. The interaction between the effects of these compounds and genetic predisposition determines the onset of the pathology. Many mechanisms contributing to smoking's adverse effects have been discovered and they are mainly related to the early steps of the atherosclerotic process. Smoking is responsible for vascular dysfunction, reduced NO production, increased expression of adhesion molecules and adherence of platelets (Messner et al., 2014). Moreover, it has been associated with the prothrombotic and the inflammatory process, as reflected by the increased levels of C-reactive protein and fibrinogen in smokers (McEvoy et al., 2015).

2. *Physical inactivity*: a sedentary lifestyle is closely associated with the onset of cardiovascular events and its connection with obesity development. Guidelines for proper cardiovascular prevention suggest mild but regular physical activity. Studies on mice revealed that physical inactivity contributes to ROS production in the endothelium and the media of blood vessels. This event triggers endothelial dysfunction and atherosclerosis (Laufs et al., 2005).

3. *Harmful use of alcohol*: alcohol consumption has been described as a “double-edged sword” because of its different effects depending on dose consumption (Massaro et al., 2012). Many studies have revealed that low levels of alcohol intake are inversely associated with total mortality but at high doses its healthy effects are overcome by the widely recognised adverse consequences, particularly increased pressure levels (Di Castelnuovo et al., 2006; Foerster et al., 2009).

#### **Metabolic risk factors:**

4. *Hypertension*: treatments aimed at reducing high blood pressure are among the most effective and used for the prevention of cardiovascular outcomes. An interplay between hypertension and diabetes has recently been observed, as hypertension is approximately twice

as frequent in patients with diabetes compared with patients without the disease (Sowers et al., 2001).

5. *Diabetes*: diabetes mellitus is a chronic state of hyperglycemia. It has been reported that CVD is the leading cause of death among people suffering from diabetes (>50%). There are two forms of diabetes: type 1 diabetes mellitus (T1DM) and type 2 diabetes mellitus (T2DM). The risk of cardiovascular events is particularly high in T1DM patients, particularly in patients under 40, who present a risk >10 fold higher than that of the general population. T2DM patients instead have threefold to fourfold increased risk of cardiovascular mortality. The general pathophysiology of the atherosclerotic process is the same as in the normal population, but insulin resistance and hyperglycemia contribute with unique characteristics to the process by impairing endothelial function, triggering low-grade inflammation, thrombosis fibrinolysis and modification of lipoprotein particles (Laakso et al., 2014).

6. *Dyslipidemia*: the term dyslipidemia refers to the abnormal amount of lipids (cholesterol, TG or phospholipids) inside blood flow. This risk factor is therefore representative of many different pathological conditions that differ in their etiology and in their contribution to CVD onset. A detailed report of dyslipidemia conditions will be discussed in the following chapter.

7. *Being overweight and obesity*: obesity is an important factor of CVD. Atherosclerosis and obesity are shown to share common pathological features. While for many years scientists believed that both these conditions were caused just by lipid accumulation, today it is evident they are both inflammatory processes, involving the activation of immune cells, cytokine production and cell death. Adipokines released by adipocytes induce many events, such as endothelial dysfunction, inflammation and insulin resistance, that can stimulate atherosclerosis development (Rocha et al., 2009).

**Other risk factors:**

8. *Poverty and low educational status*: it has been described that poverty, as well as social stress or living alone, can promote CVD onset. Mental stress is strictly connected with oxidative and hemodynamic stress, as in this condition ROS production is increased and atherosclerotic process aggravated (Inoue, 2014).

9. *Advancing age*: the atherosclerotic process may start its evolution in the early phase of life but with the passing of time it can develop and progress. Many age-related processes have been connected with atherosclerosis evolution, such as ROS production and DNA damage (Niccoli et al., 2012).

10. *Gender*: despite women sharing the same cardiovascular risk factors with men, it is well known that they have a decreased cardiovascular risk compared to men and they are protected from cardiovascular events until older age (Vaccarino et al., 2011). Many studies have investigated sex differences in CVD risk, also focusing on genetic differences (Winham et al., 2015). Different elements able to diversify men and women have been identified, such as hormone influence, artery size – being smaller in women, it allows a prompt diagnosis - and a different propensity to risk-associated behaviours, such as smoking or excessive alcohol consumption (Spence et al., 2015).

11. *Inherited (genetic) disposition*: the association between increased personal cardiovascular risk and a family history of CVD represents strong evidence underlining the important role of genetic factors in the onset of CVD. Due to the advance in sequencing technology, over the last decade many Genome Wide Association Studies (GWAS) have been performed in order to elucidate genetic variants associated with specific CVD and also with their risk factors (Smith et al., 2015). Many loci involved in the development of these diseases have been identified: for

example, loss of function mutations in APOC3 gene have been connected with a decrease in plasma TG levels and cardiovascular risk (Crosby et al., 2014).

12. *Psychological factors*: Growing evidence suggests that these factors, including stress and depression, are closely involved in the onset of cardiovascular events, especially for women. Depression is more prevalent in women than in men and affects 40% of young women with MI. Not only depression, but also anxiety, maternal stress and exposure to early life adversities are associated with cardiovascular outcomes. Finally, circumscribed events, such as sudden anger and stressful events can trigger MI or sudden cardiac death in predisposed subjects (Vaccarino et al., 2011).

### **3.1 DYSLIPIDEMIA**

Described for the first time by Fredrickson in 1965, dyslipidemia is a term referring to lipid disorders involving different lipid types (Fredrickson et al., 1965). Knowledge of the concentration of cholesterol and TG levels permits the identification of three different types of hyperlipidemia: high cholesterol levels, high TG levels and high cholesterol and TG levels in the same condition. However, as plasma lipids levels are strictly connected with the amount of circulating lipoproteins, many dyslipidemias are connected to lipoproteins disorder, so called hyperlipoproteinemias, and so a classification based on lipoprotein levels, rather than lipids alone, offers more information. Despite hyperlipoproteinemias having been studied in depth over the last 50 years, as they are extremely and directly connected with cardiovascular outcomes, their classification still remains inspired by that of Fredrickson (Beaumont et al., 1970):

- **Type I:** also known as Hyperchylomicronaemia, it is connected with an increased content of TG coming from diet and therefore with an increase in chylomicrons plasma content.
- **Type II:** this type of hyperlipoproteinemia is connected to an increase in LDL cholesterol plasma content (type IIa) and is also called hypercholesterolemia. This condition is associated with a 10 to 13-fold increase in the risk of CVD and derives mainly from genetic disorders. Common causes are mutations on LDL receptor, APOB or proprotein convertase subtilisin/kexin type 9 genes, despite many individuals with familial hypercholesterolemia phenotype having polygenic instead of monogenic mutations causing hypercholesterolemia (Santos et al., 2014). When the increase in LDL cholesterol levels is also associated with an increase in VLDL plasma levels, and therefore in TG content, this condition is called type IIb hyperlipoproteinemia.
- **Type III:** this condition is accompanied by an increase in VLDL remnants, the IDL. These lipoproteins derive from VLDL and are denser and richer in cholesterol content.
- **Type IV:** this hyperlipoproteinemia can be described as an increase in VLDL content when plasma LDL are in the normal range and chylomicrons are nearly absent.. Because of the increased VLDL, there is an increase in TG plasma levels. This condition, called hypertriglyceridemia, is strictly connected with CVD onset. For many years major efforts to prevent CVD have been made to reduce LDL cholesterol levels, e.g. with statin therapy. However, it has been established that an increase in TG plasma levels, in particular greater than 10 mmol/L can possibly lead to cardiovascular events (Nordestgaard et al., 2014). In fact, as previously mentioned, TG in plasma can trigger the atherosclerotic process similarly to LDL (Schwartz et al., 2012).
- **Type V:** hypertriglyceridemia can derive also from this last type of hyperlipoproteinemia, caused by an increase in VLDL concurrent with an increase in

chylomicrons. Increased TG derive therefore both from the exogenous and endogenous lipoprotein pathways.

**THE MAJOR ABNORMAL LIPOPROTEIN PATTERNS  
AND THEIR TYPE NUMBERS**

Type	Chylo- microns	LDL ( $\beta$ -lp)	VLDL (pre- $\beta$ -lp)	Floating $\beta$ -lipopro- teins
I	+			
IIa		+		
IIb		+	+	
III				+
IV			+	
V	+		+	

*Tab. I Fredrickson classification of dyslipidemias (Beaumont et al., 1970)*

Due to their different etiology, dyslipidemias can be divided into primary dyslipidemias, derived from a genetic defect, or secondary dyslipidemias, caused by lifestyle and unhealthy habits. Among secondary dyslipidemias there are also cases of genetic predisposition followed by incorrect dietary habits. Aside from the familiar predisposition, food intake and the consumption of specific FAs plays a major role in dyslipidemia onset and CVD outcomes.

### **3.2 FATTY ACIDS INTAKE**

The relationship between FAs and cardiovascular health has been widely investigated for many decades and a special emphasis has been given to the impact of dietary FAs on plasma levels of lipids and lipoproteins (Hegsted et al., 1993; Michas et al., 2014). Omega3 polyunsaturated fatty acids (n-3 PUFAs) have attracted growing attention over the last decade as they have gained a prominent position, presumed to be one of the healthiest nutrients. Anti-atherogenic,

anti-arrhythmic and anti-inflammatory effects of n-3 PUFAs, as well as their inverse association with death resulting from cardiovascular diseases, have been established (De Caterina, 2011). n-3 PUFAs, through the activation of PPAR $\alpha$  (Schoonjans et al., 1996), are effective in the reduction of TG plasma levels (Ito, 2015). In 2002 the American Heart Association recommended n-3 PUFA for patients with ischemic heart disease and subjects with hypertriglyceridemia, although some recent studies on patients with multiple cardiovascular risk factors and meta-analysis have questioned their real clinical usefulness for major cardiovascular outcomes (Rizos et al., 2012; Roncaglioni et al., 2013).

In addition to n-3 PUFAs, other FAs are involved in the regulation of lipid profile and cardiovascular risk. Generally, it has been proposed that mono- and poly-unsaturated fatty acids (MUFA and PUFA respectively) lower total and LDL-cholesterol, when replacing saturated fatty acids (SFA) and carbohydrates, with the latest ones having a stronger effects (Mensink et al., 2003; Mensink, 2016). MUFA in particular has been shown to increase the secretion of ApoC-III and ApoE containing VLDL and to decrease at the same time the secretion of other more slowly metabolised TRLs, a major precursor of LDL, while reducing their flux to LDL (Zheng et al., 2008). On the other hand SFA and trans unsaturated FA (TFA) - in particular those derived from industrial partially hydrogenated oils- increase ApoB, total and LDL-cholesterol and TG (Mensink, 2016; Mozaffarian, 2016). Accordingly, it has been suggested that replacing SFA and TFA with unhydrogenated, monounsaturated and polyunsaturated fats may be more effective in preventing CVD, even more than reducing overall fat intake (Hu et al., 1997; Mensink et al., 2003). In particular, reduction in SFA consumption to under 10% of total energy intake remains a regular WHO recommendation for cardiovascular prevention (Mensink, 2016; Zong et al., 2016).

Concerning the influence on cardioprotective HDL cholesterol levels, studies replacing carbohydrates intake with different FAs type, showed that HDL levels were raised by MUFA, PUFA and in particular SFA. Apo A-I levels are also increased after carbohydrates substitution

with SFA (Mensink et al., 2003; Mensink, 2016). In contrast, TFA have been reported to exert an HDL-and plasmatic Apo A-I lowering effect (Matthan et al., 2004).

Although the role of FA intake on CVD has been widely investigated, some limitations to these studies exist:

- i. The effects of dietary fat quality on health, intermediate phenotype, and subsequent disease incidence are difficult to investigate in intervention studies, partly because of short study durations. Moreover, such trials usually replaced FAs with carbohydrates (Mensink et al., 2003), thus intrinsically altering the related metabolic pathways (high-carbohydrate diets are known to induce dyslipidemia (Lichtenstein et al., 1998).
- ii. On the other hand, in epidemiological and observational studies the assessment of dietary FAs intake from different food sources with the use of food frequency questionnaires is potentially biased by substantial measurement errors (Warensjo et al., 2008; Niknam et al., 2014).
- iii. Furthermore, most of these studies considered the dietary intake of general FA classes, i.e. SFA, MUFA, and PUFA, while the distinct effects of the singles FAs, which may be biochemically highly heterogeneous even within the same category, were not taken into account and remained elusive and very difficult to disentangle.

#### **4. *IN VIVO* STUDIES ON MYRISTIC ACID ROLE IN CAD**

SFAs intake represents a well-known risk factor for CAD and their replacement with unsaturated FAs has been associated with a decreased cardiovascular risk. However, SFA are a heterogeneous FA species that differ in their structure, function and source, and recent studies have demonstrated that single SFAs also have different effects on plasma lipids as well as on subclinical inflammation (Zong et al., 2016; Santaren et al., 2017). Potential protective effects have been observed for odd chain SFA and very-long chain SFA (VLSFA), while shorter chain



SFA have been positively associated with proinflammatory markers and to incident type 2 diabetes (Forouhi et al., 2014; Santaren et al., 2017). Myristic acid is a 14-carbon saturated (C14:0) FA and is a major component of dairy fats as well as of coconut oil, nutmeg, butter and palm oil. First studies on the role of individual FAs described C14:0 as the most potent saturated FA. They reported the high cholesterolemic effects of C14:0, even in comparison with palmitic acid (C16:0) and oleic acid (C18:1) (Katan et al., 1994; Zock et al., 1994; Kris-Etherton et al., 1997). In particular, it was shown to raise both total and LDL cholesterol when substituted for C16:0 and C18:1. The same effects on total and LDL cholesterol were observed years later in large meta-analysis when carbohydrates constituting 1% of dietary energy intake were replaced with C14:0 (Mensink et al., 2003; Mensink, 2016). The intake of C14:0 has been also associated with elevated risk of CAD development (Johnson et al., 1998; Zong et al., 2016). Accordingly, it has been reported that risk for CVD, myocardial infarction and stroke can be decreased by reducing the intake of C14:0, palmitate and simple carbohydrates and improved by a greater intake of linoleic acid and marine n-3 FAs (Ebbesson et al., 2015). A moderate intake of C14:0 together with alpha-linolenic acid has however been associated with a positive increase in LCAT activity that promotes cholesterol efflux from peripheral tissues (Vaysse-Boue et al., 2007). MetS is represented by the concurrent presence of different medical conditions (such as high blood pressure, high TG plasma levels, obesity and high blood sugars) and is considered a risk factor for CVD onset (Galassi et al., 2006). Higher proportions of C14:0 plasma levels were found in people with MetS compared to healthy controls, and high proportions of C14:0 as well as of C16:0 were associated with adverse profiles of several metabolic risk factors (Mayneris-Perxachs et al., 2014). However, a recent investigation showed the association of C14:0 with decreased risk of T2DM (Ericson et al., 2015). Moreover, in recent population-based studies C14:0 has been associated with the increase of inflammatory markers, including fibrinogen and C-reactive protein (Santos et al., 2014; Santaren et al., 2017). However, only few studies focused their attention specifically on C14:0 effects on lipids and

lipoproteins levels. One of these studies demonstrated that meals enriched with C14:0 resulted in a higher increase in postprandial HDL TG plasma levels than meals enriched with stearic acid (C18:0); furthermore in the same study higher levels of HDL cholesterol 24 hours after the C14:0-enriched meal were reported (Tholstrup et al., 2003). This result is in contrast with a recent study on a Mediterranean population, in which C14:0 was found to be strongly associated with decreased plasma HDL-C levels (Noto et al., 2016). It was demonstrated that this inverse correlation could be explained with the C14:0 ability to increase HDL trapping to cell surface heparan sulphate proteoglycans in the liver and the consequent highest internalisation of HDL-derived cholesteryl esters. These recent findings revealed that, despite decades of investigation into the role of FAs in cardiovascular health, some of their cardiovascular effects - and in particular some effects of the less-studied C14:0 - remain to be disclosed.

## **CHAPTER 2**

### ***IN VIVO* INVESTIGATION OF POSSIBLE NEW ASSOCIATIONS BETWEEN CARDIOVASCULAR RISK FACTORS: THE EMERGING ROLE OF MYRISTIC ACID**

#### **1. INTRODUCTION**

The purpose of the present research project has been to discover new possible associations of FAs with lipids and apolipoprotein levels, to disclose potential underlying mechanisms related to the development of CAD.

This *in vivo* investigation of possible new associations between cardiovascular risk factors represented a broadening of my master's degree thesis, where these correlations were investigated in a limited number of subjects previously enrolled in the *Verona Heart Study* (VHS). VHS is an ongoing project which started in 1996 with the aim of creating a biobank of plasma samples to research and shed light on cardiovascular risk factors. In particular, 57 CAD patients had been enrolled in that exploratory research and for each of these patients lipid (TG, HDL, LDL and total cholesterol) and apolipoprotein (ApoA-I, A-V,B,C-III and E) levels as well as LPL activity and iron-metabolism related parameters (iron, ferritin, transferrin and hepcidin) were measured and statistically analysed to evaluate their possible correlations. The most interesting correlations emerging from that exploratory research were related to classical cardiovascular risk factors. A SFA, C14:0, showed interesting positive correlations with parameters connected with the onset of CVD (TG, ApoB and ApoC-III) and negative correlations with cardioprotective elements (HDL, ApoA-I and ApoA-V). Because of these interesting and unexpected correlations, related to classical risk factors - rather than new risk factors such as iron parameters - the present research was aimed at deepening the influence of C14:0 on lipid and apolipoproteins metabolism.

The analysis has been expanded to a larger cohort of subjects (n=1,370), to further investigate the relationships between plasma FAs and parameters related to lipid metabolism, and to validate and strengthen the previous C14:0 correlations observed in the restricted group of VHS subjects.

This phase of the project was possible thanks to a collaboration with the Laboratory of Genetic and Non-Genetic Risk Factors for Atherothrombotic Disorders, Department of Medicine, present at the LURM (University Laboratory of Medical Research) research centre of The University of Verona.

In this phase of the study a higher number of subjects enrolled in the VHS was selected and major FAs levels were analysed in the plasma sample of each patient by means of plasma FAs extraction and subsequent gas-chromatographic analysis. Correlations between all FAs and lipid and apolipoprotein (ApoA-I, B, C-III and E) were evaluated and regression analyses were used to deepen the relationships among significantly correlated lipids and FAs and to disentangle the most relevant relationships of dependency.

## **2. EXPERIMENTAL DESIGN AND PROCEDURES**

*The gas-chromatographic analyses of fatty acids and the statistical tests were performed thanks to the kind collaboration of Prof. Oliviero Olivieri's and Prof. Nicola Martinelli's laboratory (Laboratory of Genetic and Non-Genetic Risk Factors for Atherothrombotic Disorders), Department of Medicine, University of Verona.*

### **2.1 Study subjects**

Plasma samples were obtained from 1,370 subjects previously enrolled in the VHS, in collaboration with the University Hospital of Verona (AOUI). Details on the enrolment criteria have been described in previous VHS publications (Girelli et al., 1998; Olivieri et al., 2003). Patients that were candidates for coronary artery bypass grafting, with angiographically documented severe multivessel coronary atherosclerosis at the time of sampling, were gathered in the CAD group. In the control group (CAD-free group) subjects with angiographically documented normal coronary arteries were enrolled. These patients had been examined for reasons other than possible CAD and were required to have neither history nor evidence of atherosclerosis in vascular beds. For this project 1,370 samples from the VHS biobank were chosen: 1,004 samples were selected from the CAD group of patients, while 366 belonged to the group of CAD-free subjects. Both CAD patients and controls came from the same geographical area (Northern Italy), with a similar socio-economic background. Oral or written informed consent was obtained at the time of sampling for every subject after a full explanation of the study. A complete clinical history, including cardiovascular risk factors such as smoking and hypertension, was gathered for all participating subjects.

Overnight fasting plasma samples were collected in Vacutainer® tubes containing ethylenediaminetetraacetic acid (EDTA) as anticoagulant. Plasma samples were centrifuged at 3500 rpm at 4°C for 15 minutes, to remove cellular components, and stored at -80°C until use, as indicated in the following experimental design (Fig.1).

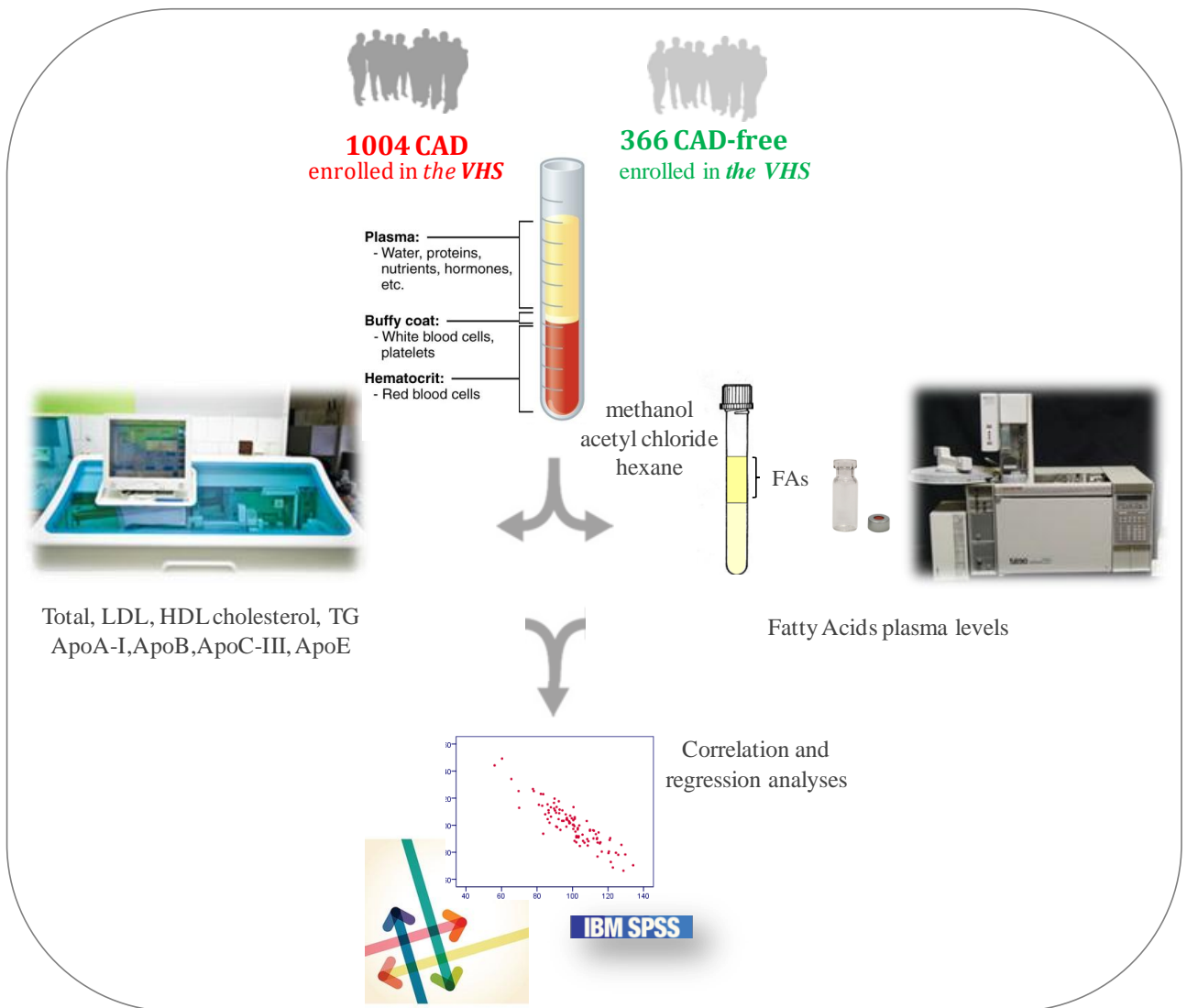


Fig.1 Experimental design.

## **2.2 Clinical chemistry analyses of plasma lipid parameters**

Plasma lipid parameters, including TG, HDL, LDL and total cholesterol, as well as ApoA-I, ApoB, ApoC-III and ApoE parameters were determined as previously described (Girelli et al., 1998) by the Analysis Laboratory of the University Hospital of Verona. Plasmatic ApoC-III was measured by a fully automated turbidimetric immunoassay. The reagents (catalog number: KAI-006) were obtained from Kamiya (Seattle, WA, USA), and the procedure described by the manufacturer was implemented on a COBAS auto analyzer e501 (Roche). Precision was assessed on three pools of control sera with low, medium and high ApoC-III values. 1.8%, 2.02% and 1.98% intra assay coefficient of variation (CV) and 4.4%, 3.4% and 2.29% inter assay CV were maintained. Plasmatic ApoA-I, ApoB and ApoE were measured by a nephelometric immunoassays on a nephelometer BNII Siemens (Dade Behring, Murbyrg, Germany). Intraassay CV -calculated on 10 control replicates- were 2.1%, 1.6% and 1.98%, while interassay CV –determined measuring duplicates over 10 days- were 3.2%, 2.36% and 3.98% for ApoA-I, ApoB and ApoE, respectively.

## **2.3 Gas-chromatography analysis of plasma fatty acid levels**

Levels of plasmatic FAs were measured as previously described (Martinelli et al., 2008). In particular, FAs were extracted from 100  $\mu$ l of plasma sample by means of a direct transesterification reaction by adding 2 ml of reaction mix containing 1.9 ml of methanol and 100  $\mu$ l of acetyl chloride (Lepage et al., 1984). 2,6-di-ter-*p*-cresol/L (BHT)(Sigma-Aldrich) was added to each vial as an antioxidant agent. The transesterification reactions were carried out for one hour at 100°C. To each cooled sample 1 ml of water and 1 ml of hexane were added and, after two minutes of centrifugation at 2500 rpm, the upper hydrophobic phase containing esterified FAs was collected, dried in a SpeedVac system, resuspended in 0.5 ml of hexane and transferred into a glass vial for further analysis. Gas-chromatography was performed by using a

Hewlett-Packard 5980 chromatograph, equipped with an HP-INNOWax Polyethylene Glycol column. Detailed instrumental conditions are reported below:

Column: HP-INNOWax Polyethylene Glycol 30.0 m x 250  $\mu$ m x 0,25  $\mu$ m phase column,

Agilent

Gas carrier: Helium

Solvent: Hexane

Oven starting temperature: 150 °C

Temperature increase: 1 °C/min

Oven final temperature: 230 °C for 90 min

Pressure of carrier: 31.39 psi

Column flux: 29.4 ml/min

Detector: FID-Flame Ionisation Detector

Hydrogen flux for FID: 30 ml/min

Air flux for FID: 400 ml/min

FID temperature: 300 °C

Injection volume: 5  $\mu$ l

Injection type: on-line

Injector: split

Split ratio: 1:10

He Split Flow: 24.3 ml/min

Peak identification was done using commercially available reference FAs (Sigma, St Louis, MO). Three vials containing 100  $\mu$ l of the standard mix solution were processed in parallel to every analysed series of plasma samples. The comparison of the retention time of the peaks in the standard mix run with retention times in the samples permitted the reliable identification of each FA. To quantify FAs, a known amount of C19:0 –FA with an odd number of carbon atoms, not present in biological samples- was used as internal standard in all samples. The peaks areas were measured and subsequently quantified using HP-3365 Chem Station software (Hewlett Packard). The estimations of FAs concentrations were performed



normalizing the intensity of each peak with the intensity of the internal standard with a known concentration. Moreover, the concentrations of each single FA were estimated by comparing the peak intensity in the sample with the intensity of the corresponding peak in the standard mix of FAs with known concentrations. In particular, this estimation was performed as follows, by means of a specific factor related to the FA in the standard mix:

$$C_{\text{sample}} = \left( \frac{C_{\text{st}}}{\frac{h_{\text{st}}}{h_{\text{C19st}}}} \right) \times \frac{h_{\text{sample}}}{h_{\text{C19sample}}}$$

Factor derived from the standard mix of FAs

Where:

- $C_{\text{sample}}$ : concentration of the FA in the plasma sample ( $\mu\text{g/ml}$  of plasma)
- $C_{\text{st}}$ : concentration of the FA in the standard mix ( $\mu\text{g/ml}$  of plasma)
- $h_{\text{st}}$ : height of the FA peak in the standard mix
- $h_{\text{C19st}}$ : height of the C19:0 (internal standard) peak in the standard mix of FAs
- $h_{\text{sample}}$ : height of the FA peak in the plasma sample
- $h_{\text{C19sample}}$ : height of the C19:0 (internal standard) peak in the plasma sample

The levels of each FA were expressed as g/100 g total FAs methyl esters (% by wt). Each sample was analyzed in duplicate and all CV were <5%.

## 2.4 Statistical analysis

The SPSS software version 22.0 statistical package (IBM Corporation, Armonk, USA) was used to perform statistical analyses. Continuous variables were expressed as mean  $\pm$  standard deviation (SD). Variables showing a skewed distribution (e.g. TG, ApoC-III and ApoE) were logarithmically transformed and therefore expressed as geometric mean with 95% confidence interval (95% CI). The correlations between plasma lipid parameters and FA profile, as well as among FAs levels, were analysed by Pearson's test. The correlations were evaluated in total subjects, as well as in population stratified on the basis of CAD pathology (CAD and CAD free), sex (male and female) and age (< 62 and > 62 years old).

The SIMCA 13.0 (Umetrics) software was used to perform the Principal Component Analysis (PCA). PCA was applied in order to obtain an overview of the results and get some insights on the data structure, clustering and correlations. All variables were autoscaled before performing PCA. The autoscaling procedure transforms the variables so that they all have a null average value and a unit variance: this last feature is fundamental since it allows all the variables to bring the same amount of information to the overall dataset. With the aim to perform a more comprehensive analysis, at first a regression model with backward stepwise selection of variables (including all the FAs showing significant correlations at univariate analysis) was performed and then a regression model with forward stepwise selection of variables, estimating  $R^2$  modification, with the aim to identify the best predictive variables. Linear regression models were also adjusted for potential confounding factors like sex, age, diabetes, diagnosis, lipid lowering therapy and body mass index (BMI). Addressing our interest in C14:0, the study population was stratified according to C14:0 quintiles. The distribution of variables across C14:0 quintiles were assessed by ANOVA with polynomial contrasts for linear trend or by  $\chi^2$ -test for linear trend. A p-value < 0.05 was considered significant.

### 3. RESULTS

#### 3.1 Clinical characteristics of the studied population

For all patients involved in the present study, data concerning sex and age were collected at the time of blood sampling. All data, in particular age and BMI, refer to the specific moment of blood sampling. Mainly middle-aged subjects were enrolled in the study (Tab. I).

	<b>Total Population (n=1,370)</b>
<b>Age (years)</b>	60.6 ± 11
<b>Male sex (%)</b>	75.8%
<b>Diabetes</b>	15.2%
<b>BMI (kg/m<sup>2</sup>)</b>	25.9 ± 4.6
<b>CAD diagnosis</b>	73.3%
<b>Lipid Lowering Therapy</b>	22.6%

*Tab. I Mean clinical characteristics of the VHS patients included in the present study.*

### 3.2 Lipid profile and apolipoprotein levels of the studied population

Characterisation of the lipid profile included TG, HDL, LDL and total cholesterol plasma levels. Mean values of these parameters in the whole population are reported in Tab. II. Together with lipid parameters, levels of Apo-I, ApoB, ApoC-III and ApoE were also measured.

<b>Total Population</b>	
<b>(n=1,370)</b>	
<b>Total cholesterol (mmol/L)</b>	5.49 ± 1.15
<b>HDL cholesterol (mmol/L)</b>	1.25 ± 0.35
<b>LDL cholesterol (mmol/L)</b>	3.64 ± 0.98
<b>Triglycerides (mmol/L)</b>	1.61 (1.57-1.64)
<b>ApoA-I (g/L)</b>	1.31 ± 0.27
<b>ApoB (g/L)</b>	1.12 ± 0.30
<b>ApoC-III (mg/dL)</b>	10.8 (10.6 – 11.0)
<b>ApoE (g/L)</b>	0.041 (0.040- 0.042)

*Tab. II Mean values related to lipid and apolipoprotein parameters in the whole studied population.*

### 3.3 Fatty acids levels in plasma of the studied population

In Fig.2 two examples of gas-chromatograms are reported, one obtained from the standard mix of FAs and one from a real plasma sample analysis.

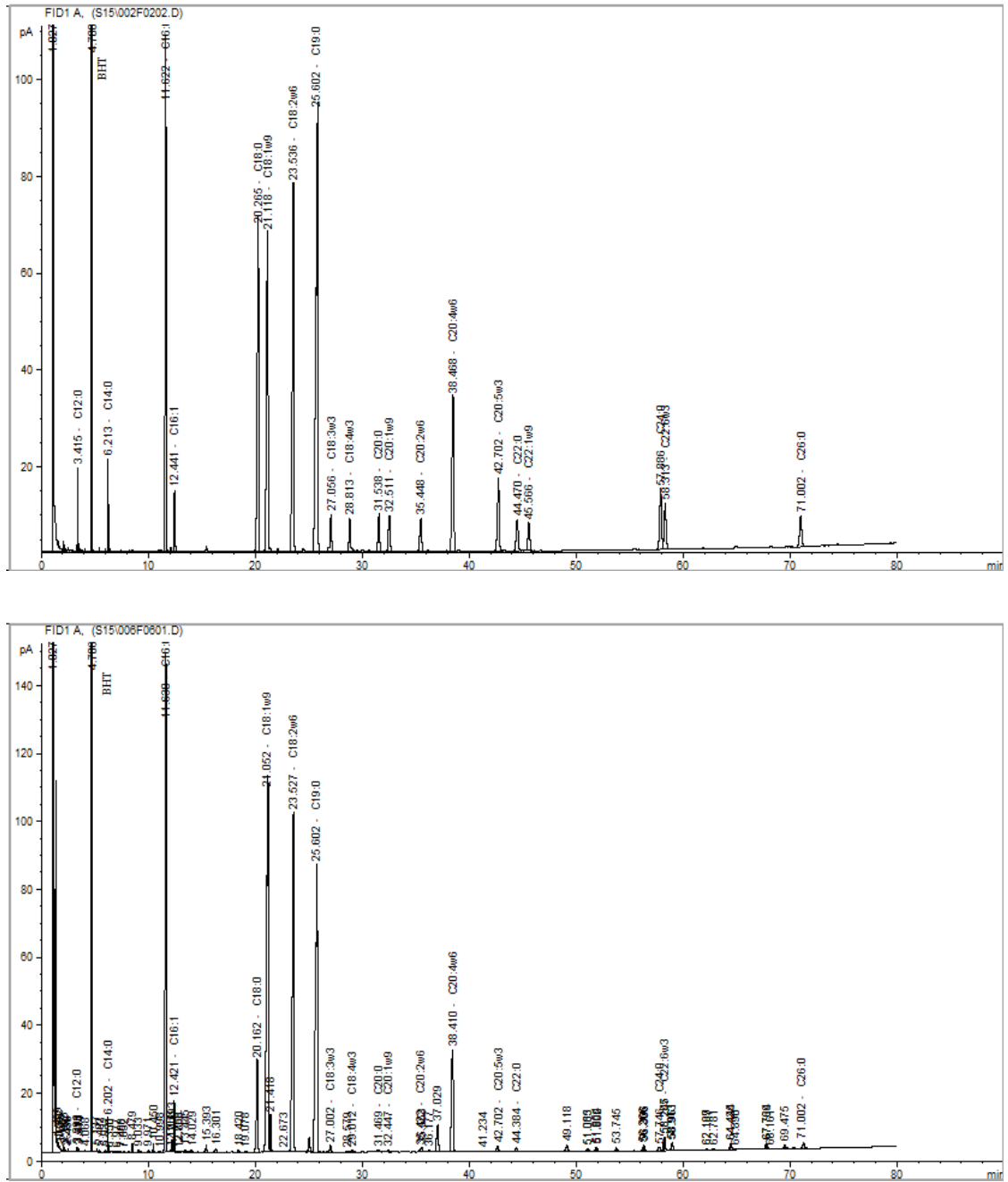


Fig.2 FA gas-chromatographic profiles obtained from the analysis of the FAs standard mix (upper image) and from the analysis of a real plasma sample of a studied patient (lower image).

Results obtained from the analysis of the 1,370 plasma samples are reported in Tab. III. They are expressed as the proportion of the specific FA of the total amount of identified FAs. Mean values with standard deviation or confidence interval for skewed values are reported for single FAs and for FA classes.

<b>Total Population (n=1,370)</b>	
<b>SFA</b>	35.2 ± 2.3
<b>C12:0</b>	0.118 (0.114-0.122)
<b>C14:0</b>	1.03 (1.01-1.06)
<b>C16:0</b>	24.0 ± 1.8
<b>C18:0</b>	8.07 (8.02- 8.13)
<b>C20:0</b>	0.34 ± 0.07
<b>C22:0</b>	0.74 ± 0.17
<b>C24:0</b>	0.73 ± 0.21
<b>UFA</b>	64.8 ± 2.2
<b>MUFA</b>	27.0 ± 4.0
<b>C16:1n-7</b>	2.02 (1.98-2.06)
<b>C18:1n-9</b>	24.5 ± 3.8
<b>C20:1n-9</b>	0.214 (0.211-0.217)
<b>C22:1n-9</b>	0.13 ± 0.11
<b>PUFA</b>	37.7 ± 4.4
<b>n-3</b>	3.76 (3.71-3.82)
<b>C18:3n-3</b>	0.386 (0.38-0.39)
<b>C18:4n-3</b>	0.26 (0.25-0.27)
<b>C20:5n-3</b>	0.68 (0.66-0.7)
<b>C22:6</b>	2.41 ± 0.77
<b>n-6</b>	33.8 ± 4.3
<b>C18:2n-6</b>	23.9 ± 3.9
<b>C20:2n-6</b>	0.229 (0.226-0.232)
<b>C20:4n-6</b>	9.68 ± 2.14

*Tab. III Mean values of identified FAs, single and as FA classes, with corresponding standard deviations or confidence intervals for skewed values.*

### **3.4 Correlation analyses**

The correlations between single FA levels are reported in Tab. IV; those found to be statistically significant are highlighted in bold type. FAs and FA classes relationships with lipid and apolipoprotein parameters were also investigated. Many statistically significant correlations were also found between lipid/apolipoprotein values and single FA levels in the total population as reported in bold in Tab. V. Moreover, possible correlation between lipid/apolipoprotein parameters were investigated taking into account the stratification of the population. In particular, results of the correlation analyses for CAD and CAD- free populations are reported in Tab.VI and VII respectively. The same type of investigations were performed also on the population partitioned according to sex (Tab.VIII and IX) and age, with results on youngest subjects (age<62) reported in Tab.X and results of the analysis on the older population (age>62) reported in Tab.XI.

	C12:0	C14:0	C16:0	C16:1	C18:0	C18:1	C18:2	C18:3	C18:4	C20:0	C20:1	C20:2	C20:4	C20:5	C22:0	C22:1	C22:6
C12:0																	
C14:0	<b>r= 0.741<sup>***</sup></b>																
C16:0	<b>r= 0.285<sup>***</sup></b>	<b>r= 0.393<sup>***</sup></b>															
C16:1	<b>r= 0.274<sup>***</sup></b>	<b>r= 0.485<sup>***</sup></b>	<b>r= 0.424<sup>***</sup></b>														
C18:0	<b>r= 0.161<sup>***</sup></b>	<b>r= 0.096<sup>***</sup></b>	<b>r= -0.111<sup>***</sup></b>	<b>r= -0.134<sup>***</sup></b>													
C18:1	<b>r= -0.068<sup>*</sup></b>	r= 0.038	<b>r= 0.091<sup>**</sup></b>	<b>r= 0.252<sup>***</sup></b>	<b>r= -0.426<sup>***</sup></b>												
C18:2	<b>r= -0.111<sup>***</sup></b>	<b>r= -0.227<sup>***</sup></b>	<b>r= -0.556<sup>***</sup></b>	<b>r= -0.492<sup>***</sup></b>	<b>r= 0.135<sup>***</sup></b>	<b>r= -0.619<sup>***</sup></b>											
C18:3	<b>r= 0.172<sup>***</sup></b>	<b>r= 0.290<sup>***</sup></b>	r= -0.035	<b>r= -0.053<sup>†</sup></b>	r= 0.027	<b>r= -0.178<sup>***</sup></b>	<b>r= 0.203<sup>***</sup></b>										
C18:4	r= 0.044	<b>r= 0.091<sup>**</sup></b>	r= 0.004	r= -0.035	<b>r= 0.090<sup>**</sup></b>	<b>r= -0.219<sup>***</sup></b>	<b>r= 0.092<sup>**</sup></b>	<b>r= 0.132<sup>***</sup></b>									
C20:0	r= -0.022	<b>r= -0.203<sup>***</sup></b>	<b>r= -0.185<sup>***</sup></b>	<b>r= -0.250<sup>***</sup></b>	<b>r= 0.210<sup>***</sup></b>	<b>r= -0.239<sup>***</sup></b>	<b>r= 0.146<sup>***</sup></b>	<b>r= -0.156<sup>***</sup></b>	r= -0.047								
C20:1	r= 0.009	<b>r= 0.089<sup>**</sup></b>	r= 0.036	<b>r= 0.153<sup>***</sup></b>	<b>r= -0.165<sup>***</sup></b>	<b>r= 0.514<sup>***</sup></b>	<b>r= -0.335<sup>***</sup></b>	r= -0.015	<b>r= -0.102<sup>***</sup></b>	r= -0.046							
C20:2	<b>r= 0.059<sup>†</sup></b>	<b>r= 0.147<sup>***</sup></b>	<b>r= -0.302<sup>***</sup></b>	r= 0.001	<b>r= 0.223<sup>***</sup></b>	<b>r= -0.293<sup>***</sup></b>	<b>r= 0.479<sup>***</sup></b>	<b>r= 0.215<sup>***</sup></b>	<b>r= 0.064<sup>**</sup></b>	r= -0.043	<b>r= 0.059<sup>*</sup></b>						
C20:4	<b>r= -0.240<sup>***</sup></b>	<b>r= -0.382<sup>***</sup></b>	<b>r= -0.141<sup>***</sup></b>	<b>r= -0.179<sup>***</sup></b>	<b>r= 0.156<sup>***</sup></b>	<b>r= -0.412<sup>***</sup></b>	<b>r= -0.094<sup>**</sup></b>	<b>r= -0.299<sup>***</sup></b>	r= 0.031	<b>r= 0.217<sup>***</sup></b>	<b>r= -0.296<sup>***</sup></b>	<b>r= -0.196<sup>***</sup></b>					
C20:5	r= 0.044	<b>r= 0.111<sup>***</sup></b>	r= 0.044	<b>r= 0.033</b>	r= 0.048	<b>r= -0.176<sup>***</sup></b>	<b>r= -0.182<sup>***</sup></b>	<b>r= 0.290<sup>***</sup></b>	<b>r= 0.118<sup>***</sup></b>	r= 0.013	r= 0.019	<b>r= -0.159<sup>***</sup></b>	<b>r= 0.120<sup>***</sup></b>				
C22:0	<b>r= -0.059<sup>*</sup></b>	<b>r= -0.184<sup>***</sup></b>	<b>r= -0.308<sup>***</sup></b>	<b>r= -0.309<sup>***</sup></b>	<b>r= 0.143<sup>***</sup></b>	<b>r= -0.434<sup>***</sup></b>	<b>r= 0.400<sup>***</sup></b>	<b>r= -0.080<sup>**</sup></b>	r= 0.021	<b>r= 0.631<sup>***</sup></b>	<b>r= -0.172<sup>***</sup></b>	<b>r= 0.063<sup>*</sup></b>	<b>r= 0.216<sup>***</sup></b>	<b>r= 0.106<sup>***</sup></b>			
C22:1	<b>r= -0.056<sup>*</sup></b>	r= -0.051	r= 0.030	<b>r= -0.121<sup>***</sup></b>	r= 0.016	<b>r= -0.176<sup>***</sup></b>	<b>r= 0.084<sup>**</sup></b>	r= -0.003	<b>r= 0.285<sup>***</sup></b>	<b>r= 0.093<sup>**</sup></b>	r= -0.015	r= -0.019	r= 0.047	r= 0.014	<b>r= 0.141<sup>***</sup></b>		
C22:6	<b>r= -0.203<sup>***</sup></b>	<b>r= -0.260<sup>***</sup></b>	r= -0.025	<b>r= -0.168<sup>***</sup></b>	<b>r= -0.056<sup>*</sup></b>	<b>r= -0.133<sup>***</sup></b>	<b>r= -0.175<sup>***</sup></b>	<b>r= 0.056<sup>*</sup></b>	<b>r= 0.062<sup>*</sup></b>	<b>r= 0.076<sup>**</sup></b>	<b>r= -0.068<sup>*</sup></b>	<b>r= -0.236<sup>***</sup></b>	<b>r= 0.261<sup>***</sup></b>	<b>r= 0.531<sup>***</sup></b>	r= -0.008	<b>r= 0.111<sup>***</sup></b>	
C24:0	r= -0.038	<b>r= -0.164<sup>***</sup></b>	<b>r= -0.131<sup>***</sup></b>	<b>r= -0.277<sup>***</sup></b>	<b>r= 0.196<sup>***</sup></b>	<b>r= -0.516<sup>***</sup></b>	<b>r= 0.272<sup>***</sup></b>	<b>r= -0.037<sup>***</sup></b>	r= 0.051	<b>r= 0.462<sup>***</sup></b>	<b>r= -0.245<sup>***</sup></b>	r= -0.005	<b>r= 0.346<sup>***</sup></b>	<b>r= 0.164<sup>***</sup></b>	<b>r= 0.729<sup>***</sup></b>	<b>r= 0.192<sup>***</sup></b>	<b>r= 0.119<sup>***</sup></b>

Tab. IV Correlations between single FAs plasma levels in the whole population. Significant correlations are in bold type.

\* = p-value < 0.05

\*\* = p-value < 0.01

\*\*\* = p-value < 0.001



	Tot chol	HDL	LDL	TG	ApoA-I	ApoB	ApoC-III	ApoE
<b>SFA</b>	r= 0.008	r= -0.050	r= <b>-0.064*</b>	r= <b>0.245***</b>	r= 0.029	r= 0.055	r= <b>0.192***</b>	r= <b>0.106***</b>
<b>C12:0</b>	r= 0.039	r= <b>-0.070*</b>	r= -0.016	r= <b>0.229***</b>	r= 0.002	r= 0.043	r= <b>0.145***</b>	r= <b>0.065*</b>
<b>C14:0</b>	r= <b>0.136***</b>	r= <b>-0.091**</b>	r= 0.048	r= <b>0.441***</b>	r= 0.049	r= <b>0.157***</b>	r= <b>0.327***</b>	r= <b>0.178***</b>
<b>C16:0</b>	r= -0.040	r= <b>-0.227***</b>	r= <b>-0.075*</b>	r= <b>0.367***</b>	r= <b>-0.150***</b>	r= <b>0.074*</b>	r= <b>0.244***</b>	r= <b>0.134***</b>
<b>C18:0</b>	r= -0.013	r= <b>0.273***</b>	r= <b>-0.063*</b>	r= <b>-0.205***</b>	r= <b>0.274***</b>	r= <b>-0.094**</b>	r= <b>-0.090**</b>	r= -0.028
<b>C20:0</b>	r= -0.008	r= <b>0.204***</b>	r= 0.040	r= <b>-0.394***</b>	r= <b>0.081**</b>	r= <b>-0.083**</b>	r= <b>-0.313***</b>	r= <b>-0.200***</b>
<b>C22:0</b>	r= <b>0.128***</b>	r= <b>0.249***</b>	r= <b>0.192***</b>	r= <b>-0.437***</b>	r= <b>0.138***</b>	r= 0.028	r= <b>-0.307***</b>	r= <b>-0.173***</b>
<b>C24:0</b>	r= <b>0.119***</b>	r= <b>0.246***</b>	r= <b>0.137***</b>	r= <b>-0.366***</b>	r= <b>0.150***</b>	r= 0.026	r= <b>-0.230***</b>	r= <b>-0.183***</b>
<b>UFA</b>	r= -0.004	r= 0.051	r= <b>0.066*</b>	r= <b>-0.242***</b>	r= -0.026	r= -0.050	r= <b>-0.189***</b>	r= <b>-0.104***</b>
<b>MUFA</b>	r= <b>-0.158***</b>	r= <b>-0.309***</b>	r= <b>-0.153***</b>	r= <b>0.380***</b>	r= <b>-0.255***</b>	r= <b>-0.067*</b>	r= <b>0.170***</b>	r= <b>0.110***</b>
<b>C16:1n-7</b>	r= <b>0.093**</b>	r= <b>-0.063*</b>	r= 0.056	r= <b>0.318***</b>	r= 0.012	r= <b>0.135***</b>	r= <b>0.249***</b>	r= <b>0.175***</b>
<b>C18:1n-9</b>	r= <b>-0.188***</b>	r= <b>-0.317***</b>	r= <b>-0.173***</b>	r= <b>0.339***</b>	r= <b>-0.279***</b>	r= <b>-0.101***</b>	r= <b>0.127***</b>	r= <b>0.078**</b>
<b>C20:1n-9</b>	r= <b>-0.129***</b>	r= <b>-0.198***</b>	r= <b>-0.161***</b>	r= <b>0.242***</b>	r= <b>-0.108***</b>	r= <b>-0.067*</b>	r= <b>0.138***</b>	r= <b>0.112***</b>
<b>C22:1n-9</b>	r= -0.007	r= <b>0.090**</b>	r= -0.009	r= <b>-0.127***</b>	r= <b>0.084**</b>	r= <b>-0.058*</b>	r= <b>-0.091**</b>	r= 0.007
<b>PUFA</b>	r= <b>0.142***</b>	r= <b>0.309***</b>	r= <b>0.170***</b>	r= <b>-0.471***</b>	r= <b>0.219***</b>	r= 0.035	r= <b>-0.253***</b>	r= <b>-0.154***</b>
<b>n-3</b>	r= <b>0.104***</b>	r= 0.039	r= <b>0.069*</b>	r= 0.001	r= 0.054	r= <b>0.163***</b>	r= <b>0.074*</b>	r= 0.046
<b>C18:3n-3</b>	r= <b>0.167***</b>	r= -0.051	r= <b>0.093**</b>	r= <b>0.299***</b>	r= 0.022	r= <b>0.194***</b>	r= <b>0.271***</b>	r= <b>0.112***</b>
<b>C18:4n-3</b>	r= -0.014	r= <b>0.122***</b>	r= -0.027	r= <b>-0.130***</b>	r= <b>0.107***</b>	r= -0.027	r= <b>-0.064*</b>	r= 0.003
<b>C20:5n-3</b>	r= <b>0.239***</b>	r= <b>0.148***</b>	r= <b>0.165***</b>	r= 0.038	r= <b>0.175***</b>	r= <b>0.245***</b>	r= <b>0.181***</b>	r= <b>0.070*</b>
<b>C22:6n-3</b>	r= -0.006	r= -0.023	r= -0.001	r= <b>-0.065*</b>	r= -0.035	r= <b>0.068*</b>	r= -0.027	r= 0.001
<b>n-6</b>	r= <b>0.122***</b>	r= <b>0.309***</b>	r= <b>0.157***</b>	r= <b>-0.482***</b>	r= <b>0.212***</b>	r= -0.003	r= <b>-0.277***</b>	r= <b>-0.170***</b>
<b>C18:2n-6</b>	r= <b>0.107***</b>	r= <b>0.252***</b>	r= <b>0.141***</b>	r= <b>-0.380***</b>	r= <b>0.172***</b>	r= -0.021	r= <b>-0.241***</b>	r= <b>-0.140***</b>
<b>C20:2n-6</b>	r= 0.027	r= <b>0.111***</b>	r= -0.008	r= -0.046	r= <b>0.188***</b>	r= -0.038	r= 0.011	r= 0.006
<b>C20:4n-6</b>	r= 0.048	r= <b>0.157***</b>	r= 0.057	r= <b>-0.273***</b>	r= <b>0.107***</b>	r= 0.033	r= <b>-0.120***</b>	r= <b>-0.086**</b>

Tab. V Correlations between plasma lipid/ apolipoprotein parameters and fatty acids profile in total population. Significant correlations are in bold type.

\* = p-value < 0.05

\*\* = p-value < 0.01

\*\*\* = p-value < 0.001

	Tot chol	HDL	LDL	TG	ApoA-I	ApoB	ApoC-III	ApoE
C12:0	<b>r= 0.066*</b>	<b>r= -0.111**</b>	r= 0.021	<b>r= 0.264***</b>	r= -0.002	<b>r= 0.088**</b>	<b>r= 0.176***</b>	<b>r= 0.081*</b>
C14:0	<b>r= 0.161***</b>	<b>r= -0.117***</b>	<b>r= 0.077*</b>	<b>r= 0.467***</b>	<b>r= 0.071*</b>	<b>r= 0.186***</b>	<b>r= 0.360***</b>	<b>r= 0.204***</b>
C16:0	r= -0.019	<b>r= -0.232***</b>	r= -0.056	<b>r= 0.366***</b>	<b>r= -0.144***</b>	<b>r= 0.094**</b>	<b>r= 0.279***</b>	<b>r= 0.161***</b>
C18:0	r= 0.019	<b>r= 0.222***</b>	r= 0.001	<b>r= -0.151***</b>	<b>r= 0.249***</b>	r= -0.035	r= -0.059	r= 0.009
C20:0	r= -0.042	<b>r= 0.191***</b>	r= 0.014	<b>r= -0.415***</b>	r= 0.048	r= -0.093**	<b>r= -0.327***</b>	<b>r= -0.223***</b>
C22:0	<b>r= 0.114***</b>	<b>r= 0.225***</b>	<b>r= 0.189***</b>	<b>r= -0.431***</b>	<b>r= 0.100**</b>	r= 0.025	<b>r= -0.332***</b>	<b>r= -0.195***</b>
C24:0	<b>r= 0.134***</b>	<b>r= 0.217***</b>	<b>r= 0.165***</b>	<b>r= -0.336***</b>	<b>r= 0.106***</b>	r= 0.057	<b>r= -0.248***</b>	<b>r= -0.198***</b>
C16:1n-7	<b>r= 0.089**</b>	<b>r= -0.071*</b>	r= 0.057	<b>r= 0.317***</b>	r= 0.026	<b>r= 0.141***</b>	<b>r= 0.282***</b>	<b>r= 0.184***</b>
C18:1n-9	<b>r= -0.228***</b>	<b>r= -0.300***</b>	<b>r= -0.234***</b>	<b>r= 0.284***</b>	<b>r= -0.273***</b>	<b>r= -0.168***</b>	<b>r= 0.104**</b>	r= 0.049
C20:1n-9	<b>r= -0.138**</b>	<b>r= -0.187***</b>	<b>r= -0.202***</b>	<b>r= 0.234***</b>	<b>r= -0.090**</b>	<b>r= -0.088**</b>	<b>r= 0.154***</b>	<b>r= 0.124***</b>
C22:1n-9	r= 0.074*	r= 0.006	<b>r= 0.100**</b>	r= -0.044	r= 0.040	<b>r= 0.071*</b>	r= -0.007	r= 0.051
C18:3n-3	<b>r= 0.179***</b>	<b>r= -0.087**</b>	<b>r= 0.101**</b>	<b>r= 0.335***</b>	r= 0.022	<b>r= 0.210***</b>	<b>r= 0.300***</b>	<b>r= 0.128***</b>
C18:4n-3	<b>r= 0.089**</b>	<b>r= 0.087**</b>	r= 0.065	r= 0.036	<b>r= 0.116**</b>	<b>r= 0.113**</b>	<b>r= 0.076*</b>	r= 0.062
C20:5n-3	<b>r= 0.224***</b>	<b>r= 0.130***</b>	<b>r= 0.125***</b>	<b>r= 0.068*</b>	<b>r= 0.169***</b>	<b>r= 0.250***</b>	<b>r= 0.192***</b>	<b>r= 0.067*</b>
C22:6n-3	r= -0.006	r= 0.007	r= -0.034	r= -0.060	r= -0.022	<b>r= 0.075*</b>	r= 0.001	r= -0.019
C18:2n-6	<b>r= 0.118***</b>	<b>r= 0.224***</b>	<b>r= 0.178***</b>	<b>r= -0.350***</b>	<b>r= 0.149***</b>	r= 0.002	<b>r= -0.267***</b>	<b>r= -0.133***</b>
C20:2n-6	r= 0.026	<b>r= 0.115***</b>	r= -0.005	r= -0.036	<b>r= 0.200***</b>	r= -0.050	r= 0.017	r= 0.014
C20:4n-6	r= 0.051	<b>r= 0.215***</b>	r= 0.044	<b>r= -0.279***</b>	<b>r= 0.135***</b>	r= 0.034	<b>r= -0.119***</b>	<b>r= -0.097**</b>

Tab. VI Correlations between plasma lipid/apolipoprotein parameters and fatty acids profile in CAD population. Significant correlations are in bold type.

\* = p-value < 0.05

\*\* = p-value < 0.01

\*\*\* = p-value < 0.001

	Tot chol	HDL	LDL	TG	ApoA-I	ApoB	ApoC-III	ApoE
C12:0	r= -0.055	r= -0.076	r= -0.108	<b>r= 0.206<sup>***</sup></b>	r= -0.039	r= -0.067	r= 0.094	r= 0.041
C14:0	r= 0.050	r= -0.087	r= -0.029	<b>r= 0.425<sup>***</sup></b>	r= -0.007	r= 0.070	<b>r= 0.253<sup>***</sup></b>	r= 0.102
C16:0	<b>r= -0.122<sup>*</sup></b>	<b>r= -0.226<sup>***</sup></b>	<b>r= -0.156<sup>**</sup></b>	<b>r= 0.369<sup>***</sup></b>	<b>r= -0.170<sup>**</sup></b>	r= -0.015	<b>r= 0.142<sup>**</sup></b>	r= 0.040
C18:0	<b>r= -0.115<sup>*</sup></b>	<b>r= 0.276<sup>***</sup></b>	<b>r= -0.210<sup>***</sup></b>	<b>r= -0.253<sup>***</sup></b>	<b>r= 0.255<sup>***</sup></b>	<b>r= -0.182<sup>**</sup></b>	<b>r= -0.107<sup>*</sup></b>	r= -0.089
C20:0	r= 0.088	<b>r= 0.210<sup>***</sup></b>	<b>r= 0.116<sup>*</sup></b>	<b>r= -0.334<sup>**</sup></b>	r= 0.101	r= -0.016	<b>r= -0.264<sup>***</sup></b>	<b>r= -0.132<sup>*</sup></b>
C22:0	<b>r= 0.183<sup>***</sup></b>	<b>r= 0.274<sup>***</sup></b>	<b>r= 0.232<sup>***</sup></b>	<b>r= -0.426<sup>***</sup></b>	<b>r= 0.196<sup>***</sup></b>	r= 0.093	<b>r= -0.218<sup>***</sup></b>	r= -0.083
C24:0	r= 0.081	<b>r= 0.228<sup>***</sup></b>	r= 0.092	<b>r= -0.381<sup>***</sup></b>	<b>r= 0.172<sup>**</sup></b>	r= 0.031	<b>r= -0.136<sup>*</sup></b>	r= -0.101
C16:1n-7	r= 0.102	r= 0.035	r= 0.029	<b>r= 0.283<sup>***</sup></b>	r= 0.041	r= 0.069	<b>r= 0.145<sup>**</sup></b>	<b>r= 0.129<sup>*</sup></b>
C18:1n-9	r= -0.079	<b>r= -0.235<sup>***</sup></b>	r= -0.069	<b>r= 0.395<sup>***</sup></b>	<b>r= -0.211<sup>**</sup></b>	r= -0.018	<b>r= 0.120<sup>*</sup></b>	<b>r= 0.110<sup>*</sup></b>
C20:1n-9	<b>r= -0.109<sup>*</sup></b>	<b>r= -0.169<sup>**</sup></b>	r= -0.085	<b>r= 0.210<sup>***</sup></b>	<b>r= -0.111<sup>*</sup></b>	r= -0.052	r= 0.070	r= 0.058
C22:1n-9	r= -0.068	r= -0.021	r= -0.046	r= -0.055	r= 0.013	r= -0.063	r= -0.070	r= 0.046
C18:3n-3	<b>r= 0.126<sup>*</sup></b>	r= -0.023	r= 0.076	<b>r= 0.238<sup>***</sup></b>	r= -0.002	<b>r= 0.173<sup>**</sup></b>	<b>r= 0.214<sup>***</sup></b>	r= 0.071
C18:4n-3	r= -0.086	<b>r= 0.122<sup>*</sup></b>	r= -0.097	<b>r= -0.165<sup>**</sup></b>	r= 0.083	r= -0.089	r= -0.094	r= 0.004
C20:5n-3	<b>r= 0.290<sup>**</sup></b>	<b>r= 0.211<sup>***</sup></b>	<b>r= 0.270<sup>**</sup></b>	r= -0.043	<b>r= 0.202<sup>***</sup></b>	<b>r= 0.248<sup>***</sup></b>	<b>r= 0.156<sup>**</sup></b>	r= 0.083
C22:6n-3	r= -0.009	r= -0.021	r= 0.069	<b>r= -0.156<sup>**</sup></b>	r= -0.035	r= 0.006	<b>r= -0.137<sup>*</sup></b>	r= 0.047
C18:2n-6	r= 0.087	<b>r= 0.188<sup>**</sup></b>	<b>r= 0.110<sup>*</sup></b>	<b>r= -0.372<sup>***</sup></b>	<b>r= 0.147<sup>**</sup></b>	r= 0.012	<b>r= -0.116<sup>*</sup></b>	<b>r= -0.120<sup>*</sup></b>
C20:2n-6	r= 0.030	r= 0.090	r= 0.001	r= -0.055	<b>r= 0.176<sup>**</sup></b>	r= 0.008	r= -0.004	r= -0.016
C20:4n-6	r= 0.040	r= 0.082	r= 0.076	<b>r= -0.289<sup>***</sup></b>	r= 0.056	r= 0.033	<b>r= -0.126<sup>*</sup></b>	r= -0.055

Tab. VII Correlations between plasma lipid/apolipoprotein parameters and fatty acids profile in CAD-free population. Significant correlations are in bold type.

\* = p-value < 0.05

\*\* = p-value < 0.01

\*\*\* = p-value < 0.001

	Tot chol	HDL	LDL	TG	ApoA-I	ApoB	ApoC-III	ApoE
C12:0	r= 0.038	r= <b>-0.075*</b>	r= -0.011	r= <b>0.204***</b>	r= 0.015	r= 0.047	r= <b>0.138***</b>	r= <b>0.068*</b>
C14:0	r= <b>0.143***</b>	r= <b>-0.097**</b>	r= 0.059	r= <b>0.424***</b>	r= <b>0.079*</b>	r= <b>0.166***</b>	r= <b>0.326***</b>	r= <b>0.199***</b>
C16:0	r= -0.011	r= <b>-0.179***</b>	r= -0.058	r= <b>0.342***</b>	r= <b>-0.106**</b>	r= <b>0.082*</b>	r= <b>0.270***</b>	r= <b>0.160***</b>
C18:0	r= -0.007	r= <b>0.248***</b>	r= -0.026	r= <b>-0.192**</b>	r= <b>0.259***</b>	r= <b>-0.082*</b>	r= <b>-0.095**</b>	r= -0.023
C20:0	r= -0.048	r= <b>0.119***</b>	r= 0.033	r= <b>-0.402***</b>	r= -0.015	r= <b>-0.081*</b>	r= <b>-0.346***</b>	r= <b>-0.224***</b>
C22:0	r= <b>0.117***</b>	r= <b>0.186***</b>	r= <b>0.220***</b>	r= <b>-0.428***</b>	r= <b>0.066*</b>	r= 0.042	r= <b>-0.333***</b>	r= <b>-0.208***</b>
C24:0	r= <b>0.129***</b>	r= <b>0.221***</b>	r= <b>0.170***</b>	r= <b>-0.348***</b>	r= <b>0.124***</b>	r= 0.040	r= <b>-0.228***</b>	r= <b>-0.206***</b>
C16:1n-7	r= <b>0.092**</b>	r= <b>-0.179***</b>	r= 0.058	r= <b>0.313***</b>	r= 0.018	r= <b>0.139***</b>	r= <b>0.259***</b>	r= <b>0.196***</b>
C18:1n-9	r= <b>-0.178***</b>	r= <b>-0.289***</b>	r= <b>-0.184***</b>	r= <b>0.325***</b>	r= <b>-0.270***</b>	r= <b>-0.105**</b>	r= <b>0.120***</b>	r= <b>0.086**</b>
C20:1n-9	r= <b>-0.110***</b>	r= <b>-0.166***</b>	r= <b>-0.151***</b>	r= <b>0.226***</b>	r= <b>-0.079*</b>	r= -0.056	r= <b>0.150***</b>	r= <b>0.142***</b>
C22:1n-9	r= 0.023	r= 0.016	r= 0.027	r= <b>-0.067*</b>	r= 0.055	r= 0.002	r= -0.036	r= 0.025
C18:3n-3	r= <b>0.168***</b>	r= <b>-0.077*</b>	r= <b>0.086*</b>	r= <b>0.325***</b>	r= 0.033	r= <b>0.196***</b>	r= <b>0.285***</b>	r= <b>0.133***</b>
C18:4n-3	r= 0.045	r= <b>0.113***</b>	r= 0.013	r= -0.027	r= <b>0.130***</b>	r= 0.059	r= 0.018	r= 0.049
C20:5n-3	r= <b>0.247***</b>	r= <b>0.114***</b>	r= <b>0.173***</b>	r= <b>0.071*</b>	r= <b>0.151***</b>	r= <b>0.264***</b>	r= <b>0.193***</b>	r= <b>0.091**</b>
C22:6n-3	r= -0.014	r= -0.050	r= -0.011	r= -0.038	r= -0.065	r= <b>0.068*</b>	r= -0.021	r= 0.018
C18:2n-6	r= <b>0.090**</b>	r= <b>0.231***</b>	r= <b>0.128***</b>	r= <b>-0.371***</b>	r= <b>0.178***</b>	r= -0.034	r= <b>-0.248***</b>	r= <b>-0.165***</b>
C20:2n-6	r= 0.013	r= <b>0.123***</b>	r= 0.004	r= <b>-0.083**</b>	r= <b>0.220***</b>	r= -0.053	r= -0.016	r= 0.005
C20:4n-6	r= 0.041	r= <b>0.140***</b>	r= <b>0.068*</b>	r= <b>-0.266***</b>	r= 0.061	r= 0.041	r= <b>-0.128***</b>	r= <b>-0.104**</b>

Tab. VIII Correlations between plasma lipid/apolipoprotein parameters and fatty acids profile in male population. Significant correlations are in bold type.

\* = p-value < 0.05

\*\* = p-value < 0.01

\*\*\* = p-value < 0.001

	Tot chol	HDL	LDL	TG	ApoA-I	ApoB	ApoC-III	ApoE
C12:0	r= 0.035	r= -0.106	r= -0.031	<b>r= 0.337***</b>	r= -0.054	r= 0.036	<b>r= 0.167**</b>	r= 0.054
C14:0	r= 0.106	<b>r= -0.153**</b>	r= 0.019	<b>r= 0.526***</b>	r= -0.062	<b>r= 0.134*</b>	<b>r= 0.329***</b>	<b>r= 0.115*</b>
C16:0	r= -0.102	<b>r= -0.296***</b>	<b>r= -0.129*</b>	<b>r= 0.423**</b>	<b>r= -0.209**</b>	r= 0.038	<b>r= 0.191**</b>	r= 0.094
C18:0	r= -0.072	<b>r= 0.275***</b>	<b>r= -0.212***</b>	<b>r= -0.226***</b>	<b>r= 0.268***</b>	<b>r= -0.123*</b>	r= -0.103	r= -0.082
C20:0	r= 0.075	<b>r= 0.332***</b>	r= 0.070	<b>r= -0.350***</b>	<b>r= 0.222***</b>	r= -0.069	<b>r= -0.258***</b>	<b>r= -0.181**</b>
C22:0	<b>r= 0.140*</b>	<b>r= 0.353***</b>	<b>r= 0.122*</b>	<b>r= -0.447***</b>	<b>r= 0.254***</b>	r= 0.007	<b>r= -0.258***</b>	<b>r= -0.112*</b>
C24:0	r= 0.096	<b>r= 0.394***</b>	r= 0.027	<b>r= -0.444***</b>	<b>r= 0.256***</b>	r= -0.024	<b>r= -0.235***</b>	<b>r= -0.118*</b>
C16:1n-7	r= 0.082	<b>r= -0.164**</b>	r= 0.054	<b>r= 0.362***</b>	r= -0.057	<b>r= 0.135*</b>	<b>r= 0.209***</b>	r= 0.108
C18:1n-9	<b>r= -0.200***</b>	<b>r= -0.357***</b>	<b>r= -0.150*</b>	<b>r= 0.369***</b>	<b>r= -0.270***</b>	r= -0.103	<b>r= 0.162**</b>	r= 0.074
C20:1n-9	<b>r= -0.167**</b>	<b>r= -0.216***</b>	<b>r= -0.204**</b>	<b>r= 0.270***</b>	<b>r= -0.118*</b>	<b>r= -0.121*</b>	<b>r= 0.121*</b>	r= 0.060
C22:1n-9	r= 0.076	<b>r= 0.147**</b>	r= 0.097	<b>r= -0.122*</b>	r= 0.108	r= 0.032	r= -0.063	r= 0.063
C18:3n-3	<b>r= 0.151**</b>	r= -0.069	<b>r= 0.120*</b>	<b>r= 0.245***</b>	r= -0.058	<b>r= 0.203***</b>	<b>r= 0.222***</b>	r= 0.045
C18:4n-3	r= 0.059	<b>r= 0.147**</b>	r= 0.031	r= -0.041	r= 0.079	r= 0.044	r= 0.031	r= 0.008
C20:5n-3	<b>r= 0.210***</b>	<b>r= 0.242***</b>	<b>r= 0.141*</b>	r= -0.063	<b>r= 0.230***</b>	<b>r= 0.193**</b>	<b>r= 0.138*</b>	r= 0.007
C22:6n-3	r= 0.025	r= 0.077	r= 0.030	r= -0.167**	r= 0.063	r= 0.062	r= -0.044	r= -0.042
C18:2n-6	<b>r= 0.143**</b>	<b>r= 0.282***</b>	<b>r= 0.183**</b>	<b>r= -0.393***</b>	<b>r= 0.135*</b>	r= 0.023	<b>r= -0.231***</b>	r= -0.093
C20:2n-6	r= 0.053	r= 0.029	r= -0.037	r= 0.083	r= 0.081	r= 0.015	r= 0.077	r= -0.002
C20:4n-6	r= 0.064	<b>r= 0.197**</b>	r= 0.030	<b>r= -0.290***</b>	<b>r= 0.207***</b>	r= 0.017	r= -0.104	r= -0.049

Tab. IX Correlations between plasma lipid/apolipoprotein parameters and fatty acids profile in females population. Significant correlations are in bold type.

\* = p-value < 0.05

\*\* = p-value < 0.01

\*\*\* = p-value < 0.001

	Tot chol	HDL	LDL	TG	ApoA-I	ApoB	ApoC-III	ApoE
C12:0	r= 0.012	r= -0.054	r= -0.064	r= <b>0.217</b> <sup>***</sup>	r= 0.020	r= -0.005	r= <b>0.176</b> <sup>***</sup>	r= <b>0.095</b> <sup>*</sup>
C14:0	r= <b>0.137</b> <sup>***</sup>	r= -0.074	r= 0.016	r= <b>0.462</b> <sup>***</sup>	r= 0.073	r= <b>0.119</b> <sup>**</sup>	r= <b>0.372</b> <sup>***</sup>	r= <b>0.242</b> <sup>***</sup>
C16:0	r= 0.010	r= <b>-0.220</b> <sup>***</sup>	r= -0.013	r= <b>0.454</b> <sup>***</sup>	r= <b>-0.099</b> <sup>*</sup>	r= <b>0.143</b> <sup>***</sup>	r= <b>0.328</b> <sup>***</sup>	r= <b>0.221</b> <sup>***</sup>
C18:0	r= <b>-0.083</b> <sup>*</sup>	r= <b>0.256</b> <sup>***</sup>	r= <b>-0.103</b> <sup>*</sup>	r= <b>-0.204</b> <sup>***</sup>	r= <b>0.242</b> <sup>***</sup>	r= <b>-0.143</b> <sup>**</sup>	r= <b>-0.083</b> <sup>*</sup>	r= -0.014
C20:0	r= -0.059	r= <b>0.196</b> <sup>***</sup>	r= 0.020	r= <b>-0.449</b> <sup>***</sup>	r= 0.042	r= <b>-0.125</b> <sup>**</sup>	r= <b>-0.366</b> <sup>***</sup>	r= <b>-0.246</b> <sup>***</sup>
C22:0	r= 0.058	r= <b>0.247</b> <sup>***</sup>	r= <b>0.160</b> <sup>***</sup>	r= <b>-0.527</b> <sup>***</sup>	r= <b>0.101</b> <sup>*</sup>	r= -0.036	r= <b>-0.372</b> <sup>***</sup>	r= <b>-0.230</b> <sup>***</sup>
C24:0	r= 0.044	r= <b>0.263</b> <sup>***</sup>	r= <b>0.149</b> <sup>***</sup>	r= <b>-0.495</b> <sup>***</sup>	r= <b>0.138</b> <sup>**</sup>	r= -0.030	r= <b>-0.315</b> <sup>***</sup>	r= <b>-0.220</b> <sup>***</sup>
C16:1n-7	r= <b>0.193</b> <sup>***</sup>	r= -0.075	r= <b>0.107</b> <sup>**</sup>	r= <b>0.427</b> <sup>***</sup>	r= 0.033	r= <b>0.226</b> <sup>***</sup>	r= <b>0.354</b> <sup>***</sup>	r= <b>0.248</b> <sup>***</sup>
C18:1n-9	r= <b>-0.091</b> <sup>*</sup>	r= <b>-0.295</b> <sup>***</sup>	r= <b>-0.130</b> <sup>**</sup>	r= <b>0.382</b> <sup>***</sup>	r= <b>-0.275</b> <sup>***</sup>	r= -0.044	r= <b>0.154</b> <sup>**</sup>	r= 0.076
C20:1n-9	r= <b>-0.100</b> <sup>**</sup>	r= <b>-0.190</b> <sup>***</sup>	r= <b>-0.151</b> <sup>***</sup>	r= <b>0.245</b> <sup>***</sup>	r= <b>-0.101</b> <sup>*</sup>	r= -0.048	r= <b>0.149</b> <sup>***</sup>	r= <b>0.090</b> <sup>*</sup>
C22:1n-9	r= -0.045	r= 0.041	r= -0.013	r= <b>-0.132</b> <sup>**</sup>	r= <b>0.086</b> <sup>*</sup>	r= -0.065	r= <b>-0.101</b> <sup>*</sup>	r= -0.028
C18:3n-3	r= <b>0.109</b> <sup>**</sup>	r= <b>-0.108</b> <sup>**</sup>	r= 0.057	r= <b>0.297</b> <sup>***</sup>	r= -0.045	r= <b>0.144</b> <sup>***</sup>	r= <b>0.247</b> <sup>***</sup>	r= <b>0.131</b> <sup>**</sup>
C18:4n-3	r= 0.029	r= <b>0.087</b> <sup>*</sup>	r= 0.010	r= -0.040	r= <b>0.114</b> <sup>**</sup>	r= 0.052	r= 0.015	r= <b>0.086</b> <sup>*</sup>
C20:5n-3	r= <b>0.171</b> <sup>***</sup>	r= <b>0.092</b> <sup>*</sup>	r= <b>0.136</b> <sup>**</sup>	r= 0.042	r= <b>0.181</b> <sup>***</sup>	r= <b>0.220</b> <sup>***</sup>	r= <b>0.178</b> <sup>***</sup>	r= 0.070
C22:6n-3	r= <b>-0.078</b> <sup>*</sup>	r= -0.047	r= -0.037	r= <b>-0.104</b> <sup>**</sup>	r= -0.039	r= 0.032	r= <b>-0.095</b> <sup>*</sup>	r= -0.057
C18:2n-6	r= 0.041	r= <b>0.235</b> <sup>***</sup>	r= <b>0.094</b> <sup>*</sup>	r= <b>-0.438</b> <sup>***</sup>	r= <b>0.137</b> <sup>**</sup>	r= -0.072	r= <b>-0.276</b> <sup>***</sup>	r= <b>-0.188</b> <sup>***</sup>
C20:2n-6	r= 0.028	r= 0.075	r= -0.029	r= -0.015	r= <b>0.174</b> <sup>***</sup>	r= -0.030	r= 0.052	r= -0.002
C20:4n-6	r= 0.011	r= <b>0.143</b> <sup>***</sup>	r= 0.071	r= <b>-0.314</b> <sup>***</sup>	r= 0.079	r= 0.007	r= <b>-0.201</b> <sup>***</sup>	r= <b>-0.091</b> <sup>*</sup>

Tab.X Correlations between plasma lipid /apolipoprotein parameters and fatty acids profile in the youngest population (age<62). Significant correlations are in bold type.

\* = p-value < 0.05

\*\* = p-value < 0.01

\*\*\* = p-value < 0.001

	Tot chol	HDL	LDL	TG	ApoA-I	ApoB	ApoC-III	ApoE
C12:0	r= 0.049	r= -0.043	r= 0.029	<b>r= 0.198<sup>***</sup></b>	r= 0.027	r= 0.070	<b>r= 0.095<sup>*</sup></b>	r= 0.039
C14:0	<b>r= 0.123<sup>**</sup></b>	<b>r= -0.082<sup>*</sup></b>	r= 0.078	<b>r= 0.394<sup>***</sup></b>	r= 0.054	<b>r= 0.183<sup>***</sup></b>	<b>r= 0.265<sup>***</sup></b>	<b>r= 0.116<sup>**</sup></b>
C16:0	<b>r= -0.095<sup>*</sup></b>	<b>r= -0.221<sup>***</sup></b>	<b>r= -0.137<sup>**</sup></b>	<b>r= 0.260<sup>***</sup></b>	<b>r= -0.185<sup>***</sup></b>	r= -0.007	<b>r= 0.146<sup>***</sup></b>	r= 0.055
C18:0	r= 0.058	<b>r= 0.324<sup>***</sup></b>	r= -0.019	<b>r= -0.238<sup>***</sup></b>	<b>r= 0.334<sup>***</sup></b>	r= -0.044	<b>r= -0.106<sup>**</sup></b>	r= -0.049
C20:0	r= 0.048	<b>r= 0.224<sup>***</sup></b>	r= 0.067	<b>r= -0.345<sup>***</sup></b>	<b>r= 0.134<sup>**</sup></b>	r= -0.037	<b>r= -0.250<sup>***</sup></b>	<b>r= -0.152<sup>**</sup></b>
C22:0	<b>r= 0.197<sup>***</sup></b>	<b>r= 0.276<sup>***</sup></b>	<b>r= 0.225<sup>***</sup></b>	<b>r= -0.366<sup>***</sup></b>	<b>r= 0.197<sup>***</sup></b>	<b>r= 0.089<sup>*</sup></b>	<b>r= -0.237<sup>***</sup></b>	<b>r= -0.116<sup>**</sup></b>
C24:0	<b>r= 0.174<sup>***</sup></b>	<b>r= 0.263<sup>***</sup></b>	<b>r= 0.122<sup>**</sup></b>	<b>r= -0.283<sup>***</sup></b>	<b>r= 0.188<sup>***</sup></b>	r= 0.061	<b>r= -0.162<sup>***</sup></b>	<b>r= -0.154<sup>***</sup></b>
C16:1n-7	r= 0.002	r= -0.070	r= 0.005	<b>r= 0.222<sup>***</sup></b>	r= -0.025	r= 0.049	<b>r= 0.131<sup>**</sup></b>	<b>r= 0.103<sup>*</sup></b>
C18:1n-9	<b>r= -0.263<sup>***</sup></b>	<b>r= -0.350<sup>***</sup></b>	<b>r= -0.213<sup>***</sup></b>	<b>r= 0.327<sup>***</sup></b>	<b>r= -0.296<sup>***</sup></b>	<b>r= -0.144<sup>***</sup></b>	<b>r= 0.108<sup>**</sup></b>	<b>r= 0.082<sup>*</sup></b>
C20:1n-9	<b>r= -0.153<sup>***</sup></b>	<b>r= -0.216<sup>***</sup></b>	<b>r= -0.171<sup>***</sup></b>	<b>r= 0.253<sup>***</sup></b>	<b>r= -0.114<sup>**</sup></b>	<b>r= -0.087<sup>*</sup></b>	<b>r= 0.125<sup>**</sup></b>	<b>r= 0.135<sup>**</sup></b>
C22:1n-9	<b>r= 0.115<sup>**</sup></b>	r= 0.049	<b>r= 0.111<sup>**</sup></b>	r= -0.024	r= 0.048	<b>r= 0.085<sup>*</sup></b>	r= 0.017	<b>r= 0.093<sup>*</sup></b>
C18:3n-3	<b>r= 0.212<sup>***</sup></b>	r= 0.015	<b>r= 0.127<sup>**</sup></b>	<b>r= 0.283<sup>***</sup></b>	<b>r= 0.108<sup>**</sup></b>	<b>r= 0.232<sup>***</sup></b>	<b>r= 0.292<sup>***</sup></b>	<b>r= 0.092<sup>*</sup></b>
C18:4n-3	r= 0.071	<b>r= 0.158<sup>***</sup></b>	r= 0.023	r= -0.022	<b>r= 0.127<sup>**</sup></b>	r= 0.058	r= 0.032	r= 0.000
C20:5n-3	<b>r= 0.286<sup>***</sup></b>	<b>r= 0.190<sup>***</sup></b>	<b>r= 0.183<sup>***</sup></b>	r= 0.031	<b>r= 0.171<sup>***</sup></b>	<b>r= 0.261<sup>***</sup></b>	<b>r= 0.185<sup>***</sup></b>	r= 0.064
C22:6n-3	r= 0.049	r= -0.017	r= 0.029	r= -0.019	r= -0.045	<b>r= 0.097<sup>*</sup></b>	r= 0.044	r= 0.044
C18:2n-6	<b>r= 0.174<sup>***</sup></b>	<b>r= 0.272<sup>***</sup></b>	<b>r= 0.191<sup>***</sup></b>	<b>r= -0.324<sup>***</sup></b>	<b>r= 0.206<sup>**</sup></b>	r= 0.038	<b>r= -0.199<sup>***</sup></b>	<b>r= -0.094<sup>*</sup></b>
C20:2n-6	r= 0.037	<b>r= 0.129<sup>***</sup></b>	r= 0.019	r= -0.062	<b>r= 0.191<sup>***</sup></b>	r= -0.032	r= -0.027	r= 0.016
C20:4n-6	<b>r= 0.081<sup>*</sup></b>	<b>r= 0.173<sup>***</sup></b>	r= 0.048	<b>r= -0.244<sup>***</sup></b>	<b>r= 0.134<sup>**</sup></b>	r= 0.056	r= -0.047	<b>r= -0.083<sup>*</sup></b>

Tab. XI Correlations between plasma lipid/apolipoprotein parameters and fatty acids profile in the oldest population (age>62). Significant correlations are in bold type.

\* = p-value < 0.05

\*\* = p-value < 0.01

\*\*\* = p-value < 0.001

### 3.5 Principal Component Analysis (PCA) results

In order to obtain a general description of the relationships existing in the present dataset, PCA analysis was performed. This analysis is based on the dimensionality reduction by using new variables, the principal components, accounting for the maximum dataset variance. The results obtained indicate that the first two PCs explain 17.9% and 11.7% of the total variance contained in the original dataset, respectively.

In particular, PCA allows the graphical representation of samples showing similar behaviours, as well as the visualization of the variables responsible for the aforementioned similarities and differences. The loading plot obtained by the PCA analysis of the whole population is reported in Fig.3.

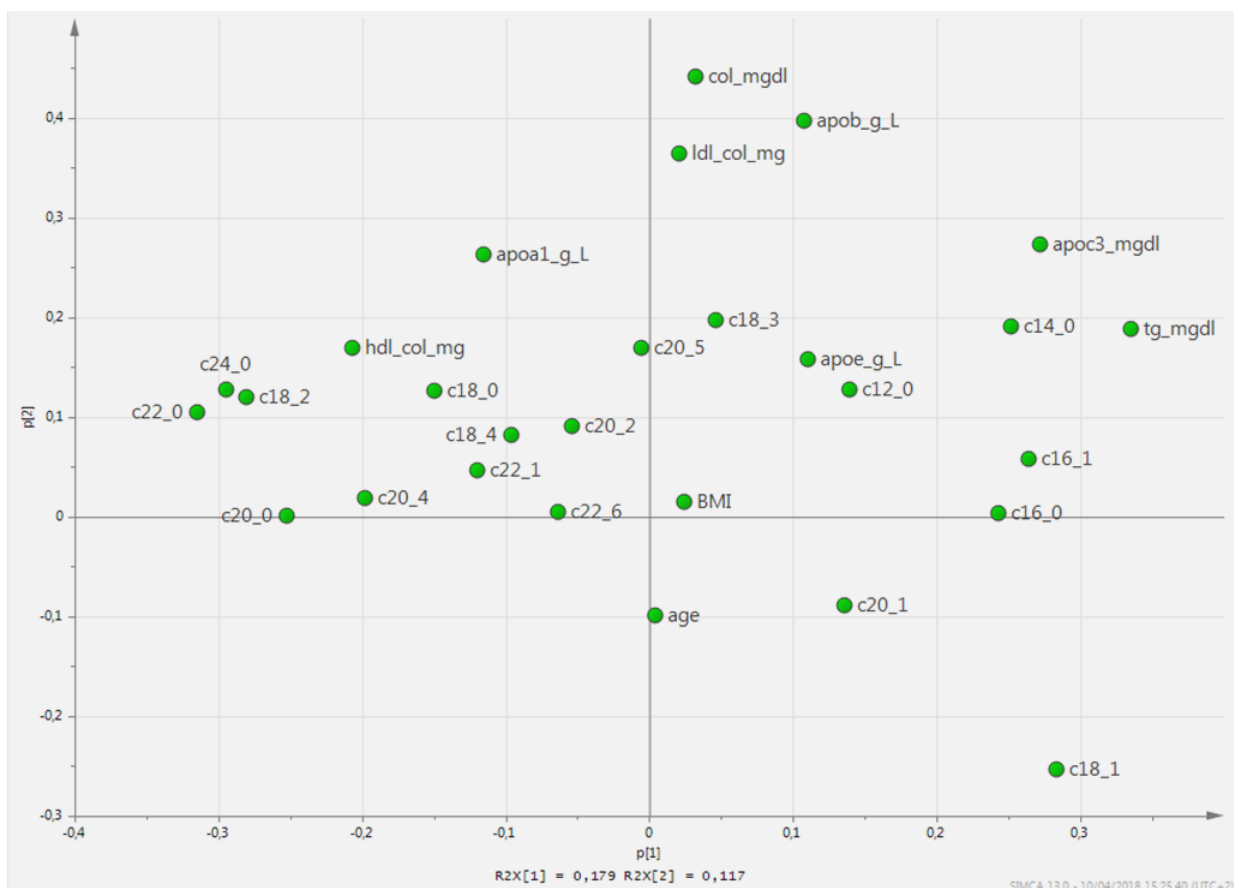


Fig.3 PCA results showing the loading plot obtained from the analysis of lipid/apolipoprotein parameters and FAs values in the whole population (n=1,370).



### 3.6 Regression analyses

To highlight the most important associations between lipid/apolipoprotein parameters and single FA, regression analyses were performed. Values of FAs that showed significant correlation with the lipid/apolipoprotein parameter in the previous analysis on the whole population (Tab. V) were involved in the regression study. Results of regression analysis for each parameter in the whole population are reported in Tab.XII. In the right part of the table the results after correction for sex, age, BMI, diabetes, CAD diagnosis, and lipid-lowering therapy are reported. In the studied population C14:0 was the main statistical predictor, among the various FAs, of both plasmatic TG and ApoC-III (Tab. XII), explaining about 20% and 10% of their variability, respectively. The significance of these relationships did not change even after adjustment for sex, age, BMI, presence of CAD pathology and use of lipid lowering therapy.

<b>Dependent variable:</b>	<b>Standardized Beta-coefficient</b>	<b>p-value *</b>	<b>R<sup>2</sup></b>	<b>R<sup>2</sup> change</b>	<b>Adjusted Standardized Beta-coefficient</b>	<b>P-value<sup>#</sup></b>
<b>Total Cholesterol</b>						
<b>C20:5n-3</b>	0.232	<0.001	0.057	0.057	0.217	<0.001
<b>C18:2n-6</b>	0.175	<0.001	0.081	0.023	0.164	<0.001
<b>C16:1n-7</b>	0.184	<0.001	0.115	0.034	0.192	<0.001
<b>C20:1n-9</b>	-0.092	0.001	0.122	0.007	-0.075	0.011
<b>C14:0</b>	0.068	0.028	0.127	0.005	0.059	0.091
<b>C22:0</b>	0.092	0.002	0.132	0.005	0.102	0.002
<b>C18:3n-3</b>	0.061	0.046	0.134	0.003	0.062	0.063
<b>HDL-C</b>						
<b>C18:1n-9</b>	0.597	<0.001	0.100	0.100	0.533	<0.001
<b>C16:0</b>	0.160	0.012	0.140	0.040	0.178	0.007
<b>C18:0</b>	0.337	<0.001	0.160	0.020	0.277	<0.001
<b>C16:1n-7</b>	0.302	<0.001	0.173	0.013	0.242	<0.001
<b>C20:0</b>	0.133	<0.001	0.183	0.011	0.106	<0.001
<b>C20:5n-3</b>	0.289	<0.001	0.194	0.010	0.257	<0.001
<b>C20:1n-9</b>	-0.077	0.009	0.200	0.006	-0.061	0.041
<b>C18:2n-6</b>	0.820	<0.001	0.206	0.006	0.730	<0.001
<b>C20:4n-6</b>	0.377	<0.001	0.221	0.016	0.356	<0.001

<b>C18:4n-3</b>	0.109	<0.001	0.231	0.009	0.095	<0.001
<b>C24:0</b>	0.099	0.003	0.236	0.006	0.097	0.003
<b>LDL-C</b>						
<b>C22:0</b>	0.135	<0.001	0.037	0.037	0.156	<0.001
<b>C20:5n-3</b>	0.150	<0.001	0.058	0.021	0.144	<0.001
<b>C20:1n-9</b>	-0.127	<0.001	0.079	0.021	-0.111	0.002
<b>C18:0</b>	-0.137	<0.001	0.091	0.012	-0.098	0.004
<b>C18:1n-9</b>	-0.089	0.022	0.095	0.004	-0.058	0.170
<b>Triglycerides</b>						
<b>C14:0</b>	0.324	<0.001	0.195	0.195	0.338	<0.001
<b>C22:0</b>	-0.112	<0.001	0.326	0.131	-0.130	<0.001
<b>C18:0</b>	-0.065	0.005	0.362	0.037	-0.041	0.093
<b>C18:3n-3</b>	0.268	<0.001	0.391	0.029	0.246	<0.001
<b>C18:1n-9</b>	0.251	<0.001	0.418	0.027	0.254	<0.001
<b>C16:0</b>	0.193	<0.001	0.442	0.024	0.173	<0.001
<b>C20:0</b>	-0.129	<0.001	0.450	0.008	-0.117	<0.001
<b>C20:4</b>	0.112	<0.001	0.458	0.007	0.108	<0.001
<b>C20:1n-9</b>	0.079	0.001	0.463	0.005	0.078	0.002
<b>C12:0</b>	-0.068	0.027	0.464	0.002	-0.090	0.005
<b>ApoA-I</b>						
<b>C18:1n-9</b>	-0.141	<0.001	0.078	0.078	0.002	<0.001
<b>C18:0</b>	0.173	<0.001	0.108	0.030	0.066	<0.001
<b>C20:5n-3</b>	0.172	<0.001	0.126	0.018	0.017	<0.001
<b>C20:2n-6</b>	0.115	<0.001	0.144	0.018	0.035	0.001
<b>C16:0</b>	-0.102	<0.001	0.154	0.009	0.004	0.006
<b>ApoB</b>						
<b>C20:5n-3</b>	0.227	<0.001	0.060	0.060	0.218	<0.001
<b>C18:3n-3</b>	0.116	<0.001	0.076	0.016	0.116	<0.001
<b>C16:1n-7</b>	0.138	<0.001	0.094	0.018	0.150	<0.001
<b>C18:0</b>	-0.155	<0.001	0.102	0.008	-0.113	<0.001
<b>C18:1n-9</b>	-0.149	<0.001	0.118	0.015	-0.143	<0.001
<b>C22:6</b>	-0.072	0.033	0.121	0.003	-0.066	0.063
<b>ApoC-III</b>						
<b>C14:0</b>	0.288	<0.001	0.107	0.107	0.310	<0.001
<b>C20:0</b>	-0.150	<0.001	0.173	0.065	-0.140	<0.001
<b>C18:3n-3</b>	0.204	<0.001	0.200	0.027	0.188	<0.001
<b>C22:0</b>	-0.096	0.008	0.214	0.014	-0.122	0.002

<b>C20:5n-3</b>	0.097	<0.001	0.230	0.016	0.074	0.011
<b>C12:0</b>	-0.112	0.003	0.237	0.007	-0.135	0.001
<b>C16:0</b>	0.109	<0.001	0.244	0.007	0.102	0.001
<b>C20:1n-9</b>	0.073	0.016	0.250	0.006	0.093	0.004
<b>C20:4</b>	0.129	<0.001	0.257	0.006	0.107	0.002
<b>C18:1n-9</b>	0.097	0.008	0.261	0.004	0.080	0.041
<b>ApoE</b>						
<b>C20:0</b>	-0.117	<0.001	0.040	0.040	-0.103	0.004
<b>C14:0</b>	0.144	0.001	0.061	0.020	0.167	0.001
<b>C24:0</b>	-0.121	0.001	0.069	0.008	-0.118	0.002
<b>C20:1n-9</b>	0.093	0.005	0.073	0.005	0.098	0.006
<b>C12:0</b>	-0.086	0.039	0.077	0.003	-0.103	0.025
<b>C18:1n-9</b>	-0.142	0.001	0.080	0.003	-0.133	0.005
<b>C18:2n-6</b>	-0.134	<0.001	0.088	0.008	-0.131	0.001
<b>C18:3n-3</b>	0.068	0.025	0.091	0.004	0.070	0.035

*Tab. XII Fatty acid predictors of plasma lipid and apolipoprotein profile by linear regression analyses. At first a regression model with backward stepwise selection of variables and then a regression model with forward stepwise selection of variables were performed.*

### **3.7 In vivo evaluation of myristic acid correlation with CAD risk factors: focus on triglycerides and ApoC-III plasma levels**

As indicated in Tab.XII C14:0 is the strongest predictor of single lipid parameters with respect to other FAs and was the first predictor of both TG and ApoC-III plasma levels. Therefore, the distribution of all lipid and apolipoprotein values were evaluated in relation to C14:0 quintiles, also taking into account the two sub-groups, CAD and CAD-free. The statistical evaluation was performed by means of ANOVA test. The mean clinical characteristics of subjects included are reported in Tab. XIII.

	<b>CAD (n=1,004)</b>	<b>CAD-free (n=366)</b>
<b>Age (years)</b>	61 ± 10	58 ± 12
<b>Male sex (%)</b>	79.8%	65%
<b>Diabetes</b>	18.1%	7,1%
<b>Lipid Lowering Therapy</b>	29.1%	4,8%
<b>Total cholesterol (mmol/L)</b>	5.50 ± 1.17	5.47 ± 1.17
<b>HDL Cholesterol (mmol/L)</b>	1.18 ± 0,3	1.42 ± 0.42
<b>LDL Cholesterol (mmol/L)</b>	3.69 ± 1	3.5 ± 0.92
<b>Triglycerides (mmol/L)</b>	1.70 (1.65-1.75)	1.37 (1.31-1.43)
<b>Apolipoprotein A-I (g/L)</b>	1.27 ± 0.24	1.39 ± 0.31
<b>Apolipoprotein B (g/L)</b>	1.16 ± 0.31	1.05 ± 0.25
<b>Apolipoprotein C-III (mg/dL)</b>	11.1 (10.8- 11.3)	10.1 (9.7- 10.5)
<b>Apolipoprotein E</b>	0.042 (0.041- 0.043)	0.039 (0.038- 0.040)

*Tab. XIII Clinical characteristics of CAD and CAD-free populations.*

As reported in Tab. XIV some parameters were found to be significantly correlated with C14:0 quintiles values, including among the most significant total cholesterol, HDL cholesterol, TG, ApoB, ApoC-III and ApoE. TG and ApoC-III plasma concentrations in the whole population were directly related with C14:0 levels divided into quintiles ( $p < 0.001$ ) (Fig.3A and Fig.4A respectively) and were both preserved either in CAD ( $p < 0.001$ ) and CAD-free subjects ( $p < 0.001$ ) when separately considered (Fig.4B-C and Fig.5B-C). This tendency remained statistically significant also after partitioning between men and women inside both populations (Fig.4D-G and Fig.5D-G), as further confirmation of the solid and independent association of plasmatic C14:0 with plasma TG and ApoC-III concentration.

<b>C 14:0 quintiles</b>						
	<b>I</b> (<0.73)	<b>II</b> (0.73-0.91)	<b>III</b> (0.91-1.13)	<b>IV</b> (1.13-1.47)	<b>V</b> (>1.47)	<b>P</b>
<b>Age (years)</b>	61.4±10.2	61.3±10.9	62.5±11	59.2±11.3	58.7±11.2	<0.001
<b>Male sex (%)</b>	81.0%	79.9%	69.0%	74.5%	74.8%	0.007
<b>CAD diagnosis (%)</b>	81.8%	69.0%	70.8%	70.1%	74.8%	0.004
<b>Total cholesterol (mmol/L)</b>	5.31±1.07	5.32±1.12	5.50±1.22	5.66±1.17	5.69±1.12	<0.001
<b>HDL cholesterol (mmol/L)</b>	1.21±0.35	1.32±0.39	1.31±0.35	1.22±0.33	1.17±0.30	<0.001
<b>LDL cholesterol (mmol/L)</b>	3.55±0.91	3.52±0.96	3.71±1.09	3.77±0.98	3.64±0.95	0.033
<b>Triglycerides (mmol/L)</b>	1.33(1.27-1.40)	1.35(1.29-1.42)	1.48(1.40-1.55)	1.80(1.72-1.89)	2.23(2.11-2.35)	<0.001
<b>Apo A-I (g/L)</b>	1.25± 0.27	1.31±0.29	1.33±0.26	1.32±0.28	1.31±0.23	0.021
<b>Apo B (g/L)</b>	1.08±0.27	1.08±0.26	1.11±0.31	1.16±0.29	1.19±0.33	<0.001
<b>Apo C-III (mg/dL)</b>	9.74(9.41-10.07)	9.77(9.40-10.15)	10.25(9.81-10.70)	11.48(11.04-11.94)	12.98(12.35-13.63)	<0.001
<b>Apo E (g/L)</b>	0.040(0.038-0.041)	0.037(0.036-0.039)	0.040(0.038-0.042)	0.042(0.040-0.044)	0.045(0.043-0.048)	<0.001

Tab. XIV. Distribution of plasma lipid and apolipoprotein parameters concentrations in relation to C14:0 quintiles.

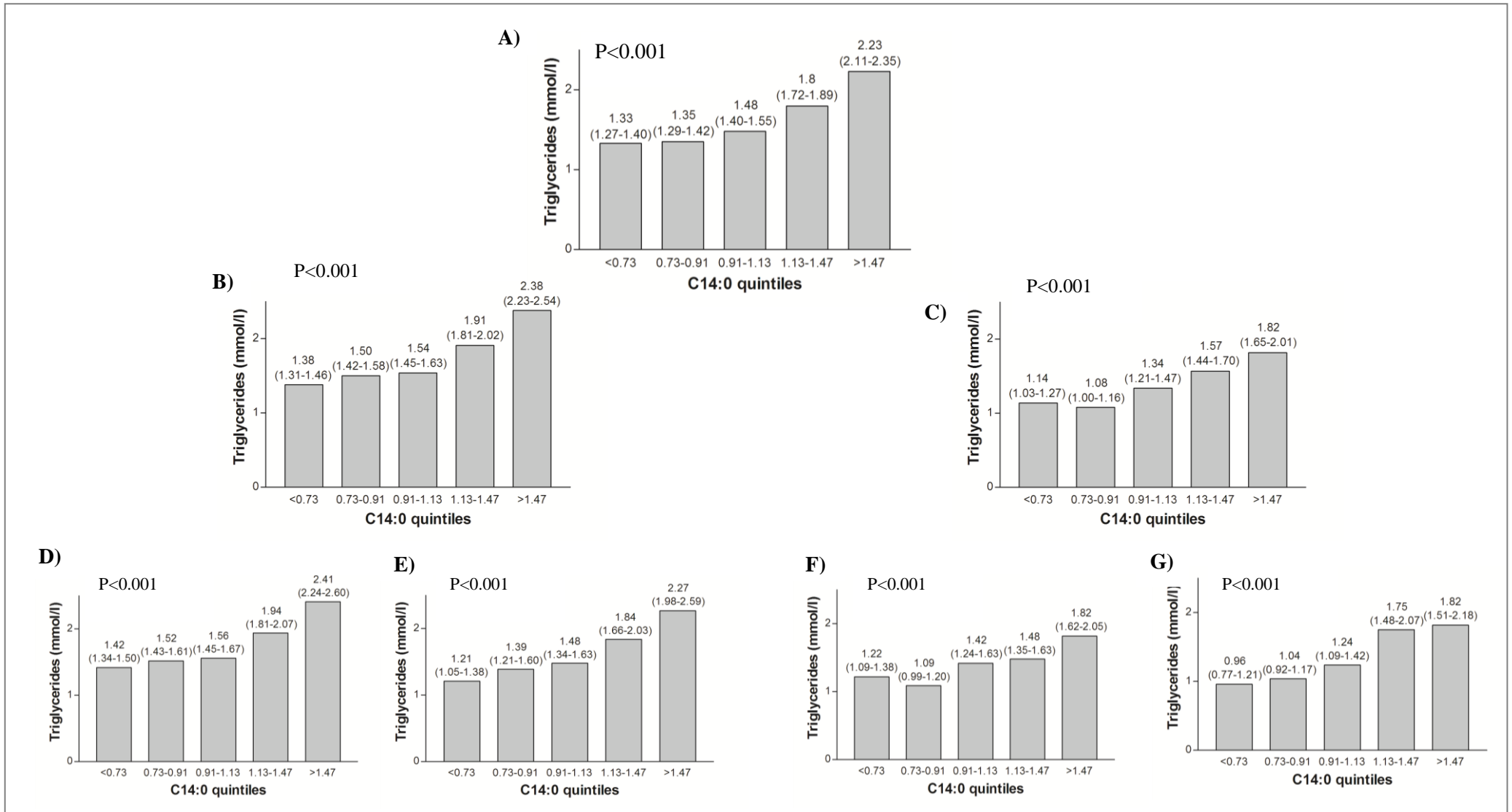


Fig.4 Representation of triglycerides distribution in relation to C14:0 quintiles in the whole population (A), in CAD patients (B) and CAD-free subject (C). Inside these two distinct populations the distribution of triglycerides was also evaluated among males (D for CAD and F for CAD free subjects) and females subjects (E for CAD and G for CAD free subjects).

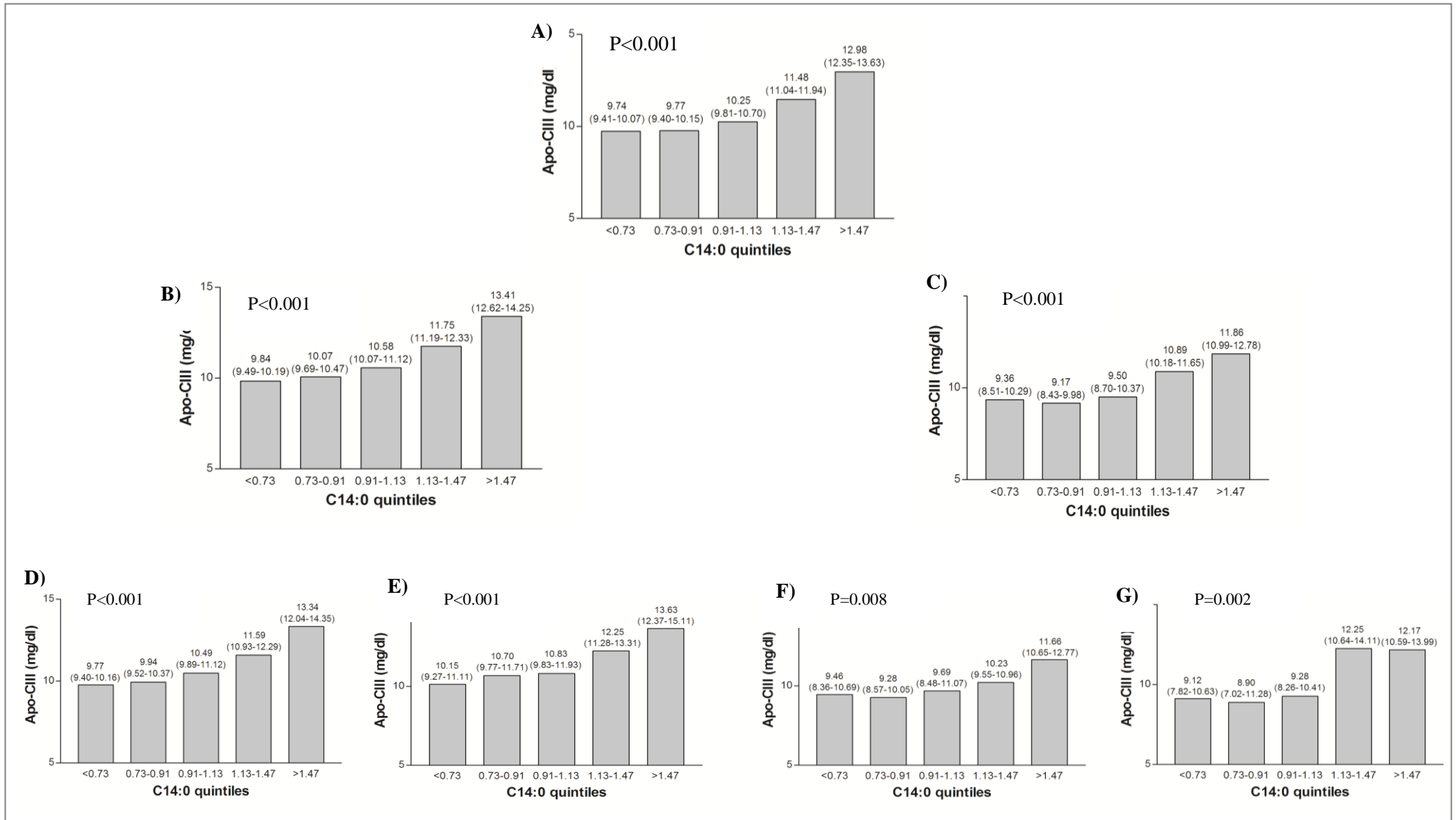


Fig.5 Representation of ApoC-III distribution in relation to C14:0 quintiles in the whole population (A), in CAD patients (B) and CAD-free subject (C). Inside these two distinct populations the distribution of ApoC-III was also evaluated among male (D for CAD and F for CAD free subjects) and female subjects (E for CAD and G for CAD free subjects).

## 4. DISCUSSION

Limitations of previous studies aimed at investigating the relationships between lipid/apolipoprotein parameters and FAs plasma levels were mentioned in the first chapter and include replacement of FA intake with carbohydrates, use of food frequency questionnaires, consideration of FA classes rather than single FAs or finally small population cohorts (Mensink et al., 2003; Warensjo et al., 2008; Niknam et al., 2014). Therefore, the present project was developed to investigate the existence of possible correlations of lipid and apolipoprotein parameters with the gas-chromatographically analysed FAs plasma levels in a large population, disclosing new possible FA-related mechanisms involved in CVD onset that are not already highlighted. Secondly, this project intended to evaluate and possibly confirm the interesting and significant correlations observed during my master's degree thesis between C14:0 plasma levels and lipid/apolipoprotein parameters on a smaller group of subjects (57 VHS CAD patients). Therefore, the correlations between lipid profile and plasmatic FAs were investigated in 1,370 subjects, with and without CAD, involved in the VHS. Correlation analyses identified a high number of significant correlations between lipid and FA levels (Tab. V) in whole as well as in stratified population.

PCA analysis, performed to obtain a general graphical representation of the relationships existing among the variables, showed and confirmed the associations of total and LDL cholesterol with ApoB -known to be the main protein component of the LDL particles- and also identified a new important cluster of variables which comprises TG, ApoC-III and C14:0 (Fig. 3). In particular, C14:0 was the FA closest to a group of connected lipid parameters, suggesting therefore a possible relationship with TG plasma levels and their regulation. Regression analyses including only significantly correlated FAs were needed to bring to light only the strongest and possibly causal associations. The results obtained from regression analysis highlighted the most significant FAs predictors of the lipid/apolipoprotein analysed. Many



associations were found, such as the one involving C18:1, the major diet monounsaturated fatty acid (MUFA). C18:1 was the first predictor both of HDL and also of ApoA-I plasma levels, the main apolipoprotein component of HDL, consistent with literature data describing the cardioprotective ability of MUFAs to increase HDL cholesterol (Michas et al., 2014). The main interesting result was however related to C14:0 associations: this FA was the strongest predictor of both a lipid and an apolipoprotein parameter. C14:0 was confirmed to be correlated with cardiovascular risk factors, but the results obtained demonstrated that C14:0 is the first FA predictor of both TG and ApoC-III plasma levels, explaining about 20% and 10% of their plasma variability, independently of any other possible influencing factor (Tab. XII). C14:0 is a SFA that is present at low concentrations in human plasma if compared to some other SFAs. In the studied population C14:0 represented only 1% of all identified FAs (Tab. III). However, it is the third most common saturated FA in the diet and the hypercholesterolemic effects of this FA on both total and LDL cholesterol are already well known. In particular, C14:0 was reported to raise LDL cholesterol levels even more than C16:0 (Zock et al., 1994; Kris-Etherton et al., 1997). Like C16:0 and stearic acid (C18:0), high levels of C14:0 have been associated with an increased CAD risk (Zong et al., 2016). Recently its negative association with HDL plasma levels in a Mediterranean population has been highlighted, in agreement with the negative correlation observed between these two parameters (Tab. V). It has been suggested that C14:0 could influence HDL trapping on liver surface (Noto et al., 2016). This recent investigation pointed out how C14:0 could still hide unknown atherogenic effects that need to be uncovered. In the present study, for the first time an important new connection between C14:0 and TG plasma levels has been demonstrated. It is possible to speculate that this mechanism could be due to a C14:0 positive influence on the plasma TG-regulator ApoC-III, which was also found to be predicted mainly by C14:0 levels in the studied population (Tab. XII).

As far as we know this is the first time that such strong associations are highlighted by means of regression analysis in a population study, and in particular it is the first time that the relation between C14:0 and ApoC-III plasma levels have been reported. These data are in agreement with some population-based studies reporting correlation analysis involving FA levels. In the study of de Oliveira et al. focused on a multiethnic cohort of 2,837 US subjects, a significant increase in the levels of plasma TG in relation to the distribution of plasma phospholipid C14:0 quintiles was reported (de Oliveira Otto et al., 2013). This trend is like that observed in Tab. XIV and Fig.4. In the following year another study based on a Mediterranean population of 427 subjects at high risk of CVD reported that higher levels of C14:0 were present in people with metabolic syndrome (Mayneris-Perxachs et al., 2014), which is strictly connected with the risk of CVD. Moreover, in this study C14:0 showed a strong correlation with TG plasma levels. Research performed on 758 Western Alaskan Native subjects showed a statistically significant correlation of TG with C14:0 extracted from red blood cells (RBCs) and this correlation was even stronger when C14:0 extracted from plasma lipids was analysed (Ebbesson et al., 2015). Furthermore, in a very recent research C14:0 was found to be correlated to TG levels, together with C16:0 and C18:0, and with the presence of atherosclerosis (Polonskaya et al., 2017). Unfortunately, dietary supplementation studies failed to reveal the potential TG raising effect of C14:0. Zock et al. compared the effect of diet rich in C14:0, C16:0 and C18:1 on plasma lipids when supplied by means of synthetic fats accounting for 10% of total energy intake. They reported only a slight increase in TG levels following C14:0 diet compared with C18:1 diet, but no differences in TG levels when compared with C16:0 supplementation (Zock et al., 1994). However, the study of Zock et al. was limited by a very small sample size (59 subjects). In a large meta-analysis including 60 controlled trials, as well as in a recent WHO report based on 84 different studies the isocalorical replacement of 1% of total energy in the diet coming from carbohydrates with C14:0 was negatively associated with TG plasma levels in a slightly significant manner (Mensik et al. 2003, Mensik 2016). However, this study also had

limitations. This effect might be explained by the replacement nutrient used, as in the same report the replacement of SFA with carbohydrates caused an increase in total plasma TG concentration. The TG raising effect of the replacement nutrient used in this study - carbohydrates- could therefore interfere with the detection of the actual C14:0 impact on TG plasma levels.

The fact that C14:0 was simultaneously the first predictor of ApoC-III plasma levels, explaining also in this case a high portion of its plasma variability, represents further evidence supporting the association observed with TG plasma levels. As already mentioned, ApoC-III is a potent plasma regulator of TG levels, and loss-of-function mutations in APOC-III gene have had a favorable effect on the overall cardiovascular risk due to their reducing effect on TG plasma levels (Crosby et al., 2014). The important role played by ApoC-III in CAD has already been reported and recently our group has investigated the different sialylated isoforms of ApoC-III in CAD patients (Olivieri et al., 2002; Olivieri et al., 2003; Martinelli et al., 2007; Olivieri Oliviero, 2017). A very recent study reported ApoC-III among the three apolipoproteins most significantly associated with incident CVD, together with ApoC-II and ApoE (Pechlaner et al., 2017), which was predicted by C14:0 levels in this PhD thesis. The authors suggested that targeting TRLs would probably be a better solution for cardiovascular treatment, compared to the classical approach focused only on LDL cholesterol levels and measurement of classical ApoA-I and ApoB. While reducing LDL cholesterol represented an effective method for cardiovascular prevention, many patients maintain a significant residual risk. This observation is shifting the medical management of the cardiovascular risk through the reduction of TG plasma levels, therefore current therapy for reducing ApoC-III plasma levels include statins, fibrates, thiazolidinediones, niacin and antisense oligonucleotide currently under phase III study (Khetarpal et al., 2016). However, it is already known that ApoC-III plasma levels are also regulated by FAs and n-3 PUFA. At high pharmaceutical doses n-3

PUFA can decrease TG plasma levels through many mechanisms also involving ApoC-III reduction (Ooi et al., 2015; Khetarpal et al., 2016). The transcription of ApoC-III gene is also negatively mediated by the PPAR $\alpha$ , which is activated by n-3 PUFA (Duval et al., 2007; Ooi et al., 2015).

Interestingly, C14:0 has already been reported to modulate the apolipoprotein metabolism. In particular, *in vitro* experiments revealed that C14:0 treatments can increase ApoB secretion, while reducing its degradation, in HepG2 cells and in rat hepatoma cells (Arrol et al., 2000; Kummrow et al., 2002). Moreover, a slight negative influence on PPAR $\alpha$  activity has also been reported when C14:0 has been supplied at high concentrations in HepG2 culture media, despite other FAs showing an even greater influence on the receptor activity (Popeijus et al., 2014). The disclosure that C14:0 could have an influence on ApoC-III levels, as suggested by the data presented in the present PhD thesis, would represent important information that could direct a proper cardiovascular prevention.

In conclusion, this is the first time that regression analyses on such a large number of patients have demonstrated that C14:0 is the first FA predictor of TG plasma levels. Importantly, this result concurs with some correlation population-based studies supporting a positive association between C14:0 and TG. It seems reasonable to hypothesise a possible positive C14:0-related influence on TG plasma levels. Furthermore, the strong association observed with the potent TG plasma regulator ApoC-III represents an extremely important element in support of this theory. The important association found in this first part of the study therefore opened the road to further studies aimed at disclosing the possible influence of C14:0 on ApoC-III expression. An *in vitro* validation of this relationship could confirm the potential C14:0 effect on TG plasma levels, mediated by the hypothesised influence on ApoC-III levels, and will be presented in the following chapter.

## **CHAPTER 3**

### **ANALYSIS OF THE ASSOCIATION BETWEEN MYRISTIC ACID AND APOC-III IN A HEPG2 CELL MODEL**

#### **1. INTRODUCTION**

The intake of specific FAs has been connected with the onset of different chronic diseases, including CVD. In recent years the understanding of the biological effects of FAs and of their mechanisms of action has been improved and the concept of “fatty acids sensing” has emerged. With this expression it is possible to refer to the ability of FAs to influence biological processes by acting as signaling molecules interacting with intra and extracellular receptor systems (Georgiadi et al., 2012). For example, the PPAR are nuclear hormone receptors that, also acting as transcription factors, regulate the expression of genes involved in lipid-related pathways, when activated by long-chain PUFA (Adkins et al., 2010). Other cellular receptor systems involved in the response to FAs levels include Toll-like Receptor 4 (TLR4), Sterol-Regulatory element Binding Protein 1 (SRBP1), Hepatocyte Nuclear factor 4 $\alpha$  and other nuclear receptors (Georgiadi et al., 2012).

To date information on the influence of FAs on apolipoprotein expression mainly refer to the negative effect of n-3 PUFA on ApoC-III protein levels and therefore on TG (Ito, 2015). n-3 PUFA are considered one of the main cardioprotective nutrients. In 2002 the American Heart Association recommended n-3 PUFA for patients with ischaemic heart disease and subjects with hypertriglyceridemia (De Caterina, 2011), although some recent data have questioned their real clinical usefulness (Rizos et al., 2012; Roncaglioni et al., 2013).

In the present PhD thesis significant relationships between C14:0 and TG plasma levels, as well as between C14:0 and ApoC-III, in plasma of CAD and CAD free subjects have been identified. The consequent hypothesis is that these associations could hide a possible still unknown influence of this FA on the expression of ApoC-III, that could therefore trigger an effect on TG plasma levels. The confirmation of the existence of a positive C14:0 effect on the levels of ApoC-III would suggest a consequent reasonable influence on TG plasma levels, which were found to be mainly predicted by C14:0 in the plasma of analysed subjects. To disclose this possible association, the effects of different concentrations of C14:0 have been investigated by the *in vitro* experiments described in the present chapter.

Since apolipoproteins are mainly secreted at hepatic levels, for the *in vitro* investigation of C14:0 effect on ApoC-III expression the hepatocellular carcinoma cells (HepG2) have been used. HepG2 represent a well-established cellular model for the study of lipoprotein metabolism (Meex et al., 2011) and they have been used in many studies on lipoprotein synthesis and metabolism, as well as in apolipoprotein expression experiments (Naem et al., 2013; Wu et al., 2013; Parseghian et al., 2014; Noto et al., 2016).

## **2. EXPERIMENTAL DESIGN AND PROCEDURES**

*The experimental part, and in particular the mass-spectrometry analysis, was performed thanks to the kind collaboration with Prof. Ruth Birner-Gruenberger and her group, who hosted me for three months in their Laboratory of “Functional Proteomics and Metabolic Pathways” at the Medical University of Graz, Austria. This placement was supported by the CooperInt exchange programme of the University of Verona.*

### **2.1 Cell culture and myristic acid conditioning**

HepG2 hepatoma cells were propagated in RPMI medium (RPMI 1640, Sigma Aldrich) supplemented with 10% fetal bovine serum (FBS), 100 U/ml penicillin, 100 µg/ml streptomycin and 4mM L-glutamine. Cells were maintained in a humidified incubator at 37°C with 5% CO<sub>2</sub>. For the experiment HepG2 cells were grown in a 75 cm<sup>2</sup> flask (three replicas for each treatment) until they were 70% confluent and six hours before the experiment the medium was replaced by serum-free media. The treatment was performed by using C14:0 (Sigma Aldrich) complexed with fatty acids-free Bovine Serum Albumin (BSA, Sigma Aldrich) in a 6:1 molar ratio. C14:0 was dissolved in 0.1 M NaOH (55°C) and added to a previously prepared 10% FA-free BSA solution, stirred for one hour at 37 °C. The filtered solution containing C14:0-BSA complex was supplemented into the serum-free media to obtain the following concentrations: 50, 125, 250 and 500 µM of C14:0. Control cells were supplemented with BSA alone. After 24 hours of incubation, cells were harvested using trypsin. A small amount of cells was used to measure cell viability and growth, which were assessed using CASY technology (Roche). The viability measurement of this instrument is based on electrical current exclusion, since the status and the integrity of the cell membrane distinctively affects the electrical signal generated. The percentage of cell viability was expressed as the ratio of total viable cells to the sum of total of cells. Remaining cells were washed three times with cold PBS and cell pellets were stored at -20°C until further use, as indicated in the experimental design (Fig.1).

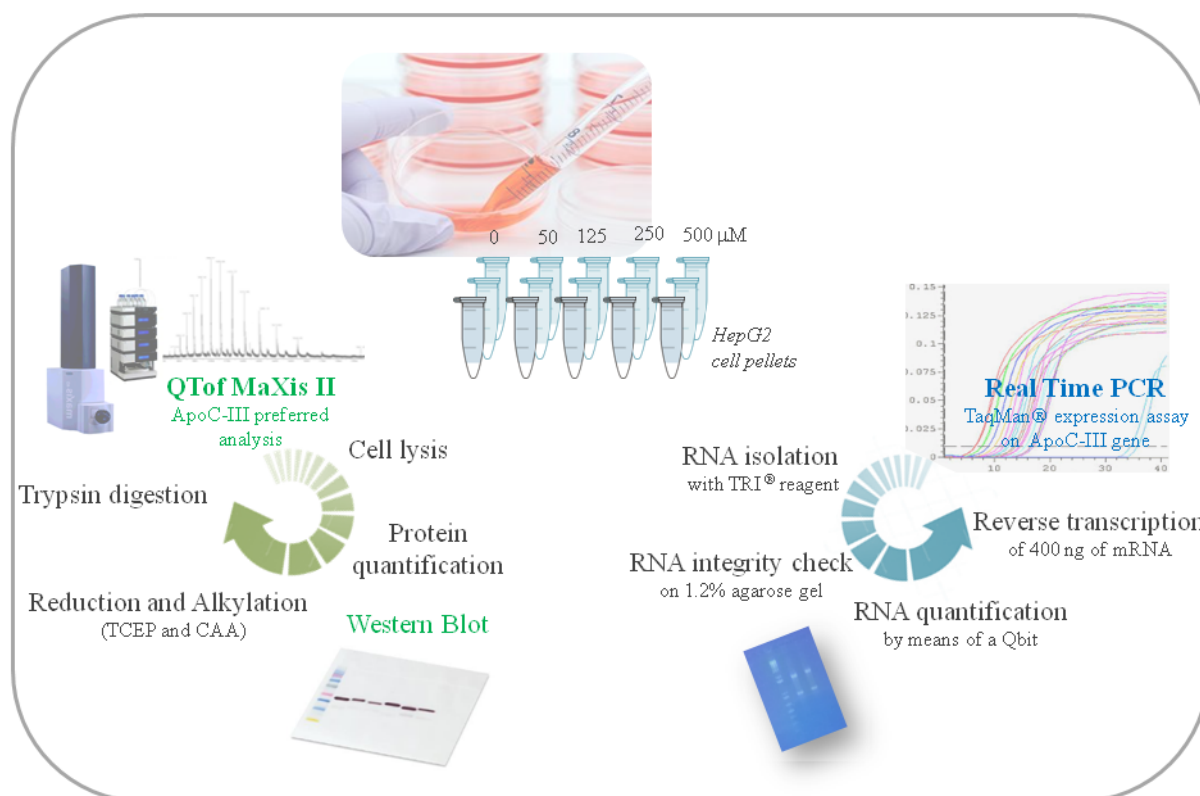


Fig.1 Experimental workflow

## 2.2 Western Blot analyses on ApoC-III

For Western Blot analyses cells were lysated directly in culture dish by adding RIPA buffer (Sigma Aldrich) on the PBS washed adherent cells. After an incubation step of five minutes in ice, cells were rapidly scraped and cell lysate was then transferred to a tube on ice. Sample was then subjected to ten minutes at 8000g at 4°C to remove cell debris. Protease inhibitors were added to the protein lysates. Protein samples from cell lysate (up to 100 μg) and 1 μl of human plasma, loaded as positive control, were diluted in Laemmli's sample buffer (62.5 mM Tris-HCl, pH 6.8, 25% glycerol, 2% SDS, 0.01% Bromophenol Blue), boiled for three minutes and separated by SDS/polyacrylamide gel electrophoresis (PAGE) on 12% T acrylamide gels in Tris/glycine/SDS buffer. Proteins were then electroblotted onto a polyvinylidene fluoride (PVDF) membrane (Bio-Rad) at 80 V for two hours at 4°C. Amido-black staining was used to confirm equal protein loading in different lanes. Non-specific sites were blocked by incubating the membranes with 5% non-fat dried milk and 0.05% Tween-20 (Sigma-Adrich) in Tris-



buffered saline at 37°C for 45 min. The membrane was incubated with the anti-ApoC-III antibody (ab108205, Abcam) at the dilution 1:1000 in 1% non-fat dried milk, 0.05% Tween-20 in Tris-buffered saline for three hours at room temperature. The membrane was then incubated for 45 minutes at room temperature with the appropriate horseradish peroxidase (HRP)-conjugated secondary anti-rabbit antibody. The immunocomplexes were visualised by chemiluminescence using the Chemidoc MP imaging system (Bio-Rad).

### **2.3 Protein digestion for mass spectrometry analysis**

HepG2 cell lysis was performed by sonication, using an ultrasonic probe with an amplitude of 70% for few seconds. Cell debris was removed by centrifugation at 3000g for 10 minutes at 4°C. For each sample 10 µg of protein were taken for digestion. Tris-HCl-TFE buffer (25% trifluoroethanol, 25% H<sub>2</sub>O, 50% Tris-HCl 100 mM, pH 8.5) was added to dilute each sample at least 1:4. Reduction step was performed using 10 mM TCEP (tris(2-carboxyethyl)phosphine) pH 8.5. Chloroacetamide 40 mM pH 8.5 was used for alkylation. After 10 minutes at 95°C, by shaking it was diluted to 10% TFE with 50 mM ammonium bicarbonate. For protein digestion Trypsin was used. In particular, 1 µg of trypsin was added to 50 µg of total protein and the digestion was performed overnight at 37 °C. The peptides obtained were then diluted in solvent A (0,3% FA, 5% ACN) and stored at -20 °C until further LC-MS/MS analysis was performed.

### **2.4 LC-MS/MS targeted analysis of ApoC-III**

An aliquot of 500 ng of each sample was injected in a nano-HPLC (Dionex Ultimate 3000) equipped with a C18, 5 µm, 100 Å, 5 x 0.3 mm, enrichment column and an Acclaim PepMap RSLC nanocolumn (C18, 2 µm, 100 Å, 500 x 0.075 mm) (Thermo Fisher Scientific, Waltham, USA). Samples were concentrated on the enrichment column for six min at a flow rate of 5 µl/min with 0.1 % heptafluorobutyric acid as isocratic solvent. Separation was carried out on the nanocolumn at a flow rate of 300 nl/min at 60 °C using the following gradient, where

solvent A is 0.1 % formic acid in water and solvent B is acetonitrile containing 0.1 % formic acid: 0-6 min: 4 % B; 6-94 min: 4-25 % B; 94 -99 min: 25-95 % B, 99 – 109 min: 95 % B; 109.1-124 min: 4 % B; The maXis II<sup>TM</sup> ETD high-resolution LC-QTOF mass spectrometer (Bruker Daltonics , Bremen, Germany) was operated with the captive source in positive mode with the following settings: mass range: 200 - 2000 m/z, 2 Hz, capillary 1300V, dry gas flow 3 L/min with 150 °C, nanoBooster 0.2 bar, precursor acquisition control top17 (CID). For preferred fragmentation of ApoC-III peptides, previously measured peptide m/z were added to a preference mass list using a width of 0.02 m/z (R.GWVTDGFSSLK.D 2+, K.DALSSVQESQVAQQAR.G 2+/3+, K.DYWSTVK.D 2+, K.TAKDALSSVQESQVAQQAR.G 3+, R.GWVTDGFSSLKDYWSTVK.D 2+). The MS/MS data were analysed for protein identification and quantification using data analysis software (Bruker), Sum Peak algorithm, and by MaxQuant 1.5.3.30 (Cox et al., 2014) against the human public database SwissProt database with taxonomy homo sapiens (downloaded on 11.06.2015, 42150 sequences) and common contaminants. Carbamidomethylation on Cys was entered as fixed modification, oxidation on methionine as variable modification. Detailed search criteria were used as follows: trypsin, max. missed cleavage sites: 2; search mode: MS/MS ion search with decoy database search included; precursor mass tolerance +/- 0.006 Da; product mass tolerance +/- 40 ppm; acceptance parameters for identification: 1 % PSM FDR; 1 % protein FDR. In addition, a label free quantitation including the Match between runs feature of MaxQuant was performed (Cox et al., 2014) requiring a minimum of 1 ratio counts of quantified razor and unique peptides. Data processing was performed using Perseus software version 1.5.0.31. Contaminants and reverse protein sequences created during the database search were removed. For data analysis ApoC-III intensities were normalised on the intensities of all peptides identified in each samples and statistical analysis was performed by t-test comparison.

## **2.5 Real Time PCR analysis of ApoC-III**

mRNA isolation was carried out adding TRI<sup>®</sup> reagent (T9424, Sigma Aldrich) to cell pellets according to the producer's instructions. Total RNA amount was quantified by means of a QBit 3.0 fluorometer coupled with specific Qubit RNA BR or HS Assay Kit (Thermo Fisher Scientific). Before the reverse transcription step, the purity and integrity of the extracted RNA was checked loading 2 µg of RNA on 1.2% agarose gel. For the reverse transcription reaction, a total of 400 ng of mRNA for each sample were used and cDNA was synthesised using SuperScript<sup>™</sup> Vilo<sup>™</sup> cDNA Synthesis Kit (11754, Invitrogen). RT-PCR was performed using TaqMan<sup>®</sup> Universal Master Mix II (4440040, Applied Biosystems) and TaqMan<sup>®</sup> Gene expression assay for ApoC-III (Hs00163644\_m1, Applied Biosystems) according to the manufacturer's protocol, in a real time PCR system (ABI Prism 7500, Applied Biosystems, Carlsbad, CA, USA). Relative quantification of the expression levels of transcript in each sample was normalised on GAPDH mRNA level, using Human GAPDH endogenous control (4326317E, Applied Biosystems). For each treatment RT-PCR were run on three biological replicates and on each sample in duplicate. Comparisons of ApoC-III expression levels between treated and control samples were performed using Student T-test on ddCt values and fold changes were calculated using the 2<sup>(-ddCt)</sup> method for relative gene expression quantification (Schmittgen et al., 2008).

### 3. RESULTS

#### 3.1 Effect of myristic acid treatments on HepG2 cells viability and growth

After 24 hours of treatments with 0, 50, 125, 250 and 500  $\mu\text{M}$  C14:0, cells were taken for viability and growth assessment by means of CASY technology. As reported in Fig.2, cell viability, assessed based on measurement of cells membrane integrity, remained above 90% for each C14:0 treatment used, although slightly decreasing with higher C14:0 concentrations. Measure of cell numbers after 24 hours of incubation with different concentrations of C14:0 revealed a slight decrease in cell number, and therefore in cell growth, following increasing concentration of C14:0 (Fig.3).

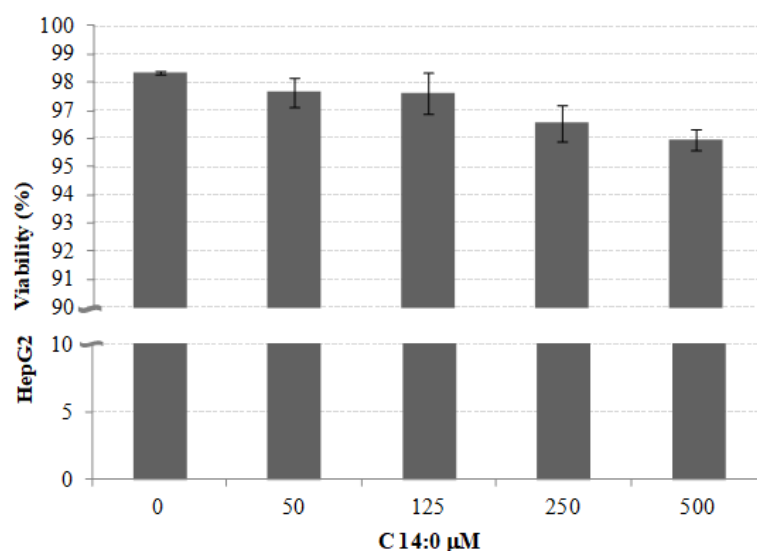


Fig.2 HepG2 viability, measured using CASY, after 24h treatment with different C14:0 concentrations.

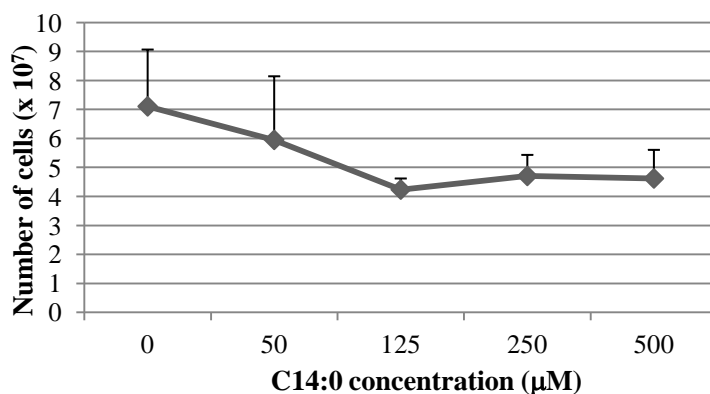
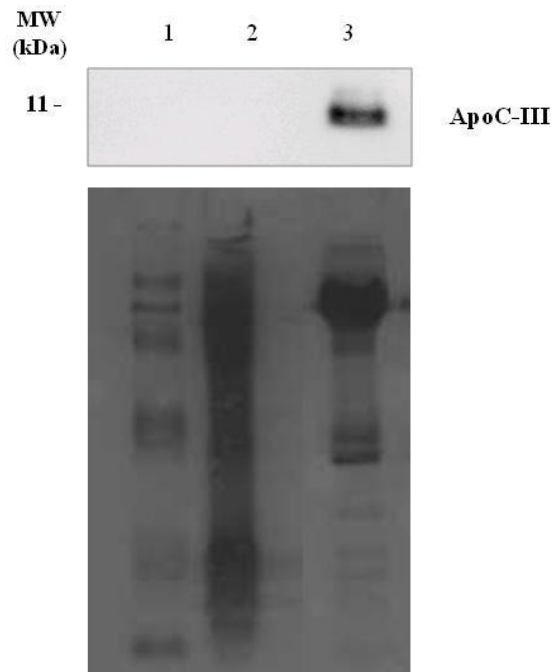


Fig.3 HepG2 numbers, estimated using CASY, after 24h treatment with different C14:0 concentrations.

### 3.2 Modulation of ApoC-III protein in HepG2 cells treated with myristic acid

Despite the efforts, Western blot analyses failed to detect the presence of ApoC-III in the whole cellular lysate of HepG2 cells treated with different concentrations of C14:0, even when a higher amount of total protein was loaded and antibodies dilution increased. As reported in Fig.4 it was impossible to detect the presence of ApoC-III in the lysate of 250  $\mu$ M C14:0 treated HepG2 cells (used as representative of all treatments), while ApoC-III was immunodetected in the sample of plasma used as positive control.



*Fig.4 Western Blot analysis of ApoC-III. Lane 1 from the left: marker. Lane 2: lysate of HepG2 cells treated with 250 $\mu$ M C14:0. Lane 3: plasma sample as positive control.*

To obtain information on ApoC-III protein, the analysis on HepG2 lysate proteins was performed using a maXis II<sup>TM</sup> ETD high-resolution LC-QTOF mass spectrometer (Bruker Daltonics), by performing a targeted analysis adding previously identified m/z values of ApoC-III in the preferred list for better and more precise identification. By using this technique, it was possible to reveal the presence of intracellular ApoC-III, even though present at very low

concentration in samples of HepG2 cell lysates (Fig.6). The identification was possible with just one peptide in each sample and in the 0 and 50  $\mu\text{M}$  C14:0 treated cells the identification of ApoC-III was possible in only one of the three biological replicates analysed. However, the data obtained highlighted a slight and gradual increase in ApoC-III protein content following increasing C14:0 treatment, which was of statistical significance at 125  $\mu\text{M}$  C14:0.

### **3.3 Modulation of ApoC-III mRNA in HepG2 cells treated with myristic acid**

To assess the possible influence of C14:0 on ApoC-III mRNA, the expression levels of ApoC-III were assessed by means of reverse transcription and Real Time PCR following 24-hour treatment of HepG2 cells with 0, 50, 125, 250, 500  $\mu\text{M}$  C14:0. Before proceeding with the reverse transcription of mRNA, the purity of total RNA extracted from HepG2 cell lysates was assessed by running 2  $\mu\text{g}$  on a 1.2% agarose gel. The integrity and purity of total RNA was confirmed as shown in Fig.5. Results of the expression analysis were normalized on the expression levels of GAPDH housekeeping gene and were expressed as ApoC-III fold change as reported in Fig.6 (dark grey bars). It is possible to observe a gradual and slight rise in ApoC-III fold change following the increasing concentration of C14:0. At 250  $\mu\text{M}$  C14:0 a statistically significant increase was observed ( $p=0.030$ ). Interestingly, the general trend in ApoC-III mRNA expression levels agreed with the trend observed for the protein levels detected by means of MS/MS analysis.

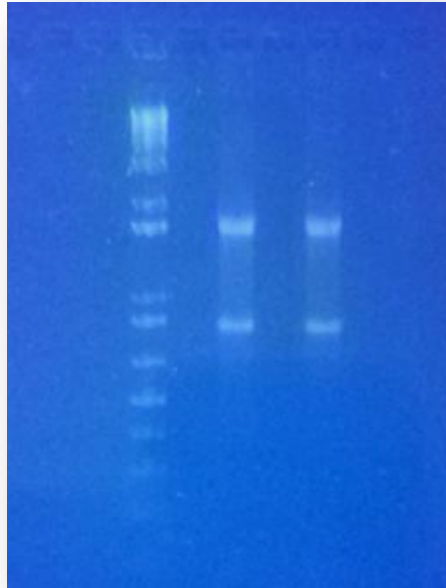


Fig.5 Control of RNA purity and integrity following total RNA extraction. The loading of two exemplifying RNA samples extracted from HepG2 cells is reported.

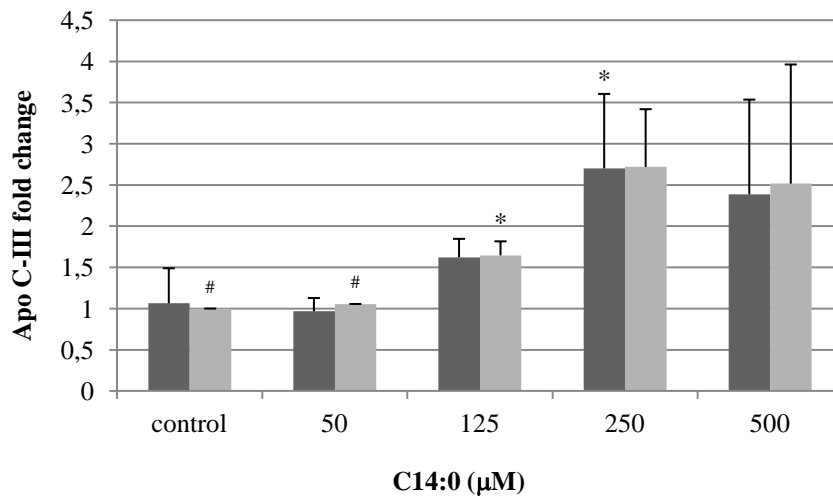


Fig.6 ApoC-III protein modulation in HepG2 treated cells measured by high-resolution MS (light grey) and ApoC-III mRNA modulation in the same samples, measured by RealTime PCR (dark grey). Data are represented as mean  $\pm$  SD. Three independent samples per each C14:0 treatment were used. Significant changes were determined by t-test. \*  $p < 0,05$  relative to the control group, # ApoC-III peptide identified in just one of the three biological replicates used.

## 4. DISCUSSION

The role of plasma FAs on cardiovascular risk factors and on cardiovascular risk itself has been widely studied in previous decades (Mensink et al., 2003; Michas et al., 2014). The ability of n-3 PUFAs of acting on ApoC-III and consequently on TG plasma levels, actually decreasing cardiovascular risk, is already known (De Caterina, 2011). However recent publications about well-known FAs have pointed out how these FAs may still have unknown important effects on cardiovascular parameters (Noto et al., 2016). This observation led to the development of the present project that, as shown in the first chapter, was initially aimed at revealing possible new links between lipid/apolipoprotein parameters and FAs plasma levels and as a consequence possible new FA-related cardiovascular risk mechanisms. Due to the important correlations involving C14:0 in the plasma of CAD and CAD-free subjects observed in the previous chapter of this thesis, in the present part of the project the possible influence of C14:0 on levels of ApoC-III was investigated in an *in vitro* cell model. The aim was to investigate the C14:0 influence on both ApoC-III protein and mRNA levels. To assess the influence on protein concentrations, intracellular ApoC-III protein levels were investigated at first by means of Western Blot analysis. However, as reported in Fig.4, this technique failed to detect ApoC-III in HpeG2 cell lysate, possibly because of the extremely low protein levels. A different approach was then selected, consisting of high-resolution mass spectrometry analysis with the m/z values of some previously identified ApoC-III peptides in the preferred list for a better identification of the protein. This approach is very similar to targeted mass spectrometry and succeeded in the identification of ApoC-III protein as shown in Fig.6. As a confirmation of the initial hypothesis, the concentration of this protein was gradually increased following C14:0 dosage, being particularly significant at 125  $\mu$ M. This observation supports the *in vivo* finding that C14:0 is the first predictor of both ApoC-III and TG plasma levels. However, some limitations in this study must be highlighted, including the identification of the protein with just



one peptide, when normally in mass spectrometry analysis at least two peptides are necessary for a proper protein identification (Kalli et al., 2012). Furthermore, ApoC-III was identified in just one of the three biological replicates for both controls and in the C14:0 50  $\mu$ M treated cells. However, the finding obtained by mass-spectrometry (MS) could be seen as a verification that, for those C14:0 concentrations (0 and 50  $\mu$ M), ApoC-III was present at lower concentrations, being therefore hardly detectable. On the other hand, in cells treated with the highest concentrations of C14:0 the identification of ApoC-III was possible in all the replicates, probably due to a strong C14:0 influence on ApoC-III protein levels. Finally, it should be noticed that the analysis was focused on the intracellular ApoC-III, while as described in the first chapter this is also a secreted protein. We decided as a first step to analyse the intracellular ApoC-III since it has been reported that that culture conditions have an influence on ApoC-III secretion by HepG2 cells which, differently to ApoC-III mRNA, is controlled by unknown serum factors (Clavey et al., 1999). Some FBS used for cell culture can impair ApoC-III secretion, but others cannot, and when changing the cell medium the secretion could not be restored. Importantly, this effect was also present if the experimental media - as in the present project - was without FBS, to avoid direct effect of serum on the secretion. Moreover, it was reported that in absence of FAs HepG2 cells secrete more LDL-like particle than normal hepatocytes that instead secrete buoyant VLDL particles (Ellsworth et al., 1986) and this feature could have led to questionable results and probably misinterpretations. For all these reasons the present part of the project was focused on the intracellular portion of ApoC-III.

To have more in-depth results concerning C14:0 influence on ApoC-III expression, its effects on the mRNA levels were investigated (Fig.6) confirming the hypothesis of a positive influence of this FA on Apo C-III expression at mRNA level. Despite its gradual and slight rise, the expression level of ApoC-III actually increased with high concentrations of C14:0 and the increase in the mRNA fold change was statistically significant at 250  $\mu$ M.

To date this is the first time that ApoC-III protein and mRNA expression have been assessed following C14:0 supplementation in a cell culture system. Taken together, these *in vitro* findings suggest a probable influence of C14:0 on ApoC-III expression levels and support the positive correlations observed *in vivo* in plasma of CAD and CAD free patients, where C14:0 resulted the first predictor of both ApoC-III and TG plasma levels. Further *in vitro* investigations would be necessary to clarify the exact mechanisms through which C14:0 can influence ApoC-III expression. The expression of this apolipoprotein is modulated by many transcription factors and it is negatively regulated by PPAR $\alpha$  (Ooi et al., 2008). Interestingly, in HepG2 cells C14:0 showed the ability to lower the activity of this transcription factor even though the effect was reduced in comparison with some other FA such as C16:0 (Popeijus et al., 2014). Moreover, ApoC-III is positively regulated by insulin levels (Ooi et al., 2008), and accordingly SFAs are strictly connected with the onset of insulin resistance (Kennedy et al., 2009; Sears et al., 2015). A possible major role of C14:0 on insulin resistance would need to be investigated in further *in vitro* experiments. An *in vivo* confirmation of a possible direct relationship between C14:0 consumption and TG plasma levels, as already done for n-3 PUFA (Tang et al., 2012), would also be needed. As hypertriglyceridemia is an important risk factor for CVD onset (Nordestgaard et al., 2014) and ApoC-III an important target to contrast this dangerous condition (Zheng, 2014; Khetarpal et al., 2016), the confirmation of a possible *in vivo* direct relationship between C14:0 consumption and TG plasma levels would represent an important landmark for proper and more complete cardiovascular prevention and treatment.

## **5. Concluding remarks**

Both the *in vivo* and *in vitro* data obtained demonstrated an important role of the SFA C14:0 in the regulation of plasma TG levels. The results obtained suggest that this relationship could be mediated by a possible influence of C14:0 on the TG plasma regulator ApoC-III. Further

studies in this direction could help the elucidation of the negative role of C14:0 on cardiovascular health, probably confirming the opposite effect that C14:0 may have on TG plasma levels when compared with the well-known effect of n-3 PUFAs.

## **SECTION 2**

## CHAPTER 1

### **PROTEOMICS AND FATTY ACIDS**

#### **1. Proteomics investigations of fatty acids effects**

Over last few years the role of FAs has been studied and today the important influence of FA intake on many chronic diseases, including also CVD, has been established. For this reason, the importance of detecting and identifying biomarkers that can predict FA influence on specific diseases has emerged. Modulations in the protein expressions as well as in their post-translational modifications in tissues and in biofluids (mainly plasma and urine) may highlight the real consequences of the intake of specific FAs, providing important information about their mechanisms of action. The disclosure of this information would be essential for proper prevention and precise treatment of many chronic diseases. Proteomic approaches today offer important opportunities to deepen our understanding of the mechanisms of action of different FAs and accordingly the number of proteomic investigations on FAs effect has increased over the last few years (de Roos et al., 2012). First studies in this direction took advantage of the use of the two-dimensional gel electrophoresis (2-DE) for the visualisation of differently modulated proteins after specific FAs treatments, followed by an identification step using MS instruments. They investigated the modulations in tissues or biofluid proteomes of human or animal models. For example, the role of long chain n-3 PUFA intake on the levels of serum proteins was evaluated in a double blind randomised trial on 81 healthy volunteers (de Roos et al., 2008). 2-DE followed by MS technique revealed that some proteins such as ApoA-I, serum amyloid P and antithrombin III- like protein were down-regulated in the serum of those subjects who had fish oil supplements, demonstrating that fish oil activated anti-inflammatory and lipid-related mechanisms. The effects of n-3 PUFA was studied also on tissues by Sidhu et al. who studied the proteomics modulation following Docosahexenoic acid (DHA) supplementation on mouse brain synaptic plasma membrane (Sidhu et al., 2011). The authors

of this research found that 18 proteins, important for synaptic physiology, were significantly downregulated, including CREB and caspase-3 related proteins, and they suggest that this mechanism could be relevant for a suboptimal brain function. Furthermore, many studies investigated the roles of other FAs, and in particular of cis-9 trans-11-conjugated linoleic acid (CLA). The results of these analyses are controversial compared to studies highlighting the improvement of systemic insulin sensitivity in obesity-induced diabetes and others reporting no plasma proteome changes (de Roos et al., 2011; Rungapamestry et al., 2012). The analysis of mouse colon tissue proteome was also performed to shed light on the effects of n-3 and n-6 PUFAs on bacterially induced intestinal inflammation. This study demonstrated the increase of proteins with anti-inflammatory activity following n-3 PUFA administrations and the modulation of proteins involved in cytoskeletal organisation and cellular stress after n-6 PUFA exposure (Cooney et al., 2012). Another study compared changes induced by the intake of different FA classes (SFA, MUFA and long-chain n-3PUFA) in the proteome of peripheral blood mononuclear cells (PBMC) of metabolic syndrome patients. Results of this study highlighted the increase in the expression of proteins related to oxidative stress, degradation of ubiquitinated proteins and DNA repair following SFA diet; these changes in the proteomic profile were associated with an increase in CVD risk factors (Rangel-Zuniga et al., 2015).

Many researches were also focused on proteome changes in different cell culture models induced by FA treatments. As high levels of FAs play a role in inducing loss of function in pancreatic beta-cells, the effects of C18:1 in combination with glucose were studied in INS-1E model cells (Maris et al., 2011). Results showed that the treatment with oleate down-regulates chaperones impairing insulin signaling and proteasome degradation and provided an important insight into the molecular mechanism through which oleate induces beta cells dysfunction. More recent studies substituted the use of 2-DE technique with LC-MS/MS methods, as in the case of Sargsyan et al., who in 2016 proceeded with the study of FA effects on beta cells

(Sargsyan et al., 2016). The results of their study showed that C18:1 plays a pro-survival role targeting ER stress proteins and protecting beta cells from the toxic effects of C16:0. This case highlighted how proteomics can provide a complete overview of molecular mechanisms involved in pathological conditions. FAs have not only an important role in insulin secretion at pancreatic level, but also play a fundamental role in insulin sensitivity in many part of the body, such as in muscles. Last year a study investigated the effects of C16:0 and C18:1 on mouse C2C12 myoblasts (Chen et al., 2016). C18:1 was shown to revert the toxic effects of C16:0 in this type of cells, lowering levels of Cox-2, previously found to be strongly up-regulated by C16:0. The overall positive effect of C18:1 therefore lies in the ability of relieving cellular stress and restoring insulin sensitivity. A very recent study instead investigated the role of Eicosapentaenoic acid (EPA), an n-3 PUFA, on the proteome of HUVEC cells stimulated with TNF $\alpha$  in order to simulate a model of endothelial activation (Zhang et al., 2017). Many enriched pathways were identified, such as glutathione metabolism, oxidation reduction, and DNA replication, giving important insights into the protective role of n-3 PUFA in the atherosclerotic process. All this research underlines how FAs have important effects on many different mechanisms taking place in different organs and how proteomics may represent a crucial technique for their detection.

During the last few years many proteomic studies have also aimed at investigating the effects of FA intake at hepatic level (Tab. I). The liver is involved in the absorption of chylomicrons lipids and in the simultaneous secretion of VLDL with their related apolipoproteins, representing an important hub in lipid metabolism and metabolic disorders - as described in detail in the first section. Furthermore, the understanding of the molecular changes in response to FA intake could help the treatment and prevention of Nonalcoholic fatty liver disease (NAFLD), the most common form of liver disease in the US (Charlton, 2004). This is a pathological condition where fat accumulates in the liver in patients with no history of

excessive alcohol consumption. NAFLD is characterised by a wide spectrum of liver diseases, ranging from simple steatosis to nonalcoholic steatohepatitis (NASH) which can eventually evolve into fibrosis and cirrhosis and liver cancer. The strong interplay between NAFLD and MetS has been described and both disorders can predict T2DM and CVD (Yki-Jarvinen, 2014). It has been demonstrated that NAFLD can be detected in a high percentage of patients with documented CAD (Baharvand-Ahmadi et al., 2016). Dietary FA composition seems to be involved in the pathogenesis of hepatic steatosis (Ferramosca et al., 2014), having a central role in fat accumulation, and for this reason many studies have focused on the study of FA effects on hepatic metabolism (Malhi et al., 2006; Ricchi et al., 2009; Mei et al., 2011; Hetherington et al., 2016). Because of their roles in lipid metabolism - and therefore on CVD -, and for their influence on NAFLD, the role of FAs on liver metabolism has also been analysed during the last few years with proteomic approaches. In some studies, high-fat diet mice were used as models of NASH, and their proteome changes were analysed in comparison to control groups. Results highlighted the activation of some pathways following high-fat diet, involving xenobiotic, lipid metabolism, inflammatory response and cell-cycle control (Kirpich et al., 2011). Moreover, the specific proteomic analysis of liver mitochondria from rats with NASH confirmed the involvement of lipid metabolism and cell cycle control pathways and highlighted some new pathways, for example FAs  $\beta$ -oxidation and cell polarity maintenance (Li et al., 2014). The proteomic effects of n-3 PUFA- rich diet was also investigated on mouse liver samples, to elucidate their beneficial health effects (Ahmed et al., 2014). Several novel proteins were found to be modulated by this treatment, such as regucalcin, an important protein involved in lipid metabolism. Other proteins were found to be deregulated, mainly involved in the regulation of lipid and carbohydrate metabolism, one carbon-metabolism, citric cycle and protein synthesis. The strength of this research lies in the use of a proteomic approach, which highlighted both specific proteins involved in the beneficial effects of n-3 PUFA and general pathways. The anti-inflammatory properties of n-3 PUFA were confirmed at molecular levels



in another proteomic investigation on ApoE-knockdown mice (Huang et al., 2015). They demonstrated that n-3 PUFA are involved in many steps of the hepatic metabolism and they also verified the exact anti-inflammatory molecular mechanism in HepG2 cells, reporting that n-3 PUFA can actually inhibit nuclear factor- $\kappa$ B (NF- $\kappa$ B) activation. HepG2 represent an important cellular model for the study of liver metabolism; due to the scarce availability of human hepatocytes for research purposes, they are generally used (Ramboer et al., 2015). Even though some limitations when using this type of cells should be borne in mind, as there are also some differences in comparison with hepatocytes from a proteomic point of view (Wisniewski et al., 2016), HepG2 showed more proteomic features characteristic of hepatocytes than other hepatoma cell lines (Slany et al., 2010). Over the last few years HepG2 cells have been used as a model to investigate the proteomic hepatic response to elaidic acid, in combination with lipidomic and transcriptomic approaches (Vendel Nielsen et al., 2013). HepG2 were also used as cellular model in a subsequent study on the effects of TFA (Krogager et al., 2015). The effects of elaidic and trans-vaccenic acids were compared at proteomic levels. A notable adverse effect of elaidic acid was demonstrated, as only this FA induced an increase in proteins involved in cholesterol synthesis and transport.

All these findings emphasise the importance and opportunities offered by proteomics in the study of metabolism disorders and especially in FA effects. Furthermore, recent studies aimed at investigating molecular mechanisms related to lipid metabolism and NAFLD introduced the use of HepG2 cells as a model for the investigation of FA response from a proteomic point of view. However, to date only the proteomic effects of some specific FAs – but not of C14:0 - have been analysed and more investigations in this direction are necessary.

Fatty acid supplementation/ Diet	Sample analysed	Proteomic approach	Reference
High-fat diet	Mice liver	2D-DIGE MALDI-TOF/MS-MS	<i>Kirpich, 2011</i>
High-fat diet	Mice liver mitochondria	2DE MALDI-TOF/MS-MS	<i>Li, 2014</i>
Diets high or low in <i>n</i> -3 PUFA	C57BL/6 mice liver	2D-PAGE MALFI TOF MS	<i>Ahmed, 2014</i>
PUFA	ApoE-knockout mice liver HepG2 cells	2DE Ion trap LC/MS	<i>Huang, 2015</i>
Elaidic acid	HepG2	SILAC DIGE	<i>Vendel Nielsen, 2013</i>
Elaidic acid <i>and</i> <i>trans</i> -vaccenic acid	HepG2	SILAC TRIPLE-TOF MS	<i>Krogager, 2015</i>

Tab. I Most recent proteomic research analysing the influence of fatty acids and fats on liver metabolism.

## 2. *In-vitro* studies on myristic acid

Myristic acid (C14:0) is a saturated FA, present in many oils and particularly dairy fats. The *in vivo* effects of this FA have been studied over the years in population-based studies, as described in detail in the first section of the present thesis. However, *in vitro* investigations were performed - mainly on hepatoma cell lines - to elucidate C14:0 molecular mechanisms and interactions. Some studies aimed at investigating its possible influence on lipid metabolism showed that incubation of McA-RH7777 cells with C14:0 caused the secretion of dense ApoB containing lipoproteins (Kummrow et al., 2002). A reduction in ApoB degradation was also reported, together with an increase in its secretion (Arrol et al., 2000; Kummrow et al., 2002). Subsequent research in this direction recently confirmed the increase in VLDL after C14:0 treatment in primary hepatocytes (Tiwari et al., 2016). Moreover, it was reported that C14:0 enhances VLDL transport vesicle budding and the recruitment of their main protein small valosin-containing protein-interacting protein (SVIP) to the ER. An increased secretion

of ApoB in presence of C14:0 was also observed both in HepG2 and McA-RH7777, together with a decrease in ApoB degradation in the latter cells (Arrol et al., 2000; Kummrow et al., 2002). Furthermore, like other FAs, C14:0 showed an influence on ApoA-I by decreasing Sp1 binding to APOA-1 promoter and therefore its synthesis (Haas et al., 2004). This apolipoprotein is among the main proteins of HDL, as described in the first section. HDL metabolism seems to be influenced by C14:0 administration. Recently it has been reported that C14:0 increases HDL binding to HepG2 cells by a nonsaturable pathway suggesting a possible explanation for the association with decreased HDL levels found in plasma of the Mediterranean population (Noto et al., 2016). Moreover, the expression of ApoA-I - as for other apolipoproteins, such as ApoC-III - is controlled by Peroxisome Proliferator Activated Receptors, principally the PPAR $\alpha$  form (Duval et al., 2007; Ooi et al., 2008). Like other SFAs, C14:0 showed the ability to decrease the activity of this ligand-activated receptor when supplied in a concentration greater than 10  $\mu$ M in HepG2 culture media (Popeijus et al., 2014). C14:0 seems to have a role not only in molecular mechanisms underlying lipid metabolism but also in the insulin pathway. Human G protein-coupled receptor 40 (hGPR40), also known as free fatty acid receptor 1, is an important player in the glucose-dependent insulin secretion in pancreatic  $\beta$ -cells and a recent study investigated its binding affinity for 18 FAs (Ren et al., 2016). FAs with carbon chain longer than C14:0 had molecular size too large for entering the receptor binding pocket, while among shorter FAs C14:0 showed the highest affinity for the receptor, suggesting a potential important involvement in insulin secretion. Moreover, C14:0 seems to play an important role in the skeletal muscle, the major insulin-target organ involved in glucose uptake. In mouse C2C12 myotubes C14:0 was seen to increase by 1.4 fold the insulin-dependent glucose uptake, increasing the expression of diacylglycerol kinase (DGK)  $\delta$  (Wada et al., 2016). This evidence suggested an important aspect of C14:0 that would therefore protect and improve glucose homeostasis in T2DM.

Besides being one of their target molecule, C14:0 has an important influence on desaturases activities (Rioux et al., 2011). In 2004 an increase in  $\Delta 6$ -desaturase activity in a dose dependent manner when cultured rat hepatocytes were incubated with C14:0 was reported (Jan et al., 2004). This evidence highlighted the important role of this FA in the regulation of PUFA bioavailability. Some years later the Rioux research group found that the activity of Sphingolipid  $\Delta 4$  desaturase 1 (DES1) was increased in presence of increasing concentrations of C14:0 in COS-7 cells (Beauchamp et al., 2007). As DES-1 is an enzyme involved in the catalysis of the last step of the de novo ceramide biosynthesis, through the introduction of a trans  $\Delta 4$ -double bond in the carbon chain of the dihydroceramide, this evidence suggested an important role of C14:0 in the biosynthesis of ceramide and in sphingolipid metabolism. Some years later, they demonstrated that the treatment with C14:0 targeted DES1, initially present in the ER, to the mitochondrial membrane, causing an increase in ceramide levels and apoptotic consequences (Beauchamp et al., 2009). Later on, the increase in DES1 activity and the consequent increase in the number of apoptotic cells were confirmed in culture rat hepatocytes (Ezanno et al., 2012). A further study reported that C14:0 is not lipotoxic to primary mouse hepatocytes but can potentiate C16:0-mediated apoptosis, ER stress, cytochrome c release and caspase-3 activation (Martinez et al., 2015). These findings were confirmed *in vivo* in mice fed with a combination of palmitic and C14:0, exhibiting a wide range of effects, including lipodystrophy, hepatosplenomegaly, increased liver ceramide content and cholesterol levels, ER stress, liver damage, inflammation and fibrosis.

The effects of C14:0 on DES1 are due to the N-myristoylation of the enzyme (Rioux et al., 2011). Through the irreversible covalent linkage to the N-terminal glycine of many eukaryotic and viral proteins - called myristoylation - C14:0 can regulate many protein features, including protein subcellular localisation, protein-protein interaction and protein-membrane interactions (Martin et al., 2011). As C14:0 is hydrophobic by nature, myristoylated proteins are targeted to hydrophobic regions, such as lipid rafts, plasma membrane, Golgi, ER, nuclear membrane and

mitochondria. Due to the specific localisation of these proteins, C14:0 can regulate different cellular functions. While in the beginning this modification was described as a co-translational reaction, it was further observed as a post-translational event in apoptotic cells. N-myristoyltransferase (NMT) is the enzyme that catalyses the irreversible attachment of C14:0 to an N-terminal - or internal when the myristoylation occurs post-translationally - glycine of the target protein; in some rare cases the attachment can also occur in correspondence with an internal lysine by means of an amide bond. NMT inhibition causes loss of N-myristoylation and cytotoxicity in cancer cells and a recent proteomic study revealed that this inhibition has important consequences in HeLa cells, such as ER stress, cell cycle arrest and apoptosis (Thinon et al., 2016). Another previous proteomic study showed, by means of a chemistry-based approach, more than 100 protein myristoylated in HeLa cells during normal growth and apoptosis (Thinon et al., 2014). Among those proteins they found nucleolar proteins that mediate nuclear process, component of the ubiquitination machinery, proteins involved in cell cycle regulation, in microtubule dynamics and in many other cell functions. Studies specifically aimed at identifying the N-terminally myristoylated protein in the liver used cultured rat hepatocytes as a model and found both signal transduction proteins, such as the  $\alpha$  subunit of the heterotrimeric G protein, and also cytoskeleton proteins, such as actin and cytokeratin (Rioux et al., 2002). Recent research has highlighted the role of myristoylation in carcinogenesis and in immune functions, due to its ability to modulate immune cell signaling cascade (Udenwobele et al., 2017). However, even though this modification has many cellular consequences, it should be noted that only 0.05% of the radiolabeled C14:0 added in cell culture media is used for N-myristoylation (Martin et al., 2011).

In conclusion, even though many studies investigated the effects of C14:0 on different cellular pathways, data are to date fragmentary and a complete overview of its biochemical effects does not exist. As mentioned above, proteomics techniques represent an efficient tool to study the effects of FAs at molecular level from a global point of view. Therefore, the use of these

techniques would be essential for the study of overall C14:0 effects, particularly on liver cells where this FA may mediate pathological conditions such as cardiovascular disease, following perturbation of lipid metabolism, and NAFLD.

## **CHAPTER 2**

### ***IN VITRO* PROTEOMIC ANALYSIS OF HEPG2 CELLS TREATED WITH MYRISTIC ACID**

#### **1. INTRODUCTION**

As mentioned in Chapter 1 a general and complete overview of the proteomic effects of C14:0 on liver cells does not exist.

*In vivo* studies described C14:0 as an independent predictor of the liver pathology NASH (Tomita et al., 2011). Moreover, in the first section of the present thesis, evidence supporting its involvement in the regulation of ApoC-III and plasma TG levels -and therefore in cardiovascular health- have been reported. This suggests that the influence of this FA on lipid metabolism to date is still only partially disclosed. For this reason, a more in-depth investigation of C14:0 effects, in particular at liver level, is required to elucidate the association of this FA with NASH and cardiovascular disease.

The proteome, as well as the secretome, of C14:0-treated HepG2 cells have been investigated, with the aim of disclosing the overall proteomic and biochemical effects linking this unhealthy FA with pathological conditions. This type of investigation could contribute to a better understanding of the molecular mechanisms behind clinical findings related to the plasmatic C14:0 levels and its adverse health effects.

## 2. EXPERIMENTAL DESIGN AND PROCEDURES

*This experimental part, and in particular the MS analysis, was performed thanks to the kind collaboration with Prof. Ruth Birner-Gruenberger and her group, Medical University of Graz, Austria.*

### 2.1 Cell culture and treatment with myristic acid

HepG2 cells were cultured in RPMI 1640 media (Sigma-Aldrich), supplemented with 10% FBS, 100 U/ml penicillin and 100 µg/ml streptomycin, 4 mM L-glutamine and were maintained in a humidified incubator at 37°C in an atmosphere of 5% CO<sub>2</sub>. The FBS was removed from the HepG2 culture media six hours before C14:0 treatments. C14:0 was complexed to Bovine Serum Albumin (Fatty Acid Free BSA, Sigma-Aldrich) by mixing a solution 10 mM C14:0 (previously dissolved in NaOH 0.1M at 55°C) with a solution of 10% BSA and stirring one hour at 37°C, as previously described (Noto et al., 2016). A lipid solution was obtained and was then filtered with 0.22 µm filters. The C14:0-BSA solution obtained was added to cell culture FBS-free media at the following concentrations: 50, 125, 250 µM and 500 µM. 10% BSA was added to controls. C14:0-BSA incubation was performed for 24 hours. To ensure no interference of the BSA at proteomic analysis level, for the secretome analysis C14:0 was dissolved in dimethyl sulfoxide (DMSO), as previously described (Popeijus et al., 2014). The C14:0 dissolved in DMSO was added to cell culture FBS-free media at 50, 125, 250 µM while to obtain controls only DMSO was added to the medium. Notably, the same quantity of DMSO (0.5%) was used for all treatments, in order to exclude possible DMSO effects. For this analysis the incubation was also performed for 24 hours. Three biological replicates for each C14:0 concentration were used both for the proteome and secretome analyses. Immediately after the incubation the cells were washed twice with PBS, and the viability was checked by analysing three times an aliquot of cells with CASY Cell Counter and Analyzer. Then the cells were subjected to the experimental workflow indicated in Fig.1. The viability measurement of this instrument is based on the electrical current exclusion, since the status and the integrity of the



cell membrane distinctively affects the electrical signal generated. The percentage of cell viability was expressed as the ratio of total viable cells to the sum of total cells.

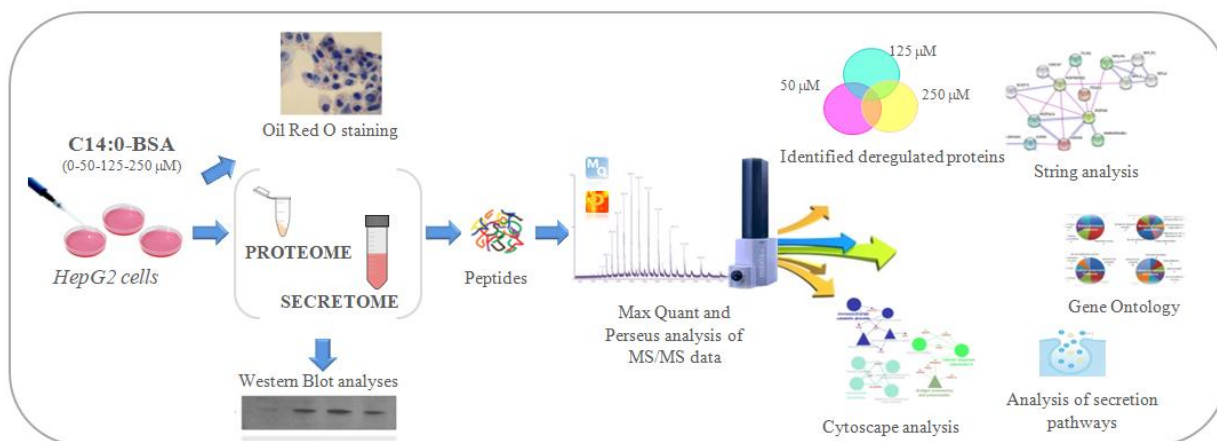


Fig.1 Experimental Workflow

## 2.2 Oil Red O staining

HepG2 cells were grown on a cover slip inside a 6-well plate. Cells were incubated with C14:0-BSA at the concentrations mentioned above for 24 hours, washed with phosphate-buffered saline (PBS) and then fixed with 4% formaldehyde solution for five min at room temperature. After fixation, cells were washed gently with 60% isopropanol and stained with the working solution of 0.6 % Oil Red O in 60% isopropanol for 15 min. The HepG2 stained cells were washed with distilled water several times to remove unincorporated dye. Then, the samples were stained with hematoxylin for 4 min for nuclei visualisation. Slides were examined using a light microscope with 100X magnification.

## 2.3 Proteome and Secretome sample Preparation

C14:0 treated cells were harvested using trypsin and centrifuged at 3000g for 10 min at 4°C to discard RPMI media. After two washes with cold PBS, cells were lysed in PBS by sonication, using an ultrasonic probe with an amplitude of 70% for few seconds. Cell debris was removed

with centrifugation at 3000g for 10 minutes at 4°C. For secretome preparation, the HepG2 cell media containing secreted proteins were collected by centrifugation at 5,000g for 10 min to pellet floating cells. Proteins in the media were concentrated using Amicon Ultra-4 filters 3K (Merk Millipore, Darmstadt, Germany) to reduce sample volume. Protein concentrations were determined using Bradford Protein assay (Bio-Rad). 10 µg of protein were taken from each sample for protein digestion, as described in Paragraph 2.3, Chapter 3 of Section 1. Tris-HCl-TFE buffer (25% trifluoroethanol, 25% H<sub>2</sub>O, 50% Tris-HCl 100 mM) was added to dilute each sample at least 1:4. Reduction step was performed using TCEP, (tris(2-carboxyethyl)phosphine), 10 mM final concentration. CAA (chloroacetamide) 40 mM was used for alkylation. Samples were shaken 10 minutes at 95° and diluted to 10% TFE with 50 mM ammonium bicarbonate. Proteins digestion was performed by adding 1µg/µL of trypsin to every 50 µg of proteins and an overnight incubation at 37 °C was performed. Obtained peptides were then diluted in solvent A (0.3% FA, 5% ACN) and stored at -20 °C until further LC-MS/MS analysis.

#### **2.4 LC-MS/MS and data analysis**

Label free mass spectrometry analysis and protein identification were performed as described in Chapter 2 Section 1. An aliquot of 500 ng of each sample was injected in a nano-HPLC (Dionex Ultimate 3000) equipped with a C18, 5 µm, 100 Å, 5 x 0.3 mm, enrichment column and an Acclaim PepMap RSLC nanocolumn (C18, 2 µm, 100 Å, 500 x 0.075 mm) (Thermo Fisher Scientific, Waltham, USA). Separation was carried out on the nanocolumn at a flow rate of 300 nl/min at 60 °C using an acetonitrile and formic acid gradient. The maXis II<sup>TM</sup> ETD high-resolution LC-QTOF mass spectrometer (Bruker Daltonics, Bremen, Germany) was operated with the captive source in positive mode.

The MS/MS data were analysed for protein identification and quantification using Data analysis software (Bruker), Sum Peak algorithm, and by MaxQuant 1.5.3.30 against the human public database SwissProt database with taxonomy homo sapiens (downloaded on 11.06.2015, 42150 sequences) and common contaminants. Carbamidomethylation on Cys was entered as fixed modification, oxidation on methionine as variable modification. In addition, a label free quantification including the match between runs of MaxQuant was performed (Cox et al., 2014) requiring a minimum of two ratio counts of quantified razor and unique peptides. Data processing was performed using Perseus software version 1.5.0.31. Contaminants and reverse protein sequences created during database search were removed. LFQ intensities were  $\log_2$  transformed to lower the effect of the outlier values. Filtering for three valid values in at least one condition - C14:0 concentration - was used for both proteome and secretome analysis. For protein groups missing LFQ values, this value was obtained by means of an imputation step in which the values were replaced with random values taken from the Gaussian distribution of values, to simulate an LFQ value for those low abundant protein groups. Perseus default parameters (width of 0.3 and downshift of 1.8 separately for each column) were maintained during this passage. For each protein group log differences were calculated as the difference between the averages of  $\log_2$  LFQ intensities of the treated samples and the average of  $\log_2$  LFQ intensities of the controls. R software (RCoreTeam, 2015) was employed for statistical analysis. ANOVA with subsequent multiple testing correction with Benjamini-Hochberg method was used to identify altered protein groups (Benjamini et al., 1995). Tukey's Honest Significant Differences test on protein groups significant after the ANOVA was used for the comparison of protein groups among different samples. Only proteins with p-value  $< 0.05$  and fold change  $\geq 1.3$  in both directions were considered significantly modulated.

## **2.5 Protein annotation, secretion prediction, protein networks and pathways analysis**

The analysis of identified proteins was performed according to Gene Ontology (GO) using the DAVID v6.8 Functional Annotation Bioinformatics Tools (<https://david.ncifcrf.gov/>) (Huang et al., 2009). Using this tool, the enrichment analysis for GO cellular component, biological process and molecular function was performed by comparing the GO terms of identified proteins against the rest of the genome. This analysis revealed the over-represented GO terms ( $p < 0.05$ ) in the submitted dataset.

In order to investigate the secretion mechanisms of the proteins found to be modulated in the secretome of C14:0-treated HepG2 cells, the potential secretion pathways were predicted by using the SecretomeP v2.0 server (Bendtsen et al., 2004) (<http://www.cbs.dtu.dk/services/SecretomeP/>). This tool predicted classically and non-classically secreted proteins. For those proteins predicted to be secreted by non-classical secretion pathways, the potential exosomal and microvesicle release was investigated by annotation on the ExoCarta database (Mathivanan et al., 2009) (<http://exocarta.ludwig.edu.au/>). To investigate possible interaction networks between the proteins modulated by C14:0, the STRING database v10.5 (<http://string-db.org>) (Snel et al., 2000) was used. The network was built using associations with a medium score ( $\geq 0.4$ ) based exclusively on experimental and database knowledge while excluding all other prediction methods implemented in STRING (such as text-mining and co-expression). Additional white nodes and network depth were kept to the minimum value (5 and 1 respectively), to exclude as many false positive interactions as possible.

In addition, ClueGO v2.3.3 (Bindea et al., 2009), a Cytoscape v3.5.1 plug-in, was used for analysing significantly enriched GO biological process and KEGG pathways ( $p$ -value  $< 0.05$ ) by using the human genome as background. In ClueGO settings the kappa score level was set to 0.4 and the GO Tree Levels ranged from levels 3–8.

## 2.6 Western Blot analysis of selected proteins

To confirm the protein trend detected by MS/MS and deepen the effect of C14:0 on ER stress, western blot analyses were performed. Samples from two different biological replicates were diluted 1:1 with Laemmli's sample buffer (62.5 mM Tris-HCl, pH 6.8, 25% glycerol, 2% SDS, 0.01% Bromophenol Blue), kept at 95°C for seven minutes and separated by SDS/polyacrylamide gel electrophoresis on 12% T acrylamide gels in Tris/glycine/SDS buffer. Proteins were then electroblotted onto polyvinylidene fluoride membranes (Bio-Rad) at 80 V for two hours at 4°C. Amido black staining was used to confirm equal protein loading in different lanes. Non-specific sites were blocked by incubating the membranes with 5% non-fat dried milk and 0.05% Tween-20 (Sigma Adrich) in Tris-buffered saline at 37°C for 45 min. Membranes were incubated with the different primary antibodies at the appropriate dilutions (as reported in Tab. I) in 1% non-fat dried milk, 0.05% Tween-20 in Tris-buffered saline.

Antibody	Gene Name	Source	Supplier	Dilution
<b>Perilipin 2</b>	PLIN2	mouse	Santa Cruz Biotechnology (sc-377429)	1:100
<b>Vesicle associated membrane protein associated protein B/C</b>	VAPB	mouse	Santa Cruz Biotechnology (sc-293364)	1:100
<b>Eukaryotic peptide chain release factor GTP-binding subunit ERF3A</b>	GSPT1	mouse	Santa Cruz Biotechnology (sc-515615)	1:1000
<b>β-Actin</b>	ACTB	mouse	Sigma A2228	1:3000
<b>Fatty Acids Synthase</b>	FASN	mouse	Santa Cruz Biotechnology (sc-55580)	1:1000
<b>Heterogeneous nuclear ribonucleoprotein A2/B1</b>	HNRNPA2B1	mouse	Santa Cruz Biotechnology (sc-374053)	1:1000
<b>Heat shock cognate 71 KDa protein</b>	HSPA8	mouse	Santa Cruz Biotechnology (sc-7298)	1:1000
<b>Complement C4</b>	C4A/B	mouse	Santa Cruz Biotechnology (sc-271181)	1:100
<b>Retinol Binding Protein 4</b>	RBP4	mouse	Santa Cruz Biotechnology (sc-48384)	1:100

<b>Cyclic AMP-dependent transcription factor ATF-6 alpha</b>	ATF-6 $\alpha$	mouse	Santa Cruz Biotechnology (sc-166659)	1:100
<b>Serine/threonine-protein kinase/endoribonuclease IRE1<math>\alpha</math></b>	ERN1	mouse	Santa Cruz Biotechnology (sc-390960)	1:100
<b>Eukaryotic translation initiation factor 2-alpha kinase 3 PERK</b>	EIF2AK3	mouse	Santa Cruz Biotechnology (sc-377400)	1:100

*Tab. 1 Primary antibodies used for Western Blot analysis.*

The incubation lasted for three hours at room temperature, except for Vesicle associated membrane protein associated protein B/C (VAPB) for which an overnight incubation was used. Blots were then incubated for 45 minutes at room temperature with horseradish peroxidase (HRP)-conjugated secondary antibody (Santa Cruz Biotechnology, sc-2005, diluted 1:5000). The immunocomplexes were visualised by chemiluminescence using the Chemidoc™ MP Imaging System (Bio-Rad, Hercules, USA).

### 3. RESULTS

#### 3.1 Effects of myristic acid on HepG2 viability and on lipid droplets accumulation

The effects of different concentrations of C14:0 (50-125-250-500  $\mu\text{M}$ ) on HepG2 cell viability were determined after 24 hours' incubation by means of CASY technology, based on cell membrane integrity assessment (Section1, Chapter 3, Fig.2). Cell viability remained above 90% after 24 hours' incubation with each C14:0 treatment used. The effect on cell viability of different dosages of C14:0 when dissolved in DMSO - used for secretome analysis - was also assessed (Fig.2). The results obtained indicated that C14:0 showed no toxicity to HepG2 cells. Nevertheless, at 500  $\mu\text{M}$  C14:0-BSA there was a slight (although statistically not significant) decrease of cell viability. For this reason, samples treated with C14:0 500  $\mu\text{M}$  were excluded from subsequent analyses.

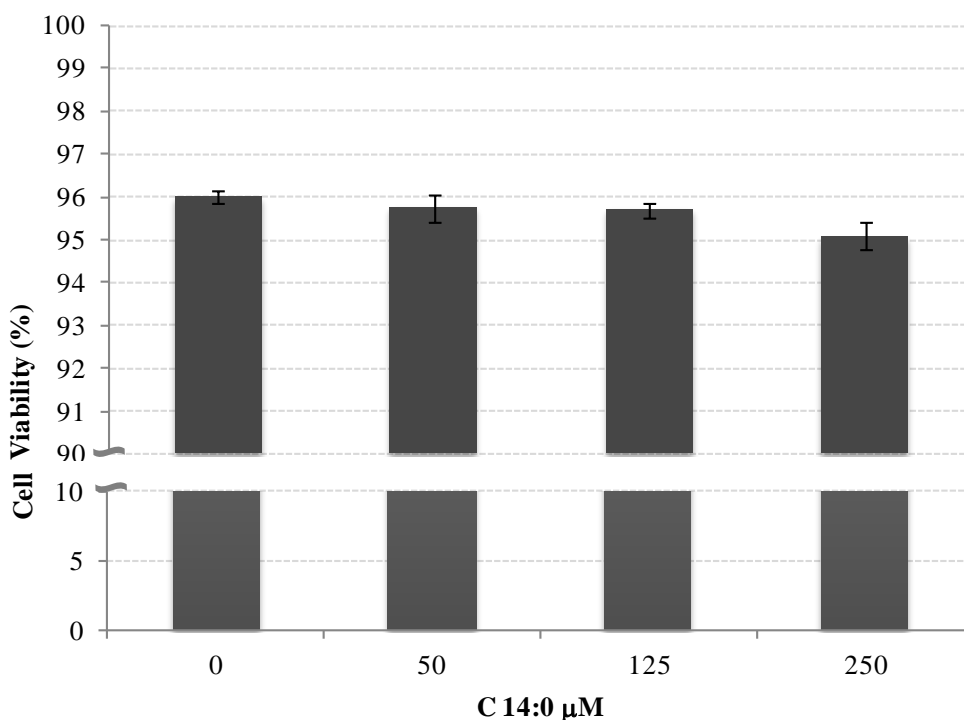
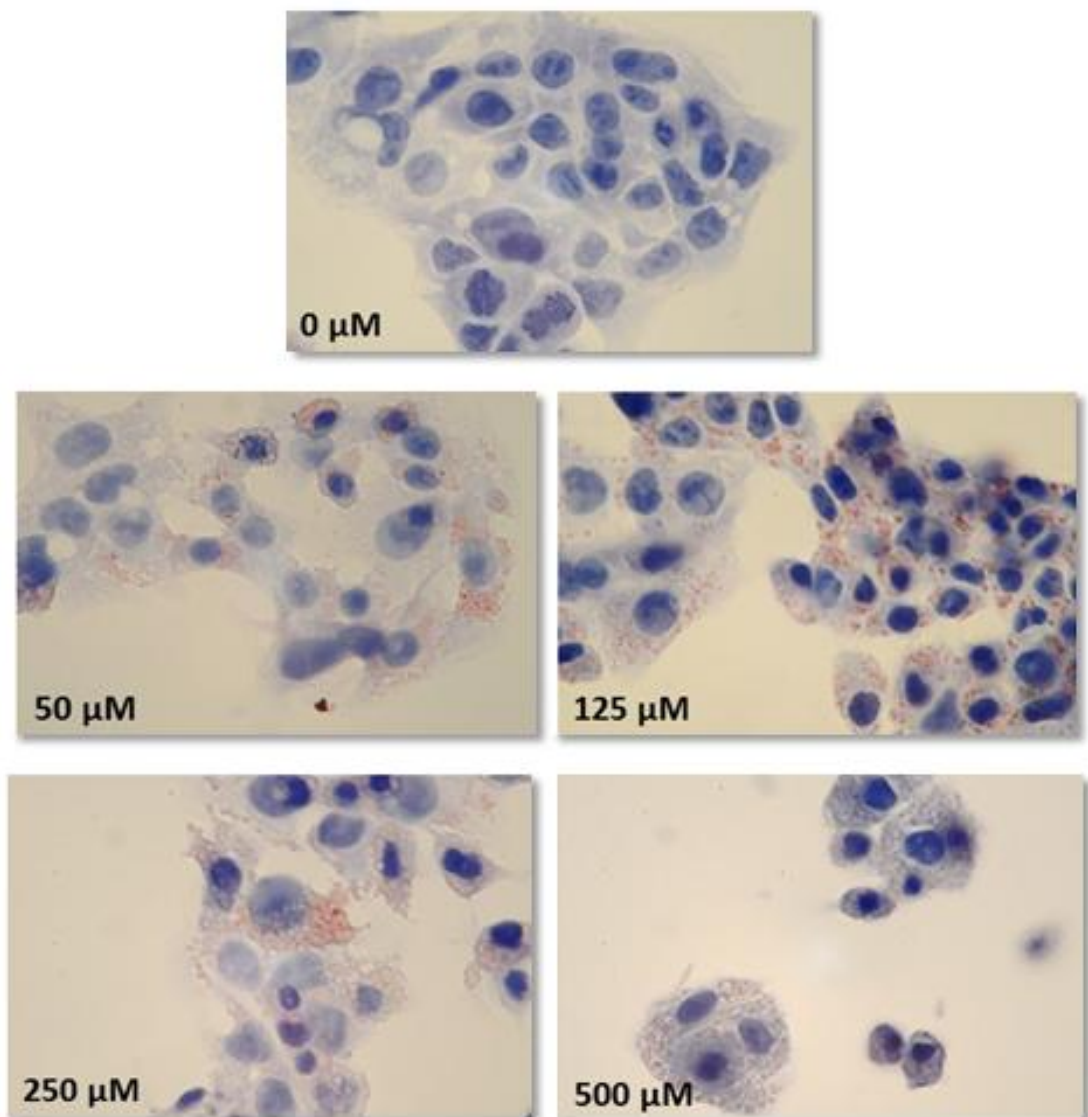


Fig.2 HepG2 cell viability, measured by using CASY technology, after 24h treatment with different concentration of C14:0 (0, 125, 250  $\mu\text{M}$ ) dissolved in DMSO. All experiments were repeated in triplicate.

The evaluation of C14:0 effect on HepG2 cells was also performed by analyzing the lipid droplet (LD) accumulation. Cells were stained with Oil Red O solution (pink dye) for intracellular neutral lipid and hematoxylin (blue) for nuclei visualisation and were observed by microscopy at 100X magnification (Fig.3). While there were no visible lipid droplets in the untreated control cells, C14:0 treatment for 24 hours induced the accumulation of lipid droplets in HepG2 cells even at the lowest concentration (50  $\mu\text{M}$ ). Lipid droplets were particularly evident and distinct at 125  $\mu\text{M}$ .



*Fig.3 Intracellular lipid droplets in HepG2 cells stained with Oil Red O. No lipid droplets were observed in HepG2 cells in the control group (upper image), while they were present in HepG2 cells*



*after myristic acid treatments (50, 125, 250 and 500  $\mu$ M). Cells were observed under 100X magnification.*

### **3.2 Quantitative analysis of proteins deregulated by myristic acid in HepG2 proteome and secretome.**

To elucidate the effects of C14:0 treatments (50, 125 and 250  $\mu$ M for 24h) on HepG2 cells proteome and secretome, separated proteomics investigations were performed on cell lysates and secreted proteins in culture media respectively. Protein expression in biological triplicates from C14:0-treated and untreated cells was compared. For each sample equal amounts of digested protein were subjected to MS/MS analysis. Output data were analysed by MaxQuant software package employing label-free quantification (LFQ) of areas of extracted ion chromatograms of peptides from MS1 spectra to compare relative abundances of proteins between groups. Proteins with a minimum fold-change of 1.3 and an ANOVA p-value < 0.05 in the post hoc test were considered deregulated.

As concerns the proteome analysis, a total of 1,937 proteins with at least 99% confidence (FDR < 1%) were identified. After filtering for contaminants, for sequences read in the reverse direction and finally for proteins identified in all three biological replicates in at least one condition – C14:0 concentration -, a total of 1,362 proteins were found. Among these 47 intracellular proteins showed fold change greater or equal of  $\pm$  1.3 when compared to controls and concurrent significantly altered levels of expression following ANOVA and Tukey's comparison post hoc test (p < 0.05). Control versus 50  $\mu$ M C14:0 analysis revealed 12 up and two down-regulated, control versus 125  $\mu$ M C14:0 26 up and five down-regulated, and control versus 250  $\mu$ M C14:0 30 up and eight down-regulated proteins (Tab. IIa and b). The most modulated intracellular protein (Eukaryotic peptide chain release factor GTP-binding subunit ERF3A) was five times induced in all C14:0 treated cells compared to the controls, as well as the most down-regulated intracellular protein (Protein-L-isoaspartate(D-aspartate) O-methyltransferase).

Majority Protein ID	Protein name	Gene name	ANOVA	Fold change 0-50	p adj 0-50	Fold change 0-125	p adj 0-125	Fold change 0-250	p adj 0-250
P15170	Eukaryotic peptide chain release factor GTP-binding subunit ERF3A	GSPT1	0.0121	<b>5.48</b>	<b>0.000</b>	<b>5.83</b>	<b>0.000</b>	<b>5.33</b>	<b>0.000</b>
Q9P035	Very-long-chain (3R)-3-hydroxyacyl-CoA dehydratase 3	HACD3	0.029	<b>3.04</b>	<b>0.025</b>	<b>5.08</b>	<b>0.003</b>	<b>4.95</b>	<b>0.003</b>
O95292	Vesicle-associated membrane protein-associated protein B/C	VAPB	0.0005	<b>3.58</b>	<b>0.000</b>	<b>4.03</b>	<b>0.000</b>	<b>4.07</b>	<b>0.000</b>
O75356	Ectonucleoside triphosphate diphosphohydrolase 5	ENTPD5	0.0171	<b>2.71</b>	<b>0.002</b>	<b>3.30</b>	<b>0.000</b>	<b>3.04</b>	<b>0.001</b>
P0COL5	Complement C4-B	C4B	0.0171	<b>2.61</b>	<b>0.001</b>	<b>2.97</b>	<b>0.001</b>	<b>2.97</b>	<b>0.001</b>
Q15424	Scaffold attachment factor B1	SAFB	0.0309	<b>2.60</b>	<b>0.008</b>	<b>2.92</b>	<b>0.004</b>	<b>2.96</b>	<b>0.004</b>
Q96CN7	Isochorismatase domain-containing protein 1	ISOC1	0.0199	<b>3.93</b>	<b>0.001</b>	<b>3.91</b>	<b>0.002</b>	<b>2.91</b>	<b>0.007</b>
O43765	Small glutamine-rich tetratricopeptide repeat-containing protein alpha	SGTA	0.0281	<b>2.71</b>	<b>0.004</b>	<b>2.46</b>	<b>0.007</b>	<b>2.83</b>	<b>0.003</b>
Q9H444	Charged multivesicular body protein 4b	CHMP4B	0.0383	<b>2.78</b>	<b>0.007</b>	<b>2.64</b>	<b>0.010</b>	<b>2.75</b>	<b>0.008</b>
Q99541	Perilipin-2	PLIN2	0.0001	1.28	0.000	<b>1.90</b>	<b>0.000</b>	<b>2.18</b>	<b>0.000</b>
P61011	Signal recognition particle 54 kDa protein	SRP54	0.0191	<b>2.28</b>	<b>0.001</b>	<b>2.25</b>	<b>0.001</b>	<b>2.06</b>	<b>0.002</b>
Q9NX63	MICOS complex subunit MIC19	CHCHD3	0.0191	1.25	0.116	<b>1.63</b>	<b>0.002</b>	<b>1.74</b>	<b>0.001</b>
P35580	Myosin-10	MYH10	0.0199	1.18	0.263	<b>1.53</b>	<b>0.004</b>	<b>1.65</b>	<b>0.001</b>
Q16186	Proteasomal ubiquitin receptor ADRM1	ADRM1	0.0238	<b>1.64</b>	<b>0.004</b>	<b>1.78</b>	<b>0.002</b>	<b>1.63</b>	<b>0.004</b>
P10606	Cytochrome c oxidase subunit 5B, mitochondrial	COX5B	0.015	1.19	0.038	<b>1.37</b>	<b>0.001</b>	<b>1.56</b>	<b>0.000</b>
P02671	Fibrinogen $\alpha$ chain	FGA	0.0245	1.04	0.951	<b>1.33</b>	<b>0.024</b>	<b>1.53</b>	<b>0.002</b>
P10412	Histone H1.4	HIST1H1E	0.031	<b>1.32</b>	<b>0.014</b>	<b>1.33</b>	<b>0.011</b>	<b>1.46</b>	<b>0.002</b>
Q9UJZ1	Stomatin-like protein 2, mitochondrial	STOML2	0.0199	1.19	0.080	<b>1.42</b>	<b>0.002</b>	<b>1.45</b>	<b>0.001</b>
P01023	Alpha-2-macroglobulin	A2M	0.0272	1.29	0.023	<b>1.47</b>	<b>0.002</b>	<b>1.43</b>	<b>0.003</b>
P02787	Serotransferrin	TF	0.0171	1.12	0.096	1.20	0.007	<b>1.39</b>	<b>0.000</b>
P29966	Myristoylated alanine-rich C-kinase substrate	MARCKS	0.0353	1.01	0.998	1.10	0.523	<b>1.39</b>	<b>0.004</b>
P04040	Catalase	CAT	0.031	1.20	0.048	1.29	0.008	<b>1.37</b>	<b>0.002</b>
P07305	Histone H1.0	H1F0	0.0245	1.07	0.584	1.10	0.280	<b>1.36</b>	<b>0.001</b>
P08195	4F2 cell-surface antigen heavy chain	SLC3A2	0.0171	1.13	0.069	1.27	0.002	<b>1.35</b>	<b>0.000</b>
P35613	Basigin	BSG	0.015	1.11	0.076	1.28	0.001	<b>1.35</b>	<b>0.000</b>
P07306	Asialoglycoprotein receptor 1	ASGR1	0.0171	1.12	0.079	1.27	0.001	<b>1.35</b>	<b>0.000</b>
O60573	Eukaryotic translation initiation factor 4E type 2	EIF4E2	0.031	0.97	0.953	1.01	0.995	<b>1.34</b>	<b>0.006</b>

P05023	Sodium/potassium-transporting ATPase subunit alpha-1	ATP1A1	0.0287	1.19	0.045	<b>1.32</b>	<b>0.003</b>	<b>1.34</b>	<b>0.003</b>
Q8WWI1	LIM domain only protein 7	LMO7	0.039	1.16	0.142	<b>1.33</b>	<b>0.006</b>	<b>1.31</b>	<b>0.007</b>
P02649	Apolipoprotein E	APOE	0.015	1.09	0.063	1.21	0.001	<b>1.30</b>	<b>0.000</b>
P05362	Intercellular adhesion molecule 1	ICAM1	0.023	1.11	0.251	<b>1.36</b>	<b>0.001</b>	1.29	0.005
Q8IY81	pre-rRNA processing protein FTSJ3	FTSJ3	0.0226	1.20	0.022	<b>1.36</b>	<b>0.001</b>	1.29	0.003
Q5JTV8	Torsin-1A-interacting protein 1	TOR1AIP1	0.039	1.15	0.133	<b>1.34</b>	<b>0.003</b>	1.23	0.021
O43719	HIV Tat-specific factor 1	HTATSF1	0.0475	0.97	0.995	<b>1.61</b>	<b>0.015</b>	0.97	0.995
Q7Z7A1	Centriolin	CNTRL	0.0195	1.09	0.991	<b>4.44</b>	<b>0.004</b>	0.65	0.486

Tab. IIa Proteins significantly up-regulated by different concentrations of C14:0 in HepG2 cell proteome with relative fold change compared to controls (ANOVA p-value adjusted with Benjamini-Hochberg method; Tukey's HSD p-value adjusted for multiple comparisons (10 comparisons)). Significant p-values and fold change greater than 1.3 are highlighted in bold type.

Majority Protein ID	Protein name	Gene name	ANOVA	Fold change 0-50	p adj 0-50	Fold change 0-125	p adj 0-125	Fold change 0-125	p adj 0-250
P22061	Protein-L-isoaspartate(D-aspartate) O-methyltransferase	PCMT1	0.0462	-1.02	1.000	-1.77	0.421	<b>-5.02</b>	<b>0.008</b>
P50570	Dynamin-2	DNM2	0.0366	-1.01	1.000	-1.43	0.559	<b>-3.67</b>	<b>0.005</b>
Q96FC7	Phytanoyl-CoA hydroxylase-interacting protein-like	PHYHIPL	0.0464	-1.49	0.422	<b>-2.93</b>	<b>0.010</b>	<b>-2.84</b>	<b>0.012</b>
P02753	Retinol-binding protein 4	RBP4	0.015	<b>-1.40</b>	<b>0.024</b>	<b>-1.64</b>	<b>0.002</b>	<b>-2.31</b>	<b>0.000</b>
P48147	Prolyl endopeptidase	PREP	0.0272	-1.21	0.412	-1.21	0.424	<b>-2.04</b>	<b>0.001</b>
Q15003	Condensin complex subunit 2	NCAPH	0.014	-1.07	0.654	-1.12	0.236	<b>-1.67</b>	<b>0.000</b>
Q8NEV1	Casein kinase II subunit alpha 3	CSNK2A3	0.0172	-1.21	0.013	-1.27	0.004	<b>-1.44</b>	<b>0.000</b>
Q9BQE3	Tubulin alpha-1C chain	TUBA1C	0.0482	-1.24	0.062	-1.27	0.040	<b>-1.43</b>	<b>0.005</b>
O43852	Calumenin	CALU	0.0195	-1.27	0.002	<b>-1.31</b>	<b>0.001</b>	-1.22	0.005
P60981	Dextrin	DSTN	0.0464	-1.94	0.469	<b>-7.62</b>	<b>0.007</b>	-1.17	0.983
O94903	Proline synthase co-transcribed bacterial homolog protein	PROSC	0.029	<b>-2.27</b>	<b>0.014</b>	-0.79	0.652	-0.79	0.657
Q9BRA2	Thioredoxin domain-containing protein 17	TXNDC17	0.0367	-3.88	0.068	<b>-5.14</b>	<b>0.028</b>	-0.59	0.661

Tab. IIb Proteins significantly down-regulated by different concentrations of C14:0 in HepG2 cell proteome with corresponding fold change (ANOVA p-value adjusted with Benjamini-Hochberg method; Tukey's HSD p-value adjusted for multiple comparisons (10 comparisons)). Significant p-values and fold change lower than -1.3 are highlighted in bold type.

Regarding the secretome analysis of HepG2 cells after C14:0 treatment, a total of 475 proteins were identified by MS/MS analysis. After applying the same filtering conditions also used for the proteome analysis, 282 proteins were detected as deregulated in their secretion in all three biological replicates of at least one condition with at least 99% confidence (FDR < 1%). Among these a total of 32 unique secreted proteins were found to be deregulated by C14:0 (p-value < 0.05 and 1.3 fold-change) as compared to controls. At 50  $\mu$ M C14:0 four proteins had a reduced secretion, at 125  $\mu$ M C14:0 eight proteins were over-secreted and three had lower secretion while at 250  $\mu$ M C14:0 22 proteins were over-secreted and seven less secreted (Tab. IIIa and b). The most deregulated secreted protein (UDP-glucose 6-dehydrogenase) was two times more secreted in 250  $\mu$ M C14:0 treated cells as compared to controls, while the most down-regulated secreted proteins were 60S acidic ribosomal protein P0 at 50  $\mu$ M C14:0 with a fold change of six and Phosphatidylcholine-sterol acyltransferase with a fold change of four at 250  $\mu$ M C14:0.

Majority Protein ID	Protein name	Gene name	ANOVA	Fold change 0-50	p adj 0-50	Fold change 0-125	p adj 0-125	Fold change 0-250	p adj 0-250
O60701	UDP-glucose 6-dehydrogenase	UGDH	0.007	0.84	0.569	1.31	0.252	<b>2.48</b>	<b>0.001</b>
O14745	Na(+)/H(+) exchange regulatory cofactor NHE-RF1	SLC9A3R1	0.006	1.02	0.998	<b>1.61</b>	<b>0.012</b>	<b>2.41</b>	<b>0.000</b>
P22626	Heterogeneous nuclear ribonucleoprotein A2/B1	HNRNPA2B1	0.001	0.98	0.995	<b>1.62</b>	<b>0.001</b>	<b>2.28</b>	<b>0.000</b>
P49327	Fatty acid synthase	FASN	0.008	1.14	0.568	<b>1.46</b>	<b>0.023</b>	<b>2.20</b>	<b>0.000</b>
O75874	Isocitrate dehydrogenase [NADP] cytoplasmic	IDH1	0.044	0.99	1.000	1.50	0.159	<b>2.19</b>	<b>0.007</b>
P61981	14-3-3 protein $\gamma$	YWHAG	0.022	0.54	0.095	1.47	0.386	<b>2.16</b>	<b>0.037</b>
Q16658	Fascin	FSCN1	0.046	0.91	0.936	1.36	0.301	<b>1.98</b>	<b>0.013</b>
P06733	Alpha-enolase	ENO1	0.012	1.13	0.570	<b>1.45</b>	<b>0.014</b>	<b>1.84</b>	<b>0.001</b>
P30086	Phosphatidyl ethanolamine-binding protein 1	PEBP1	0.046	1.02	0.999	1.44	0.101	<b>1.84</b>	<b>0.008</b>
P11142	Heat shock cognate 71 kDa protein	HSPA8	0.006	1.11	0.484	<b>1.34</b>	<b>0.013</b>	<b>1.83</b>	<b>0.000</b>
P00338	L-lactate dehydrogenase A	LDHA	0.009	0.95	0.966	<b>1.74</b>	<b>0.004</b>	<b>1.82</b>	<b>0.003</b>

P02545	Prelamin-A/C	LMNA	0.026	1.07	0.932	1.28	0.176	<b>1.81</b>	<b>0.002</b>
P38646	Stress-70 protein. mitochondrial	HSPA9	0.004	1.26	0.012	<b>1.36</b>	<b>0.002</b>	<b>1.78</b>	<b>0.000</b>
P08238	Heat shock protein HSP 90-beta	HSP90AB1	0.026	0.72	0.185	1.16	0.737	<b>1.74</b>	<b>0.021</b>
P50395	Rab GDP dissociation inhibitor beta	GDI2	0.009	0.92	0.740	1.30	0.063	<b>1.69</b>	<b>0.001</b>
P21333	Filamin-A	FLNA	0.012	0.86	0.400	1.07	0.876	<b>1.64</b>	<b>0.003</b>
P30101	Protein disulfide-isomerase A3	PDIA3	0.048	0.87	0.691	1.12	0.809	<b>1.63</b>	<b>0.020</b>
P68363	Tubulin alpha-1B chain	TUBA1B	0.044	0.91	0.842	1.12	0.748	<b>1.62</b>	<b>0.012</b>
P0DMV8	Heat shock 70 kDa protein 1A	HSPA1A	0.026	0.81	0.316	1.15	0.651	<b>1.60</b>	<b>0.015</b>
P15311	Ezrin	EZR	0.013	0.99	1.000	1.26	0.063	<b>1.59</b>	<b>0.001</b>
P00352	Retinal dehydrogenase 1	ALDH1A1	0.006	1.06	0.674	<b>1.41</b>	<b>0.001</b>	<b>1.54</b>	<b>0.000</b>
P14618	Pyruvate kinase PKM	PKM	0.035	0.97	0.988	1.16	0.395	<b>1.54</b>	<b>0.006</b>

Tab. IIIa Proteins significantly modulated by different concentrations of C14:0 in HepG2 cell secretome with relative fold change (ANOVA p-value adjusted with Benjamini-Hochberg method; Tukey's HSD p-value adjusted for multiple comparisons (10 comparisons)). Significant p-values and fold change greater than 1.3 are highlighted in bold type.

Majority Protein ID	Protein name	Gene name	ANOVA	Fold change 0-50	p adj 0-50	Fold change 0-125	p adj 0-125	Fold change 0-250	p adj 0-250
P04180	Phosphatidylcholine-sterol acyltransferase	LCAT	0.007	-0.93	0.987	-1.11	0.962	<b>-4.50</b>	<b>0.001</b>
Q9BRK5	45 kDa calcium-binding protein	SDF4	0.044	<b>-5.24</b>	<b>0.008</b>	-0.96	1.000	-2.78	0.090
P02750	Leucine-rich alpha-2-glycoprotein	LRG1	0.014	-1.12	0.523	<b>-1.37</b>	<b>0.016</b>	<b>-1.67</b>	<b>0.001</b>
P01033	Metalloproteinase inhibitor 1	TIMP1	0.008	-1.04	0.951	<b>-1.46</b>	<b>0.003</b>	<b>-1.58</b>	<b>0.001</b>
Q6H9L7	Isthmin-2	ISM2	0.019	-1.13	0.284	-1.31	0.010	<b>-1.48</b>	<b>0.001</b>
P02654	Apolipoprotein C-I	APOC1	0.046	<b>-1.57</b>	<b>0.004</b>	-1.30	0.072	<b>-1.42</b>	<b>0.017</b>
P07942	Laminin subunit beta-1	LAMB1	0.008	-1.25	0.002	-1.25	0.002	<b>-1.34</b>	<b>0.000</b>
P04004	Vitronectin	VTN	0.019	-1.26	0.005	-1.21	0.013	<b>-1.34</b>	<b>0.001</b>
Q92563	Testican-2	SPOCK2	0.046	<b>-1.37</b>	<b>0.022</b>	-0.94	0.903	-0.93	0.818
P05388	60S acidic ribosomal protein P0	RPLP0	0.001	<b>-6.34</b>	<b>0.000</b>	-0.92	0.963	-0.80	0.593

Tab. IIIb Proteins significantly modulated by different concentrations of C14:0 in HepG2 cell secretome with relative fold change (ANOVA p-value adjusted with Benjamini-Hochberg method; Tukey's HSD p-value adjusted for multiple comparisons (10 comparisons)). Significant p-values and fold change lower than -1.3 are highlighted in bold type.

Both in the proteome and in the secretome analysis the number of modulated proteins increased with the increasing concentration of C14:0 and many proteins were shared among the three different C14:0 treatments, as reported in Fig.4.

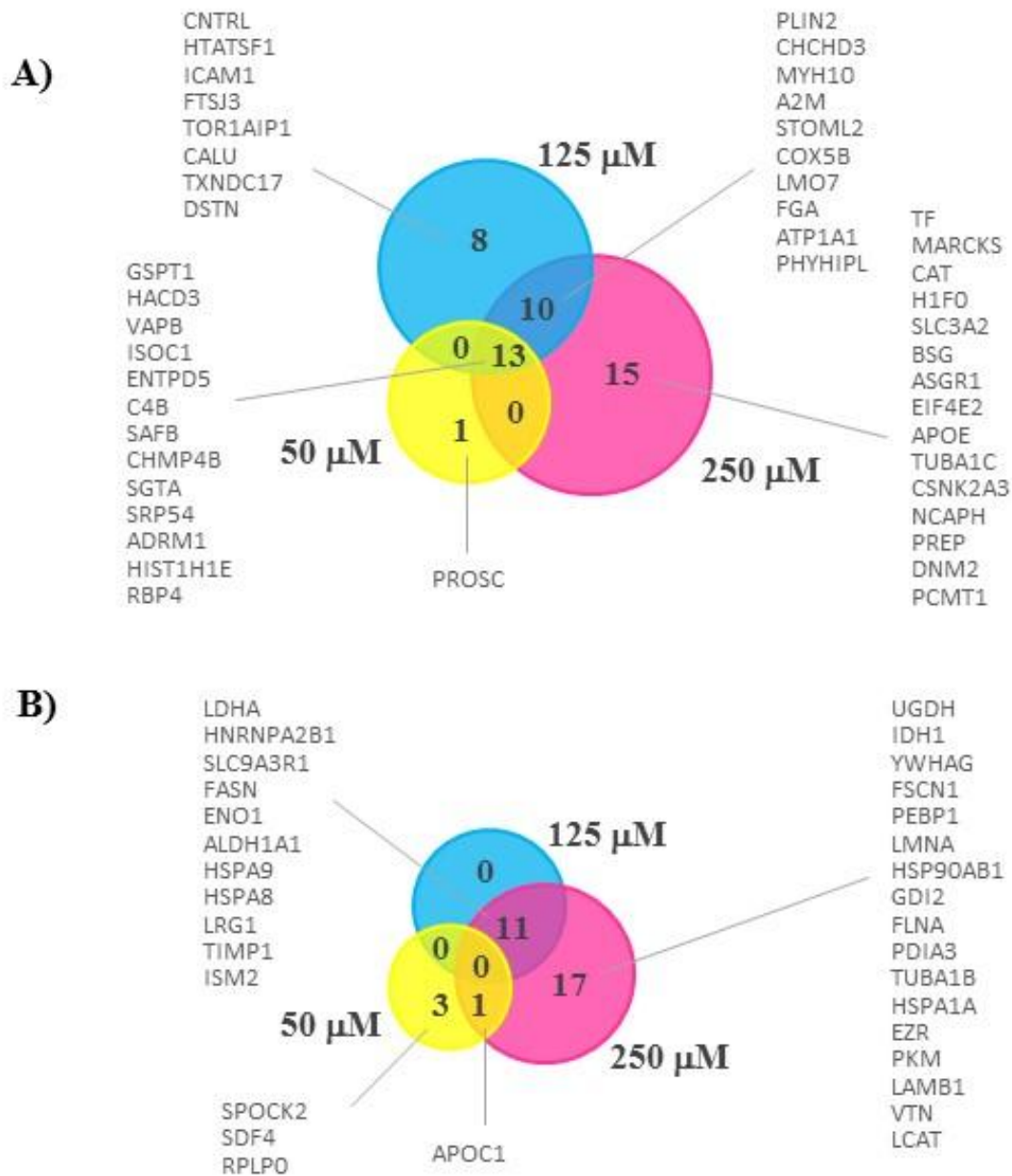


Fig.4 Venn diagrams summarising the overlapping proteins among the three different C14:0 treatments, identified in proteome (A) and secretome (B) samples. Proteins were identified with a minimum of two unique peptides per protein.

Some of these identified proteins were further selected as representative for Western Blotting analysis. Different parameters were used for protein selection, such as the degree of the C14:0-induced deregulation, over-secretion, novelty and biological relevance. The following intracellular deregulated proteins were selected: Eukaryotic peptide chain release factor GTP-binding subunit ERF3A (eRF3a), Vesicle-associated membrane protein-associated protein B/C (VAP-B/C), Perilipin-2 (ADRP), Retinol-binding protein 4 (RBP4), Apolipoprotein E (APOE) and Complement C4 alpha (C4A) (Fig.5).

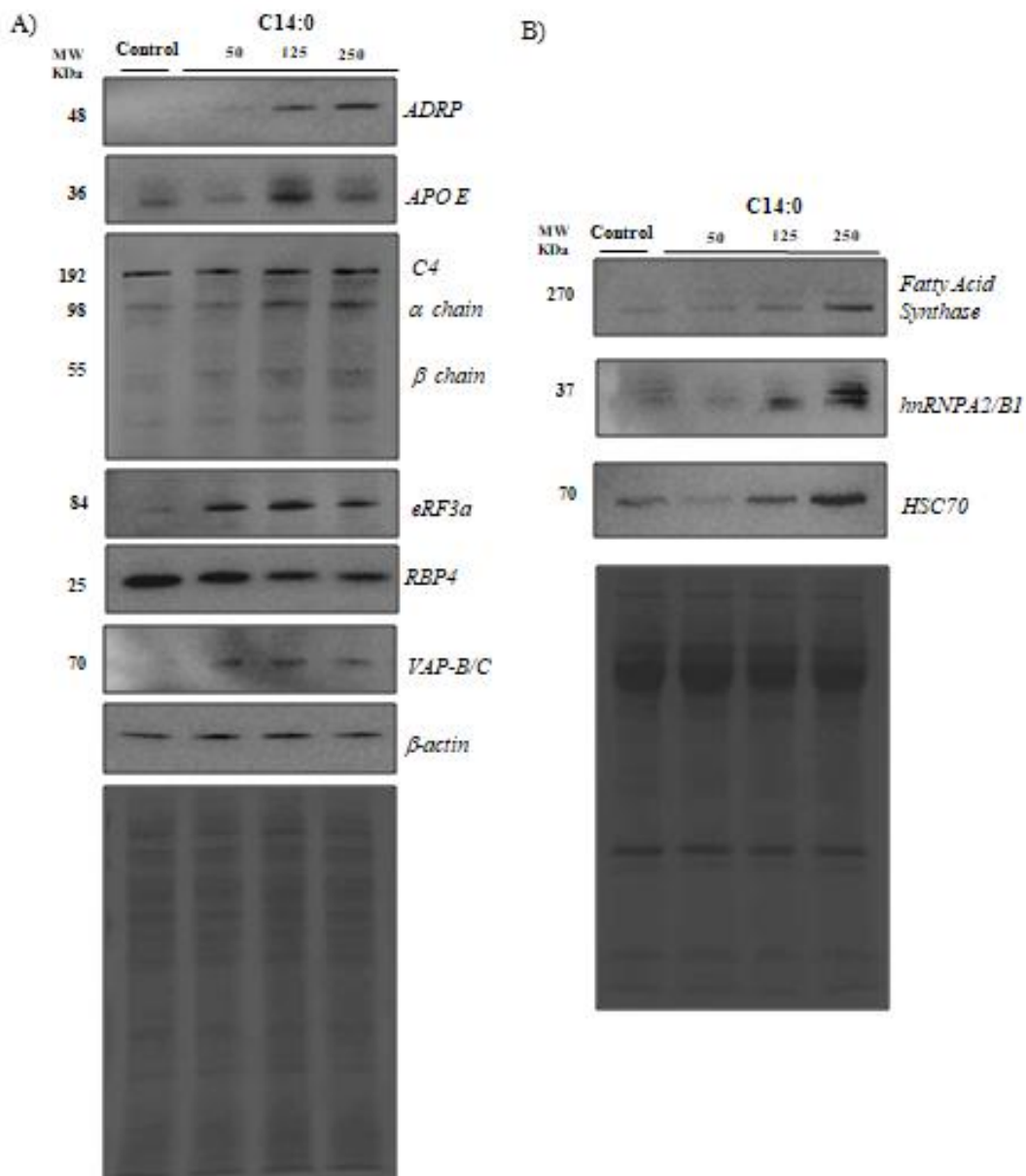


Fig.5 Validation of some intracellular (A) and secreted (B) proteins modulated in HepG2 following myristic acid treatments (from 50 to 250  $\mu$ M) by means of Western Blot technique.

For the validation of the modulated proteins found in the HepG2 secretome Fatty acid Synthase, Heterogeneous nuclear ribonucleoproteins A2/B1 (hnRNP A2/B1) and Heat shock cognate 71 kDa protein (HSC70) were selected. The levels of these proteins in two biological replicates of HepG2 control and C14:0 treated cells were compared. The level of expression of ADRP, ApoE, eRF3a and C4 (also of its isoforms alpha and beta) increased markedly as expected, while the level of VAP-B/C increased only slightly, and its detection was also difficult to obtain probably due to the lower abundance of the protein in HepG2 cell lysates. The Western Blotting analysis on the intracellular down-regulated protein RBP4 showed a marked signal coming from the protein and a significant decrease in its expression concurrent with the increase in C14:0 concentration in HepG2 culture media; instead, a marked increase in the secretion of all the three proteins analysed from secretome samples was observed. Overall these proteins investigated by Western Blotting technique confirmed the modulations observed in HepG2 cell proteome and secretome following C14:0 administration, corroborating in this manner the reliability of the MS/MS data.

### **3.3 Prediction of secretion pathways**

To predict if the 35 proteins found to be modulated in the secretome of the C14:0 treated HepG2 cells are secreted through the classical (involving signal peptide) or non-classical pathway (not signal peptide) the on-line prediction server SecretomeP 2.0 was used. This tool relies on a large number of other feature prediction servers to obtain information on various post-translational and localisation aspects of the investigated protein, which are then integrated into the final prediction of secretion (Caccia et al., 2013). For those deregulated proteins predicted to be secreted by means of a non-classical pathway the Exocarta database was consulted. Exocarta is a manually curated exosomes database collecting proteins identified in exosome vesicles by different experiments on different cell types (Keerthikumar et al., 2016). According to Exocarta results, the majority of the deregulated secreted proteins identified (~



69%) were already found to be secreted through exosome release in other experiments. 22 proteins out of the 32 modulated secreted proteins were found to be exosome released proteins. Only ~ 31% proteins were predicted to be secreted by classical pathways with an N-terminal signal peptide by Secteome P 2.0 investigation (Tab. IV).

Protein name	Majority Protein IDs	Gene names	SecretomeP	ExoCarta
Retinal dehydrogenase 1	P00352	ALDH1A1		Present
Apolipoprotein C-I	P02654	APOC1	SP	
Alpha-enolase	P06733	ENO1		Present
Ezrin	P15311	EZR		Present
Fatty acid synthase	P49327	FASN		Present
Filamin-A	P21333	FLNA		Present
Fascin	Q16658	FSCN1		Present
Rab GDP dissociation inhibitor beta	P50395	GDI2		Present
Heterogeneous nuclear ribonucleoproteins A2/B1	P22626	HNRNPA2B1		Present
Heat shock protein HSP 90-beta	P08238	HSP90AB1		Present
Heat shock 70 kDa protein 1A	P0DMV8	HSPA1A		Present
Heat shock cognate 71 kDa protein	P11142	HSPA8		Present
Stress-70 protein, mitochondrial	P38646	HSPA9		Present
Isocitrate dehydrogenase [NADP] cytoplasmic	O75874	IDH1		Present
Isthmin-2	Q6H9L7	ISM2	SP	
Laminin subunit beta-1	P07942	LAMB1	SP	
Phosphatidylcholine-sterol acyltransferase	P04180	LCAT	SP	
L-lactate dehydrogenase A chain	P00338	LDHA		Present
Prelamin-A/C	P02545	LMNA		Present
Leucine-rich alpha-2-glycoprotein	P02750	LRG1	SP	
Protein disulfide-isomerase A3	P30101	PDIA3	SP	
Phosphatidylethanolamine-binding protein 1	P30086	PEBP1		Present
Pyruvate kinase PKM	P14618	PKM		Present
60S acidic ribosomal protein P0	P05388	RPLP0		Present
45 kDa calcium-binding protein	Q9BRK5	SDF4	SP	
Na(+)/H(+) exchange regulatory cofactor NHE-RF1	O14745	SLC9A3R1		Present
Testican-2	Q92563	SPOCK2	SP	
Metalloproteinase inhibitor 1	P01033	TIMP1	SP	
Tubulin alpha-1B chain	P68363	TUBA1B		Present
UDP-glucose 6-dehydrogenase	O60701	UGDH		Present
Vitronectin	P04004	VTN	SP	
14-3-3 protein gamma	P61981	YWHAG		Present

Tab. IV Investigation of proteins secretion pathways by using SecretomeP server and Exocarta database (SP: Signal Peptide).

### **3.4 Modulation of biological processes and pathways induced by myristic acid**

To disclose the interaction networks between the modulated proteins and to better elucidate biological process and molecular pathways involved in the response of HepG2 cells to C14:0 treatments, specific bioinformatics analyses were performed. Different tools were used, including DAVID, STRING on-line database and Cytoscape software. This analysis promoted the illustration of biological context, association with diverse physiological pathways and network interactions of proteins whose expression was found to be influenced by C14:0.

The GO analysis was performed by using DAVID on-line bioinformatics tool. As reported in Fig.6, Cellular Component analysis revealed that both in the proteome and in the secretome, most of the proteins are proteins commonly found in extracellular exosome. Many other proteins were reported to be present in the membrane fraction and cytosol in both types of samples and while in the proteome some proteins were typical of the endoplasmic reticulum and mitochondrion, in the secretome many proteins were typical of cellular junction, focal adhesion and extracellular space. The analysis of the Biological Process revealed that most deregulated intracellular and secreted proteins are involved in cell-cell adhesion. Moreover, deregulated intracellular proteins are also involved in the response to drug, while the secreted proteins in oxidation-reduction process, cell response to interleukin-4, as well as in protein folding. Finally, according to the Molecular Function analysis, most of the deregulated intracellular and secreted proteins exhibited “binding” activity, namely protein binding, poly(A) RNA binding, and cadherin binding involved in cell-cell adhesion.

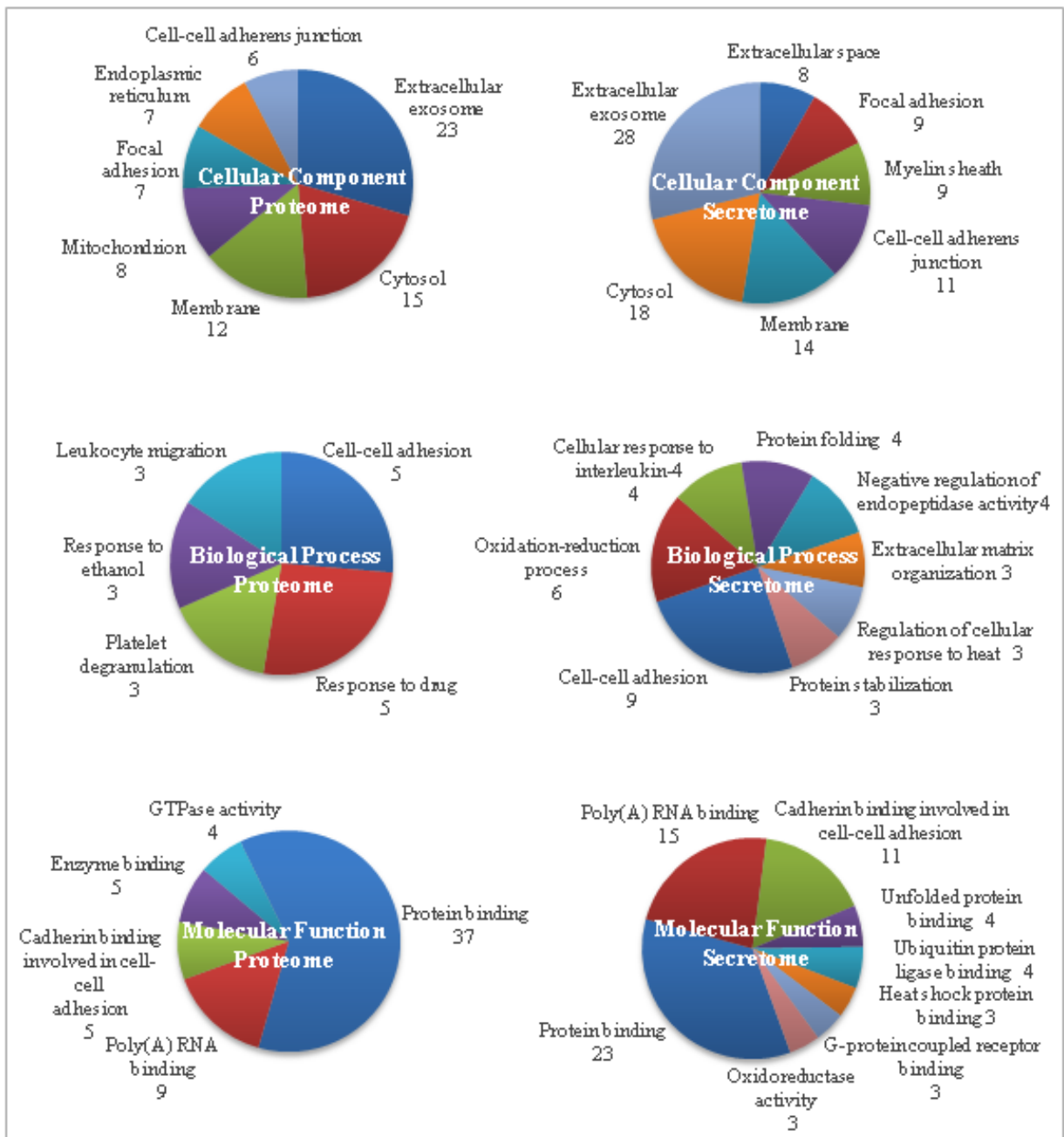


Fig.6 Gene Ontology analysis of the HepG2 proteome (left) and secretome (right) deregulated after myristic acid treatment. Only overrepresented categories with  $p$ -value  $< 0.05$  are shown. The area of each sector is proportional to the number of genes annotated to the corresponding GO category (i.e. cellular components, biological processes and molecular functions) which is also indicated.

STRING search tool was used to identify interaction networks of the proteins perturbed after C14:0 treatments. Two STRING criteria were selected: “database” based on the observation that functionally associated proteins have known interactions from curated databases and “experiments,” i.e. experimentally proven interactions from published studies. Among the 47 proteins differentially expressed in the proteome, only 18 were connected in the String output and many interactions were highlighted mainly between pairs of proteins (for example between VAPB and COX5B, but also TF and DNMT2, as well as between SLC3A2 and BSG) (Fig.7A). Two small clusters were identified that are related to cytoskeleton organisation and to proteins targeted to endoplasmic reticulum and/or proteasome (including for example TUBA1C, DSTN, and SGTA), as well as to complement and coagulation cascades (A2M, FGA, and ICAM1). In comparison with the proteome, the secretome showed the highest percentage of physically connected proteins; 15 out of 32 proteins found to be modulated by different concentrations of C14:0 were present in the String output (Fig.7B). HSPA8 (heat shock cognate 71 kDa protein, HSC70) was an important hub in this interaction network connecting a total of six proteins, suggesting that it may play an important role in mediating the effects of C14:0. Indeed, HSPA8 resulted in a cluster involving proteins related to mRNA processing, translation, and protein folding (HNRNPA2B1, RPLP0, PDIA3), as well as including other heat shock proteins (HSP90AB1, HSPA1A, and HSPA9) which are key mediators of stress response, intracellular trafficking, cell proliferation. Moreover, the network produced by String contained a highly connected subnetwork of metabolism-associated enzymes (ALDH1A1, LDHA, PKM, ENO1) connected to scaffold proteins that regulate surface expression of plasma membrane proteins (EZR, SLC9A3R1, GDI2).

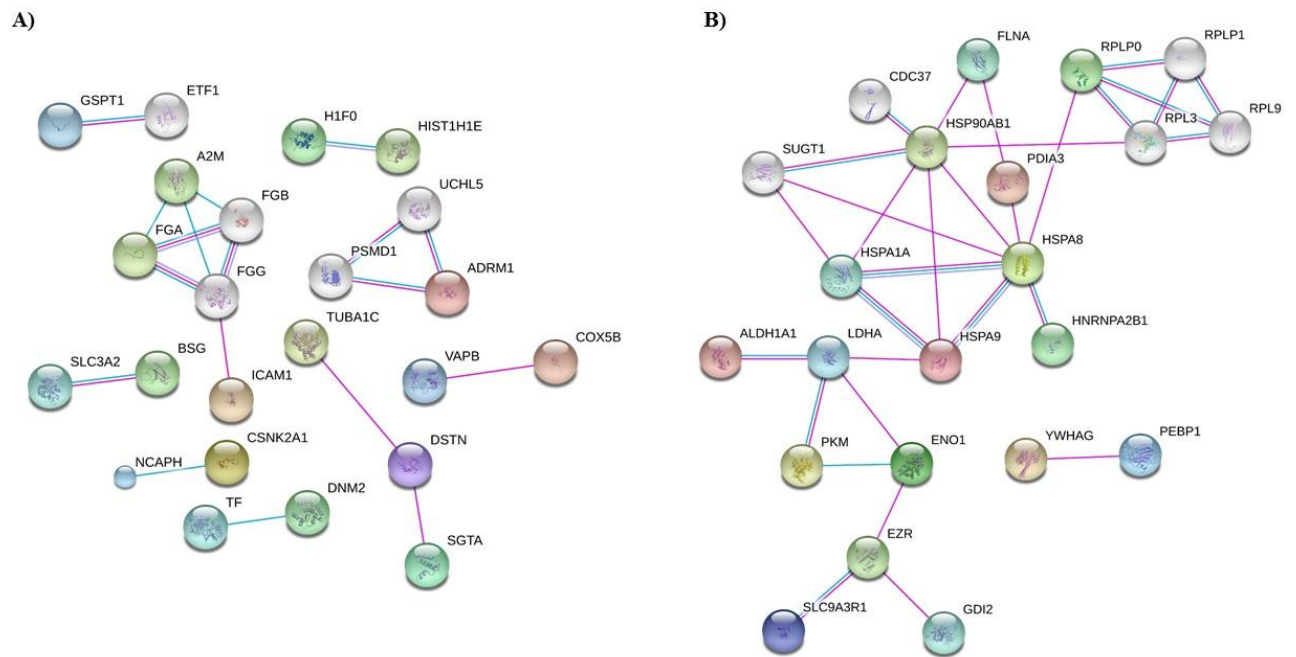


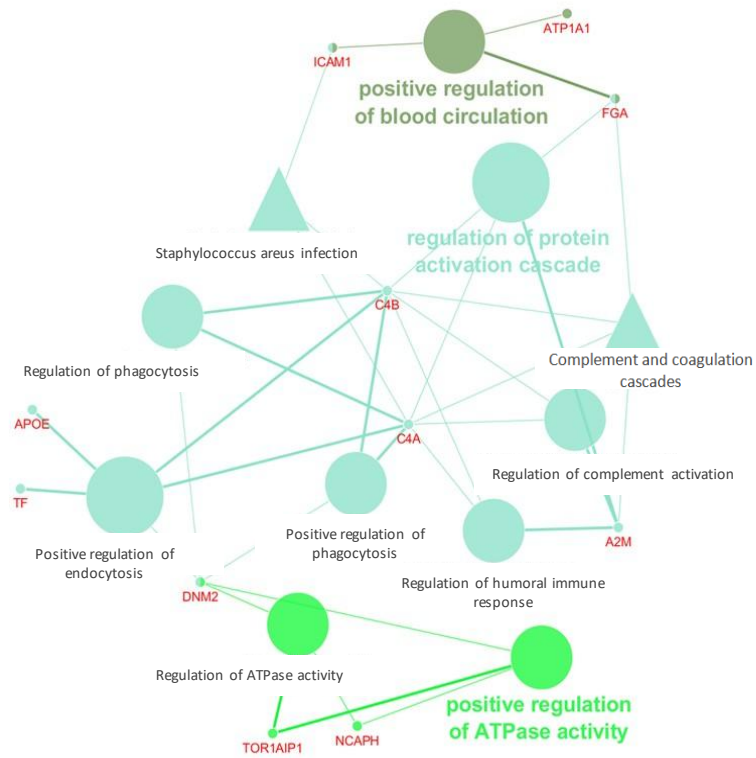
Fig.7 Analysis of interactions among the HepG2 intracellular (A) and secreted (B) proteins deregulated after myristic acid treatment. The predicted protein interactions that were found in the STRING interaction database were restricted to the categories “database” and “experiments”. Additional nodes are indicated as white nodes.

In order to highlight the enriched biological processes and molecular pathways involving the proteins that exhibited a changed abundance in HepG2 cell proteome and secretome after C14:0 treatments, ClueGO plugin for Cytoscape was used with *GO biological process* and *KEGG database* selection. Only enriched pathways with  $p < 0.05$  and a Kappa score threshold of 0.4 were considered. Different biological processes were found to be enriched when deregulated intracellular proteins were analysed, including positive regulation of ATPase activity and blood circulation, as well as regulation of protein activation cascade (Fig.8A). As concerns enriched KEGG pathways, positive regulation of complement activation was found to be involved in the response to C14:0 treatment.

Cytoscape analysis of the deregulated secreted proteins influenced by C14:0 treatments revealed three main biological processes, namely response to interleukin-4, microvillus assembly and monosaccharide catabolic process, to be significantly enriched (Fig.8B). In the last biological process, glycolysis/gluconeogenesis and catabolism of hexose were the

dominant processes. Moreover, the main KEGG pathway related to secreted proteins modulated by C14:0 was antigen processing and presentation, grouping together many Heat Shock proteins.

A)



B)

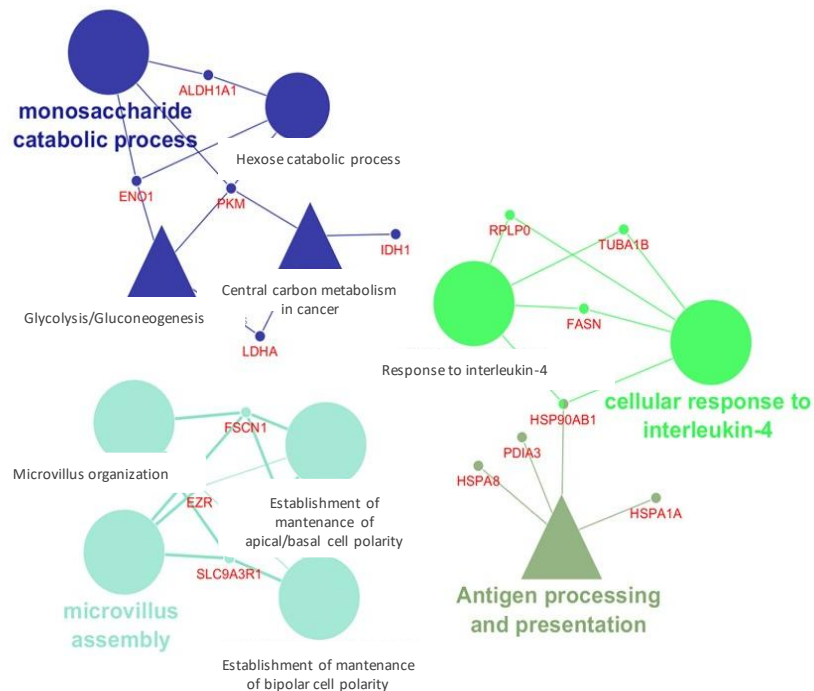


Fig.8 Results of ClueGo clustering analysis with Cytoscape for the visualisation of significantly enriched biological process (circles) and KEGG pathways (triangles) related to deregulated proteome

(A) and secretome (B) in HepG2 cells treated with myristic acid. Node size represents the enrichment of that specific process/pathway and the lines connecting different nodes indicate that these categories share gene(s). The group name is the leading group term based on highest significance (*p* -value corrected with Benjamini- Hochberg).

### 3.5 Myristic acid influence on ER stress

SFAs are known to cause ER stress in different cell types (Hetherington et al., 2016; Sramek et al., 2017). Accordingly, the proteome analysis revealed some proteins involved in protein homeostasis while in the secretome some stress signaling proteins – such as heat shock proteins - were found to be oversecreted. Therefore, the intracellular expression of some intracellular ER stress markers was investigated by means of Western Blot analysis. The expression of Cyclic AMP-dependent transcription factor ATF-6 alpha (ATF-6 $\alpha$ ) was investigated. This protein is a membrane-bound transcription factor that upon ER stress conditions is cleaved by Site-1 protease (S1P) and Site-2 protease (S2P). Cleaved forms can enter the nucleus and activate Unfolding Protein Response (UPR) genes (Yoshida et al., 2000). Western blotting detection of the cleaved forms of this protein is used as a marker of ER stress (Osowski et al., 2011). As visible in Fig.9 two bands were detected when the expression of ATF6 $\alpha$  was investigated in HepG2 cell lysates after C14:0 supplementations. Interestingly, the analysis revealed the presence of two bands. The molecular weights of these two bands correspond to the kDa of the two ATF6 $\alpha$  cleaved subunits detected also by Mao et al. rather than the full form of the protein (Mao et al., 2007). The lower isoform showed an increase after C14:0 250  $\mu$ M. The expression of two other ER stress markers was investigated. Both Serine/threonine-protein kinase/endoribonuclease (IRE1 $\alpha$ ) and Eukaryotic translation initiation factor 2-alpha kinase 3 (PERK), whose expression has already been used as ER stress markers (Hu et al., 2015), showed an increase in their expression in HepG2 cells treated with C14:0. The Western

Blotting investigation of PERK showed the appearance of supplementary bands, which could be ascribed to the increase in PERK dimerisation in presence of ER stress (Liu et al., 2000).

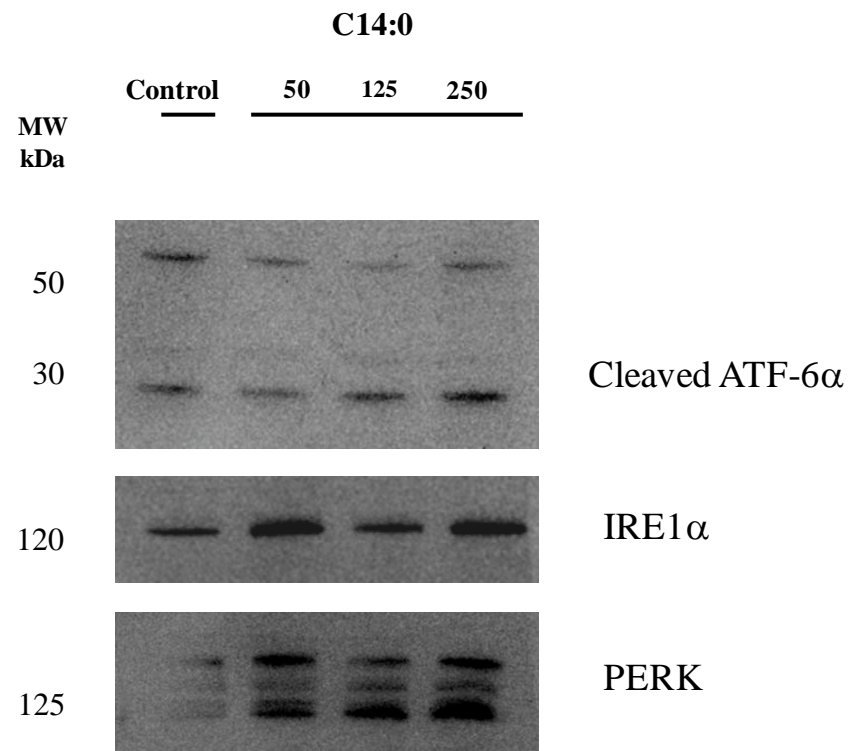


*Fig.9 Investigation of the effects of different concentrations of C14:0 on ER stress markers in HepG2 cells.*



## 4. DISCUSSION

### 4.1 Myristic acid induces lipid droplets formation, cytoskeleton reorganisation and ER stress

To date only few studies have analysed the overall response of HepG2 cell to enhanced FA intake from a proteomic point of view (Vendel Nielsen et al., 2013; Krogager et al., 2015). Moreover, despite the fact that C14:0 is a minor plasma FA, it has attracted growing attention because of its ability to decrease HDL plasma levels and also as predictor of NASH, the most extreme form of NAFLD (Tomita et al., 2011; Noto et al., 2016). However, to date only few studies have investigated the biochemical effects of C14:0 when supplied in cell culture media. To date there have been no investigations of C14:0 effect from a proteomic point of view. Therefore, this is the first proteomic study describing and investigating both the proteomic (Fig.10) and secretomic effects of different concentrations of C14:0 on HepG2 cell model.

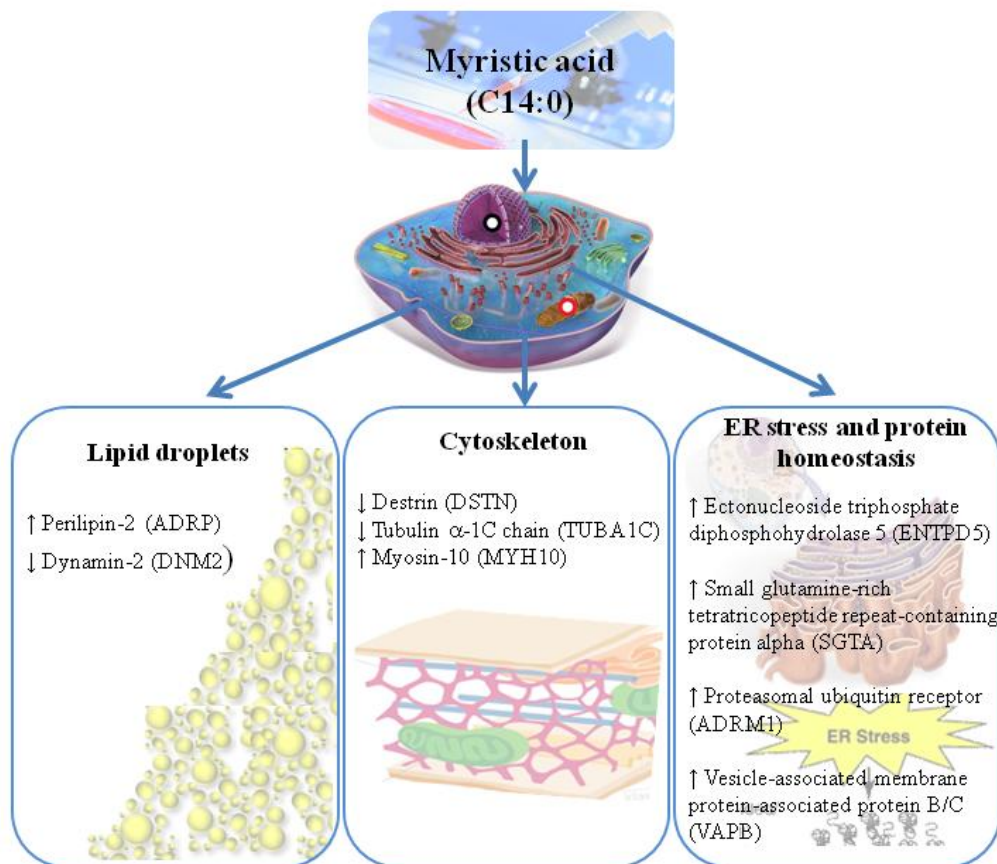


Fig.10 Main effects of myristic acid on HepG2 cells proteome.

### 4.1.1 Lipid droplets

Before performing the proteomic investigation, the dose-dependent absorption of C14:0 when dissolved in BSA was assessed. As can be observed in Fig.3 the treatment caused, in particular at concentration 125  $\mu$ M, the accumulation of LD, dynamic structures involved in lipid storage, metabolism as well as in many other cellular functions (Hashemi et al., 2015). These data are in agreement with the accumulation of LD observed in response to HepG2 supplementation with other FAs, in particular with C18:1 (Mei et al., 2011; Hetherington et al., 2016). These data are also in agreement with the C14:0-induced mild steatosis observed in primary mouse hepatocytes (Martinez et al., 2015). Nevertheless, this is the first time that LD formation has been reported after C14:0 treatment in a HepG2 cell model.

Interestingly, among the deregulated intracellular proteins identified in this PhD research project, there was Perilipin2 (ADRP). ADRP is the most abundant protein on LD surface, (Sletten et al., 2014) and was found up-regulated with an increased fold change as a consequence of the increased C14:0 dosage used for cell treatment (Tab. IIa). While at 50  $\mu$ M C14:0 the increase was not statistically significant, at 125 and 250  $\mu$ M C14:0 ADRP was significantly increased as also confirmed also with Western Blotting analysis (Fig.5).

As mentioned before, LD represent dynamic structures that, depending on nutrient availability, can undergo cycles of synthesis and catabolism through lipophagy. During this process LD are enclosed inside autophagosomes where lipids are depredated by hydrolases and later autolysosomal membranes are converted into a new lysosome for a new LD degradation cycle. An important role in this process is played by Dynamin-2 (DNM2), a regulator of vesicle trafficking that contributes to the generation of new protolysosomes; inhibition of its activity impairs generation of new protolysosomes and therefore LD catabolic process (Schulze et al., 2014). Interestingly, DNM2 was found to be strongly down-regulated by 250  $\mu$ M C14:0 treatment in HepG2 cell lysate – nearly four times as much. These data could be indicative of a

probable decrease in LD catabolism because of the cellular need to enhance LD formation and TG storage. A physical interaction among this protein, DNM2, and transferrin (TF) was highlighted by the STRING analysis, because of the involvement of DNM2 in TF endocytosis (Cao et al., 2010). In contrast with DNM2 decrease, the expression of TF increased following C14:0 250  $\mu$ M treatment. Accordingly, it has been demonstrated that iron-supplementation, as well as holotransferrin supplementation, can protect beta-cells from the lipotoxic effect of C16:0 (Jung et al., 2015). These findings suggest that the increased expression of this protein could represent a cell effort to overcome C14:0-induced stressful effect.

#### **4.1.2 Cytoskeleton remodelling**

In the proteome of HepG2 cell treated with C14:0 a decrease in the expression of some proteins involved in cytoskeleton remodeling, such as destrin (DSTN) and tubulin alpha-1C chain (TUBA1C) was observed (Tab. IIb). Interestingly, depletion of DSTN has been connected with the formation of contractile actin stress fibre associated with enlarged focal adhesion at the plasma membrane (Kanellos et al., 2015). Interestingly, these structures have already been identified in hepatic stellate cells treated with C16:0 (Hetherington et al., 2016). An increase in myosin-10 (MYH10) content in HepG2 cells treated with 125 and 250  $\mu$ M C14:0 was also observed. As myosin is able to compete with DSTN for the binding to actin stress fibres, also causing nuclear deformation (Kanellos et al., 2015), this event could be connected with a possible increase in cell contractility.

#### **4.1.3 ER stress and protein homeostasis**

SFAs, in particular C16:0, were described as being involved in ER stress development and in the consequent UPR in many tissue and cell types, also including HepG2 (Cao et al., 2012; Hetherington et al., 2016; Liu et al., 2016). As far as we know, to date the probable effect of C14:0 on ER stress has never been investigated on HepG2 cell model. However, this effect could be considered as a plausible consequence, also in light of the fact that C14:0 was shown

to enhance C16:0-induced ER stress in primary mouse hepatocytes (Martínez et al., 2015). When supplied alone in culture media, C14:0 caused a lower but significant increase in the expression of ER stress marker, as CCAAT/enhancer-binding protein homologous protein (CHOP) and X-box-binding protein 1 (XBP-1), common targets of canonical cell sensors of ER stress. Accordingly, in the present proteomic investigation an effect of C14:0 on intracellular proteins involved in protein folding homeostasis was observed. As reported in Tab. IIa all the different concentrations used of C14:0 induced an increase in the protein expression of the ectonucleoside triphosphate diphosphohydrolase 5 (ENTPD5), an ER protein which promotes protein N-glycosylation and folding in the ER. Literature data already connected perturbation in the expression of this protein with the ER stress; the knockdown of ENTPD5 in PTEN null cells caused ER stress while the increase of ENTPD5 was shown to prevent ER stress and consequent apoptosis in cancer cells (Fang et al., 2010; Shen et al., 2011). Small glutamine-rich tetratricopeptide repeat-containing protein alpha (SGTA) is another protein whose expression was found to be increased by C14:0 (50-250  $\mu$ M). This protein is involved in the regulation and maintenance of cellular proteostasis, as its main action is to act as a co-chaperone, binding mislocalised membrane proteins and maintaining them in a non-ubiquitylated state, so increasing their opportunity to be delivered to the ER (Wunderley et al., 2014; Roberts et al., 2015). An increase in the expression of this protein already at low concentration of C14:0 (Tab. IIa) could be due to cells' necessity to increase the possibilities of proteins to complete a proper folding, increasing their delivery to the ER. The STRING analysis does not highlight the important physical interaction of SGTA with the proteasomal ubiquitin receptor ADRM1 (also known as hRpn13) already known from literature data (Leznicki et al., 2015; Thapaliya et al., 2016). It seems that SGTA can regulate the access of mislocalised membrane proteins to the proteasome, selectively modulating its substrate degradation. Interestingly, as SGTA, the expression of ADRM1 was also found to be stimulated by all C14:0 treatments in HepG2 cells. These findings give rise to the hypothesis that C14:0 may provoke ER stress due to an increase

in misfolded proteins that could enhance a more stringent control on cellular proteostasis through the increased expression of these key proteins. Proteasomal degradation by means of ERAD is a cellular response following ER stress caused by the accumulation of misfolded proteins (Vembar et al., 2008). As reported in Tab. IIa and from the weak but increasing signal detected in the Western Blot (Fig.5) Vesicle-associated membrane protein-associated protein B/C (VAPB) is another protein found to be modulated by C14:0 treatment. This protein is an ER protein involved in vesicle-trafficking, ER-mitochondrion connection, calcium homeostasis, autophagy and also in the UPR following ER stress as already observed in literature data (Kanekura et al., 2006; Kanekura et al., 2009; Gomez-Suaga et al., 2017). As one of the UPR adaptive response involves the upregulation of molecular chaperones and protein processing enzymes to increase protein folding and handling efficacy (Osowski et al., 2011), the observation of a C14:0 influence on the expression of the mentioned proteins involved in the maintenance of cell proteostasis led to the hypothesis that C14:0 could stimulate ER stress in HepG2 cells, as already observed in primary mouse hepatocytes (Martinez, 2015). Therefore, to detect the UPR possible activation level a Western Blotting investigation was conducted on the expression of the three main ER membrane stress sensors: ATF6 $\alpha$ , IRE1 $\alpha$  and PERK. As can be inferred from Fig.9 this analysis confirmed the activation of the UPR due to the increased signal coming from these proteins in response to C14:0 treatments. When activated by the accumulation of unfolding proteins in the ER, ATF6 $\alpha$  is transported to the Golgi where it is cleaved by site-1 protease (S1P) and site-2 protease (S2P) releasing a 50kDa fragment that migrates to the nucleus and activates a group of genes coding for chaperones and folding enzymes (Zhang et al., 2006). In the present investigation the 90 kDa form of ATF6 $\alpha$  was not detected while two cleaved forms were present in all samples, also including the one present at 36 kDa already reported also in a previous paper (Mao et al., 2007). The signal coming from this cleaved form seems to increase slightly at 250  $\mu$ M C14:0, as a possible sign of increased

ATF6 $\alpha$  cleavage following ER stress. Moreover, when the expression of IRE1 $\alpha$  was investigated an increase in its expression was detected compared to the control sample. Notably, IRE1 $\alpha$  is a ER transmembrane protein that, when activated by the accumulation of unfolded proteins, dimerises and autophosphorylates to become active. Activated IRE1 $\alpha$  splices X-box binding protein 1 (XBP1) mRNA, that in turn encodes a transcription factor that activates UPR target genes; among them there are also genes involved in protein folding, such as Protein Disulfide Isomerase (PDI) (Lee et al., 2003), whose secretion was indeed found to be stimulated by C14:0 in the present investigation (Tab. IIIa). The main marker of UPR activation after C14:0 was the increase in the expression of PERK. This protein is an ER transmembrane protein and, when activated, it oligomerises and autophosphorylates. The present investigation demonstrated for the first time the induction of PERK expression following increasing concentration of C14:0 supplementation and, as visible in Fig.9, a possible increase in the dimeric form was also observed, similar to the one previously observed in literature (Vatolin et al., 2016). Accordingly, previous investigations on the effects of palmitate on HepG2 cell model confirmed the activation of ER stress through the induction of PERK signaling pathway (Cao et al., 2012). Activated PERK inhibits protein biosynthesis through the phosphorylation of the eukaryotic translation initiator factor eIF2 $\alpha$  and the inhibiting the formation of the ternary translation initiation complex eIF2 $\alpha$ /GTP/Met-tRNA. Interestingly, in the present proteome analysis the increased expression of eukaryotic peptide chain release factor GTP-binding subunit ERF3A (eRF3a) (Fig.5) was also reported; this protein has a role in the formation of a complex involved in the protein translation termination (Chauvin et al., 2005) and was the most induced intracellular protein following C14:0 supplementation.

#### 4.1.4 Other effects of myristic acid

In addition, as also reported in the STRING analysis, the expression of Cytochrome c oxidase subunit 5B (COX5B), a component of the mitochondrial cytochrome c oxidase complex, was slightly and gradually increased following C14:0 treatment. Notably, SFAs have already been connected with mitochondrial dysfunction, cause of oxidative stress and mtDNA oxidative damage, and C16:0 was shown to impair the oxidative phosphorylation system (OXPHOS) activity, decreasing the expression of its subunits and accelerating the degradation of OXPHOS complex (Garcia-Ruiz et al., 2015). The slight and gradual increase in COX5B expression could therefore be ascribed to a mechanism activated by HepG2 cells in order to limit ROS generation following C14:0 supplementation (Campian et al., 2007). Interestingly, at 250  $\mu$ M C14:0, and even more at 500  $\mu$ M C14:0 (data not shown), there was a slight increase in the expression of Apolipoprotein E (ApoE). These data are not only in agreement with a previous proteomic analysis showing the increase in ApoE levels in the liver of mice fed with a high-fat diet (Kirpich et al., 2011), but also with the *in vivo* study reported in the first part of the present thesis, where C14:0 was shown to be the second predictor of ApoE in the plasma of analysed patients. This was therefore also a confirmation of the close connection existing between the *in vivo* and *in vitro* part of the study. As reported in the first chapter of the present thesis ApoE, a component of lipoproteins such as chylomicrons and VLDL, has an important role in lipid metabolism and its antioxidant activity has also been described in brain, plasma and adipose tissue (Miyata et al., 1996; Mabile et al., 2003; Davignon, 2005; Tarnus et al., 2009). The increase in ApoE expression can be interpreted both as a consequence of lipid metabolism alteration induced by C14:0 supplementation and also as an effort by cells to counteract the increasing oxidative stress.

SFA have already been connected with the development of inflammation (Fritsche, 2015). In HepG2 cells treated with C14:0 a slight increase in protein connected with the inflammation pathway was observed. This may suggest that high concentrations of C14:0 are stressful for

HepG2 cells, as can be inferred from the slight reduction in cell viability and cell number following C14:0 incubation. In the present PhD thesis a slight increase in proteins connected with the acute phase response has been observed, such as complement C4 (Fig.5), fibrinogen alpha chain (FGA) and the negative acute phase TF protein. Interestingly, these proteins were found to be modulated in the secretome of HepG2 cells when treated with TFA, suggesting that SFA as well as TFA, both known for their adverse effects on cardiovascular health, have an influence on inflammation pathways (Krogager et al., 2015). Another protein involved in acute phase response and modulated by C14:0 treatment was alpha 2- macroglobulin (A2M), whose expression has already been described in HuH7 hepatocarcinoma cells treated cells following FA treatment (Chavez-Tapia et al., 2012).

Finally, the proteomic investigation highlighted an important decrease in Retinol Binding Protein (RBP) in HepG2 cell proteome (Fig.5). RBP4 has been correlated during previous years with enhanced metabolic risk and atherogenesis (Dessein et al., 2014) as well as with hepatic steatosis and also mitochondrial dysfunction (Liu et al., 2016; Meex et al., 2017). Interestingly, as opposed to the expectations, this investigation revealed a decreasing trend of this protein, suggesting a positive influence of C14:0 on mitochondrial dysfunction and fatty liver, that could differentiate it from C16:0 lipotoxic action.

#### **4.2 Myristic acid causes deregulation of secreted proteins involved in exosome and extracellular miRNA sorting**

In the present project the analysis of the differently secreted proteins following C14:0 supplementation was also reported for the first time (Tab. IIIa and IIIb). As highlighted by the DAVID GO analysis (Fig.6) of cellular components, both intracellular proteins and secreted deregulated proteins were described to be exosomes component. Accordingly, the analysis of secretion pathways using both SecretomeP tool and Exocarta database (Tab. IV) confirmed that most of the secreted proteins were proteins already found by literature papers to be secreted by



means of exosome release (Fig.11). Moreover, many of these proteins have already been identified specifically in hepatocytes exosomes (Conde-Vancells et al., 2008).

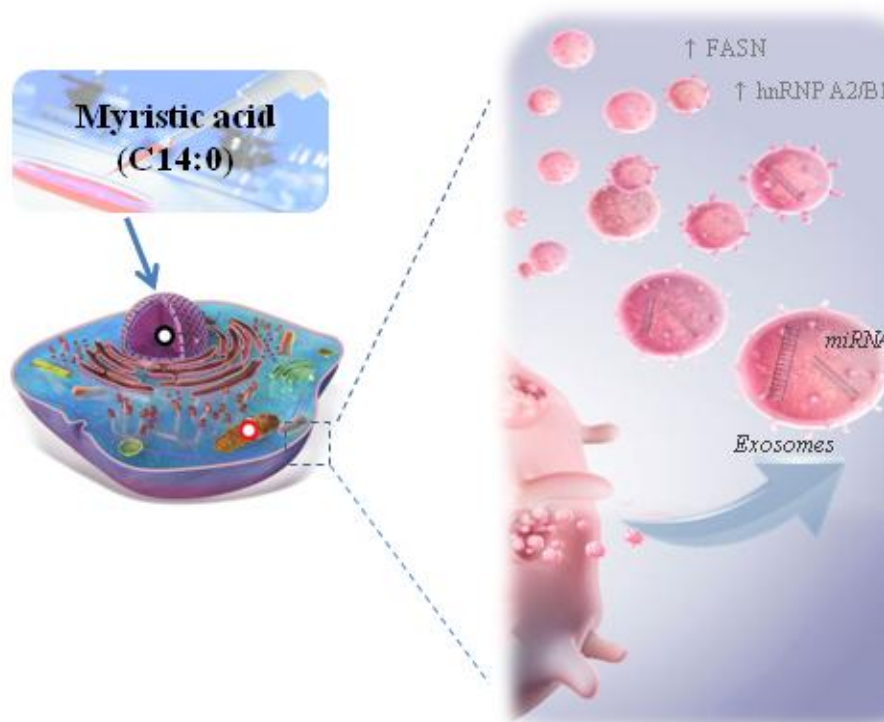


*Fig.11 Myristic acid effects on the secretion of exosome proteins and miRNA sorting in HepG2 cells.*

#### **4.2.1 Proteins related to exosomes**

Fatty acid synthase (FASN) was one of the proteins whose secretion was significantly increased following C14:0 treatment, particularly at 125 and 250 $\mu$ M, as also confirmed by Western Blot investigation (Fig.5). This enzyme has a well-known intracellular role, being involved in the formation of long-chain fatty acids. However, its secretion by means of exosomes has already been demonstrated in cancer cell line, suggesting an extracellular role for this protein (Duijvesz et al., 2013). Interestingly circulating FASN has also been detected in serum of patients and its levels have been described as a possible marker of insulin resistance (Fernandez-Real et al., 2010). Moreover, FASN serum levels were found to be elevated in

patients with liver injury, mainly steatohepatitis (Marsillach et al., 2009); this observation led therefore to the hypothesis that C14:0 could be connected with the development of liver injury.

#### **4.2.2 miRNA sorting**

As confirmed by Western Blot analysis (Fig.5) an increase in the secretion of Heterogeneous nuclear ribonucleoproteins A2/B1 (hnRNPA2/B1) was observed. The hnRNP family is comprised of >20 proteins that contribute to the complex around nascent pre-mRNA and are thus able to modulate RNA processing. It has been described that secreted hnRNPA2B1 is a key player in miRNA sorting into exosomes and is released by cells during this process (Villarroya-Beltri et al., 2013). hnRNPA1, another protein of the same family similar in its structure to hnRNPA2B1, showed increased translocation from the nucleus to the cytosol following ER stress and in particular following FAs supplementation in HepG2 cells (Damiano et al., 2013; Siculella et al., 2016). It is therefore possible to hypothesise that C14:0 also has an influence on the increased cell localisation of hnRNPA2B1 that can cause an increase in its exosomal loading. The presence of hnRNP A2/B1 in the secretome of HepG2 treated cells supported the evidence of increased protein secretion through exosomes following C14:0 supplementation. Interestingly, in the last few years microRNA and exosomes have emerged as important players in the atherosclerotic process (Huber et al., 2015; Loyer et al., 2015) and the involvement of C14:0 in their liver release would be an important aspect for further research..

#### **4.2.3 Other effects of myristic acid**

Interestingly, the secretion of many interacting Heat Shock Proteins (HSPs) was induced by C14:0, including Heat Shock protein 70 (HSPA1), Heat shock cognate protein 71 (HSPA8), Heat Shock Protein Family A Member 9 (HSPA9) and Heat Shock protein HSP 90-beta (HSP90AB1) (Fig.8B). HSPs are molecular chaperones and their intracellular role is connected with the response to various stress stimuli. Recent investigations however have highlighted the extracellular role of these proteins: they have described HSPs as “alert stress signals” secreted

by non-conventional pathways, that can inform other cells - in particular immune system cells - about the stressor presence, avoiding the propagation of the stress insult and increasing stress resistance (De Maio et al., 2013; Santos et al., 2017). Although the role of HSPs in atherosclerosis remains controversial, HSPs were thought to act as autoantigens, and trigger both cell- and antibody-mediated immune responses (Lu et al., 2010). In particular, Hsp70 represented an important node in this hub, as it has been proposed as a predictor of acute coronary syndrome risk and was found to be elevated in patients with chronic heart failure (Genth-Zotz et al., 2004; Zhang et al., 2010). Taken together these observations on the increased secretion of HSPs confirmed the conclusion of a stressful influence of C14:0 on HepG2 cells, that could eventually enhance the atherosclerotic process.

The over-secretion of Protein Disulfide-Isomerase A3 (PDIA3) was also observed at 250  $\mu$ M C14:0. Interestingly, previous studies demonstrated that treatment of liver cells with saturated fatty acids cause ER stress, UPR and apoptosis together with an increase in the expression of PDIA3, a protein involved in protein folding; moreover this protein was found to be induced in liver samples of patients affected by NAFLD (Wang et al., 2010; Zhang et al., 2015). These studies highlight an important role of PDIA3 in the development of steatosis. In addition, according to the present obtained data, this protein could play an important part in the extracellular environment, as it has already been demonstrated that the ER stress attenuates the secretion of misfolded proteins and prevent their extracellular aggregation through the secretion of molecular chaperones (Genereux et al., 2015). The presence of this protein among the over-secreted following C14:0 treatment strengthens the demonstration of ER stress induction and the evidence supporting the influence on UPR on the regulation of extracellular protein homeostasis.

As reported in the Cytoscape analysis in Fig.8B, another cluster of over-secreted proteins following C14:0 supplementations included enzymes involved in carbohydrate metabolism,

such as Enolase-1 (ENO1), Lactate dehydrogenase (LDHA) and Pyruvate kinase (PKM). The presence of these proteins in the secretome of HepG2 should not come as a surprise as they have been previously identified in the exosomes derived from hepatocytes (Conde-Vancells et al., 2008). Glycolytic enzymes can have important extracellular roles such as cell-cell communication and infections (Gomez-Arreaza et al., 2014). ENO-1 in particular has been described as a multifunctional protein, with an important role in pathophysiological situations (Diaz-Ramos et al., 2012). It is also expressed on the surface of many cell types and has been defined as a marker of pathological stress. Moreover, the secretion by HepG2 cells of ENO1 has already been described following viral cell infection (Higa et al., 2014). Taking together these observations led to the assumption that the secretion of glycolytic enzymes can also represent a cell stress signal following increasing concentration of C14:0 in cell culture media.

In summary, this proteomic research permitted for the first time the detection of both intracellular and secreted proteins deregulated by C14:0 in HepG2 cells. These findings certainly contribute to the disclosure of the biological effects induced by C14:0 at a molecular level, involved in its adverse health effects on the atherosclerotic process, in the development of NAFLD, and consequently in the onset of CAD. While in the proteome of HepG2 cells some proteins involved in cytoskeleton reorganisation and ER stress response were found to be modulated indicating their possible involvement in the development of NAFLD, in the secretome of HepG2 cells many proteins involved in cellular stress have been reported that could in the future be evaluated as a possible marker of liver stress and steatosis.

## **CHAPTER 3**

# **COMPARATIVE PROTEOMIC STUDY OF THE BIOCHEMICAL EFFECTS INDUCED BY MYRISTIC, OLEIC AND PALMITIC ACIDS**

## **1. INTRODUCTION**

While the molecular effects induced by C14:0 treatment of HepG2 cells are still poorly known, the effects of C16:0 and C18:1 have been analysed in depth during the last few years. The investigations relating to the effects of these two FAs mainly aimed at elucidating cellular mechanisms involved in FA-related hepatic lipotoxicity and in the consequent development of NAFLD. The earliest studies investigated the effects induced by the combination of these two FAs on hepatic lipotoxicity. In particular, Feldstein et al. used a combination of C18:1 and C16:0 (2:1 ratio) on the HepG2 cell model and reported an increase in lysosomal permeabilisation and an NF- $\kappa$ B-dependent stimulation of TNF- $\alpha$  expression, an important mediator of insulin resistance, TG accumulation and hepatic steatosis (Feldstein et al., 2004). Further studies reported that the same combination of FAs induces LD accumulation in HepG2 cells in a concentration-dependent manner (Yao et al., 2011). The authors also reported induction of nuclear condensation and fragmentation typical of late apoptosis and necrosis confirming the lipotoxic effect triggered by FAs.

However, C16:0 and C18:1 behave extremely different as they belong to two different FA classes. C18:1, an important component of many vegetable oils, such as olive oil, represents the MUFA, with C18:1 being the most abundant MUFA in human plasma. Accordingly, (as reported in Tab. III Chapter 2 Section1 of the present thesis) C18:1 was the most abundant unsaturated FA in the studied population, representing 24.5% of total detected FAs.

On the other hand, C16:0, present in cheese, meat, butter and in some oils, is the most abundant SFA (24% of total FA plasma content) and is a representative of the SFAs class. When the cellular effects of FAs were compared in the HepG2 cell model, by means of DAPI staining of

apoptotic nuclei and measuring caspase activation, all the individual FAs induced cellular steatosis but saturated FAs, including C16:0 and stearic acid (C18:0), caused increased toxicity and apoptosis (Malhi et al., 2006). Cell death was caspase-dependent and associated with mitochondrial membrane depolarisation and cytochrome c release. Further comparative studies demonstrated that steatosis extent was greater in presence of C18:1 in cell culture media, but cell apoptosis was inversely proportional to LD accumulation (Ricchi et al., 2009). Therefore, while C16:0 increased the rate of apoptosis and impaired insulin signaling, C18:1 showed a more steatogenic but less apoptotic behaviour. A subsequent study confirmed the higher ability of C18:1 to induce TG-enriched LD formation when compared to C16:0 treatment (Mei et al., 2011). Moreover, together with LD accumulation the appearance of autophagosomes was observed in C18:1-treated HepG2 cells. On the other hand, C16:1 was found to be poorly converted into TG-enriched LD, to suppress autophagy and induce a caspase-dependent cleavage of Beclin-1, suggesting a connection between the apoptotic and autophagic processes. This study highlighted the fact that C18:1 LD formation and autophagy induction could represent an important protective mechanism against FAs-induced lipotoxicity. A more recent comparative study confirmed the cytotoxicity induced only by C16:0 supplementation in cell culture media and showed that this FA induced ER stress in both HepG2 and primary human activated hepatic stellate cells (Hetherington et al., 2016). The influence of C16:0 on ER stress markers had been already demonstrated by previous studies that reported the concurrent decrease of Hypoxia-inducible factor-1 (HIF-1 $\alpha$ ), a transcription factor that acts as regulator of oxygen homeostasis (Yoo et al., 2014). Mitochondrial dysfunction, oxidative stress, decreased mitochondrial DNA damage and a decrease in OXPHOS activity were also described as key features of HepG2 cell supplemented with SFAs (Garcia-Ruiz et al., 2015). Taken together, C16:0 and C18:1 have been found to have divergent cellular effects, with C16:0 inducing ER stress, ROS and apoptosis and C18:1 enhancing TG formation, lipoproteins assembly and LD accumulation as well as autophagy (Fig.1).

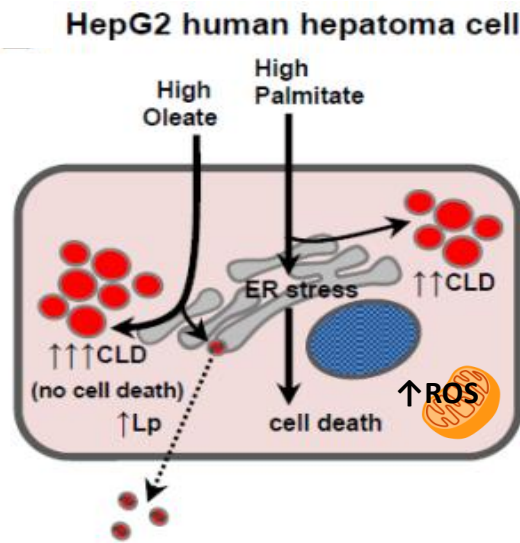


Fig.1 Main known effects induced by palmitic and oleic acid on HepG2 cell model. Adapted from Hetherington, 2016. CLD: cytosolic lipid droplets, ER: endoplasmic reticulum; Lp: lipoproteins; ROS: Reactive Oxygen Species.

However, a comprehensive investigation and comparison of the overall effects of these FAs on the HepG2 cellular proteome is still missing. Therefore, the aim of the following investigation was to assess the effects of C14:0, C16:0, or C18:1 on protein expression of HepG2 cells as determined by shotgun LC-MS/MS analysis. In the present chapter the proteomic effects of C14:0 were compared with those of these two well-known FAs, in order to highlight proteomic modulations and molecular mechanisms shared among all the three FAs, SFAs and to identify in particular proteome changes specifically induced by C14:0. This additional comparison could therefore be essential in order to better describe the specific and unique effects of C14:0 at cellular levels, facilitating elucidation of C14:0-related biological process and pathological consequences.

## 2. EXPERIMENTAL DESIGN AND PROCEDURES

*This experimental part, and in particular the MS analysis, was performed thanks to the kind collaboration of Prof. Ruth Birner-Gruenberger laboratory (Laboratory of “Functional Proteomics and Metabolic Pathways” at the Medical University of Graz, Austria).*

### 2.1 Cell culture and fatty acid conditioning

HepG2 cells were grown in the same conditions mentioned in the previous chapter (Chapter 2 Section 2). Briefly, they were cultured in RPMI 1640 media (Sigma-Aldrich), supplemented with 10% FBS, 100 U/ml penicillin and 100 µg/ml streptomycin, 4mM L-glutamine and were maintained in a humidified incubator at 37°C in an atmosphere of 5% CO<sub>2</sub>. The FBS was removed from the HepG2 culture media six hours before FA conditioning. C16:0 and C18:1 were complexed to Bovine Serum Albumin (Fatty Acid Free BSA, Sigma-Aldrich) in a 6:1 molar ratio, similarly to the C14:0 solution and as previously described (Pike et al., 2011). Sodium palmitate and oleate (Sigma-Aldrich) were dissolved in 150 mM sodium chloride stirring at 70°C in water bath. FAs solutions were then added dropwise to a previously prepared BSA solution dissolved in 150mM NaCl, and stirred one hour at 37°C. The obtained C16:0-BSA and C18:1-BSA stock solutions 1mM were filtered and stored at -20°C until further use. At the time of the experiments the solutions of FAs conjugated with BSA were added to cell culture FBS-free media at the following concentrations: 50, 125, 250 µM and 500 µM, while only the BSA was added to controls. Again, incubations were carried out for 24 hours and three biological replicates were used for each FAs concentration. As performed for C14:0 samples, after the incubation cells were washed with PBS solution and harvested using trypsin. Cell viability and number were evaluated by means of CASY technology and then samples were subjected to the following experimental workflow (Fig.2):



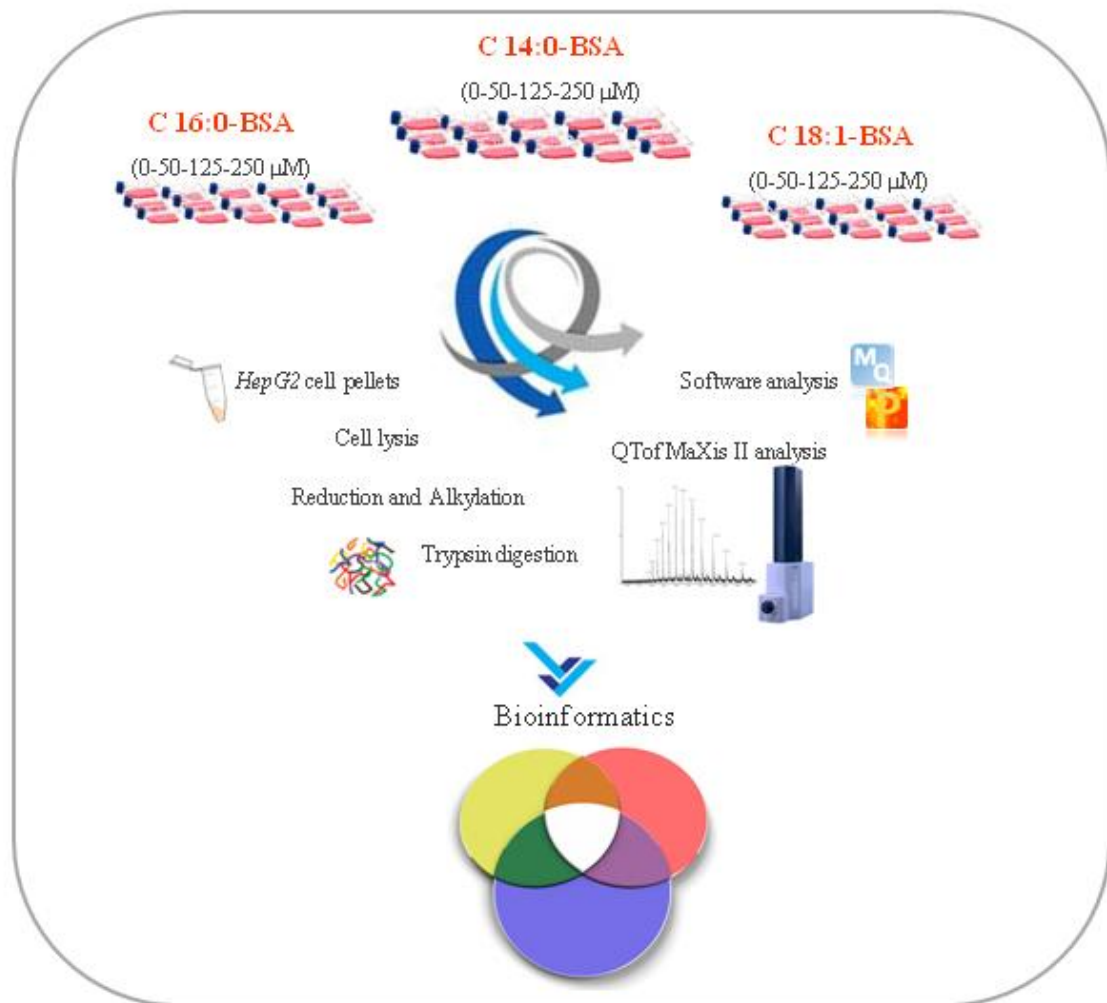


Fig.2 Experimental workflow

## 2.2 Oil Red O staining

To assess C16:0 and C18:1 incorporation the LD formation was investigated by means of Oil Red O solution, as performed for C14:0-treated HepG2 and described in Chapter 2 Section 2. Briefly, HepG2 cells were grown on a cover slip inside a 6-well plate and incubated with C16:0-BSA and C18:1-BSA at the highest concentration used for the analysis for 24 hours. After fixation, cells were stained with a solution of 0.6 % Oil Red O in 60% isopropanol for 15 minutes, for LD visualisation and with hematoxylin for 4 minutes highlight cell nuclei. Slide were removed from the well and examined using 100X magnification under light microscope.

### 2.3 Sample preparation and mass spectrometry analysis

Due to the negative effect of high concentrations of FAs on cell viability and to maintain the same concentrations of FAs used in the C14:0 investigation, only treatments with 50, 125 and 250  $\mu\text{M}$  FAs were selected for the proteomic analysis. The procedure used for sample preparation and analysis by means of mass spectrometry was the same as used for C14:0-treated HepG2 cells sample preparation, described in Chapter 2 of the present section. Cells were lysed in PBS by sonication and cell debris was removed with centrifugation at 3000g for ten minutes at 4°C. Protein concentrations were determined using Bradford Protein assay (Bio-Rad). 10  $\mu\text{g}$  of protein was taken from each sample for protein digestion. Tris-HCl-TFE buffer pH 8.5 (25% trifluoroethanol, 25%  $\text{H}_2\text{O}$ , 50% Tris-HCl 100 mM) was added to each sample. Reduction step was performed using TCEP, (tris(2-carboxyethyl)phosphine), pH 8.5 10mM final concentration. CAA (chloroacetamide) 40 mM dissolved in Tris-HCl pH 8.5 was used for alkylation. Samples were shaken for ten minutes at 95°C and diluted to have 10% TFE with 50mM ammonium bicarbonate. Protein digestion was performed by adding 1 $\mu\text{g}/\mu\text{L}$  of trypsin to every 50  $\mu\text{g}$  of proteins and an overnight incubation at 37 °C was performed. Obtained peptides were then diluted in solvent A (0.3% FA, 5% ACN) and stored at -20 °C until further LC-MS/MS analysis. For each sample an aliquot of 500 ng of each sample was injected in a nano-HPLC (Dionex Ultimate 3000) equipped with a C18, 5  $\mu\text{m}$ , 100 Å, 5 x 0.3 mm, enrichment column and an Acclaim PepMap RSLC nanocolumn (C18, 2  $\mu\text{m}$ , 100 Å, 500 x 0.075 mm) (Thermo Fisher Scientific). Each sample was then analysed by means of an II<sup>TM</sup> ETD high-resolution LC-QTOF mass spectrometer (Bruker Daltonics). Details on the enrichment and settings of the mass spectrometry instrument are reported in Chapter 2 of the present section. The MS/MS data were analysed for protein identification and quantification using Data analysis software (Bruker), Sum Peak algorithm, and by MaxQuant 1.5.3.30 against the human public database SwissProt database with taxonomy homo sapiens (downloaded on

11.06.2015, 42150 sequences) and common contaminants. Modification settings and search criteria were maintained equal to the C14:0 samples analysis described above. Importantly, two identified peptides were used as minimum requirement for protein identification. Data processing was performed with Perseus software version 1.5.0.31. Known contaminants were removed from the result list. LFQ intensities were  $\log_2$  transformed to lower the effect of the outlier values.

The protein lists were filtered to keep only protein groups with at least three valid values in at least one FA concentration, meaning that in at least one FA treatment the protein had to be identified in all three biological replicates. For protein groups missing LFQ values, this value was obtained by means of an imputation step with Perseus software in which the values were replaced with random values taken from the Gaussian distribution of values, to simulate an LFQ value for those low abundant protein groups. Perseus default parameters -width of 0.3 and downshift of 1.8 separately for each column - were used for imputation. For each protein group  $\log_2$  differences were calculated as the difference between the averages of  $\log_2$  LFQ intensities of the treated samples and controls. For statistical analysis R software (RCoreTeam, 2015) was employed. ANOVA with subsequent multiple testing correction with Benjamini-Hochberg (Benjamini et al., 1995) method was used to identify altered protein groups. Tukey's Honest Significant Differences test on protein groups significant after the ANOVA was used for the comparison of protein groups among different samples. Only proteins with p-value  $< 0.05$  and fold change greater than  $\pm 1.3$  were considered significantly modulated both in C16:0 and C18:1 treated samples.

#### **2.4 Comparative proteomic analysis to assess the effects of myristic, oleic and palmitic acid**

The analysis of deregulated proteins shared among different FA treatments was performed by means of Functional Enrichment Analysis Tool (FunRich) (<http://www.funrich.org/>) which was

used for the generation of Venn diagrams (Pathan et al., 2015). The Gene Ontology (Finegold et al.) analyses were performed on proteins specifically regulated by single FAs by means of the DAVID v6.8 Functional Annotation Bioinformatics Tools (<https://david.ncifcrf.gov/>) (Huang da et al., 2009) as previously described (Chapter 2, Section 2).

### 3. RESULTS

#### 3.1 Effects of palmitic and oleic acid on HepG2 cell viability and lipid droplets

The effects of C16:0 and C18:1 (50-125-250-500  $\mu\text{M}$ ) on HepG2 cell viability after 24 hours of incubations were investigated by means of CASY technology. Graphical representation of the results of viability measurements following C16:0 and C18:1 supplementations are reported in Fig.3 and Fig.4 respectively.

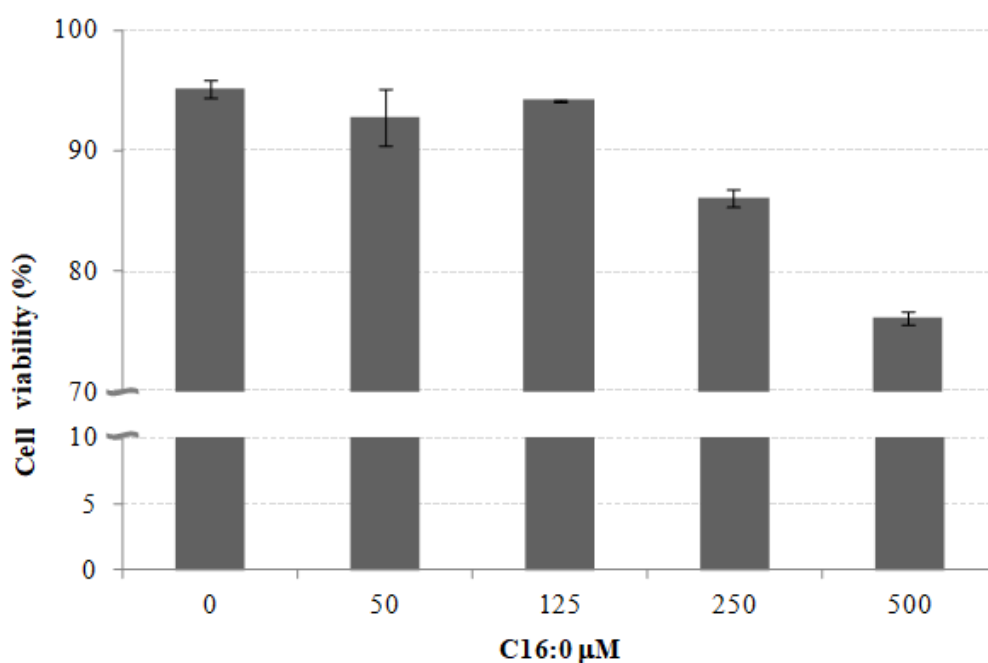


*Fig.3 HepG2 cell viability, measured by using CASY technology, after 24h treatment with different concentrations of C16:0 (0, 50, 125, 250 and 500  $\mu\text{M}$ ) conjugated with BSA. All experiments were performed at least in triplicate.*

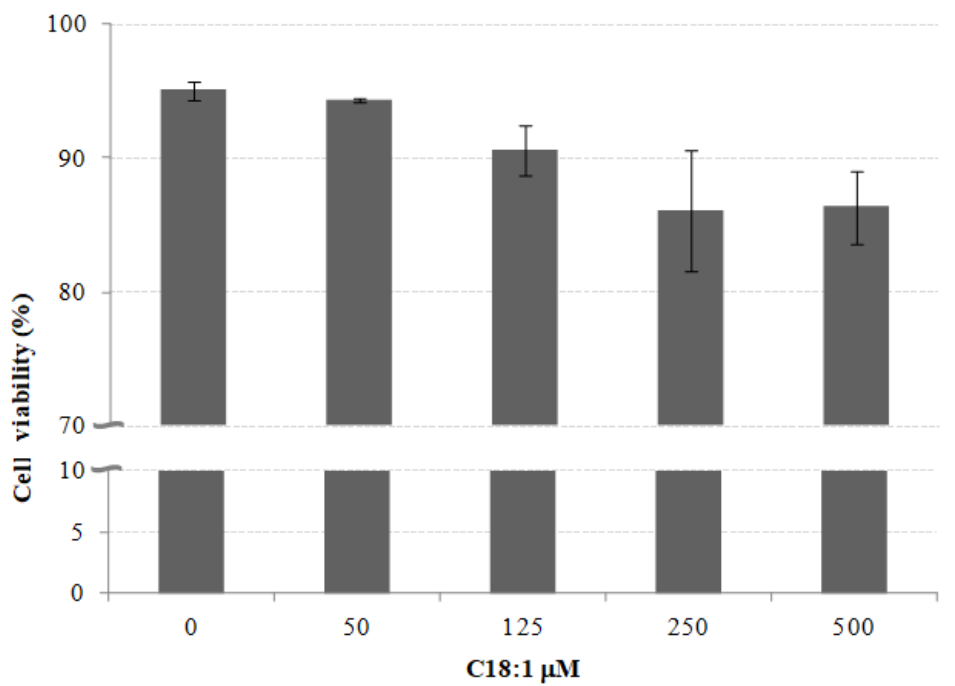


*Fig.4 HepG2 cell viability, measured by using CASY technology, after 24h treatment with different concentrations of C18:1 (0, 50, 125, 250 and 500  $\mu\text{M}$ ) conjugated with BSA. All experiments were repeated at least in triplicate.*

HepG2 cell viability decreased with both FAs treatments and this was particularly true in a concentration dependent manner for C18:1. However, while a slight decrease in cell viability was observed with the highest concentration of C18:1, the viability decreased significantly with the highest concentration of C16:0 treatment to 76%.

To be able to confirm the cellular uptake of FAs dissolved in BSA from the culture media and their incorporation into TG and LD, HepG2 treated with both FAs were stained with the lipid-soluble Oil Red O, as previously performed on C14:0-treated cells. C16:0 induced a significant accumulation of LD inside cell cytoplasm (Fig.5B) and condensed hematoxylin-stained nuclei when compared to control cells (Fig.5A). C18:1 induced an even more pronounced increase in LD content, and LD reached greater dimensions and highest number per single cell (Fig.5C) when compared to C16:0.

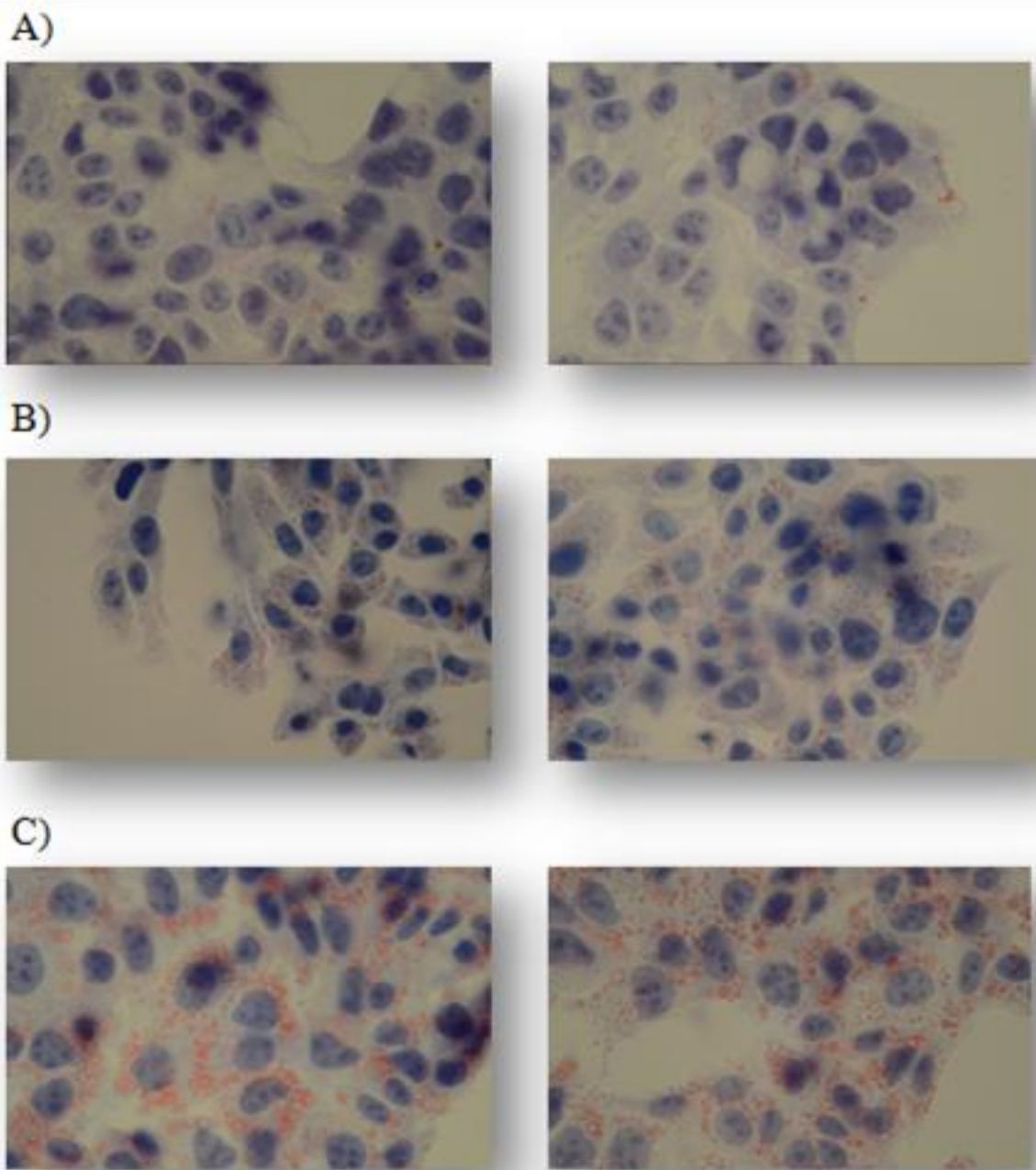


*Fig.5 Effects of C16:0 and C18:1 loading on lipids and LD accumulation. A) control HepG2 cells, B) C16:0-treated HepG2 cells and C) C18:1-treated HepG2 cells.*

### 3.2 Quantitative analysis of proteins deregulated by palmitic and oleic acid in HepG2 cell proteome

MS analyses were performed on HepG2 cells treated with C16:0 and C18:1 (0-50-125-250  $\mu$ M). Only protein groups identified with at least three valid values in one condition –at least one concentration in which the identification succeeded in all three biological replicates- were considered for further analyses. The abundance of proteins was determined by label free MS1-based quantitation and subjected to statistical analysis, namely ANOVA test followed by Tukey's Honest Significant Differences test, to disclose proteins differently modulated in HepG2 cells by C16:0 and C18:1. The 37 proteins whose expression was found to be increased by C16:0 in culture media are reported in Tab. I, while the 34 down-regulated proteins are reported in Tab. II. The expressions of 80 proteins were found to be modulated by C18:1 treatments in HepG2 cells. Details on the 40 up-regulated proteins are reported in Tab. III while the 40 down-regulated proteins are listed in Tab. IV.

Major Protein ID	Protein name	Gene name	ANOVA	50-0 p adj	Fold change 0-50	125-0 p adj	Fold change 0-125	250-0 p adj	Fold change 0-250
Q99541	Perilipin-2	PLIN2	<b>0.0003</b>	0.433	0.60	0.139	<b>2.11</b>	<b>0.001</b>	<b>5.76</b>
Q15043	Zinc transporter ZIP14	SLC39A14	<b>0.0007</b>	0.498	<b>1.43</b>	<b>0.024</b>	<b>2.27</b>	<b>0.000</b>	<b>5.08</b>
P07305	Histone H1.0	H1FO	<b>0.0031</b>	<b>0.003</b>	<b>3.05</b>	<b>0.008</b>	<b>2.65</b>	<b>0.000</b>	<b>4.41</b>
P13995	Bifunctional methylenetetrahydrofolate dehydrogenase/cyclohydrolase. mitochondrial	MTHFD2	<b>0.0000</b>	<b>0.000</b>	<b>2.74</b>	<b>0.000</b>	<b>2.83</b>	<b>0.000</b>	<b>3.60</b>
P09874	Poly [ADP-ribose] polymerase 1	PARP1	<b>0.0076</b>	0.178	<b>1.59</b>	0.132	<b>1.66</b>	<b>0.001</b>	<b>3.22</b>
Q9HCU5	Prolactin regulatory element-binding protein	PREB	<b>0.0048</b>	0.767	<b>1.37</b>	0.301	<b>1.75</b>	<b>0.035</b>	<b>2.59</b>
P43307	Translocon-associated protein subunit alpha	SSR1	<b>0.0000</b>	<b>0.010</b>	<b>1.52</b>	<b>0.033</b>	<b>1.41</b>	<b>0.000</b>	<b>2.57</b>
P61803	Dolichyl-diphosphooligosaccharide--protein glycosyltransferase subunit DAD1	DAD1	<b>0.0397</b>	1.000	1.00	1.000	1.01	<b>0.034</b>	<b>2.29</b>
Q9Y2V2	Calcium-regulated heat stable protein 1	CARHSP1	<b>0.0204</b>	0.246	<b>1.76</b>	<b>0.017</b>	<b>2.77</b>	0.087	<b>2.11</b>
O95573	Long-chain-fatty-acid--CoA ligase 3	ACSL3	<b>0.0042</b>	0.840	1.20	<b>0.028</b>	<b>1.90</b>	<b>0.014</b>	<b>2.06</b>
P08195	4F2 cell-surface	SLC3A2	<b>0.0000</b>	<b>0.003</b>	<b>1.43</b>	<b>0.005</b>	<b>1.40</b>	<b>0.000</b>	<b>2.01</b>



	antigen heavy chain								
Q7L0Y3	Mitochondrial ribonuclease P protein 1	TRMT10C	<b>0.0037</b>	0.139	<b>1.72</b>	<b>0.044</b>	<b>2.01</b>	0.056	<b>1.95</b>
Q9NVI7	ATPase family AAA domain-containing protein 3A	ATAD3A	<b>0.0152</b>	0.462	<b>1.41</b>	0.312	<b>1.51</b>	<b>0.049</b>	<b>1.94</b>
P05141	ADP/ATP translocase 2	SLC25A5	<b>0.0000</b>	0.201	1.26	0.376	1.20	<b>0.001</b>	<b>1.83</b>
P22695	Cytochrome b-c1 complex subunit 2. mitochondrial	UQCRC2	<b>0.0002</b>	0.683	1.24	0.565	1.28	<b>0.032</b>	<b>1.78</b>
P52292	Importin subunit alpha-1	KPNA2	<b>0.0001</b>	<b>0.002</b>	<b>2.19</b>	<b>0.024</b>	<b>1.69</b>	<b>0.019</b>	<b>1.73</b>
P06576	ATP synthase subunit beta. mitochondrial	ATP5B	<b>0.0000</b>	0.354	1.12	0.078	1.20	<b>0.000</b>	<b>1.71</b>
P21796	Voltage-dependent anion-selective channel protein 1	VDAC1	<b>0.0009</b>	1.000	0.98	0.993	1.06	<b>0.026</b>	<b>1.67</b>
Q9HDC9	Adipocyte plasma membrane-associated protein	APMAP	<b>0.0000</b>	0.800	1.07	0.430	1.12	<b>0.000</b>	<b>1.66</b>
P84098	60S ribosomal protein L19	RPL19	<b>0.0012</b>	0.185	1.26	<b>0.028</b>	<b>1.42</b>	<b>0.003</b>	<b>1.63</b>
P28331	NADH-ubiquinone oxidoreductase 75 kDa subunit. mitochondrial	NDUFS1	<b>0.0000</b>	0.119	1.23	<b>0.049</b>	1.29	<b>0.001</b>	<b>1.62</b>
Q9UHG3	Prenylcysteine oxidase 1	PCYOX1	<b>0.0052</b>	1.000	1.01	0.912	1.12	<b>0.039</b>	<b>1.57</b>
P00387	NADH-cytochrome b5 reductase 3	CYB5R3	<b>0.0033</b>	0.960	1.06	0.621	1.14	<b>0.010</b>	<b>1.48</b>
P25705	ATP synthase subunit alpha. mitochondrial	ATP5A1	<b>0.0000</b>	1.000	1.00	1.000	1.00	<b>0.002</b>	<b>1.48</b>
P10606	Cytochrome c oxidase subunit 5B. mitochondrial	COX5B	<b>0.0000</b>	1.000	1.01	0.983	0.95	<b>0.038</b>	<b>1.44</b>
P04843	Dolichyl-diphosphooligosaccharide--protein glycosyltransferase subunit 1	RPN1	<b>0.0008</b>	0.986	1.05	0.729	1.14	<b>0.046</b>	<b>1.44</b>
Q9UJS0	Calcium-binding mitochondrial carrier protein Aralar2	SLC25A13	<b>0.0005</b>	0.976	0.95	1.000	1.01	<b>0.035</b>	<b>1.38</b>
P40939	Trifunctional enzyme subunit alpha. mitochondrial	HADHA	<b>0.0000</b>	0.819	1.04	0.913	1.03	<b>0.000</b>	<b>1.37</b>
P55084	Trifunctional enzyme subunit beta. mitochondrial	HADHB	<b>0.0004</b>	0.969	0.95	0.991	1.03	<b>0.016</b>	<b>1.37</b>
P10809	60 kDa heat shock protein. mitochondrial	HSPD1	<b>0.0001</b>	0.682	1.13	0.737	1.12	<b>0.045</b>	<b>1.36</b>
Q16822	Phosphoenolpyruvate carboxykinase [GTP]. mitochondrial	PCK2	<b>0.0000</b>	0.890	0.94	0.309	1.14	<b>0.005</b>	<b>1.35</b>
Q6UB35	Monofunctional C1-tetrahydrofolate synthase. mitochondrial	MTHFD1L	<b>0.0003</b>	0.888	1.07	0.045	1.29	<b>0.019</b>	<b>1.34</b>
O75390	Citrate synthase. mitochondrial	CS	<b>0.0000</b>	0.974	1.04	0.998	0.98	<b>0.006</b>	<b>1.33</b>
P24752	Acetyl-CoA acetyltransferase. mitochondrial	ACAT1	<b>0.0000</b>	0.999	0.98	0.999	0.98	<b>0.044</b>	<b>1.33</b>
P49748	Very long-chain specific acyl-CoA dehydrogenase. mitochondrial	ACADVL	<b>0.0000</b>	0.999	0.99	0.087	1.18	<b>0.004</b>	<b>1.32</b>

Q9NX58	Cell growth-regulating nucleolar protein	LYAR	<b>0.0006</b>	<b>0.001</b>	<b>2.36</b>	<b>0.002</b>	<b>2.17</b>	0.828	1.16
P53396	ATP-citrate synthase	ACLY	<b>0.0104</b>	<b>0.031</b>	<b>1.40</b>	0.387	1.19	0.737	1.12

Tab. 1 Proteins significantly up-regulated by different concentrations of C16:0 treatment in HepG2 cell proteome with relative fold change compared to controls (ANOVA p-value adjusted with Benjamini-Hochberg method; Tukey's HSD p-value adjusted for multiple comparisons). Significant p-values and fold changes higher than 1.3 are highlighted in bold type.

Major Protein ID	Protein name	Gene name	ANOVA	50-0 p adj	fold change 0-50	125-0 p adj	fold change 0-125	250-0 p adj	fold change 0-250
P62854	40S ribosomal protein S26	RPS26	<b>0.0221</b>	<b>0.028</b>	<b>-9.36</b>	0.694	<b>-2.22</b>	<b>0.018</b>	<b>-11.18</b>
P62318	Small nuclear ribonucleoprotein Sm D3	SNRPD3	<b>0.0340</b>	0.583	<b>-2.49</b>	<b>0.021</b>	<b>-10.31</b>	<b>0.021</b>	<b>-10.30</b>
O43852	Calumenin	CALU	<b>0.0091</b>	1.000	-1.07	0.588	<b>-1.90</b>	<b>0.013</b>	<b>-5.99</b>
P62266	40S ribosomal protein S23	RPS23	<b>0.0254</b>	0.714	<b>-1.76</b>	0.956	-1.35	<b>0.019</b>	<b>-5.63</b>
O14980	Exportin-1	XPO1	<b>0.0008</b>	0.994	1.10	1.000	-1.00	<b>0.001</b>	<b>-4.13</b>
O43493	Trans-Golgi network integral membrane protein 2	TGOLN2	<b>0.0080</b>	0.786	<b>-1.34</b>	0.149	<b>-1.96</b>	<b>0.003</b>	<b>-3.75</b>
Q9NVS9	Pyridoxine-5-phosphate oxidase	PNPO	<b>0.0088</b>	0.945	-1.27	0.980	-1.19	<b>0.022</b>	<b>-3.45</b>
Q9UHB9	Signal recognition particle subunit SRP68	SRP68	<b>0.0000</b>	1.000	1.01	1.000	-1.00	<b>0.000</b>	<b>-3.16</b>
P50552	Vasodilator-stimulated phosphoprotein	VASP	<b>0.0168</b>	<b>0.028</b>	<b>-2.58</b>	0.076	<b>-2.18</b>	<b>0.012</b>	<b>-3.00</b>
Q9H773	dCTP pyrophosphatase 1	DCTPP1	<b>0.0104</b>	0.987	1.14	0.922	-1.24	<b>0.042</b>	<b>-2.47</b>
P02751	Fibronectin	FN1	<b>0.0288</b>	<b>0.042</b>	<b>-3.27</b>	0.291	<b>-2.08</b>	0.240	<b>-2.18</b>
Q9BY77	Polymerase delta-interacting protein 3	POLDIP3	<b>0.0006</b>	0.643	-1.18	0.774	-1.15	<b>0.001</b>	<b>-2.13</b>
Q86TG7	Retrotransposon-derived protein PEG10	PEG10	<b>0.0060</b>	<b>0.035</b>	<b>-1.88</b>	0.014	<b>-2.10</b>	<b>0.039</b>	<b>-1.85</b>
Q00839	Heterogeneous nuclear ribonucleoprotein U	HNRNPU	<b>0.0007</b>	0.997	-1.05	0.899	-1.12	<b>0.007</b>	<b>-1.83</b>
P63261	Actin, cytoplasmic 2	ACTG1	<b>0.0168</b>	0.219	<b>-1.31</b>	0.263	-1.29	<b>0.016</b>	<b>-1.61</b>
P63162	Small nuclear ribonucleoprotein-associated protein N	SNRPN	<b>0.0267</b>	0.447	<b>-1.80</b>	<b>0.022</b>	<b>-3.61</b>	0.640	<b>-1.60</b>
Q16181	Septin-7	SEPT7	<b>0.0398</b>	<b>0.045</b>	<b>-1.73</b>	0.996	-1.06	0.148	<b>-1.52</b>
Q7L5N1	COP9 signalosome complex subunit 6	COPS6	<b>0.0062</b>	0.925	-1.08	0.976	1.05	<b>0.008</b>	<b>-1.51</b>
Q9BQP7	Mitochondrial genome maintenance exonuclease 1	MGME1	<b>0.0029</b>	<b>0.022</b>	<b>-2.20</b>	0.372	-1.48	0.340	<b>-1.51</b>
P22626	Heterogeneous nuclear ribonucleoproteins A2/B1	HNRNPA2B1	<b>0.0000</b>	0.908	-1.08	0.253	-1.22	<b>0.014</b>	<b>-1.45</b>
Q13428	Treacle protein	TCOF1	<b>0.0000</b>	0.572	-1.14	0.620	-1.13	<b>0.017</b>	<b>-1.40</b>
Q16698	2,4-dienoyl-CoA reductase, mitochondrial	DECR1	<b>0.0033</b>	<b>0.034</b>	<b>-1.70</b>	0.575	-1.26	0.273	<b>-1.38</b>

P11717	Cation-independent mannose-6-phosphate receptor	IGF2R	<b>0.0182</b>	0.129	-1.22	<b>0.006</b>	<b>-1.42</b>	<b>0.015</b>	<b>-1.35</b>
Q04828	Aldo-keto reductase family 1 member C1	AKR1C1	<b>0.0246</b>	<b>0.019</b>	<b>-1.48</b>	0.449	-1.19	0.081	<b>-1.35</b>
P27797	Calreticulin	CALR	<b>0.0161</b>	0.995	-1.03	<b>0.022</b>	-1.31	<b>0.013</b>	<b>-1.35</b>
P14174	Macrophage migration inhibitory factor	MIF	<b>0.0367</b>	0.788	-1.12	<b>0.020</b>	<b>-1.49</b>	0.162	-1.29
P22307	Non-specific lipid-transfer protein	SCP2	<b>0.0122</b>	0.111	-1.25	<b>0.007</b>	<b>-1.44</b>	0.121	-1.24
Q9H8Y8	Golgi reassembly-stacking protein 2	GORASP2	<b>0.0011</b>	0.402	-1.20	<b>0.036</b>	<b>-1.42</b>	0.282	-1.24
Q06830	Peroxiredoxin-1	PRDX1	<b>0.0017</b>	<b>0.006</b>	<b>-1.31</b>	0.125	-1.17	<b>0.030</b>	-1.23
Q16555	Dihydropyrimidinase-related protein 2	DPYSL2	<b>0.0335</b>	<b>0.009</b>	<b>-1.40</b>	0.053	-1.28	0.221	-1.19
Q09666	Neuroblast differentiation-associated protein AHNAK	AHNAK	<b>0.0377</b>	<b>0.012</b>	<b>-1.41</b>	0.092	-1.26	0.698	-1.11
P07339	Cathepsin D	CTSD	<b>0.0002</b>	<b>0.022</b>	<b>-1.44</b>	0.629	-1.15	0.825	-1.11
O75521	Enoyl-CoA delta isomerase 2, mitochondrial	ECI2	<b>0.0076</b>	1.000	-1.00	<b>0.024</b>	<b>-3.46</b>	1.000	-1.01
O14949	Cytochrome b-c1 complex subunit 8	UQCRQ	<b>0.0000</b>	0.648	1.22	<b>0.023</b>	<b>-1.72</b>	1.000	1.02

Tab. II Proteins significantly down-regulated by different concentrations of C16:0 treatment in HepG2 cell proteome with relative fold change compared to controls (ANOVA p-value adjusted with Benjamini-Hochberg method; Tukey's HSD p-value adjusted for multiple comparisons). Significant p-values and fold changes lower than -1.3 are highlighted in bold type.

Majority Protein ID	Protein name	Gene name	ANOVA	50-0 p adj	fold change 0-50	125-0 p adj	fold change 0-125	250-0 p adj	fold change 0-250
Q99541	Perilipin-2	PLIN2	<b>0.0000</b>	<b>0.006</b>	<b>3.06</b>	<b>0.000</b>	<b>7.45</b>	<b>0.000</b>	<b>18.94</b>
P60228	Eukaryotic translation initiation factor 3 subunit E	EIF3E	<b>0.0247</b>	<b>0.004</b>	<b>4.20</b>	<b>0.010</b>	<b>3.47</b>	<b>0.002</b>	<b>4.90</b>
P30046	D-dopachrome decarboxylase	DDT	<b>0.0371</b>	0.404	<b>1.77</b>	0.942	0.80	<b>0.020</b>	<b>3.33</b>
P09874	Poly [ADP-ribose] polymerase 1	PARP1	<b>0.0056</b>	<b>0.012</b>	<b>1.83</b>	<b>0.003</b>	<b>2.13</b>	<b>0.000</b>	<b>3.27</b>
O14929	Histone acetyltransferase type B catalytic subunit	HAT1	<b>0.0140</b>	<b>0.002</b>	<b>2.41</b>	<b>0.001</b>	<b>2.85</b>	<b>0.001</b>	<b>2.62</b>
P11388	DNA topoisomerase 2-alpha	TOP2A	<b>0.0275</b>	<b>0.011</b>	<b>2.47</b>	<b>0.004</b>	<b>2.90</b>	<b>0.010</b>	<b>2.51</b>
P28288	ATP-binding cassette sub-family D member 3	ABCD3	<b>0.0323</b>	0.137	<b>1.48</b>	0.083	<b>1.56</b>	<b>0.001</b>	<b>2.42</b>
P62805	Histone H4	HIST1H4A	<b>0.0140</b>	0.757	1.17	<b>0.003</b>	<b>1.98</b>	<b>0.001</b>	<b>2.26</b>
P16401	Histone H1.5	HIST1H1B	<b>0.0130</b>	<b>0.005</b>	<b>2.03</b>	<b>0.000</b>	<b>2.74</b>	<b>0.003</b>	<b>2.16</b>
Q9Y5B9	FACT complex subunit SPT16	SUPT16H	<b>0.0024</b>	<b>0.002</b>	<b>1.65</b>	<b>0.000</b>	<b>2.36</b>	<b>0.000</b>	<b>2.11</b>
O75367	Core histone macro-H2A.1	H2AFY	<b>0.0247</b>	<b>0.028</b>	<b>1.58</b>	<b>0.005</b>	<b>1.82</b>	<b>0.001</b>	<b>2.11</b>

Q15785	Mitochondrial import receptor subunit TOM34	TOMM34	<b>0.0495</b>	<b>0.010</b>	<b>2.02</b>	<b>0.012</b>	<b>2.00</b>	<b>0.008</b>	<b>2.08</b>
P52292	Importin subunit alpha-1	KPNA2	<b>0.0004</b>	<b>0.000</b>	<b>2.46</b>	<b>0.000</b>	<b>2.58</b>	<b>0.005</b>	1.75
Q99879	Histone H2B type 1-M	HIST1H2BM	<b>0.0140</b>	0.789	0.90	<b>0.038</b>	<b>1.40</b>	<b>0.003</b>	<b>1.65</b>
P02679	Fibrinogen gamma chain	FGG	<b>0.0034</b>	0.997	1.03	0.807	1.10	<b>0.002</b>	<b>1.62</b>
P02647	Apolipoprotein A-I	APOA1	<b>0.0006</b>	0.970	0.94	0.814	1.12	<b>0.014</b>	<b>1.55</b>
P04844	Dolichyl-diphosphooligosaccharide--protein glycosyltransferase subunit 2	RPN2	<b>0.0250</b>	0.186	1.19	0.057	1.25	<b>0.002</b>	<b>1.46</b>
P26196	Probable ATP-dependent RNA helicase DDX6	DDX6	<b>0.0063</b>	<b>0.002</b>	1.29	<b>0.002</b>	<b>1.30</b>	<b>0.000</b>	<b>1.46</b>
Q01581	Hydroxymethylglutaryl-CoA synthase. cytoplasmic	HMGCS1	<b>0.0065</b>	<b>0.010</b>	<b>2.14</b>	<b>0.025</b>	<b>1.92</b>	0.340	<b>1.41</b>
P09525	Annexin A4	ANXA4	<b>0.0476</b>	0.997	0.97	0.078	1.27	<b>0.012</b>	<b>1.39</b>
Q14152	Eukaryotic translation initiation factor 3 subunit A	EIF3A	<b>0.0324</b>	0.452	1.10	<b>0.012</b>	1.27	<b>0.002</b>	<b>1.36</b>
P05141	ADP/ATP translocase 2	SLC25A5	<b>0.0052</b>	<b>0.001</b>	1.26	<b>0.000</b>	<b>1.34</b>	<b>0.000</b>	<b>1.35</b>
Q15392	Delta(24)-sterol reductase	DHCR24	<b>0.0360</b>	0.939	1.05	0.050	1.25	<b>0.008</b>	<b>1.35</b>
P32754	4-hydroxyphenylpyruvate dioxygenase	HPD	<b>0.0243</b>	<b>0.005</b>	<b>1.35</b>	<b>0.003</b>	<b>1.38</b>	0.005	<b>1.34</b>
P78527	DNA-dependent protein kinase catalytic subunit	PRKDC	<b>0.0147</b>	<b>0.004</b>	1.29	<b>0.001</b>	<b>1.37</b>	<b>0.001</b>	<b>1.34</b>
P49748	Very long-chain specific acyl-CoA dehydrogenase. mitochondrial	ACADVL	<b>0.0360</b>	0.485	1.15	0.865	1.08	<b>0.038</b>	<b>1.33</b>
P51149	Ras-related protein Rab-7a	RAB7A	<b>0.0147</b>	<b>0.020</b>	1.20	0.181	1.12	<b>0.002</b>	<b>1.30</b>
Q13765	Nascent polypeptide-associated complex subunit alpha	NACA	<b>0.0493</b>	<b>0.005</b>	<b>1.38</b>	<b>0.008</b>	<b>1.35</b>	<b>0.024</b>	1.29
Q02809	Procollagen-lysine,2-oxoglutarate 5-dioxygenase 1	PLOD1	<b>0.0250</b>	<b>0.002</b>	<b>1.31</b>	<b>0.006</b>	1.25	<b>0.007</b>	1.25
P25205	DNA replication licensing factor MCM3	MCM3	<b>0.0275</b>	<b>0.007</b>	<b>1.39</b>	<b>0.005</b>	<b>1.42</b>	0.068	1.25
Q6UB35	Monofunctional C1-tetrahydrofolate synthase. mitochondrial	MTHFD1L	<b>0.0370</b>	<b>0.004</b>	1.29	<b>0.003</b>	<b>1.30</b>	<b>0.024</b>	1.22
Q9Y2X3	Nucleolar protein 58	NOP58	<b>0.0175</b>	<b>0.001</b>	<b>1.35</b>	<b>0.005</b>	1.26	<b>0.035</b>	1.18
O60841	Eukaryotic translation initiation factor 5B	EIF5B	<b>0.0235</b>	<b>0.002</b>	<b>1.32</b>	<b>0.004</b>	<b>1.30</b>	<b>0.062</b>	1.18
P02786	Transferrin receptor protein 1	TFRC	<b>0.0010</b>	<b>0.000</b>	<b>1.65</b>	0.387	1.12	0.148	1.17
P49327	Fatty acid synthase	FASN	<b>0.0061</b>	<b>0.001</b>	<b>1.32</b>	<b>0.007</b>	1.23	0.154	1.12
Q03252	Lamin-B2	LMNB2	<b>0.0332</b>	<b>0.002</b>	<b>1.35</b>	<b>0.049</b>	1.20	0.328	1.11
P31930	Cytochrome b-c1 complex subunit 1. mitochondrial	UQCRC1	<b>0.0140</b>	<b>0.000</b>	<b>1.34</b>	<b>0.006</b>	1.22	0.173	1.11
P17844	Probable ATP-dependent RNA helicase DDX5	DDX5	<b>0.0065</b>	<b>0.000</b>	<b>1.38</b>	<b>0.014</b>	1.22	0.434	1.09

O94906	Pre-mRNA-processing factor 6	PRPF6	<b>0.0147</b>	<b>0.005</b>	<b>1.31</b>	0.843	1.06	0.387	0.90
P78330	Phosphoserine phosphatase	PSPH	<b>0.0056</b>	<b>0.004</b>	<b>2.70</b>	1.000	1.01	0.188	0.62

Tab. III Proteins significantly up-regulated by different concentrations of C18:1 treatment in HepG2 cell proteome with relative fold change compared to controls (ANOVA p-value adjusted with Benjamini-Hochberg method; Tukey's HSD p-value adjusted for multiple comparisons). Significant p-values and fold changes higher than 1.3 are highlighted in bold type.

Majority Protein ID	Protein name	Gene name	ANOVA	50-0 p adj	fold change 0-50	125-0 p adj	fold change 0-125	250-0 p adj	fold change 0-250
Q13148	TAR DNA-binding protein 43	TARDBP	0.0052	0.317	<b>-1.36</b>	0.437	<b>-1.30</b>	<b>0.000</b>	<b>-2.91</b>
Q15020	Squamous cell carcinoma antigen recognized by T-cells 3	SART3	<b>0.0493</b>	<b>0.012</b>	<b>-2.85</b>	<b>0.031</b>	<b>-2.46</b>	0.075	<b>-2.13</b>
Q00839	Heterogeneous nuclear ribonucleoprotein U	HNRNPU	<b>0.0422</b>	0.757	-1.18	0.176	<b>-1.40</b>	<b>0.005</b>	<b>-1.95</b>
Q86TG7	Retrotransposon-derived protein PEG10	PEG10	<b>0.0006</b>	<b>0.000</b>	<b>-1.78</b>	<b>0.000</b>	<b>-1.96</b>	0.000	<b>-1.85</b>
Q8NC51	Plasminogen activator inhibitor 1 RNA-binding protein	SERBP1	<b>0.0161</b>	0.306	-1.24	0.452	-1.20	<b>0.001</b>	<b>-1.83</b>
P22307	Non-specific lipid-transfer protein	SCP2	<b>0.0275</b>	0.709	-1.15	<b>0.018</b>	<b>-1.52</b>	<b>0.002</b>	<b>-1.80</b>
P84090	Enhancer of rudimentary homolog	ERH	<b>0.0161</b>	<b>0.004</b>	<b>-1.69</b>	<b>0.001</b>	<b>-1.97</b>	<b>0.003</b>	<b>-1.74</b>
Q9Y2W1	Thyroid hormone receptor-associated protein 3	THRAP3	<b>0.0403</b>	1.000	-1.01	0.136	-1.28	<b>0.005</b>	<b>-1.57</b>
Q15942	Zyxin	ZYX	<b>0.0056</b>	1.000	1.00	<b>0.020</b>	-1.26	<b>0.000</b>	<b>-1.56</b>
Q9BXP5	Serrate RNA effector molecule homolog	SRRT	<b>0.0422</b>	0.732	-1.13	<b>0.036</b>	<b>-1.40</b>	<b>0.008</b>	<b>-1.54</b>
Q32MZ4	Leucine-rich repeat flightless-interacting protein 1	LRRFIP1	<b>0.0447</b>	0.385	-1.20	1.000	1.01	<b>0.015</b>	<b>-1.50</b>
P23588	Eukaryotic translation initiation factor 4B	EIF4B	<b>0.0070</b>	0.606	-1.09	<b>0.007</b>	<b>-1.30</b>	<b>0.000</b>	<b>-1.49</b>
P50552	Vasodilator-stimulated phosphoprotein	VASP	<b>0.0363</b>	<b>0.022</b>	<b>-3.69</b>	<b>0.003</b>	<b>-5.88</b>	0.776	<b>-1.48</b>
P06730	Eukaryotic translation initiation factor 4E	EIF4E	<b>0.0100</b>	0.777	-1.09	0.469	-1.13	<b>0.002</b>	<b>-1.48</b>
P27797	Calreticulin	CALR	<b>0.0275</b>	<b>0.009</b>	<b>-1.35</b>	<b>0.005</b>	<b>-1.38</b>	<b>0.002</b>	<b>-1.45</b>
Q13428	Treacle protein	TCOF1	<b>0.0006</b>	0.173	-1.09	<b>0.000</b>	<b>-1.40</b>	<b>0.000</b>	<b>-1.44</b>
Q15370	Transcription elongation factor B polypeptide 2	TCEB2	<b>0.0195</b>	<b>0.003</b>	<b>-3.44</b>	0.995	1.10	0.647	<b>-1.40</b>
Q9P2E9	Ribosome-binding protein 1	RRBP1	<b>0.0002</b>	0.070	-1.09	<b>0.000</b>	-1.22	<b>0.000</b>	<b>-1.38</b>
P14314	Glucosidase 2 subunit beta	PRKCSH	<b>0.0403</b>	1.000	1.00	0.616	-1.10	<b>0.006</b>	<b>-1.36</b>
P14174	Macrophage migration inhibitory factor	MIF	<b>0.0000</b>	<b>0.001</b>	<b>-1.92</b>	<b>0.031</b>	<b>-1.49</b>	0.104	<b>-1.36</b>
P08621	U1 small nuclear ribonucleoprotein 70 kDa	SNRNP70	<b>0.0059</b>	1.000	1.01	<b>0.004</b>	-1.26	<b>0.001</b>	<b>-1.36</b>

P04040	Catalase	CAT	<b>0.0052</b>	<b>0.003</b>	-1.24	<b>0.000</b>	<b>-1.37</b>	<b>0.000</b>	<b>-1.36</b>
Q9NZT2	Opioid growth factor receptor	OGFR	<b>0.0403</b>	0.457	1.16	0.904	-1.07	0.030	<b>-1.35</b>
P38919	Eukaryotic initiation factor 4A-III	EIF4A3	<b>0.0097</b>	0.945	1.04	0.124	-1.15	<b>0.002</b>	<b>-1.35</b>
Q9Y4L1	Hypoxia up-regulated protein 1	HYOU1	<b>0.0059</b>	0.050	1.22	0.999	1.01	0.006	<b>-1.33</b>
P61916	Epididymal secretory protein E1	NPC2	<b>0.0296</b>	<b>0.031</b>	-1.26	<b>0.002</b>	<b>-1.44</b>	<b>0.022</b>	-1.28
P51665	26S proteasome non-ATPase regulatory subunit 7	PSMD7	<b>0.0052</b>	0.637	-1.18	<b>0.012</b>	<b>-1.64</b>	0.599	-1.19
Q04828	Aldo-keto reductase family 1 member C1	AKR1C1	<b>0.0052</b>	<b>0.002</b>	<b>-1.47</b>	<b>0.001</b>	<b>-1.48</b>	0.236	-1.17
O96008	Mitochondrial import receptor subunit TOM40 homolog	TOMM40	<b>0.0173</b>	<b>0.030</b>	<b>-2.20</b>	<b>0.001</b>	<b>-3.62</b>	0.953	-1.16
P07910	Heterogeneous nuclear ribonucleoproteins C1/C2	HNRNPC	<b>0.0422</b>	<b>0.015</b>	<b>-1.31</b>	<b>0.016</b>	<b>-1.31</b>	0.248	-1.16
P01023	Alpha-2-macroglobulin	A2M	<b>0.0021</b>	<b>0.028</b>	<b>-1.45</b>	<b>0.003</b>	<b>-1.68</b>	0.741	-1.13
P63220	40S ribosomal protein S21	RPS21	<b>0.0000</b>	0.839	1.13	<b>0.000</b>	<b>-11.01</b>	0.932	-1.10
O75477	Erlin-1	ERLIN1	<b>0.0250</b>	0.931	1.17	<b>0.005</b>	<b>-2.70</b>	1.000	-1.02
P62333	26S protease regulatory subunit 10B	PSMC6	<b>0.0498</b>	<b>0.006</b>	<b>-1.58</b>	0.882	-1.10	1.000	-1.01
P08758	Annexin A5	ANXA5	<b>0.0323</b>	0.121	-1.16	<b>0.004</b>	-1.31	1.000	1.01
Q14137	Ribosome biogenesis protein BOP1	BOP1	<b>0.0328</b>	0.187	-1.28	<b>0.004</b>	<b>-1.65</b>	0.999	1.03
P02751	Fibronectin	FN1	<b>0.0147</b>	<b>0.036</b>	<b>-7.71</b>	0.127	<b>-4.77</b>	1.000	1.03
Q96IX5	Up-regulated during skeletal muscle growth protein 5	USMG5	<b>0.0494</b>	<b>0.013</b>	<b>-5.62</b>	0.469	-2.02	1.000	1.04
P11766	Alcohol dehydrogenase class-3	ADH5	<b>0.0422</b>	<b>0.014</b>	<b>-1.33</b>	0.806	-1.08	0.745	1.09
Q13724	Mannosyl-oligosaccharide glucosidase	MOGS	<b>0.0360</b>	<b>0.010</b>	<b>-2.76</b>	0.928	-1.20	0.950	1.18

Tab. IV Proteins significantly down-regulated by different concentrations of C18:1 treatment in HepG2 cell proteome with relative fold change compared to controls (ANOVA p-value adjusted with Benjamini-Hochberg method; Tukey's HSD p-value adjusted for multiple comparisons). Significant p-values and fold changes lower than -1.3 are highlighted in bold type.

### 3.3 Comparison between proteins modulated by myristic, palmitic and oleic acids

To detect which C14:0 modulated proteins were unique for this FA or shared with other FAs, a comparative analysis was performed between proteins deregulated by C14:0, C16:0 and C18:1. By means of FunRich bioinformatics tool a Venn diagram (Fig.6) was generated in order to graphically illustrate common and unique proteins whose expression was significantly altered in HepG2 cells after FAs treatments. Interestingly, the analysis revealed that only the expression of one single protein, Perilipin2, was modulated by all three FAs and the shared

proteins were only few with respect to the number of total of proteins modulated by each FA. While 14 proteins were shared between C16:0 and C18:1, C14:0 shared only four proteins exclusively with C16:0 and two proteins exclusively with C18:1. Therefore 40 out of 47 proteins whose expression were found to be altered by C14:0 treatment were exclusively modulated by this saturated FA.

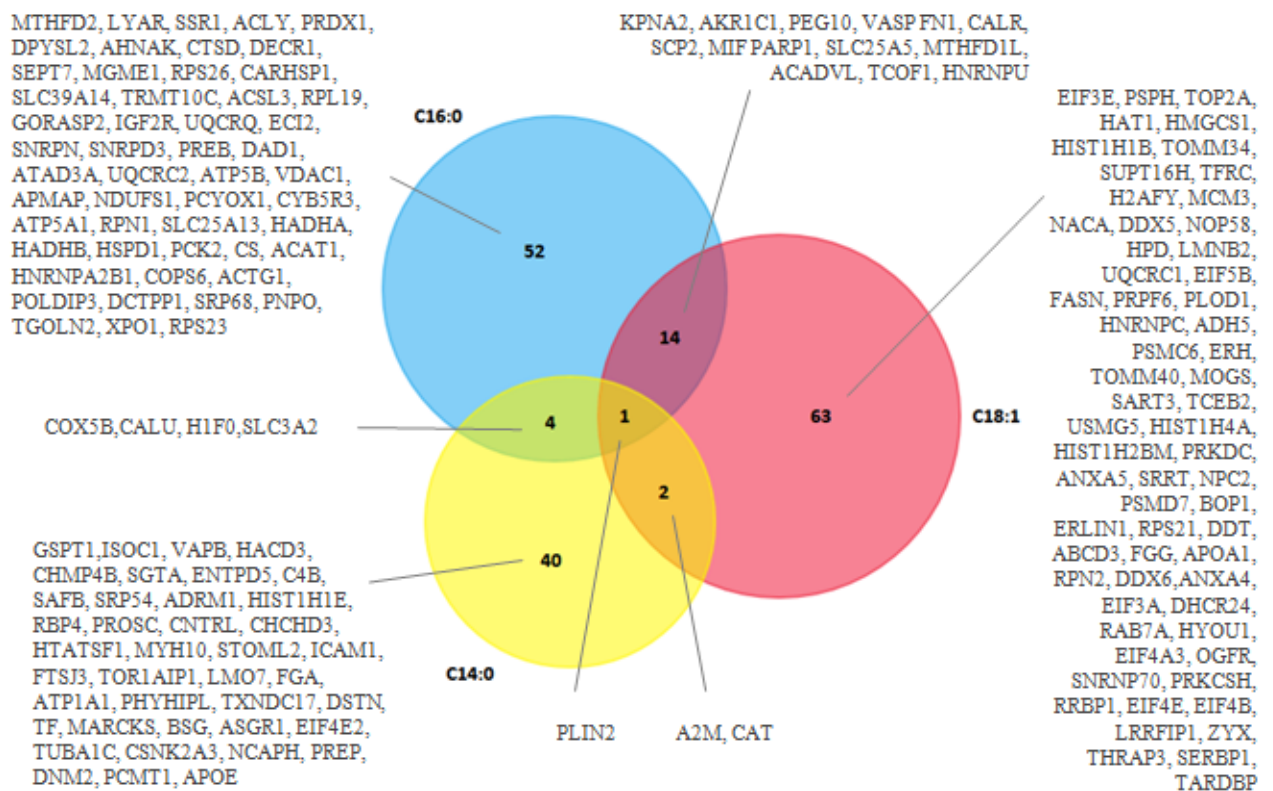


Fig.6 Graphical representation of unique and overlapping proteins whose expression was found to be modulated by myristic (C14:0), palmitic (C16:0) and oleic acid (C18:1).

### **3.4 Biological processes exclusively modulated by myristic, palmitic or oleic acid**

The results obtained showed a high number of “specifically altered” proteins, for each FA treatment, suggesting specific actions of the individual FAs analysed. To disclose the specific effects of each of these FAs, and in particular the biological processes involved in the specific response to C14:0 treatment, GO analyses were performed of up- and down-regulated proteins specifically modulated by the individual FAs analysed. Results of DAVID GO analysis on proteins specifically modulated by C14:0 are reported in Fig.7. Regulation of calcium ion homeostasis, cellular matrix organisation and negative regulation of the apoptotic process were among the biological processes mainly up-regulated by C14:0.



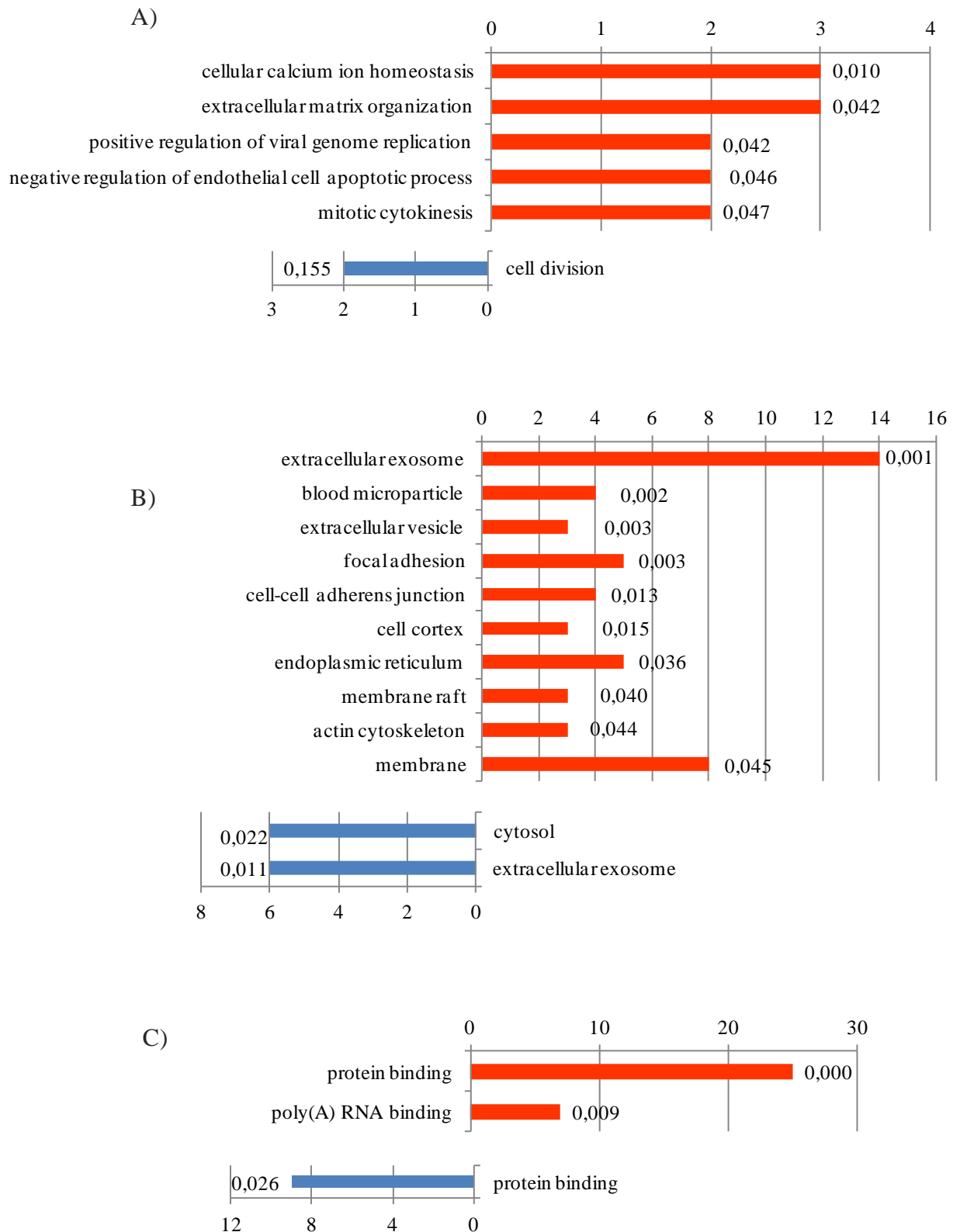


Fig.7 Gene Ontology analysis of HepG2 proteins modulated exclusively by C14:0. In blue down-regulated and in red up-regulated protein biological processes (A), cellular components (B) and molecular functions (C) are reported. Horizontal axis represents the number of proteins involved and enrichment p-value is reported at the end of each bar.

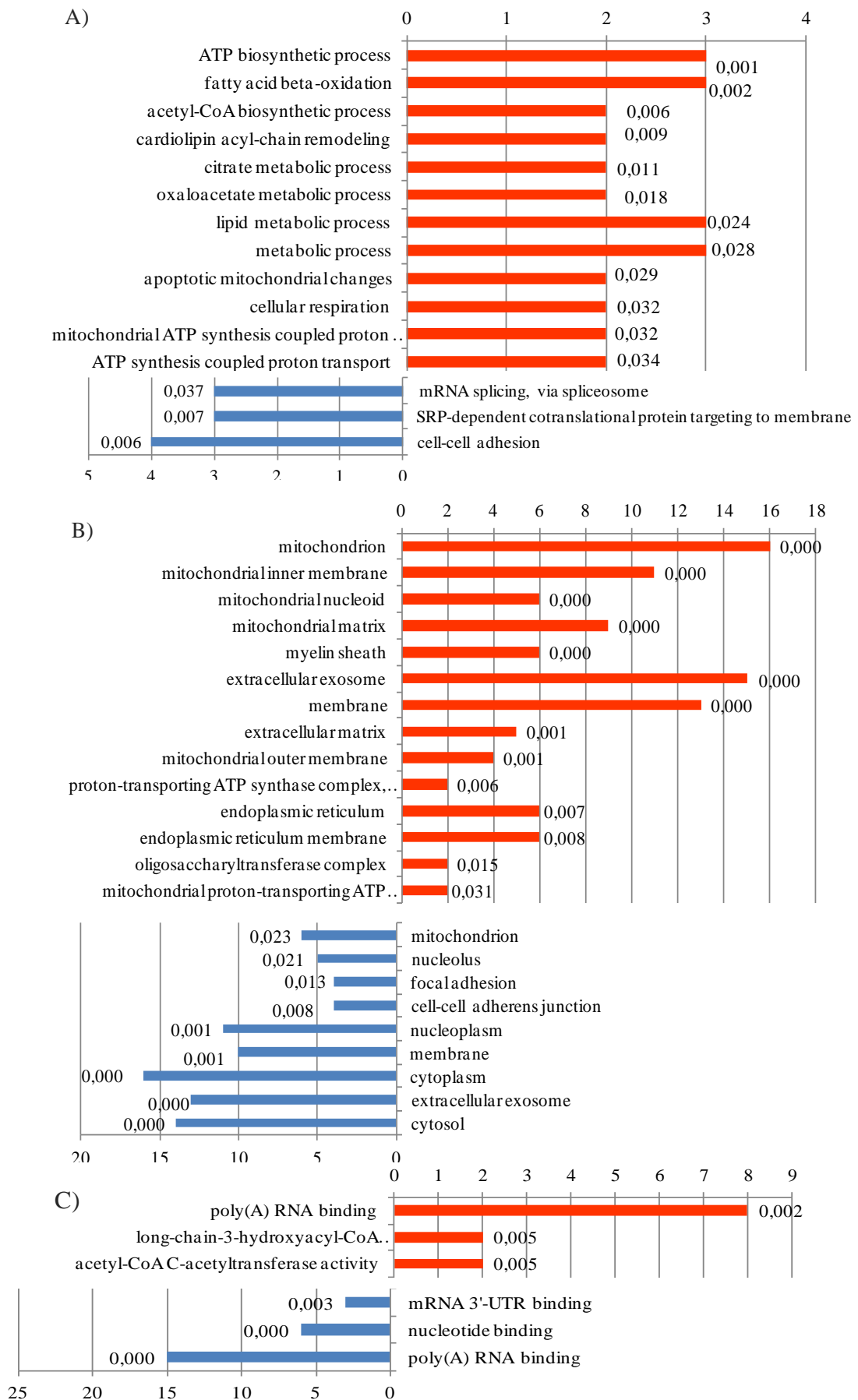


Fig.8 Gene Ontology analysis of HepG2 proteins modulated exclusively by C16:0. In blue down-regulated and in red up-regulated protein biological processes (A), cellular components (B) and molecular functions (C) are reported. Horizontal axis represents the number of proteins involved and enrichment p-value is reported at the end of each bar.

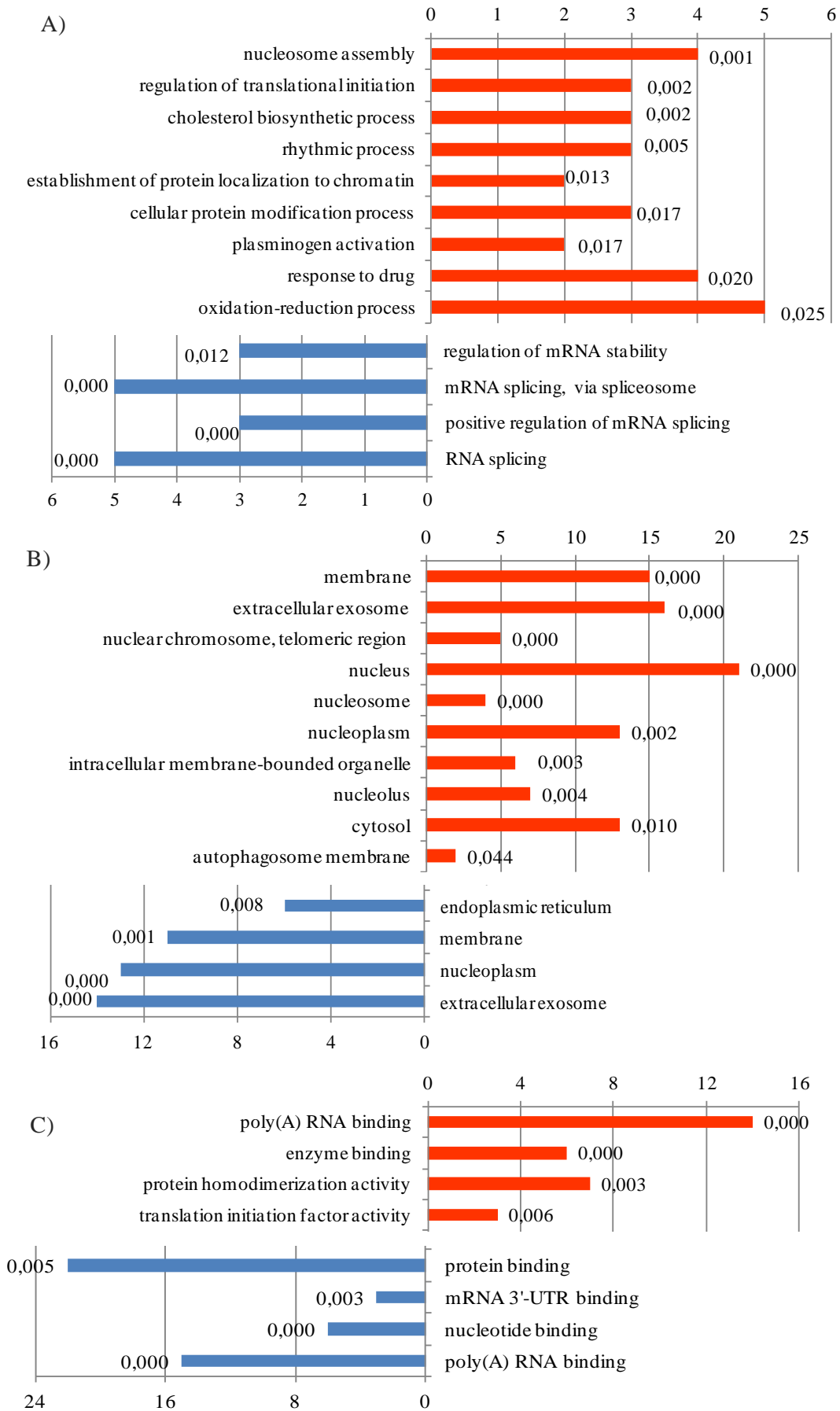


Fig.9 Gene Ontology analysis of HepG2 proteins modulated exclusively by C18:1. In blue down-regulated and in red up-regulated protein biological processes (A), cellular components (B) and molecular functions (C) are reported. Horizontal axis represents the number of proteins involved and enrichment p-value is reported at the end of each bar.

Proteins specifically up-regulated by C14:0 were mainly present in exosome compartment as described in the cellular component GO analysis (Fig.7B). Many other cellular compartment proteins were also found to be significantly up-regulated by C14:0 treatments such as focal adhesion proteins, endoplasmic reticulum proteins and actin cytoskeleton proteins. Concerning proteins specifically up-regulated by C16:0, the GO analysis revealed that the pool of proteins was particularly enriched in proteins involved in ATP biosynthetic process, fatty acid beta-oxidation - more in general lipid metabolic processes - apoptotic mitochondrial changes and cellular respiration (Fig.8A). Down-regulated proteins were instead involved in mRNA splicing, protein targeting to membrane and cell-cell adhesion. In line with the GO biological process analysis, the cellular component analysis demonstrated that the majority of the up-regulated proteins were mitochondrial proteins and they were mitochondrial membrane, membrane and nucleoid proteins (Fig.8B). Moreover, extracellular exosome, membrane and endoplasmic reticulum proteins were also significantly up-regulated. Some proteins of the mitochondrion were also found to be significantly present in C16:0 down-regulated proteins, together with nuclear proteins, focal adhesion proteins, membrane proteins and cytoplasm protein. Molecular functions of up-regulated proteins involved many specific function, such as poly(A)RNA binding, long-chain 3 hydroxyacyl-CoA dehydrogenase activity and protein transporting ATPsynthase activity (Fig.8C). Poly(A) RNA binding, nucleotide binding and mRNA 3' -UTR binding were some of the molecular functions involving proteins downregulated by C16:0. Regarding proteins involved in C18:1 response, the GO analysis revealed that main up-regulated biological processes involved nucleosome assembly, regulation of translational initiation, cholesterol biosynthetic process, protein localisation to chromatin, response to drug and oxidation-reduction process (Fig.9A). On the other hand, down-regulated proteins involved mRNA processing and stability, translational initiation and mRNA splicing. The proteins up-regulated by C18:1 mainly belonged to membranes, extracellular exosomes, nucleus, cytosol and autophagosome membranes while down regulated proteins were

principally extracellular exosome, nucleoplasm and membrane proteins (Fig.9B). Molecular functions of significantly C18:1 up-regulated proteins were poly(A) RNA binding, enzyme binding and protein homodimerization activity (Fig.9C).

## 4. DISCUSSION

A correlation of C14:0 to NASH and lipid metabolism - strictly connected with the onset of cardiovascular diseases – has recently been highlighted (Tomita et al., 2011; Noto et al., 2016). C14:0-induced proteomic modulations on HepG2 cells intracellular proteins were investigated in depth for the first time in this PhD research project. In the present chapter, the HepG2 proteome changes following C16:0 and C18:1 supplementation were also analysed. Even though the mechanisms underlying their effects on liver metabolism have been studied in depth during recent years (Hetherington et al., 2016) a complete investigation on their proteomic effects still lacked. The comparison of proteome modulations induced in HepG2 after C14:0, or after C16:0, C18:1 treatments, shown for the first time in the present part of the thesis, helped the identification of proteins that are exclusively modulated by C14:0, as well as proteins that are deregulated not only by C14:0 but also by C16:0 and/or C18:1.

The present investigation revealed a surprisingly scarce overlap between proteins modulated by all three FAs, which was limited to just one protein (Fig.6). This important result underlines that these molecules, all belonging to the family of FAs, behave very differently and have distinct effects on liver metabolism. Interestingly, the protein whose expression was up-regulated by all three FAs treatment was the Perilipin 2 (ADRP) (in Fig.6 illustrated with its corresponding gene name PLIN2), the main structural protein of LD. This data is therefore in line with the dose-dependent appearance of cytosolic LD following C14:0 (Fig.3 Chapter 2), C16:0 and C18:1 treatments (Fig.5) and represents a confirmation of the reliability of the obtained MS/MS proteomic data. The increase in the protein expression levels of ADRP was especially elevated in presence of C18:1 at 250  $\mu$ M in HepG2 culture media, with its fold change increasing nearly 19-fold by the treatment (Tab. III). As can also be seen from the Oil Red O staining (Fig.5), C18:1 was the most steatogenic FA and has the highest propensity for LD formation compared to C14:0 and C16:0. This data is in agreement with the Ricchi et al.

investigation, reporting a greater accumulation of LD in C18:1-treated HepG2 cells, together with an increase in TG accumulation, when compared to C16:0 treated HepG2 cells (Ricchi et al., 2009). They finally speculated that this property protects C18:1-treated cell against FA's pro-apoptotic effects.

#### **4.1 Proteins modulated exclusively by myristic acid**

The present investigation was aimed at disclosing proteins specifically modulated by C14:0. The proteomic comparison performed revealed a total of 40 proteins whose expression is regulated in HepG2 cells specifically by the C14:0. The GO analysis indicated the up-regulation of protein involved in calcium homeostasis. The Vesicle-associated membrane protein-associated protein B/C (VAPB), already mentioned in the previous chapter as involved in calcium homeostasis regulation, was found to be modulated exclusively by C14:0. Interestingly, this protein is involved in the protection of ER-stress and has been reported to be activated by the UPR (Kanekura et al., 2009). Loss of function of this protein has been connected to ER-stress related death (Suzuki et al., 2009). This may suggest that the increase in this protein may be a mechanism specific to C14:0-treated HepG2 cells, to counteract ER stress and survive general stress conditions, that is not activated in presence of C16:0, which also induces ER stress (as showed in Fig.1 of Introduction, Chapter 3, Section 2). Moreover, another protein involved in cell calcium homeostasis is Stomatin-like protein 2 (STOML2), up-regulated only in presence of C14:0. Interestingly, this protein has been found to be important for the mitochondrial respiratory chain (Mitsopoulos et al., 2015). This may therefore have an essential role in contrasting the mitochondrial stress and ROS generation induced by SFA (as showed in Fig.1 of Introduction, Chapter 3, Section 2), possibly distinguishing C14:0 to C16:0 mechanisms. The previously described Small glutamine-rich tetratricopeptide repeat-containing protein alpha (SGTA) and proteasomal ubiquitin receptor ADRM1 are proteins also found to be

regulated exclusively by C14:0. As described in the previous chapter, SGTA is involved in the regulation of the ubiquitination state of the proteins and in the maintenance of the cellular proteostasis by selectively modulating proteasomal substrate degradation (Wunderley et al., 2014; Roberts et al., 2015). Proteasomal degradation by means of ERAD is a cellular response following ER stress conditions. The presence of these proteins among the proteins up-regulated exclusively by C14:0 led to the hypothesis that this process could help HepG2 cells to maintain cellular proteostasis, decreasing the cytotoxicity that is induced by SFA. Moreover, Ectonucleoside triphosphate diphosphohydrolase 5 (ENTPD5) was another protein found to be specifically modulated by C14:0 in HepG2 cells. This protein, also described in the previous chapter, is important for a proper protein N-glycosylation and folding in the ER compartment and its increase has been reported to counteract ER stress in cancer cells (Fang et al., 2010; Shen et al., 2011). The concurrent up-regulation of all these proteins, involved in the maintenance of a proper cell protein homeostasis, could therefore suggest the activation of a peculiar mechanism aimed at opposing C14:0-induced ER stress in HepG2 cells.

Furthermore, the GO analysis on proteins modulated specifically by C14:0 revealed that many proteins up-regulated by this FA are present in extracellular exosomes, confirming the data observed in the previous chapter regarding the exosomal origin of many C14:0-deregulated secreted proteins detected by the MS/MS analysis.

Finally, another protein specifically induced by C14:0 is Apolipoprotein E (ApoE). As described in detail in Chapter 1 Section 1 of the present thesis, this protein is present on many lipoprotein types and has many important physiological roles. Interestingly, the analysis performed in Chapter 2 Section 1 of the present thesis showed that – besides its important role on ApoC-III plasma levels - C14:0 was the second FA predictor of ApoE plasma levels. The present data, showing the exclusive influence of C14:0 on HepG2 cellular levels, suggest a positive influence of C14:0 on ApoE levels. Plasma levels of ApoE have been described as



regulators of TRLs metabolism, explaining 20-40% of plasma TG variability in humans (Mahley et al., 2009). *In vivo* studies on animal models also demonstrated that ApoE plasma levels are strictly connected with the development of hypertriglyceridemia. In particular, the overexpression of ApoE3 in transgenic rabbits caused hypertriglyceridemia through the increase in VLDL production (Huang et al., 1999). On the contrary, the effects of the ApoE deficiency on the secretion of VLDL-associated TG was investigated in mice and a 46% reduction in VLDL-TG was observed compared to controls (Kuipers et al., 1997). The same study reported a 23% reduction in VLDL-TG in cultured ApoE-deficient mouse hepatocytes. An important effect of ApoE on VLDL assembly and secretion has therefore been established. Moreover, the influence of this apolipoprotein on TG levels is also due to its ability to impair VLDL lipolysis (Huang et al., 1998). As reported by Jong et al., the increased amount of ApoE particles on nascent VLDL significantly decreased TG lipolysis when compared to ApoE-deficient VLDL (Jong et al., 1997). The presence of ApoE on lipoproteins can therefore decrease their suitability for lipolysis in a dose-dependent manner. Taken together, these studies confirm an important influence of ApoE on cholesterol and TG plasma levels. Interestingly, in Chapter 2 Section 1 of the present thesis the most important statistical relationship observed *in vivo* was between C14:0 and plasma TG levels. The present *in vitro* proteomics research highlighted that, beyond the positive influence demonstrated on ApoC-III plasma levels, C14:0 may be connected to TG metabolism through the regulation of ApoE levels. The positive influence of C14:0 on both ApoC-III and ApoE levels could therefore represent a partial explanation of the statistical correlation observed between C14:0 and TG levels in the plasma of studied subjects.

## **4.2 Proteins modulated by both myristic and palmitic acid**

C14:0-treated HepG2 cells shared more modulated proteins with the saturated FA C16:0 than with C18:0, providing proteomic evidences of common mechanisms induced by the two saturated FAs. In the present investigation four proteins were found to be modulated by both C14:0 and by C16:0 with the same trend. Among these, the Cytochrome c oxidase subunit 5B, mitochondrial (COX5B), the component of the terminal oxidase in the mitochondrial electron transport was found to be down-regulated. The presence of this protein suggests a common propensity for the production of ROS by both FAs. This process has also been reported in C14:0 treated primary mouse hepatocytes (Martínez, 2015). Another protein found to be down-regulated by both C14:0 and C16:0 was Calumenin (CALU), a calcium-binding protein located in the ER membrane. This protein is involved in the alleviation of ER-stress in rat cardiomyocytes and exerts chaperone-like properties (Lee et al., 2013; Tripathi et al., 2014). The slight decrease in Calumenin induced by C14:0 (1.3 fold lower in 125  $\mu$ M C14:0 HepG2 cell proteome) as compared to the strong decrease observed with C16:0 (almost six times lower in the 250  $\mu$ M) could suggest an important difference between the effects of these two FAs, on ER-stress and cytotoxicity. The 4F2 cell-surface antigen heavy chain (SLC3A2) is another protein up-regulated by both C14:0 and C16:0 treatments. This protein is involved in amino acids transport but a recent investigation based on RNA-sequencing revealed the presence of SLC3A2 among the new genes involved in the ER-stress response of rat cardiomyocytes. Taken together these proteins found to be modulated by both C14:0 and C16:0 treatments suggest a common involvement on ROS production and in ER-stress.

### **4.3 Proteins modulated by both myristic and oleic acid**

Only two of the C18:1 modulated proteins were also found to be deregulated by C14:0 treatment: Alpha-2-macroglobulin (A2M) and Catalase (Santos-Gallego et al.) (Fig.6). Catalase is important for its role in protecting cells from the toxic effects of ROS generation, particularly from hydrogen peroxide. Interestingly, the treatment with C18:1 decreased the expression of this protein while C14:0 slightly and gradually increased it (even more at 500  $\mu$ M, data not shown). The decrease in antioxidant molecules following HepG2 treatment with C18:1 has already been reported, together with the increase in LD and TG accumulation (Vidyashankar et al., 2013). The increase in the expression of Catalase, after C14:0 treatment, could instead represent the activation of a cell mechanism to counteract the oxidative stress induced by the treatment with this FA and could help explain the limited degree of cytotoxicity induced by C14:0 in HepG2 when compared with other saturated FAs.

### **4.4 Proteins modulated exclusively by palmitic and oleic acid**

The comparison performed has also permitted the identification of proteins which are specifically modulated by C16:0 and C18:1. C16:0 is the major saturated FA in human plasma and previous investigations reported its poor ability to increase LD and TG accumulation in favour of more pro-apoptotic and cytotoxic behavior (Ricchi et al., 2009; Mei et al., 2011). Its positive influence on PPAR $\alpha$  and therefore on  $\beta$ -oxidation has been reported (Ricchi et al., 2009) and is in line with the result obtained in the present investigation, where  $\beta$ -oxidation was among the first biological processes up-regulated in presence of C16:0 in HepG2 cell culture (Fig.8A). It has been demonstrated that increased  $\beta$ -oxidation by C16:0 causes excess electron flux in the mitochondrial respiratory chain yielding an increase in ROS generation (Nakamura et al., 2009). In agreement with this data, the present GO analysis reported an increase in the ATP biosynthetic process and in the respiratory chain proteins. Furthermore, the cellular

component analysis revealed that the most up-regulated proteins following C16:0 treatment in HepG2 cells were mitochondrial proteins, confirming the important effect of this FA on mitochondrial processes. The GO analysis reported the enrichment in proteins involved in apoptotic mitochondrial changes that were up-regulated following C16:0 supplementation. One of these proteins is the Voltage-dependent anion-selective channel protein 1 (VDAC1) that is involved in the regulation of mitochondrion pore formation during the apoptotic process and in the release of pro-apoptotic proteins (Ben-Hail et al., 2016). The slight dose-dependent increase in the expression of this protein confirmed the cytotoxic effects of this FA (shown in Fig.3). The most down-regulated proteins by C16:0 treatment were found to be two subunits of the 40S ribosomal protein S26 (RPS26 and RPS23), with a negative fold change of -11 in the treatment with 250  $\mu$ M C16:0. The ubiquitination of these proteins has been reported during UPR, which triggers elevated protein folding capacity and attenuated protein synthesis (Higgins et al., 2015). The reduction in 40S ribosomal proteins could therefore be due to ER-stress induced by C16:0, which activates the UPR. Another protein whose expression was found to be decreased up to ten times in C16:0 treated HepG2 cell was the Small Nuclear Ribonucleoprotein SmD3 (SNRPD3). This protein is a component of the spliceosome machinery and has been described as a mediator of the metabolic stress response (Scruggs et al., 2012). Interestingly, it has been shown that cells with SmD3 haploinsufficiency acquire resistance to palmitate-induced cell death as SmD3 disruption protects cells from generalised oxidative stress and its strong decrease in the present proteomic investigation may represent a cellular effort to counteract C16:0-induced oxidative stress.

On the other hand, C18:1, representing the category of MUFA, showed to regulate the highest number of proteins in HepG2 cells when compared with the other two fatty acids. After ADRP the second most up-regulated protein in C18:1 treated HepG2 cells was the eukaryotic translation initiation factor 3 subunit E (EIF3E), implicated in the organisation of initiation

factor and ribosome required for protein translation and in the control of specific mRNA involved in growth control processes (Lee et al., 2015). Together with the GO analysis, showing the regulation of translational initiation among first biological processes up regulated by C18:1, this evidence suggests an involvement of this unsaturated FA in the protein translation process. Moreover, another protein up-regulated by C18:1 was ApoA-I. This data was consistent with both the *in vivo* results obtained from regression analysis between FAs and lipid plasma levels in Chapter 2 Section 1 of the present PhD thesis - where C18:1 resulted as the first FA predictor of ApoA-I plasma levels - and also with the reported influence of MUFA on HDL levels (Michas et al., 2014). In addition, some lipogenic proteins were found to be up-regulated by the treatment with C18:1, such as FASN involved in fatty acids synthesis and Hydroxymethylglutaryl-CoA synthase (HMGCS1) involved in cholesterol biosynthesis. Accordingly, the GO analysis highlighted the regulation of cholesterol biosynthetic process among the most significantly up-regulated biological process following C18:1 supplementation. These data are in agreement with previously reported investigations on HepG2 cells, where FASN protein and gene expression were found to be up-regulated by the presence of C18:1 (Kang et al., 2013; Hwang et al., 2014) and also with previous observations on its positive influence on the expression of lipogenic genes (e.g. SREBP-1) rather than  $\beta$ -oxidation stimulating genes (Ricchi et al., 2009).

In conclusion, this investigation provided evidence for the first time elucidating the specific proteomics effects induced by C14:0, as well as the non-specific proteomics modulation induced by C14:0 but also by C16:0 and/or by C18:1.

The results obtained revealed that C14:0 shared a higher number of proteins with the saturated C16:0 compared to the unsaturated C18:1, mainly involved in ER-stress and ROS production. However, this research also highlighted the unique influence of C14:0 on different stress-

mitigating proteins that could make this FA less cytotoxic in comparison to C16:0. Finally, the specific C14:0 influence on ApoE, strictly connected with TG plasma levels, has also been revealed, shedding light on the possible mechanism showing the significant association observed in the first section of the present thesis between C14:0 and TG plasma levels, and possibly CAD.

## **5. Concluding remarks**

For the first time the overall effects of different concentration C14:0 on HepG2 cell proteome and secretome have been evidenced in the present PhD thesis. Furthermore, the specific proteomic modulation induced by this FA on HepG2 cell proteome, when compared to the effects induced by the better studied C16:0 and C18:1, have been shown for the first time. Results highlighted a limited overlapping of proteins modulated by the three different FAs, demonstrating the unique influence of C14:0 on the expression of 40 proteins. This investigation contributes to elucidating the overall proteomic modulation induced by this less studied FA, providing important clues for a deeper comprehension of the possible mechanisms connecting C14:0 with steatohepatitis and CAD.

## Acknowledgments

Questi tre anni di dottorato sono stati anni molto intensi, serviti indubbiamente per la mia crescita professionale e personale. Desidero quindi ringraziare profondamente tutti coloro che mi hanno assistita e sostenuta durante questi anni e che hanno reso possibile la stesura di questa tesi.

Un ringraziamento particolare a Daniela, relatrice di questa tesi, per il tempo che ha dedicato alla mia ricerca, per la pazienza, la precisione e la disponibilità che mi ha sempre dimostrato. Grazie anche per avermi sempre aiutata e stimolata a trovare la strada per proseguire anche nei momenti più difficili.

Un grazie molto sentito anche a Ruth, che mi ha ospitata nel suo laboratorio con grande affetto e disponibilità. Grazie in particolare per l'incoraggiamento, lo stimolo e il desiderio di scoprire che mi ha sempre trasmesso. Un ringraziamento anche al suo laboratorio ed ai "Proteomics Pirates", avrò sempre un bellissimo ricordo dei mesi passati a lavorare insieme. Posso dire di aver trovato non solo dei colleghi ma un gruppo molto affiatato che, in quei mesi freddi, è diventato anche la mia famiglia.

Un ringraziamento particolare a Nicola, che con infinita pazienza e determinazione mi ha sempre seguita ed aiutata nel mio percorso di ricerca, sacrificando talvolta il suo tempo prezioso. Grazie davvero, il tempo trascorso insieme è stato fonte di grande apprendimento per me. Un ringraziamento speciale anche ad Annalisa, che mi ha sempre seguita e motivata, credendo sempre nelle mie capacità. Un grazie di cuore anche alla grande famiglia del LURM che mi ha sempre accolta con grandissimo calore ed affetto. Il vostro sostegno è sempre stato per me molto importante.

Grazie inoltre anche alle mie colleghe di laboratorio, Jessica e Claudia per aver condiviso insieme a me parte del mio percorso. Grazie in particolare a Jessica per avermi sempre sostenuta ed aiutata a scegliere la strada migliore da perseguire. La tua esperienza è stata per me fonte di sicurezza.

Grazie poi anche ad Elena, la mia compagna di avventure da sempre. Lo sai, il tuo sostegno è stato indispensabile durante questi tre anni. Grazie davvero di esserci stata e di esserci sempre.

Infine grazie alla mia famiglia per il sostegno che mi ha sempre dimostrato ed a Simone per la sua infinita pazienza e soprattutto per il forte incoraggiamento che ho sempre ricevuto da parte tua in ogni mio passo ed in ogni mia decisione.

Credo di poter dire che questi tre anni di dottorato non siano stati solo un'esperienza professionale ma un'esperienza di vita, che mi ha arricchita molto. Per questo motivo devo ringraziare di cuore tutte le persone elencate sopra e quelle che, per motivi di spazio, non sono riuscita ad inserire ma che hanno lasciato un segno indelebile nel mio percorso.



## **Bibliography**

Adkins, Y. and D. S. Kelley (2010). "Mechanisms underlying the cardioprotective effects of omega-3 polyunsaturated fatty acids." J Nutr Biochem **21**(9): 781-792.

Ahmed, A. A., K. A. Balogun, N. V. Bykova and S. K. Cheema (2014). "Novel regulatory roles of omega-3 fatty acids in metabolic pathways: a proteomics approach." Nutr Metab (Lond) **11**(1): 6.

Andersen, L. H., A. R. Miserez, Z. Ahmad and R. L. Andersen (2016). "Familial defective apolipoprotein B-100: A review." J Clin Lipidol **10**(6): 1297-1302.

Arrol, S., M. I. Mackness and P. N. Durrington (2000). "The effects of fatty acids on apolipoprotein B secretion by human hepatoma cells (HEP G2)." Atherosclerosis **150**(2): 255-264.

Baharvand-Ahmadi, B., K. Sharifi and M. Namdari (2016). "Prevalence of non-alcoholic fatty liver disease in patients with coronary artery disease." ARYA Atheroscler **12**(4): 201-205.

Beauchamp, E., D. Goenaga, J. Le Bloc'h, D. Catheline, P. Legrand and V. Rioux (2007). "Myristic acid increases the activity of dihydroceramide Delta4-desaturase 1 through its N-terminal myristoylation." Biochimie **89**(12): 1553-1561.

Beauchamp, E., X. Tekpli, G. Marteil, D. Lagadic-Gossmann, P. Legrand and V. Rioux (2009). "N-Myristoylation targets dihydroceramide Delta4-desaturase 1 to mitochondria: partial involvement in the apoptotic effect of myristic acid." Biochimie **91**(11-12): 1411-1419.

Beaumont, J. L., L. A. Carlson, G. R. Cooper, Z. Fejfar, D. S. Fredrickson and T. Strasser (1970). "Classification of hyperlipidaemias and hyperlipoproteinaemias." Bull World Health Organ **43**(6): 891-915.

Ben-Hail, D. and V. Shoshan-Barmatz (2016). "VDAC1-interacting anion transport inhibitors inhibit VDAC1 oligomerization and apoptosis." Biochim Biophys Acta **1863**(7 Pt A): 1612-1623.

Bendtsen, J. D., L. J. Jensen, N. Blom, G. Von Heijne and S. Brunak (2004). "Feature-based prediction of non-classical and leaderless protein secretion." Protein Eng Des Sel **17**(4): 349-356.

Benjamini, Y. and Y. Hochberg (1995). "Controlling the False Discovery Rate: A Practical and Powerful Approach to Multiple Testing." Journal of the Royal Statistical Society **57**(1): 289-300.

Benn, M., B. G. Nordestgaard, G. B. Jensen and A. Tybjaerg-Hansen (2007). "Improving prediction of ischemic cardiovascular disease in the general population using apolipoprotein B: the Copenhagen City Heart Study." Arterioscler Thromb Vasc Biol **27**(3): 661-670.

Bindea, G., B. Mlecnik, H. Hackl, P. Charoentong, M. Tosolini, A. Kirilovsky, W. H. Fridman, F. Pages, Z. Trajanoski and J. Galon (2009). "ClueGO: a Cytoscape plug-in to decipher functionally grouped gene ontology and pathway annotation networks." Bioinformatics **25**(8): 1091-1093.

Boudoulas, K. D., F. Triposciadis, P. Geleris and H. Boudoulas (2016). "Coronary Atherosclerosis: Pathophysiologic Basis for Diagnosis and Management." Prog Cardiovasc Dis **58**(6): 676-692.

Caccia, D., M. Dugo, M. Callari and I. Bongarzone (2013). "Bioinformatics tools for secretome analysis." Biochim Biophys Acta **1834**(11): 2442-2453.

Campian, J. L., X. Gao, M. Qian and J. W. Eaton (2007). "Cytochrome C oxidase activity and oxygen tolerance." J Biol Chem **282**(17): 12430-12438.

Cao, H., J. Chen, E. W. Krueger and M. A. McNiven (2010). "SRC-mediated phosphorylation of dynamin and cortactin regulates the "constitutive" endocytosis of transferrin." Mol Cell Biol **30**(3): 781-792.

Cao, J., D. L. Dai, L. Yao, H. H. Yu, B. Ning, Q. Zhang, J. Chen, W. H. Cheng, W. Shen and Z. X. Yang (2012). "Saturated fatty acid induction of endoplasmic reticulum stress and apoptosis in human liver cells via the PERK/ATF4/CHOP signaling pathway." Mol Cell Biochem **364**(1-2): 115-129.

Charlton, M. (2004). "Nonalcoholic fatty liver disease: a review of current understanding and future impact." Clin Gastroenterol Hepatol **2**(12): 1048-1058.

Chauvin, C., S. Salhi, C. Le Goff, W. Viranaicken, D. Diop and O. Jean-Jean (2005). "Involvement of human release factors eRF3a and eRF3b in translation termination and regulation of the termination complex formation." Mol Cell Biol **25**(14): 5801-5811.

Chavez-Tapia, N. C., N. Rosso and C. Tiribelli (2012). "Effect of intracellular lipid accumulation in a new model of non-alcoholic fatty liver disease." BMC Gastroenterol **12**: 20.

Chen, X., S. Xu, S. Wei, Y. Deng, Y. Li, F. Yang and P. Liu (2016). "Comparative Proteomic Study of Fatty Acid-treated Myoblasts Reveals Role of Cox-2 in Palmitate-induced Insulin Resistance." Sci Rep **6**: 21454.

Chroni, A., T. J. Nieland, K. E. Kypreos, M. Krieger and V. I. Zannis (2005). "SR-BI mediates cholesterol efflux via its interactions with lipid-bound ApoE. Structural mutations in SR-BI diminish cholesterol efflux." Biochemistry **44**(39): 13132-13143.

Clavey, V., C. Copin, M. C. Mariotte, E. Bauge, G. Chinetti, J. Fruchart, J. C. Fruchart, J. Dallongeville and B. Staels (1999). "Cell culture conditions determine apolipoprotein CIII secretion and regulation by fibrates in human hepatoma HepG2 cells." Cell Physiol Biochem **9**(3): 139-149.

Conde-Vancells, J., E. Rodriguez-Suarez, N. Embade, D. Gil, R. Matthiesen, M. Valle, F. Elortza, S. C. Lu, J. M. Mato and J. M. Falcon-Perez (2008). "Characterization and comprehensive proteome profiling of exosomes secreted by hepatocytes." J Proteome Res **7**(12): 5157-5166.

Cooney, J. M., M. P. Barnett, D. Brewster, B. Knoch, W. C. McNabb, W. A. Laing and N. C. Roy (2012). "Proteomic analysis of colon tissue from interleukin-10 gene-deficient mice fed polyunsaturated Fatty acids with comparison to transcriptomic analysis." J Proteome Res **11**(2): 1065-1077.

Cox, J., M. Y. Hein, C. A. Luber, I. Paron, N. Nagaraj and M. Mann (2014). "Accurate proteome-wide label-free quantification by delayed normalization and maximal peptide ratio extraction, termed MaxLFQ." Mol Cell Proteomics **13**(9): 2513-2526.

Crosby, J., G. M. Peloso, P. L. Auer, D. R. Crosslin, N. O. Stitzel, L. A. Lange, Y. Lu, Z. Z. Tang, H. Zhang, G. Hindy, N. Masca, K. Stirrups, S. Kanoni, R. Do, G. Jun, Y. Hu, H. M. Kang, C. Xue, A. Goel, M. Farrall, S. Duga, P. A. Merlini, R. Asselta, D. Girelli, O. Olivieri, N. Martinelli, W. Yin, D. Reilly, E. Speliotes, C. S. Fox, K. Hveem, O. L. Holmen, M. Nikpay, D. N. Farlow, T. L. Assimes, N. Franceschini, J. Robinson, K. E. North, L. W. Martin, M. DePristo, N. Gupta, S. A. Escher, J. H. Jansson, N. Van Zuydam, C. N. Palmer, N. Wareham, W. Koch, T. Meitinger, A. Peters, W. Lieb, R. Erbel, I. R. Konig, J. Kruppa, F. Degenhardt, O. Gottesman, E. P. Bottinger, C. J. O'Donnell, B. M. Psaty, C. M. Ballantyne, G. Abecasis, J. M. Ordovas, O. Melander, H. Watkins, M. Orho-Melander, D. Ardisino, R. J. Loos, R. McPherson, C. J. Willer, J. Erdmann, A. S. Hall, N. J. Samani, P. Deloukas, H. Schunkert, J. G. Wilson, C. Kooperberg, S. S. Rich, R. P. Tracy, D. Y. Lin, D. Altshuler, S. Gabriel, D. A. Nickerson, G. P. Jarvik, L. A. Cupples, A. P. Reiner, E. Boerwinkle, S. T. a. H. W. G. o. t. E. S. P. Kathiresan, N. H. Lung and I. Blood (2014). "Loss-of-function mutations in APOC3, triglycerides, and coronary disease." N Engl J Med **371**(1): 22-31.

Damiano, F., A. Rochira, R. Tocci, S. Alemanno, A. Gnoni and L. Siculella (2013). "hnRNP A1 mediates the activation of the IRES-dependent SREBP-1a mRNA translation in response to endoplasmic reticulum stress." Biochem J **449**(2): 543-553.

Dashti, M., W. Kulik, F. Hoek, E. C. Veerman, M. P. Peppelenbosch and F. Rezaee (2011). "A phospholipidomic analysis of all defined human plasma lipoproteins." Sci Rep **1**: 139.

Davignon, J. (2005). "Apolipoprotein E and atherosclerosis: beyond lipid effect." Arterioscler Thromb Vasc Biol **25**(2): 267-269.

Dawber, T. R., G. F. Meadors and F. E. Moore, Jr. (1951). "Epidemiological approaches to heart disease: the Framingham Study." Am J Public Health Nations Health **41**(3): 279-281.

de Beer, M. C., D. M. Durbin, L. Cai, A. Jonas, F. C. de Beer and D. R. van der Westhuyzen (2001). "Apolipoprotein A-I conformation markedly influences HDL interaction with scavenger receptor BI." J Lipid Res **42**(2): 309-313.

De Caterina, R. (2011). "n-3 fatty acids in cardiovascular disease." N Engl J Med **364**(25): 2439-2450.

De Maio, A. and D. Vazquez (2013). "Extracellular heat shock proteins: a new location, a new function." Shock **40**(4): 239-246.

de Oliveira Otto, M. C., J. A. Nettleton, R. N. Lemaitre, L. M. Steffen, D. Kromhout, S. S. Rich, M. Y. Tsai, D. R. Jacobs and D. Mozaffarian (2013). "Biomarkers of dairy fatty acids and risk of cardiovascular disease in the Multi-ethnic Study of Atherosclerosis." J Am Heart Assoc **2**(4): e000092.

de Roos, B., A. Geelen, K. Ross, G. Rucklidge, M. Reid, G. Duncan, M. Caslake, G. Horgan and I. A. Brouwer (2008). "Identification of potential serum biomarkers of inflammation and lipid modulation that are altered by fish oil supplementation in healthy volunteers." Proteomics **8**(10): 1965-1974.

de Roos, B. and D. F. Romagnolo (2012). "Proteomic approaches to predict bioavailability of fatty acids and their influence on cancer and chronic disease prevention." J Nutr **142**(7): 1370S-1376S.

de Roos, B., A. J. Wanders, S. Wood, G. Horgan, G. Rucklidge, M. Reid, E. Siebelink and I. A. Brouwer (2011). "A high intake of industrial or ruminant trans fatty acids does not affect the plasma proteome in healthy men." Proteomics **11**(19): 3928-3934.

Dessein, P. H., L. Tsang, G. R. Norton, A. J. Woodiwiss and A. Solomon (2014). "Retinol binding protein 4 concentrations relate to enhanced atherosclerosis in obese patients with rheumatoid arthritis." PLoS One **9**(3): e92739.

Di Castelnuovo, A., S. Costanzo, V. Bagnardi, M. B. Donati, L. Iacoviello and G. de Gaetano (2006). "Alcohol dosing and total mortality in men and women: an updated meta-analysis of 34 prospective studies." Arch Intern Med **166**(22): 2437-2445.

Diaz-Ramos, A., A. Roig-Borrellas, A. Garcia-Melero and R. Lopez-Aleman (2012). "alpha-Enolase, a multifunctional protein: its role on pathophysiological situations." J Biomed Biotechnol **2012**: 156795.

Ditiatkovski, M., J. Palsson, J. Chin-Dusting, A. T. Remaley and D. Sviridov (2017). "Apolipoprotein A-I Mimetic Peptides: Discordance Between In Vitro and In Vivo Properties-Brief Report." Arterioscler Thromb Vasc Biol **37**(7): 1301-1306.

Dominiczak, M. H. and M. J. Caslake (2011). "Apolipoproteins: metabolic role and clinical biochemistry applications." Ann Clin Biochem **48**(Pt 6): 498-515.

Dose, J., P. Huebbe, A. Nebel and G. Rimbach (2016). "APOE genotype and stress response - a mini review." Lipids Health Dis **15**: 121.

Duijvesz, D., K. E. Burnum-Johnson, M. A. Gritsenko, A. M. Hoogland, M. S. Vredenburg-van den Berg, R. Willemsen, T. Luider, L. Pasa-Tolic and G. Jenster (2013). "Proteomic profiling of exosomes leads to the identification of novel biomarkers for prostate cancer." PLoS One **8**(12): e82589.

Duval, C., M. Muller and S. Kersten (2007). "PPARalpha and dyslipidemia." Biochim Biophys Acta **1771**(8): 961-971.

Ebbesson, S. O., V. S. Voruganti, P. B. Higgins, R. R. Fabsitz, L. O. Ebbesson, S. Laston, W. S. Harris, J. Kennish, B. D. Umans, H. Wang, R. B. Devereux, P. M. Okin, N. J. Weissman, J. W. MacCluer, J. G. Umans and B. V. Howard (2015). "Fatty acids linked to cardiovascular mortality are associated with risk factors." Int J Circumpolar Health **74**: 28055.

Elliott, D. A., C. S. Weickert and B. Garner (2010). "Apolipoproteins in the brain: implications for neurological and psychiatric disorders." Clin Lipidol **51**(4): 555-573.

Ellis, K. L., A. J. Hooper, J. R. Burnett and G. F. Watts (2016). "Progress in the care of common inherited atherogenic disorders of apolipoprotein B metabolism." Nat Rev Endocrinol **12**(8): 467-484.

Ellsworth, J. L., S. K. Erickson and A. D. Cooper (1986). "Very low and low density lipoprotein synthesis and secretion by the human hepatoma cell line Hep-G2: effects of free fatty acid." J Lipid Res **27**(8): 858-874.

Ericson, U., S. Hellstrand, L. Brunkwall, C. A. Schulz, E. Sonestedt, P. Wallstrom, B. Gullberg, E. Wirfalt and M. Orho-Melander (2015). "Food sources of fat may clarify the inconsistent role of dietary fat intake for incidence of type 2 diabetes." Am J Clin Nutr **101**(5): 1065-1080.

Ezanno, H., J. le Bloc'h, E. Beauchamp, D. Lagadic-Gossmann, P. Legrand and V. Rioux (2012). "Myristic acid increases dihydroceramide Delta4-desaturase 1 (DES1) activity in cultured rat hepatocytes." Lipids **47**(2): 117-128.

Fang, M., Z. Shen, S. Huang, L. Zhao, S. Chen, T. W. Mak and X. Wang (2010). "The ER UDPase ENTPD5 promotes protein N-glycosylation, the Warburg effect, and proliferation in the PTEN pathway." Cell **143**(5): 711-724.

Feldstein, A. E., N. W. Werneburg, A. Canbay, M. E. Guicciardi, S. F. Bronk, R. Rydzewski, L. J. Burgart and G. J. Gores (2004). "Free fatty acids promote hepatic lipotoxicity by stimulating TNF-alpha expression via a lysosomal pathway." Hepatology **40**(1): 185-194.

Fernandez-Real, J. M., J. A. Menendez, J. M. Moreno-Navarrete, M. Blüher, A. Vazquez-Martin, M. J. Vazquez, F. Ortega, C. Dieguez, G. Frühbeck, W. Ricart and A. Vidal-Puig (2010). "Extracellular fatty acid synthase: a possible surrogate biomarker of insulin resistance." Diabetes **59**(6): 1506-1511.

Ferramosca, A. and V. Zara (2014). "Modulation of hepatic steatosis by dietary fatty acids." World J Gastroenterol **20**(7): 1746-1755.

Finegold, J. A., P. Asaria and D. P. Francis (2013). "Mortality from ischaemic heart disease by country, region, and age: statistics from World Health Organisation and United Nations." Int J Cardiol **168**(2): 934-945.

Fisher, E., E. Lake and R. S. McLeod (2014). "Apolipoprotein B100 quality control and the regulation of hepatic very low density lipoprotein secretion." J Biomed Res **28**(3): 178-193.

Foerster, M., P. Marques-Vidal, G. Gmel, J. B. Daeppen, J. Cornuz, D. Hayoz, A. Pecoud, V. Mooser, G. Waeber, P. Vollenweider, F. Paccaud and N. Rodondi (2009). "Alcohol drinking and cardiovascular risk in a population with high mean alcohol consumption." Am J Cardiol **103**(3): 361-368.

Forouhi, N. G., A. Koulman, S. J. Sharp, F. Imamura, J. Kroger, M. B. Schulze, F. L. Crowe, J. M. Huerta, M. Guevara, J. W. Beulens, G. J. van Woudenberg, L. Wang, K. Summerhill, J. L. Griffin, E. J. Feskens, P. Amiano, H. Boeing, F. Clavel-Chapelon, L. Dartois, G. Fagherazzi, P. W. Franks, C. Gonzalez, M. U. Jakobsen, R. Kaaks, T. J. Key, K. T. Khaw, T. Kuhn, A. Mattiello, P. M. Nilsson, K. Overvad, V. Pala, D. Palli, J. R. Quiros, O. Rolandsson, N. Roswall, C. Sacerdote, M. J. Sanchez, N. Slimani, A. M. Spijkerman, A. Tjonneland, M. J. Tormo, R. Tumino, A. D. van der, Y. T. van der Schouw, C. Langenberg, E. Riboli and N. J. Wareham (2014). "Differences in the prospective association between individual plasma phospholipid saturated fatty acids and incident type 2 diabetes: the EPIC-InterAct case-cohort study." Lancet Diabetes Endocrinol **2**(10): 810-818.

Fredrickson, D. S. and R. S. Lees (1965). "A System for Phenotyping Hyperlipoproteinemia." Circulation **31**: 321-327.

Fritsche, K. L. (2015). "The science of fatty acids and inflammation." Adv Nutr **6**(3): 293S-301S.

Galassi, A., K. Reynolds and J. He (2006). "Metabolic syndrome and risk of cardiovascular disease: a meta-analysis." Am J Med **119**(10): 812-819.

Garcia-Ruiz, I., P. Solis-Munoz, D. Fernandez-Moreira, T. Munoz-Yague and J. A. Solis-Herruzo (2015). "In vitro treatment of HepG2 cells with saturated fatty acids reproduces mitochondrial dysfunction found in nonalcoholic steatohepatitis." Dis Model Mech **8**(2): 183-191.

Genereux, J. C., S. Qu, M. Zhou, L. M. Ryno, S. Wang, M. D. Shoulders, R. J. Kaufman, C. I. Lasmezas, J. W. Kelly and R. L. Wiseman (2015). "Unfolded protein response-induced ERdj3 secretion links ER stress to extracellular proteostasis." EMBO J **34**(1): 4-19.

Genth-Zotz, S., A. P. Bolger, P. R. Kalra, S. von Haehling, W. Doehner, A. J. Coats, H. D. Volk and S. D. Anker (2004). "Heat shock protein 70 in patients with chronic heart failure: relation to disease severity and survival." Int J Cardiol **96**(3): 397-401.

Georgiadi, A. and S. Kersten (2012). "Mechanisms of gene regulation by fatty acids." Adv Nutr **3**(2): 127-134.

Girelli, D., S. Friso, E. Trabetti, O. Olivieri, C. Russo, R. Pessotto, G. Faccini, P. F. Pignatti, A. Mazzucco and R. Corrocher (1998). "Methylenetetrahydrofolate reductase C677T mutation, plasma homocysteine, and folate in subjects from northern Italy with or without angiographically documented severe coronary atherosclerotic disease: evidence for an important genetic-environmental interaction." Blood **91**(11): 4158-4163.

Glass, C. K. and J. L. Witztum (2001). "Atherosclerosis. the road ahead." Cell **104**(4): 503-516.

Goldstein, J. L. and M. S. Brown (2009). "The LDL receptor." Arterioscler Thromb Vasc Biol **29**(4): 431-438.

Gomez-Arreaza, A., H. Acosta, W. Quinones, J. L. Concepcion, P. A. Michels and L. Avilan (2014). "Extracellular functions of glycolytic enzymes of parasites: unpredicted use of ancient proteins." Mol Biochem Parasitol **193**(2): 75-81.

Gomez-Suaga, P., S. Paillusson and C. C. J. Miller (2017). "ER-mitochondria signaling regulates autophagy." Autophagy **13**(7): 1250-1251.

Gordts, P. L., R. Nock, N. H. Son, B. Ramms, I. Lew, J. C. Gonzales, B. E. Thacker, D. Basu, R. G. Lee, A. E. Mullick, M. J. Graham, I. J. Goldberg, R. M. Crooke, J. L. Witztum and J. D. Esko (2016). "ApoC-III inhibits clearance of triglyceride-rich lipoproteins through LDL family receptors." J Clin Invest **126**(8): 2855-2866.

Greenow, K., N. J. Pearce and D. P. Ramji (2005). "The key role of apolipoprotein E in atherosclerosis." J Mol Med (Berl) **83**(5): 329-342.

Haas, M. J., M. H. Horani, N. C. Wong and A. D. Mooradian (2004). "Induction of the apolipoprotein AI promoter by Sp1 is repressed by saturated fatty acids." Metabolism **53**(10): 1342-1348.

Hansson, G. K. (2005). "Inflammation, atherosclerosis, and coronary artery disease." N Engl J Med **352**(16): 1685-1695.

Hansson, G. K. and A. Hermansson (2011). "The immune system in atherosclerosis." Nat Immunol **12**(3): 204-212.

Hashemi, H. F. and J. M. Goodman (2015). "The life cycle of lipid droplets." Curr Opin Cell Biol **33**: 119-124.

Hayek, T., J. Oiknine, J. G. Brook and M. Aviram (1994). "Increased plasma and lipoprotein lipid peroxidation in apo E-deficient mice." Biochem Biophys Res Commun **201**(3): 1567-1574.

Hegsted, D. M., L. M. Ausman, J. A. Johnson and G. E. Dallal (1993). "Dietary fat and serum lipids: an evaluation of the experimental data." Am J Clin Nutr **57**(6): 875-883.

Hetherington, A. M., C. G. Sawyez, E. Zilberman, A. M. Stoianov, D. L. Robson and N. M. Borradaile (2016). "Differential Lipotoxic Effects of Palmitate and Oleate in Activated Human Hepatic Stellate Cells and Epithelial Hepatoma Cells." Cell Physiol Biochem **39**(4): 1648-1662.

Higa, L. M., B. M. Curi, R. S. Aguiar, C. C. Cardoso, A. G. De Lorenzi, S. L. Sena, R. B. Zingali and A. T. Da Poian (2014). "Modulation of alpha-enolase post-translational modifications by dengue virus: increased secretion of the basic isoforms in infected hepatic cells." PLoS One **9**(8): e88314.

Higgins, R., J. M. Gendron, L. Rising, R. Mak, K. Webb, S. E. Kaiser, N. Zuzow, P. Riviere, B. Yang, E. Fenech, X. Tang, S. A. Lindsay, J. C. Christianson, R. Y. Hampton, S. A. Wasserman and E. J. Bennett (2015). "The Unfolded Protein Response Triggers Site-Specific Regulatory Ubiquitylation of 40S Ribosomal Proteins." Mol Cell **59**(1): 35-49.

Hu, F. B., M. J. Stampfer, J. E. Manson, E. Rimm, G. A. Colditz, B. A. Rosner, C. H. Hennekens and W. C. Willett (1997). "Dietary fat intake and the risk of coronary heart disease in women." N Engl J Med **337**(21): 1491-1499.

Hu, R., Z. F. Chen, J. Yan, Q. F. Li, Y. Huang, H. Xu, X. P. Zhang and H. Jiang (2015). "Endoplasmic Reticulum Stress of Neutrophils Is Required for Ischemia/Reperfusion-Induced Acute Lung Injury." J Immunol **195**(10): 4802-4809.

Huang, C. Y., W. M. Chen, Y. G. Tsay, S. C. Hsieh, Y. Lin, W. J. Lee, W. H. Sheu and A. N. Chiang (2015). "Differential regulation of protein expression in response to polyunsaturated fatty acids in the liver of apoE-knockout mice and in HepG2 cells." J Biomed Sci **22**: 12.

Huang da, W., B. T. Sherman and R. A. Lempicki (2009). "Systematic and integrative analysis of large gene lists using DAVID bioinformatics resources." Nat Protoc **4**(1): 44-57.

Huang, Y., Z. S. Ji, W. J. Brecht, S. C. Rall, Jr., J. M. Taylor and R. W. Mahley (1999). "Overexpression of apolipoprotein E3 in transgenic rabbits causes combined hyperlipidemia by

stimulating hepatic VLDL production and impairing VLDL lipolysis." Arterioscler Thromb Vasc Biol **19**(12): 2952-2959.

Huang, Y., X. Q. Liu, S. C. Rall, Jr. and R. W. Mahley (1998). "Apolipoprotein E2 reduces the low density lipoprotein level in transgenic mice by impairing lipoprotein lipase-mediated lipolysis of triglyceride-rich lipoproteins." J Biol Chem **273**(28): 17483-17490.

Huber, H. J. and P. Holvoet (2015). "Exosomes: emerging roles in communication between blood cells and vascular tissues during atherosclerosis." Curr Opin Lipidol **26**(5): 412-419.

Huff, M. W., N. H. Fidge, P. J. Nestel, T. Billington and B. Watson (1981). "Metabolism of C-apolipoproteins: kinetics of C-II, C-III1 and C-III2, and VLDL-apolipoprotein B in normal and hyperlipoproteinemic subjects." J Lipid Res **22**(8): 1235-1246.

Hwang, Y. J., H. R. Wi, H. R. Kim, K. W. Park and K. A. Hwang (2014). "Pinus densiflora Sieb. et Zucc. alleviates lipogenesis and oxidative stress during oleic acid-induced steatosis in HepG2 cells." Nutrients **6**(7): 2956-2972.

Inoue, N. (2014). "Stress and atherosclerotic cardiovascular disease." J Atheroscler Thromb **21**(5): 391-401.

Ito, M. K. (2015). "Long-chain omega-3 fatty acids, fibrates and niacin as therapeutic options in the treatment of hypertriglyceridemia: a review of the literature." Atherosclerosis **242**(2): 647-656.

Jan, S., H. Guillou, S. D'Andrea, S. Daval, M. Bouriel, V. Rioux and P. Legrand (2004). "Myristic acid increases delta6-desaturase activity in cultured rat hepatocytes." Reprod Nutr Dev **44**(2): 131-140.

Johnson, R. K., A. E. Black and T. J. Cole (1998). "Dietary fat intake and the risk of coronary heart disease in women." N Engl J Med **338**(13): 918-919.

Jong, M. C., V. E. Dahlmans, M. H. Hofker and L. M. Havekes (1997). "Nascent very-low-density lipoprotein triacylglycerol hydrolysis by lipoprotein lipase is inhibited by apolipoprotein E in a dose-dependent manner." Biochem J **328** ( Pt 3): 745-750.

Jung, I. R., S. E. Choi, J. G. Jung, S. A. Lee, S. J. Han, H. J. Kim, D. J. Kim, K. W. Lee and Y. Kang (2015). "Involvement of iron depletion in palmitate-induced lipotoxicity of beta cells." Mol Cell Endocrinol **407**: 74-84.

Kalli, A. and S. Hess (2012). "Effect of mass spectrometric parameters on peptide and protein identification rates for shotgun proteomic experiments on an LTQ-orbitrap mass analyzer." Proteomics **12**(1): 21-31.

Kanekura, K., I. Nishimoto, S. Aiso and M. Matsuoka (2006). "Characterization of amyotrophic lateral sclerosis-linked P56S mutation of vesicle-associated membrane protein-associated protein B (VAPB/ALS8)." J Biol Chem **281**(40): 30223-30233.

Kanekura, K., H. Suzuki, S. Aiso and M. Matsuoka (2009). "ER stress and unfolded protein response in amyotrophic lateral sclerosis." Mol Neurobiol **39**(2): 81-89.

Kanellos, G., J. Zhou, H. Patel, R. A. Ridgway, D. Huels, C. B. Gurniak, E. Sandilands, N. O. Carragher, O. J. Sansom, W. Witke, V. G. Brunton and M. C. Frame (2015). "ADF and Cofilin1 Control Actin Stress Fibers, Nuclear Integrity, and Cell Survival." Cell Rep **13**(9): 1949-1964.

Kang, O. H., S. B. Kim, Y. S. Seo, D. K. Joung, S. H. Mun, J. G. Choi, Y. M. Lee, D. G. Kang, H. S. Lee and D. Y. Kwon (2013). "Curcumin decreases oleic acid-induced lipid accumulation via AMPK phosphorylation in hepatocarcinoma cells." Eur Rev Med Pharmacol Sci **17**(19): 2578-2586.

- Katan, M. B., P. L. Zock and R. P. Mensink (1994). "Effects of fats and fatty acids on blood lipids in humans: an overview." Am J Clin Nutr **60**(6 Suppl): 1017S-1022S.
- Kawakami, A., M. Aikawa, P. Alcaide, F. W. Lusinskas, P. Libby and F. M. Sacks (2006). "Apolipoprotein CIII induces expression of vascular cell adhesion molecule-1 in vascular endothelial cells and increases adhesion of monocytic cells." Circulation **114**(7): 681-687.
- Kawakami, A., M. Aikawa, N. Nitta, M. Yoshida, P. Libby and F. M. Sacks (2007). "Apolipoprotein CIII-induced THP-1 cell adhesion to endothelial cells involves pertussis toxin-sensitive G protein- and protein kinase C alpha-mediated nuclear factor-kappaB activation." Arterioscler Thromb Vasc Biol **27**(1): 219-225.
- Kawakami, A. and M. Yoshida (2009). "Apolipoprotein CIII links dyslipidemia with atherosclerosis." J Atheroscler Thromb **16**(1): 6-11.
- Keerthikumar, S., D. Chisanga, D. Ariyaratne, H. Al Saffar, S. Anand, K. Zhao, M. Samuel, M. Pathan, M. Jois, N. Chilamkurti, L. Gangoda and S. Mathivanan (2016). "ExoCarta: A Web-Based Compendium of Exosomal Cargo." J Mol Biol **428**(4): 688-692.
- Kennedy, A., K. Martinez, C. C. Chuang, K. LaPoint and M. McIntosh (2009). "Saturated fatty acid-mediated inflammation and insulin resistance in adipose tissue: mechanisms of action and implications." J Nutr **139**(1): 1-4.
- Khetarpal, S. A., A. Qamar, J. S. Millar and D. J. Rader (2016). "Targeting ApoC-III to Reduce Coronary Disease Risk." Curr Atheroscler Rep **18**(9): 54.
- Kindel, T., D. M. Lee and P. Tso (2010). "The mechanism of the formation and secretion of chylomicrons." Atheroscler Suppl **11**(1): 11-16.
- Kinnunen, P. K. and C. Ehnolm (1976). "Effect of serum and C-apoproteins from very low density lipoproteins on human postheparin plasma hepatic lipase." FEBS Lett **65**(3): 354-357.
- Kirpich, I. A., L. N. Gobejishvili, M. Bon Homme, S. Waigel, M. Cave, G. Arteel, S. S. Barve, C. J. McClain and I. V. Deaciuc (2011). "Integrated hepatic transcriptome and proteome analysis of mice with high-fat diet-induced nonalcoholic fatty liver disease." J Nutr Biochem **22**(1): 38-45.
- Krauss, R. M. (2010). "Lipoprotein subfractions and cardiovascular disease risk." Curr Opin Lipidol **21**(4): 305-311.
- Kris-Etherton, P. M. and S. Yu (1997). "Individual fatty acid effects on plasma lipids and lipoproteins: human studies." Am J Clin Nutr **65**(5 Suppl): 1628S-1644S.
- Krogager, T. P., L. V. Nielsen, D. Kahveci, T. F. Dyrland, C. Scavenius, K. W. Sanggaard and J. J. Enghild (2015). "Hepatocytes respond differently to major dietary trans fatty acid isomers, elaidic acid and trans-vaccenic acid." Proteome Sci **13**: 31.
- Kuipers, F., M. C. Jong, Y. Lin, M. Eck, R. Havinga, V. Bloks, H. J. Verkade, M. H. Hofker, H. Moshage, T. J. Berkel, R. J. Vonk and L. M. Havekes (1997). "Impaired secretion of very low density lipoprotein-triglycerides by apolipoprotein E- deficient mouse hepatocytes." J Clin Invest **100**(11): 2915-2922.
- Kummrow, E., M. M. Hussain, M. Pan, J. B. Marsh and E. A. Fisher (2002). "Myristic acid increases dense lipoprotein secretion by inhibiting apoB degradation and triglyceride recruitment." J Lipid Res **43**(12): 2155-2163.



- Laakso, M. and J. Kuusisto (2014). "Insulin resistance and hyperglycaemia in cardiovascular disease development." Nat Rev Endocrinol **10**(5): 293-302.
- Laufs, U., S. Wassmann, T. Czech, T. Munzel, M. Eisenhauer, M. Bohm and G. Nickenig (2005). "Physical inactivity increases oxidative stress, endothelial dysfunction, and atherosclerosis." Arterioscler Thromb Vasc Biol **25**(4): 809-814.
- Lee, A. H., N. N. Iwakoshi and L. H. Glimcher (2003). "XBP-1 regulates a subset of endoplasmic reticulum resident chaperone genes in the unfolded protein response." Mol Cell Biol **23**(21): 7448-7459.
- Lee, A. S., P. J. Kranzusch and J. H. Cate (2015). "eIF3 targets cell-proliferation messenger RNAs for translational activation or repression." Nature **522**(7554): 111-114.
- Lee, J. H., E. J. Kwon and D. H. Kim (2013). "Calumenin has a role in the alleviation of ER stress in neonatal rat cardiomyocytes." Biochem Biophys Res Commun **439**(3): 327-332.
- Leman, L. J., B. E. Maryanoff and M. R. Ghadiri (2014). "Molecules that mimic apolipoprotein A-I: potential agents for treating atherosclerosis." J Med Chem **57**(6): 2169-2196.
- Lepage, G. and C. C. Roy (1984). "Improved recovery of fatty acid through direct transesterification without prior extraction or purification." J Lipid Res **25**(12): 1391-1396.
- Leznicki, P., J. Korac-Prlic, K. Kliza, K. Husnjak, Y. Nyathi, I. Dikic and S. High (2015). "Binding of SGTA to Rpn13 selectively modulates protein quality control." J Cell Sci **128**(17): 3187-3196.
- Li, L., D. Z. Lu, Y. M. Li, X. Q. Zhang, X. X. Zhou and X. Jin (2014). "Proteomic analysis of liver mitochondria from rats with nonalcoholic steatohepatitis." World J Gastroenterol **20**(16): 4778-4786.
- Li, W. H., M. Tanimura, C. C. Luo, S. Datta and L. Chan (1988). "The apolipoprotein multigene family: biosynthesis, structure, structure-function relationships, and evolution." J Lipid Res **29**(3): 245-271.
- Libby, P. (2013). "Mechanisms of acute coronary syndromes and their implications for therapy." N Engl J Med **368**(21): 2004-2013.
- Libby, P., P. M. Ridker and G. K. Hansson (2011). "Progress and challenges in translating the biology of atherosclerosis." Nature **473**(7347): 317-325.
- Libby, P. and P. Theroux (2005). "Pathophysiology of coronary artery disease." Circulation **111**(25): 3481-3488.
- Lichtenstein, A. H., E. Kennedy, P. Barrier, D. Danford, N. D. Ernst, S. M. Grundy, G. A. Leveille, L. Van Horn, C. L. Williams and S. L. Booth (1998). "Dietary fat consumption and health." Nutr Rev **56**(5 Pt 2): S3-19; discussion S19-28.
- Liu, C. Y., M. Schroder and R. J. Kaufman (2000). "Ligand-independent dimerization activates the stress response kinases IRE1 and PERK in the lumen of the endoplasmic reticulum." J Biol Chem **275**(32): 24881-24885.
- Liu, Y., D. Mu, H. Chen, D. Li, J. Song, Y. Zhong and M. Xia (2016). "Retinol-Binding Protein 4 Induces Hepatic Mitochondrial Dysfunction and Promotes Hepatic Steatosis." J Clin Endocrinol Metab **101**(11): 4338-4348.
- Loyer, X., Z. Mallat, C. M. Boulanger and A. Tedgui (2015). "MicroRNAs as therapeutic targets in atherosclerosis." Expert Opin Ther Targets **19**(4): 489-496.

Lu, X. and V. Kakkar (2010). "The role of heat shock protein (HSP) in atherosclerosis: Pathophysiology and clinical opportunities." Curr Med Chem **17**(10): 957-973.

Lusis, A. J. (2000). "Atherosclerosis." Nature **407**(6801): 233-241.

Mabile, L., C. Lefebvre, J. Lavigne, L. Boulet, J. Davignon, S. Lussier-Cacan and L. Bernier (2003). "Secreted apolipoprotein E reduces macrophage-mediated LDL oxidation in an isoform-dependent way." J Cell Biochem **90**(4): 766-776.

Mahley, R. W., K. H. Weisgraber and Y. Huang (2009). "Apolipoprotein E: structure determines function, from atherosclerosis to Alzheimer's disease to AIDS." J Lipid Res **50** **Suppl**: S183-188.

Malhi, H., S. F. Bronk, N. W. Werneburg and G. J. Gores (2006). "Free fatty acids induce JNK-dependent hepatocyte lipoapoptosis." J Biol Chem **281**(17): 12093-12101.

Mao, W., S. Fukuoka, C. Iwai, J. Liu, V. K. Sharma, S. S. Sheu, M. Fu and C. S. Liang (2007). "Cardiomyocyte apoptosis in autoimmune cardiomyopathy: mediated via endoplasmic reticulum stress and exaggerated by norepinephrine." Am J Physiol Heart Circ Physiol **293**(3): H1636-1645.

Marais, A. D., J. B. Kim, S. M. Wasserman and G. Lambert (2015). "PCSK9 inhibition in LDL cholesterol reduction: genetics and therapeutic implications of very low plasma lipoprotein levels." Pharmacol Ther **145**: 58-66.

Maris, M., E. Waelkens, M. Cnop, W. D'Hertog, D. A. Cunha, H. Korf, T. Koike, L. Overbergh and C. Mathieu (2011). "Oleate-induced beta cell dysfunction and apoptosis: a proteomic approach to glucolipotoxicity by an unsaturated fatty acid." J Proteome Res **10**(8): 3372-3385.

Marsillach, J., C. Oliveras-Ferreros, R. Beltran, A. Rull, G. Aragonés, C. Alonso-Villaverde, A. Vazquez-Martin, J. Joven, J. A. Menendez and J. Camps (2009). "Serum concentrations of extracellular fatty acid synthase in patients with steatohepatitis." Clin Chem Lab Med **47**(9): 1097-1099.

Martin, D. D., E. Beauchamp and L. G. Berthiaume (2011). "Post-translational myristoylation: Fat matters in cellular life and death." Biochimie **93**(1): 18-31.

Martinelli, N., D. Girelli, G. Malerba, P. Guarini, T. Illig, E. Trabetti, M. Sandri, S. Friso, F. Pizzolo, L. Schaeffer, J. Heinrich, P. F. Pignatti, R. Corrocher and O. Olivieri (2008). "FADS genotypes and desaturase activity estimated by the ratio of arachidonic acid to linoleic acid are associated with inflammation and coronary artery disease." Am J Clin Nutr **88**(4): 941-949.

Martinelli, N., E. Trabetti, A. Bassi, D. Girelli, S. Friso, F. Pizzolo, M. Sandri, G. Malerba, P. F. Pignatti, R. Corrocher and O. Olivieri (2007). "The -1131 T>C and S19W APOA5 gene polymorphisms are associated with high levels of triglycerides and apolipoprotein C-III, but not with coronary artery disease: an angiographic study." Atherosclerosis **191**(2): 409-417.

Martinez, L., S. Torres, A. Baulies, C. Alarcon-Vila, M. Elena, G. Fabrias, J. Casas, J. Caballeria, J. C. Fernandez-Checa and C. Garcia-Ruiz (2015). "Myristic acid potentiates palmitic acid-induced lipotoxicity and steatohepatitis associated with lipodystrophy by sustaining de novo ceramide synthesis." Oncotarget **6**(39): 41479-41496.

Massaro, M., E. Scoditti, M. A. Carluccio and R. De Caterina (2012). "Alcohol and atherosclerosis: a double edged sword." Vascul Pharmacol **57**(2-4): 65-68.

Mathivanan, S. and R. J. Simpson (2009). "ExoCarta: A compendium of exosomal proteins and RNA." Proteomics **9**(21): 4997-5000.

Matthan, N. R., F. K. Welty, P. H. Barrett, C. Harausz, G. G. Dolnikowski, J. S. Parks, R. H. Eckel, E. J. Schaefer and A. H. Lichtenstein (2004). "Dietary hydrogenated fat increases high-density lipoprotein apoA-I catabolism and decreases low-density lipoprotein apoB-100 catabolism in hypercholesterolemic women." Arterioscler Thromb Vasc Biol **24**(6): 1092-1097.

Mayneris-Perxachs, J., M. Guerendiain, A. I. Castellote, R. Estruch, M. I. Covas, M. Fito, J. Salas-Salvado, M. A. Martinez-Gonzalez, F. Aros, R. M. Lamuela-Raventos, M. C. Lopez-Sabater and P. S. I. for (2014). "Plasma fatty acid composition, estimated desaturase activities, and their relation with the metabolic syndrome in a population at high risk of cardiovascular disease." Clin Nutr **33**(1): 90-97.

McEvoy, J. W., M. J. Blaha, A. P. DeFilippis, J. A. Lima, D. A. Bluemke, W. G. Hundley, J. K. Min, L. J. Shaw, D. M. Lloyd-Jones, R. G. Barr, M. J. Budoff, R. S. Blumenthal and K. Nasir (2015). "Cigarette smoking and cardiovascular events: role of inflammation and subclinical atherosclerosis from the MultiEthnic Study of Atherosclerosis." Arterioscler Thromb Vasc Biol **35**(3): 700-709.

McQueen, M. J., S. Hawken, X. Wang, S. Ounpuu, A. Sniderman, J. Probstfield, K. Steyn, J. E. Sanderson, M. Hasani, E. Volkova, K. Kazmi, S. Yusuf and I. s. investigators (2008). "Lipids, lipoproteins, and apolipoproteins as risk markers of myocardial infarction in 52 countries (the INTERHEART study): a case-control study." Lancet **372**(9634): 224-233.

Meex, R. C. R. and M. J. Watt (2017). "Hepatokines: linking nonalcoholic fatty liver disease and insulin resistance." Nat Rev Endocrinol **13**(9): 509-520.

Meex, S. J., U. Andreo, J. D. Sparks and E. A. Fisher (2011). "Huh-7 or HepG2 cells: which is the better model for studying human apolipoprotein-B100 assembly and secretion?" J Lipid Res **52**(1): 152-158.

Mei, S., H. M. Ni, S. Manley, A. Bockus, K. M. Kassel, J. P. Luyendyk, B. L. Copple and W. X. Ding (2011). "Differential roles of unsaturated and saturated fatty acids on autophagy and apoptosis in hepatocytes." J Pharmacol Exp Ther **339**(2): 487-498.

Meir, K. S. and E. Leitersdorf (2004). "Atherosclerosis in the apolipoprotein-E-deficient mouse: a decade of progress." Arterioscler Thromb Vasc Biol **24**(6): 1006-1014.

Mendis S., P. P., Norrving B. (2011). "Global atlas on cardiovascular disease prevention and control Policies, strategies and interventions." World Health Organization in collaboration with the Word Heart Federation and the Word Stroke Organization.

Mensink, R. P. (2016). "Effects of saturated fatty acids on serum lipids and lipoproteins: a systematic review and regression analysis." World Health Organization

Mensink, R. P., P. L. Zock, A. D. Kester and M. B. Katan (2003). "Effects of dietary fatty acids and carbohydrates on the ratio of serum total to HDL cholesterol and on serum lipids and apolipoproteins: a meta-analysis of 60 controlled trials." Am J Clin Nutr **77**(5): 1146-1155.

Messner, B. and D. Bernhard (2014). "Smoking and cardiovascular disease: mechanisms of endothelial dysfunction and early atherogenesis." Arterioscler Thromb Vasc Biol **34**(3): 509-515.

Michas, G., R. Micha and A. Zampelas (2014). "Dietary fats and cardiovascular disease: putting together the pieces of a complicated puzzle." Atherosclerosis **234**(2): 320-328.

Mitsopoulos, P., Y. H. Chang, T. Wai, T. Konig, S. D. Dunn, T. Langer and J. Madrenas (2015). "Stomatin-like protein 2 is required for in vivo mitochondrial respiratory chain supercomplex formation and optimal cell function." Mol Cell Biol **35**(10): 1838-1847.

Miyata, M. and J. D. Smith (1996). "Apolipoprotein E allele-specific antioxidant activity and effects on cytotoxicity by oxidative insults and beta-amyloid peptides." Nat Genet **14**(1): 55-61.

Mozaffarian, D. (2016). "Dietary and Policy Priorities for Cardiovascular Disease, Diabetes, and Obesity: A Comprehensive Review." Circulation **133**(2): 187-225.

Nabel, E. G. and E. Braunwald (2012). "A tale of coronary artery disease and myocardial infarction." N Engl J Med **366**(1): 54-63.

Naem, E., M. J. Haas, N. C. Wong and A. D. Mooradian (2013). "Endoplasmic reticulum stress in HepG2 cells inhibits apolipoprotein A-I secretion." Life Sci **92**(1): 72-80.

Nakamura, S., T. Takamura, N. Matsuzawa-Nagata, H. Takayama, H. Misu, H. Noda, S. Nabemoto, S. Kurita, T. Ota, H. Ando, K. Miyamoto and S. Kaneko (2009). "Palmitate induces insulin resistance in H4IIEC3 hepatocytes through reactive oxygen species produced by mitochondria." J Biol Chem **284**(22): 14809-14818.

Niccoli, T. and L. Partridge (2012). "Ageing as a risk factor for disease." Curr Biol **22**(17): R741-752.

Nicolardi, S., Y. E. van der Burgt, I. Dragan, P. J. Hensbergen and A. M. Deelder (2013). "Identification of new apolipoprotein-CIII glycoforms with ultrahigh resolution MALDI-FTICR mass spectrometry of human sera." J Proteome Res **12**(5): 2260-2268.

Niknam, M., Z. Paknahad, M. R. Maracy and M. Hashemi (2014). "Dietary fatty acids and inflammatory markers in patients with coronary artery disease." Adv Biomed Res **3**: 148.

Nilsson, J., H. Bjorkbacka and G. N. Fredrikson (2012). "Apolipoprotein B100 autoimmunity and atherosclerosis - disease mechanisms and therapeutic potential." Curr Opin Lipidol **23**(5): 422-428.

Nordestgaard, B. G. and A. Varbo (2014). "Triglycerides and cardiovascular disease." Lancet **384**(9943): 626-635.

Noto, D., F. Fayer, A. B. Cefalu, I. Altieri, O. Palesano, R. Spina, V. Valenti, M. Pitrone, G. Pizzolanti, C. M. Barbagallo, C. Giordano and M. R. Averna (2016). "Myristic acid is associated to low plasma HDL cholesterol levels in a Mediterranean population and increases HDL catabolism by enhancing HDL particles trapping to cell surface proteoglycans in a liver hepatoma cell model." Atherosclerosis **246**: 50-56.

Olivieri, O., A. Bassi, C. Stranieri, E. Trabetti, N. Martinelli, F. Pizzolo, D. Girelli, S. Friso, P. F. Pignatti and R. Corrocher (2003). "Apolipoprotein C-III, metabolic syndrome, and risk of coronary artery disease." J Lipid Res **44**(12): 2374-2381.

Olivieri, O., N. Martinelli, M. Baroni, A. Branchini, D. Girelli, S. Friso, F. Pizzolo and F. Bernardi (2013). "Factor II activity is similarly increased in patients with elevated apolipoprotein CIII and in carriers of the factor II 20210A allele." J Am Heart Assoc **2**(6): e000440.

Olivieri, O., C. Stranieri, A. Bassi, B. Zaia, D. Girelli, F. Pizzolo, E. Trabetti, S. Cheng, M. A. Grow, P. F. Pignatti and R. Corrocher (2002). "ApoC-III gene polymorphisms and risk of coronary artery disease." J Lipid Res **43**(9): 1450-1457.

Olivieri Oliviero, C. C., Martinelli Nicola, Castagna Annalisa, Speziali Giulia, Bassi Antonella, Ceconi Daniela, Robotti Elisa, Manfredi Marcello, Conte Eleonora, Marengo Emilio (2017). "Sialylated isoforms in patients with very low or very high apolipoprotein C-III concentrations : relationships with lipids, lipoproteins and plasma fatty acids." Submitted to Clinical Chemistry and Laboratory Medicine.

Olson, R. E. (1998). "Discovery of the lipoproteins, their role in fat transport and their significance as risk factors." J Nutr **128**(2 Suppl): 439S-443S.

Onat, A., G. Hergenc, V. Sansoy, M. Fobker, K. Ceyhan, S. Toprak and G. Assmann (2003). "Apolipoprotein C-III, a strong discriminant of coronary risk in men and a determinant of the metabolic syndrome in both genders." Atherosclerosis **168**(1): 81-89.

Ooi, E. M., P. H. Barrett, D. C. Chan and G. F. Watts (2008). "Apolipoprotein C-III: understanding an emerging cardiovascular risk factor." Clin Sci (Lond) **114**(10): 611-624.

Ooi, E. M., G. F. Watts, T. W. Ng and P. H. Barrett (2015). "Effect of dietary Fatty acids on human lipoprotein metabolism: a comprehensive update." Nutrients **7**(6): 4416-4425.

Osowski, C. M. and F. Urano (2011). "Measuring ER stress and the unfolded protein response using mammalian tissue culture system." Methods Enzymol **490**: 71-92.

Parseghian, S., L. M. Onstead-Haas, N. C. Wong, A. D. Mooradian and M. J. Haas (2014). "Inhibition of apolipoprotein A-I expression by TNF-alpha in HepG2 cells: requirement for c-jun." J Cell Biochem **115**(2): 253-260.

Patel, S., B. A. Di Bartolo, S. Nakhla, A. K. Heather, T. W. Mitchell, W. Jessup, D. S. Celermajer, P. J. Barter and K. A. Rye (2010). "Anti-inflammatory effects of apolipoprotein A-I in the rabbit." Atherosclerosis **212**(2): 392-397.

Pathan, M., S. Keerthikumar, C. S. Ang, L. Gangoda, C. Y. Quek, N. A. Williamson, D. Mouradov, O. M. Sieber, R. J. Simpson, A. Salim, A. Bacic, A. F. Hill, D. A. Stroud, M. T. Ryan, J. I. Agbinya, J. M. Mariadason, A. W. Burgess and S. Mathivanan (2015). "FunRich: An open access standalone functional enrichment and interaction network analysis tool." Proteomics **15**(15): 2597-2601.

Pechlaner, R., S. Tsimikas, X. Yin, P. Willeit, F. Baig, P. Santer, F. Oberhollenzer, G. Egger, J. L. Witztum, V. J. Alexander, J. Willeit, S. Kiechl and M. Mayr (2017). "Very-Low-Density Lipoprotein-Associated Apolipoproteins Predict Cardiovascular Events and Are Lowered by Inhibition of APOC-III." J Am Coll Cardiol **69**(7): 789-800.

Pike, L. S., A. L. Smift, N. J. Croteau, D. A. Ferrick and M. Wu (2011). "Inhibition of fatty acid oxidation by etomoxir impairs NADPH production and increases reactive oxygen species resulting in ATP depletion and cell death in human glioblastoma cells." Biochim Biophys Acta **1807**(6): 726-734.

Polonskaya, Y. V., V. S. Shramko, S. V. Morozov, E. I. Chernyak, A. M. Chernyavsky and Y. I. Ragino (2017). "Balance of Fatty Acids and Their Correlations with Parameters of Lipid Metabolism and Markers of Inflammation in Men with Coronary Atherosclerosis." Bull Exp Biol Med **164**(1): 33-35.

Popeijus, H. E., S. D. van Otterdijk, S. E. van der Krieken, M. Konings, K. Serbonij, J. Plat and R. P. Mensink (2014). "Fatty acid chain length and saturation influences PPARalpha transcriptional activation and repression in HepG2 cells." Mol Nutr Food Res **58**(12): 2342-2349.

Puranik, R., S. Bao, E. Nobecourt, S. J. Nicholls, G. J. Dusting, P. J. Barter, D. S. Celermajer and K. A. Rye (2008). "Low dose apolipoprotein A-I rescues carotid arteries from inflammation in vivo." Atherosclerosis **196**(1): 240-247.

Raitakari, O. T., V. P. Mäkinen, M. J. McQueen, J. Niemi, M. Juonala, M. Jauhiainen, V. Salomaa, M. L. Hannuksela, M. J. Savolainen, Y. A. Kesäniemi, P. T. Kovanen, J. Sundvall, T. Solakivi, B. M. Loo, J. Marniemi, J. Hernessniemi, T. Lehtimäki, M. Kahonen, M. Peltonen, J. Leiviska, A. Jula, S. S. Anand, R. Miller, S. Yusuf, J. S. Viikari and M. Ala-Korpela (2013). "Computationally estimated apolipoproteins B and A1 in predicting cardiovascular risk." Atherosclerosis **226**(1): 245-251.

- Ramboer, E., T. Vanhaecke, V. Rogiers and M. Vinken (2015). "Immortalized Human Hepatic Cell Lines for In Vitro Testing and Research Purposes." Methods Mol Biol **1250**: 53-76.
- Rangel-Zuniga, O. A., A. Camargo, C. Marin, P. Pena-Orihuela, P. Perez-Martinez, J. Delgado-Lista, L. Gonzalez-Guardia, E. M. Yubero-Serrano, F. J. Tinahones, M. M. Malagon, F. Perez-Jimenez, H. M. Roche and J. Lopez-Miranda (2015). "Proteome from patients with metabolic syndrome is regulated by quantity and quality of dietary lipids." BMC Genomics **16**: 509.
- RCoreTeam (2015). "R: A language and environment for statistical computing. ." R Foundation for Statistical Computing, Vienna, Austria (<https://www.R-project.org/>).
- Ren, X. M., L. Y. Cao, J. Zhang, W. P. Qin, Y. Yang, B. Wan and L. H. Guo (2016). "Investigation of the Binding Interaction of Fatty Acids with Human G Protein-Coupled Receptor 40 Using a Site-Specific Fluorescence Probe by Flow Cytometry." Biochemistry **55**(13): 1989-1996.
- Ricchi, M., M. R. Odoardi, L. Carulli, C. Anzivino, S. Ballestri, A. Pinetti, L. I. Fantoni, F. Marra, M. Bertolotti, S. Banni, A. Lonardo, N. Carulli and P. Loria (2009). "Differential effect of oleic and palmitic acid on lipid accumulation and apoptosis in cultured hepatocytes." J Gastroenterol Hepatol **24**(5): 830-840.
- Rioux, V., A. Galat, G. Jan, F. Vinci, S. D'Andrea and P. Legrand (2002). "Exogenous myristic acid acylates proteins in cultured rat hepatocytes." J Nutr Biochem **13**(2): 66-74.
- Rioux, V., F. Pedrono and P. Legrand (2011). "Regulation of mammalian desaturases by myristic acid: N-terminal myristoylation and other modulations." Biochim Biophys Acta **1811**(1): 1-8.
- Rizos, E. C., E. E. Ntzani, E. Bika, M. S. Kostapanos and M. S. Elisaf (2012). "Association between omega-3 fatty acid supplementation and risk of major cardiovascular disease events: a systematic review and meta-analysis." JAMA **308**(10): 1024-1033.
- Roberts, J. D., A. Thapaliya, S. Martinez-Lumbreras, E. M. Krysztofinska and R. L. Isaacson (2015). "Structural and Functional Insights into Small, Glutamine-Rich, Tetratricopeptide Repeat Protein Alpha." Front Mol Biosci **2**: 71.
- Robertson, T. A., N. S. Dutton, R. N. Martins, K. Taddei and J. M. Papadimitriou (2000). "Comparison of astrocytic and myocytic metabolic dysregulation in apolipoprotein E deficient and human apolipoprotein E transgenic mice." Neuroscience **98**(2): 353-359.
- Rocha, V. Z. and P. Libby (2009). "Obesity, inflammation, and atherosclerosis." Nat Rev Cardiol **6**(6): 399-409.
- Roncaglioni, M. C., M. Tombesi, F. Avanzini, S. Barlera, V. Caimi, P. Longoni, I. Marzona, V. Milani, M. G. Silletta, G. Tognoni and R. R. a. P. S. C. G. Marchioli (2013). "n-3 fatty acids in patients with multiple cardiovascular risk factors." N Engl J Med **368**(19): 1800-1808.
- Roselaar, S. E. and A. Daugherty (1998). "Apolipoprotein E-deficient mice have impaired innate immune responses to *Listeria monocytogenes* in vivo." J Lipid Res **39**(9): 1740-1743.
- Rosenson, R. S., H. B. Brewer, Jr., B. J. Ansell, P. Barter, M. J. Chapman, J. W. Heinecke, A. Kontush, A. R. Tall and N. R. Webb (2016). "Dysfunctional HDL and atherosclerotic cardiovascular disease." Nat Rev Cardiol **13**(1): 48-60.
- Rousan, T. A., S. T. Mathew and U. Thadani (2017). "Drug Therapy for Stable Angina Pectoris." Drugs **77**(3): 265-284.

Rungapamestry, V., J. McMonagle, C. Reynolds, G. Rucklidge, M. Reid, G. Duncan, K. Ross, G. Horgan, S. Toomey, A. P. Moloney, B. Roos and H. M. Roche (2012). "Inter-organ proteomic analysis reveals insights into the molecular mechanisms underlying the anti-diabetic effects of cis-9, trans-11-conjugated linoleic acid in ob/ob mice." Proteomics **12**(3): 461-476.

Rye, K. A. and P. J. Barter (2004). "Formation and metabolism of prebeta-migrating, lipid-poor apolipoprotein A-I." Arterioscler Thromb Vasc Biol **24**(3): 421-428.

Sacks, F. M., P. Alaupovic, L. A. Moye, T. G. Cole, B. Sussex, M. J. Stampfer, M. A. Pfeffer and E. Braunwald (2000). "VLDL, apolipoproteins B, CIII, and E, and risk of recurrent coronary events in the Cholesterol and Recurrent Events (CARE) trial." Circulation **102**(16): 1886-1892.

Santaren, I. D., S. M. Watkins, A. D. Liese, L. E. Wagenknecht, M. J. Rewers, S. M. Haffner, C. Lorenzo, A. Festa, R. P. Bazinet and A. J. Hanley (2017). "Individual serum saturated fatty acids and markers of chronic subclinical inflammation: the Insulin Resistance Atherosclerosis Study." J Lipid Res **58**(11): 2171-2179.

Santos-Gallego, C. G., B. Picatoste and J. J. Badimon (2014). "Pathophysiology of acute coronary syndrome." Curr Atheroscler Rep **16**(4): 401.

Santos, R. D. and R. C. Maranhao (2014). "What is new in familial hypercholesterolemia?" Curr Opin Lipidol **25**(3): 183-188.

Santos, T. G., V. R. Martins and G. N. M. Hajj (2017). "Unconventional Secretion of Heat Shock Proteins in Cancer." Int J Mol Sci **18**(5).

Sargsyan, E., K. Artemenko, L. Manukyan, J. Bergquist and P. Bergsten (2016). "Oleate protects beta-cells from the toxic effect of palmitate by activating pro-survival pathways of the ER stress response." Biochim Biophys Acta **1861**(9 Pt A): 1151-1160.

Schmittgen, T. D. and K. J. Livak (2008). "Analyzing real-time PCR data by the comparative C(T) method." Nat Protoc **3**(6): 1101-1108.

Schoonjans, K., B. Staels and J. Auwerx (1996). "Role of the peroxisome proliferator-activated receptor (PPAR) in mediating the effects of fibrates and fatty acids on gene expression." J Lipid Res **37**(5): 907-925.

Schulze, R. J. and M. A. McNiven (2014). "A well-oiled machine: DNM2/dynamin 2 helps keep hepatocyte lipophagy running smoothly." Autophagy **10**(2): 388-389.

Schwartz, E. A. and P. D. Reaven (2012). "Lipolysis of triglyceride-rich lipoproteins, vascular inflammation, and atherosclerosis." Biochim Biophys Acta **1821**(5): 858-866.

Scruggs, B. S., C. I. Michel, D. S. Ory and J. E. Schaffer (2012). "SmD3 regulates intronic noncoding RNA biogenesis." Mol Cell Biol **32**(20): 4092-4103.

Sears, B. and M. Perry (2015). "The role of fatty acids in insulin resistance." Lipids Health Dis **14**: 121.

Segrest, J. P., M. K. Jones, H. De Loof, C. G. Brouillette, Y. V. Venkatachalapathi and G. M. Anantharamaiah (1992). "The amphipathic helix in the exchangeable apolipoproteins: a review of secondary structure and function." J Lipid Res **33**(2): 141-166.

Shao, B. (2012). "Site-specific oxidation of apolipoprotein A-I impairs cholesterol export by ABCA1, a key cardioprotective function of HDL." Biochim Biophys Acta **1821**(3): 490-501.

- Shen, Z., S. Huang, M. Fang and X. Wang (2011). "ENTPD5, an endoplasmic reticulum UDPase, alleviates ER stress induced by protein overloading in AKT-activated cancer cells." Cold Spring Harb Symp Quant Biol **76**: 217-223.
- Siculella, L., R. Tocci, A. Rochira, M. Testini, A. Gnani and F. Damiano (2016). "Lipid accumulation stimulates the cap-independent translation of SREBP-1a mRNA by promoting hnRNP A1 binding to its 5'-UTR in a cellular model of hepatic steatosis." Biochim Biophys Acta **1861**(5): 471-481.
- Sidhu, V. K., B. X. Huang and H. Y. Kim (2011). "Effects of docosahexaenoic acid on mouse brain synaptic plasma membrane proteome analyzed by mass spectrometry and (16)O/(18)O labeling." J Proteome Res **10**(12): 5472-5480.
- Singh, P. P., M. Singh and S. S. Mastana (2006). "APOE distribution in world populations with new data from India and the UK." Ann Hum Biol **33**(3): 279-308.
- Slany, A., V. J. Haudek, H. Zwickl, N. C. Gundacker, M. Grusch, T. S. Weiss, K. Seir, C. Rodgarkia-Dara, C. Hellerbrand and C. Gerner (2010). "Cell characterization by proteome profiling applied to primary hepatocytes and hepatocyte cell lines Hep-G2 and Hep-3B." J Proteome Res **9**(1): 6-21.
- Sletten, A., A. Seline, A. Rudd, M. Logsdon and L. L. Listenberger (2014). "Surface features of the lipid droplet mediate perilipin 2 localization." Biochem Biophys Res Commun **452**(3): 422-427.
- Smith, J. G. and C. Newton-Cheh (2015). "Genome-wide association studies of late-onset cardiovascular disease." J Mol Cell Cardiol **83**: 131-141.
- Snel, B., G. Lehmann, P. Bork and M. A. Huynen (2000). "STRING: a web-server to retrieve and display the repeatedly occurring neighbourhood of a gene." Nucleic Acids Res **28**(18): 3442-3444.
- Song, Y., M. J. Stampfer and S. Liu (2004). "Meta-analysis: apolipoprotein E genotypes and risk for coronary heart disease." Ann Intern Med **141**(2): 137-147.
- Sowers, J. R., M. Epstein and E. D. Frohlich (2001). "Diabetes, hypertension, and cardiovascular disease: an update." Hypertension **37**(4): 1053-1059.
- Spence, J. D. and L. Pilote (2015). "Importance of sex and gender in atherosclerosis and cardiovascular disease." Atherosclerosis **241**(1): 208-210.
- Sramek, J., V. Nemcova-Furstova, N. Pavlikova and J. Kovar (2017). "Effect of Saturated Stearic Acid on MAP Kinase and ER Stress Signaling Pathways during Apoptosis Induction in Human Pancreatic beta-Cells Is Inhibited by Unsaturated Oleic Acid." Int J Mol Sci **18**(11).
- St-Pierre, A. C., B. Cantin, G. R. Dagenais, J. P. Despres and B. Lamarche (2006). "Apolipoprotein-B, low-density lipoprotein cholesterol, and the long-term risk of coronary heart disease in men." Am J Cardiol **97**(7): 997-1001.
- Staels, B., N. Vu-Dac, V. A. Kosykh, R. Saladin, J. C. Fruchart, J. Dallongeville and J. Auwerx (1995). "Fibrates downregulate apolipoprotein C-III expression independent of induction of peroxisomal acyl coenzyme A oxidase. A potential mechanism for the hypolipidemic action of fibrates." J Clin Invest **95**(2): 705-712.
- Suzuki, H., K. Kanekura, T. P. Levine, K. Kohno, V. M. Olkkonen, S. Aiso and M. Matsuoka (2009). "ALS-linked P56S-VAPB, an aggregated loss-of-function mutant of VAPB, predisposes motor neurons to ER stress-related death by inducing aggregation of co-expressed wild-type VAPB." J Neurochem **108**(4): 973-985.



Tang, X., Z. J. Li, J. Xu, Y. Xue, J. Z. Li, J. F. Wang, T. Yanagita, C. H. Xue and Y. M. Wang (2012). "Short term effects of different omega-3 fatty acid formulation on lipid metabolism in mice fed high or low fat diet." Lipids Health Dis **11**: 70.

Tarnus, E., H. Wassef, J. F. Carmel, P. Rondeau, M. Roche, J. Davignon, L. Bernier and E. Bourdon (2009). "Apolipoprotein E limits oxidative stress-induced cell dysfunctions in human adipocytes." FEBS Lett **583**(12): 2042-2048.

Thapaliya, A., Y. Nyathi, S. Martinez-Lumbreras, E. M. Kryzstofinska, N. J. Evans, I. L. Terry, S. High and R. L. Isaacson (2016). "SGTA interacts with the proteasomal ubiquitin receptor Rpn13 via a carboxylate clamp mechanism." Sci Rep **6**: 36622.

Thinon, E., J. Morales-Sanfrutos, D. J. Mann and E. W. Tate (2016). "N-Myristoyltransferase Inhibition Induces ER-Stress, Cell Cycle Arrest, and Apoptosis in Cancer Cells." ACS Chem Biol **11**(8): 2165-2176.

Thinon, E., R. A. Serwa, M. Broncel, J. A. Brannigan, U. Brassat, M. H. Wright, W. P. Heal, A. J. Wilkinson, D. J. Mann and E. W. Tate (2014). "Global profiling of co- and post-translationally N-myristoylated proteomes in human cells." Nat Commun **5**: 4919.

Tholstrup, T., B. Vessby and B. Sandstrom (2003). "Difference in effect of myristic and stearic acid on plasma HDL cholesterol within 24 h in young men." Eur J Clin Nutr **57**(6): 735-742.

Tiwari, S., S. Siddiqi, O. Zhelyabovska and S. A. Siddiqi (2016). "Silencing of Small Valosin-containing Protein-interacting Protein (SVIP) Reduces Very Low Density Lipoprotein (VLDL) Secretion from Rat Hepatocytes by Disrupting Its Endoplasmic Reticulum (ER)-to-Golgi Trafficking." J Biol Chem **291**(24): 12514-12526.

Tiwari, S. and S. A. Siddiqi (2012). "Intracellular trafficking and secretion of VLDL." Arterioscler Thromb Vasc Biol **32**(5): 1079-1086.

Tomita, K., T. Teratani, H. Yokoyama, T. Suzuki, R. Irie, H. Ebinuma, H. Saito, R. Hokari, S. Miura and T. Hibi (2011). "Plasma free myristic acid proportion is a predictor of nonalcoholic steatohepatitis." Dig Dis Sci **56**(10): 3045-3052.

Tripathi, R., N. Benz, B. Culleton, P. Trouve and C. Ferec (2014). "Biophysical characterisation of calumenin as a charged F508del-CFTR folding modulator." PLoS One **9**(8): e104970.

Udenwobele, D. I., R. C. Su, S. V. Good, T. B. Ball, S. Varma Shrivastav and A. Shrivastav (2017). "Myristoylation: An Important Protein Modification in the Immune Response." Front Immunol **8**: 751.

Vaccarino, V., L. Badimon, R. Corti, C. de Wit, M. Dorobantu, A. Hall, A. Koller, M. Marzilli, A. Pries, R. Bugiardini, P. Working Group on Coronary and Microcirculation (2011). "Ischaemic heart disease in women: are there sex differences in pathophysiology and risk factors? Position paper from the working group on coronary pathophysiology and microcirculation of the European Society of Cardiology." Cardiovasc Res **90**(1): 9-17.

Valenta, D. T., J. J. Bulgrien, C. L. Banka and L. K. Curtiss (2006). "Overexpression of human ApoAI transgene provides long-term atheroprotection in LDL receptor-deficient mice." Atherosclerosis **189**(2): 255-263.

van Capelleveen, J. C., A. E. Bochem, S. M. Boekholdt, S. Mora, R. C. Hoogeveen, C. M. Ballantyne, P. M. Ridker, W. Sun, P. J. Barter, A. R. Tall, A. H. Zwinderman, J. J. P. Kastelein, N. J. Wareham, K. T. Khaw and G. K. Hovingh (2017). "Association of High-Density Lipoprotein-Cholesterol Versus Apolipoprotein A-I With Risk of Coronary Heart Disease: The European Prospective Investigation Into

Cancer-Norfolk Prospective Population Study, the Atherosclerosis Risk in Communities Study, and the Women's Health Study." J Am Heart Assoc **6**(8).

Vatolin, S., J. G. Phillips, B. K. Jha, S. Govindgari, J. Hu, D. Grabowski, Y. Parker, D. J. Lindner, F. Zhong, C. W. Distelhorst, M. R. Smith, C. Cotta, Y. Xu, S. Chilakala, R. R. Kuang, S. Tall and F. J. Reu (2016). "Novel Protein Disulfide Isomerase Inhibitor with Anticancer Activity in Multiple Myeloma." Cancer Res **76**(11): 3340-3350.

Vaysse-Boue, C., H. Dabadie, E. Peuchant, P. Le Ruyet, F. Mendy, H. Gin and N. Combe (2007). "Moderate dietary intake of myristic and alpha-linolenic acids increases lecithin-cholesterol acyltransferase activity in humans." Lipids **42**(8): 717-722.

Vembar, S. S. and J. L. Brodsky (2008). "One step at a time: endoplasmic reticulum-associated degradation." Nat Rev Mol Cell Biol **9**(12): 944-957.

Vendel Nielsen, L., T. P. Krogager, C. Young, C. Ferreri, C. Chatgialiloglu, O. Norregaard Jensen and J. J. Enghild (2013). "Effects of elaidic acid on lipid metabolism in HepG2 cells, investigated by an integrated approach of lipidomics, transcriptomics and proteomics." PLoS One **8**(9): e74283.

Vidyashankar, S., R. Sandeep Varma and P. S. Patki (2013). "Quercetin ameliorate insulin resistance and up-regulates cellular antioxidants during oleic acid induced hepatic steatosis in HepG2 cells." Toxicol In Vitro **27**(2): 945-953.

Villarroya-Beltri, C., C. Gutierrez-Vazquez, F. Sanchez-Cabo, D. Perez-Hernandez, J. Vazquez, N. Martin-Cofreces, D. J. Martinez-Herrera, A. Pascual-Montano, M. Mittelbrunn and F. Sanchez-Madrid (2013). "Sumoylated hnRNPA2B1 controls the sorting of miRNAs into exosomes through binding to specific motifs." Nat Commun **4**: 2980.

Wada, Y., S. Sakiyama, H. Sakai and F. Sakane (2016). "Myristic Acid Enhances Diacylglycerol Kinase delta-Dependent Glucose Uptake in Myotubes." Lipids **51**(8): 897-903.

Wang, C. S., W. J. McConathy, H. U. Kloer and P. Alaupovic (1985). "Modulation of lipoprotein lipase activity by apolipoproteins. Effect of apolipoprotein C-III." J Clin Invest **75**(2): 384-390.

Wang, H., P. K. Chan, S. Y. Pan, K. H. Kwon, Y. Ye, J. H. Chu, W. F. Fong, W. M. Tsui and Z. L. Yu (2010). "ERp57 is up-regulated in free fatty acids-induced steatotic L-02 cells and human nonalcoholic fatty livers." J Cell Biochem **110**(6): 1447-1456.

Warensjo, E., J. Sundstrom, B. Vessby, T. Cederholm and U. Riserus (2008). "Markers of dietary fat quality and fatty acid desaturation as predictors of total and cardiovascular mortality: a population-based prospective study." Am J Clin Nutr **88**(1): 203-209.

Weisgraber, K. H., T. L. Innerarity and R. W. Mahley (1982). "Abnormal lipoprotein receptor-binding activity of the human E apoprotein due to cysteine-arginine interchange at a single site." J Biol Chem **257**(5): 2518-2521.

WHO (2012). "WHO global report: mortality attributable to tobacco."

Winham, S. J., M. de Andrade and V. M. Miller (2015). "Genetics of cardiovascular disease: Importance of sex and ethnicity." Atherosclerosis **241**(1): 219-228.

Wisniewski, J. R., A. Vildhede, A. Noren and P. Artursson (2016). "In-depth quantitative analysis and comparison of the human hepatocyte and hepatoma cell line HepG2 proteomes." J Proteomics **136**: 234-247.

- Witztum, J. L. and D. Steinberg (1991). "Role of oxidized low density lipoprotein in atherogenesis." J Clin Invest **88**(6): 1785-1792.
- Wong, N. D. (2014). "Epidemiological studies of CHD and the evolution of preventive cardiology." Nat Rev Cardiol **11**(5): 276-289.
- Wu, C. L., S. P. Zhao and B. L. Yu (2013). "Microarray analysis provides new insights into the function of apolipoprotein O in HepG2 cell line." Lipids Health Dis **12**: 186.
- Wunderley, L., P. Leznicki, A. Payapilly and S. High (2014). "SGTA regulates the cytosolic quality control of hydrophobic substrates." J Cell Sci **127**(Pt 21): 4728-4739.
- Yao, H. R., J. Liu, D. Plumeri, Y. B. Cao, T. He, L. Lin, Y. Li, Y. Y. Jiang, J. Li and J. Shang (2011). "Lipotoxicity in HepG2 cells triggered by free fatty acids." Am J Transl Res **3**(3): 284-291.
- Yki-Jarvinen, H. (2014). "Non-alcoholic fatty liver disease as a cause and a consequence of metabolic syndrome." Lancet Diabetes Endocrinol **2**(11): 901-910.
- Yoo, W., K. H. Noh, J. H. Ahn, J. H. Yu, J. A. Seo, S. G. Kim, K. M. Choi, S. H. Baik, D. S. Choi, T. W. Kim, H. J. Kim and N. H. Kim (2014). "HIF-1 $\alpha$  expression as a protective strategy of HepG2 cells against fatty acid-induced toxicity." J Cell Biochem **115**(6): 1147-1158.
- Yoshida, H., T. Okada, K. Haze, H. Yanagi, T. Yura, M. Negishi and K. Mori (2000). "ATF6 activated by proteolysis binds in the presence of NF-Y (CBF) directly to the cis-acting element responsible for the mammalian unfolded protein response." Mol Cell Biol **20**(18): 6755-6767.
- Zhang, K. and R. J. Kaufman (2006). "The unfolded protein response: a stress signaling pathway critical for health and disease." Neurology **66**(2 Suppl 1): S102-109.
- Zhang, L., K. Xiao, X. Zhao, X. Sun, J. Zhang, X. Wang, Y. Zhu and X. Zhang (2017). "Quantitative proteomics reveals key proteins regulated by eicosapentaenoic acid in endothelial activation." Biochem Biophys Res Commun **487**(2): 464-469.
- Zhang, X., Z. Xu, L. Zhou, Y. Chen, M. He, L. Cheng, F. B. Hu, R. M. Tanguay and T. Wu (2010). "Plasma levels of Hsp70 and anti-Hsp70 antibody predict risk of acute coronary syndrome." Cell Stress Chaperones **15**(5): 675-686.
- Zhang, X. Q., Y. Pan, C. H. Yu, C. F. Xu, L. Xu, Y. M. Li and W. X. Chen (2015). "PDIA3 Knockdown Exacerbates Free Fatty Acid-Induced Hepatocyte Steatosis and Apoptosis." PLoS One **10**(7): e0133882.
- Zhang, Y., A. R. Sinaiko and G. L. Nelsestuen (2012). "Glycoproteins and glycosylation: apolipoprotein c3 glycoforms by top-down maldi-tof mass spectrometry." Methods Mol Biol **909**: 141-150.
- Zheng, C. (2014). "Updates on apolipoprotein CIII: fulfilling promise as a therapeutic target for hypertriglyceridemia and cardiovascular disease." Curr Opin Lipidol **25**(1): 35-39.
- Zheng, C., C. Khoo, J. Furtado, K. Ikewaki and F. M. Sacks (2008). "Dietary monounsaturated fat activates metabolic pathways for triglyceride-rich lipoproteins that involve apolipoproteins E and C-III." Am J Clin Nutr **88**(2): 272-281.
- Zhou, L., C. Li, L. Gao and A. Wang (2015). "High-density lipoprotein synthesis and metabolism (Review)." Mol Med Rep **12**(3): 4015-4021.

Zock, P. L., J. H. de Vries and M. B. Katan (1994). "Impact of myristic acid versus palmitic acid on serum lipid and lipoprotein levels in healthy women and men." Arterioscler Thromb **14**(4): 567-575.

Zong, G., Y. Li, A. J. Wanders, M. Alsema, P. L. Zock, W. C. Willett, F. B. Hu and Q. Sun (2016). "Intake of individual saturated fatty acids and risk of coronary heart disease in US men and women: two prospective longitudinal cohort studies." BMJ **355**: i5796.